Modelling effects of stormwater best management practices on urban stormwater runoff phosphorus

by

Bowen Zhou

A thesis
presented to the University of Waterloo
in fulfilment of the
thesis requirement for the degree of
Doctor of Philosophy
in
Earth Sciences (Water)

Waterloo, Ontario, Canada, 2024

Examining Committee Membership

The following served on the Examining Committee for this thesis. The decision of the Examining Committee is by majority vote.

External Examiner	Dr. Max Maurer Professor Department of Civil Environment and Geomatic Engineering ETH Zurich
Supervisor	Dr. Philippe Van Cappellen Professor, Canada Excellence Research Chair Department of Earth and Environmental Sciences University of Waterloo
Co-supervisor	Dr. Christopher T. Parsons Research Scientist & Adjunct Professor Watershed Hydrology and Ecology Research Division Environment and Climate Change Canada
Internal Member	Dr. Fereidoun Reza Nezhad Research Associate Professor Department of Earth and Environmental Sciences University of Waterloo
	Dr. Nandita Basu Professor Department of Civil and Environmental Engineering University of Waterloo
Internal-external Member	Dr. Bruce McVicar Associate Professor Department of Civil and Environmental Engineering University of Waterloo
Other Member	Dr. Elodie Passeport Associate Professor Department of Civil and Mineral Engineering University of Toronto

AUTHOR'S DECLARATION

This thesis consists of material all of which I authored or co-authored: see Statement of Contributions included in the thesis. This is a true copy of the thesis, including any required final revisions, as accepted by my examiners.

I understand that my thesis may be made electronically available to the public.

Statement of Contributions

This thesis consists of a series of co-authored papers. As the first author on each paper, I was primarily responsible for the study designs and execution. The following summarizes the contributions of the co-authors of each paper.

Chapter 2

I and Jovana Radosavljevic (JR) developed the research questions and performed the literature review. I extracted and analyzed the data from the International Stormwater BMP Database (ISBD). I and JR wrote the paper, with input from Stephanie Slowinski (SS), Bruce McVicar (BM), Fereidoun Rezanezhad (FR), Mahyar Shafii (MS), Sarah Kaykhosravi (SK), Chris T. Parsons (CTP), and Philippe Van Cappellen (PVC).

Chapter 3

I developed the research questions, built the model and performed the data analysis. Ariel Lisogorsky (AL) and I conducted the lab analysis of field core samples. I wrote the paper with input from PVC, MS, CTP, Elodie Passeport (EP), FR and AL, and PVC. All co-authors provided feedback on data interpretation.

Chapter 4

I developed research questions and methodology. I wrote the computer code for the extraction, cleaning and analysis of data from the ISBD, and developed the machine learning model. I wrote the paper, with input from PVC, CTP, MS, FR and EP. All co-authors provided feedback on data interpretation.

Chapter 5

I developed research questions and methodology. I wrote the computer code for the extraction, cleaning and analysis of data from the ISBD, and developed the machine learning model. I wrote the paper, with input from PVC and CTP. All co-authors provided feedback on data interpretation.

Abstract

Phosphorus (P) is a key limiting nutrient for algal growth in freshwater whose excess loading to freshwater bodies contributes to cultural eutrophication and the associated symptoms of water quality deterioration. Urban stormwater is a significant contributor of P to downstream ecosystems from various point and non-point sources and via a variety of transport and emission pathways. Stormwater best management practices (BMPs) such as stormwater ponds (SWPs, a type of traditional stormwater BMP) and bioretention cells (BRCs, a type of low-impact development (LID) BMP) have the potential to attenuate P loads from urban areas and hence mitigate eutrophication risks to aquatic ecosystems. Despite their rapidly growing implementation worldwide, the effects of these stormwater BMPs on urban stormwater P concentrations and loads remain poorly understood.

In this thesis, I assess the effects of urban stormwater BMPs on P export, with the goal of determining (1) what are the knowns and unknowns regarding the sources, pathways, and influence of stormwater BMPs on urban P export, (2) what are the dominant internal processes that control P reduction in BRC, based on process-based modelling, (3) what are the general effects of BRCs on urban stormwater runoff P and how are they different from the effects on nitrogen (N), and (4) how to predict the effects of BMPs on urban stormwater runoff P through the use of data-driven models, and what are the potential influencing factors. I address these research questions by reviewing urban P sources discussed in the literature, quantifying P mass balance in a BRC facility in Mississauga, ON, assessing effects of urban stormwater BMPs on P export based on data from the International Stormwater BMP Database, and through the development of process-based and data-driven BMP P models.

In Chapter 2, I review the existing literature and analyze data from the International Stormwater BMP Database (ISBD) to summarize the sources, pathways and speciation of urban stormwater P, and the effects of urban stormwater BMPs on P export. This study acts as an introduction to the issues of P in urban stormwater runoff and identifies the research gaps associated with understanding effects of stormwater BMPs on urban stormwater P export. I show, based on both previous literature and the data in the ISBD, that the effects of stormwater BMPs on urban P export remain highly uncertain and unknown. There is a lack of predictive tools for

estimating effects of stormwater BMPs on urban P export, and I go on to fill this research gap in Chapters 3, 4, and 5.

Following Chapter 2, I address my research questions by developing a process-based P model for a BRC facility in Mississauga, ON. This model is calibrated using field monitored data for flow, water quality and filter media soil chemistry (from core samples). In Chapter 3, the model simulates the multi-year P partitioning, accumulation and export in this stormwater BMP. I show, via the analysis of model simulation results, that exfiltration to underlying native soil was principally responsible for decreasing the surface water discharge from the BRC (63% runoff reduction), while accumulation in the filter media layer was the predominant mechanism responsible for the reduction in P outflow loading (57% retention of total P (TP) inflow load). Of the P retained within the filter media layer, only 11% was stored in easily mobilizable forms. There were no signs that the P retention capacity of the BRC was approaching saturation after 7 years of operation. Thus, my results demonstrate sustained efficient P load reduction by this BRC.

In Chapter 4 I evaluate the general effects of BRCs on urban stormwater runoff P concentration and loading by analyzing data from a large number of BRCs in the ISBD from across the United States. I further compare the influence of BRCs on P and N export. I also introduce the data-driven approach in Chapter 4 by training a random forest model to predict the reduction and enrichment effects of BRCs and compare the importance of different explanatory variables. I show that while BRCs typically enrich concentrations of TP and soluble reactive P (SRP), the corresponding outflow loads of TP and SRP, were generally lower, mainly because of reductions to surface runoff volumes via exfiltration to the subsurface. This finding raises questions regarding the relative importance of this infiltrating P to the subsurface environment and potential impacts to groundwater quality. Because they are generally more efficient in reducing N loads than P loads, BRCs tended to decrease the N:P ratio of stormwater runoff, potentially altering nutrient limitation patterns in receiving aquatic ecosystems. My findings also imply that the impacts of BRCs on P and N concentrations, speciation, and loads in urban runoff are highly variable. This variability can be partly accounted for by some explanatory variables related to the climate, watershed and BRC characteristics, and predicted by machine learning (ML) methods such as the random forest model. Random forest modeling identified inflow concentrations and

BRC age as key variables modulating the changes in TP, SRP, and total N concentrations between inflow and outflow. For dissolved inorganic N, the BRC's storage volume and drainage area also emerged as important explanatory variables.

Chapter 5 also focuses on the ISBD, similar to Chapter 4, but the analysis of P control performance is expanded to six categories of BMPs. I compare the accuracy of different data-driven models for the prediction of BMP P reduction/enrichment factors, through the use of different ML methods. I show that although LID BMPs are generally more efficient at reducing runoff quantity, they are more likely to enrich TP and SRP concentrations compared to traditional BMPs leading to poorer P load reduction performance amongst LID BMPs. Both traditional and LID BMPs are more likely to enrich SRP concentration when influent SRP concentration is low, in watersheds with higher imperviousness and in drier climates. The influence of LID BMPs on SRP concentration is also more sensitive to climate, watershed and BMP characteristics compared to traditional BMPs. I show that the random forest model provides the most accurate estimation of BMPs effects on urban stormwater P concentrations when compared to models produced using other ML methods. This study suggests that switching to LID BMPs has the potential to increase eutrophication risks and requires further examination. It also proposes that ML methods, especially use of the random forest model can represent a more robust approach to estimate the effects of stormwater BMPs on urban runoff P by accounting for both P reduction and enrichment effects.

My results show that that BRCs and other stormwater BMPs have highly variable effects on urban P export. I show that although the BRC I investigated in Mississauga, ON, exhibits efficient reduction of P export, it appears to be atypical and that BRCs and other LID BMPs are generally more likely to enrich P concentration compared to traditional BMPs based on data from a large number of BMP systems in the ISBD. This concentration enrichment may further impact the quality of groundwater and surface waterbodies. Considering the global environmental policy trend to promote replacement of traditional stormwater BMPs with LID BMPs, the findings of this thesis should serve as a caution to policy makers, as understanding of the effects of stormwater BMPs on urban P export remain incomplete.

Acknowledgments

I am grateful to the Natural Sciences and Engineering Research Council of Canada (NSERC), Global Water Future (GWF), and the University of Waterloo for funding this research.

I am indebted to Philippe Van Cappellen, my supervisor and role model in science, for offering me the opportunity to work in such a diverse, inclusive, and vibrant group. Philippe instructed me how to become a mature researcher by inspiring me to come up with more idea and guiding me to overcome the challenges through my PhD trip, with a lot of supports. Thank you, Philippe!

I extend my gratitude to my co-supervisor, Chris Thomas Parsons, for the numerous efforts he invested in my work and the exciting opportunities he created for me. Chris's insightful comments and recommendations based on his experience in both academia and government always brings me great illumination.

I would like to thank my thesis committee and collaborators: Fereidoun Reza Nezhad, Elodie Passeport, Nandita Basu, Bruce McVicar and Max Maurer. Thank you for your guidance, suggestions, criticism and encouragement to my work.

To my friends and colleagues in Ecohydrology Research Group, I am always proud to be a part of this group because of how outstanding you are. Especially, I am grateful to Shuhuan Li, who recommended me to pursue PhD in 2019, which led to all the later stories. Thank you Jovana Radosavljevic, Mahyar Shafii, Stephanie Slowinski, Ariel Lisorgorsky, Yubraj Bhusal, Sarah Kaykhosravi and Md Adbus Sabur, for the time we spent together in office, lab and field for the urban project. Thank you Jane Ye, Xiaochuang Bu, Wenkai Qiu, Qiwei Huang, Clement Alibert, Lewis Alcott, Danielle Green, Hang Nguyen, Christina Lam, Zahra Akbarzadeh, Qianlin Zheng, Qingqing Sun, Binjie Shi, Kunfu Pi and Riley Mills, for the wonderful time we spent together in the campus, gym, and trips. Thank you, Anita Ghosh-Homme, Bhaleka Persaud, Marianne Vandergriendt, Linden Fairbairn and Mickey Nielsen, for helping me with my research and life in ERG. You have all helped me grow as a researcher.

To my friends, Haoyu Gu, Chenxi Wang, Zeren Ning, Siyao Zhao, Jiangyue Ju, Haoyu Yin and everyone else I have hung out with over these years, thanks for accompanying me to climb this mountain.

Dedication

To my parents, Zhongyi Zhou and Shaomei Cao, for your unwavering support. I always remember what you told me before I started my PhD: “We encourage you to pursue the PhD, not because we want you to become wealthier or more successful, but because we hope you to do the work that makes you happy, and we hope you to enrich your life through this journey and to see a bigger world”. My life has been enriched a lot after this journey. Thank you for steadily encouraging me to pursue the enthusiasm inside my heart.

Table of Contents

List of Figures

List of Tables

List of Abbreviations

BMP	Best management practice
BRC	Bioretention cell
DIN	Dissolved inorganic nitrogen
DIP	Dissolved inorganic phosphorus
DOP	Dissolved organic phosphorus
DP	Dissolved phosphorus
DUP	Dissolved unreactive phosphorus
ISBD	International Stormwater BMP Database
LID	Low impact development
N	Nitrogen
NRP	Non-reactive phosphorus
NRN	Non-reactive nitrogen
P	Phosphorus
PIP	Particulate inorganic phosphorus
POP	Particulate organic phosphorus
PP	Particulate phosphorus
REF	Reduction/enrichment factor
SRP	Soluble reactive phosphorus
SWP	Stormwater retention pond
TN	Total nitrogen
TP	Total phosphorus

Chapter 1

General introduction

1.1 Importance of phosphorus (P) for freshwater ecosystems

Phosphorus (P) is a nutrient that is essential for all living things in the earth as it plays a major role in building genetic material (DNA and RNA), transporting cellular energy (as ATP), and forming cell membranes, bones and teeth (Schipper, 2014). Since it was first purified and found by German alchemist Hennig Brandt in late 17th century, its significance in food production was not realized until mid-19th century when the German chemist Justus von Liebig found the Law of the Minimum, which states that the plant yield is controlled by the essential nutrient, including P, that is deficient in the environment for plant growth (Cordell & White, 2011). The wide use of P in agriculture (as one of the key ingredients in fertilizer), military (*e.g.*, in white phosphorus bomb) and daily necessities (*e.g.*, detergents) give prominence to the importance of P for human society after industrial revolution (Ashley et al., 2011). Although P is abundant in the earth's crust, it has been considered as a scarce resource in recent years due to the limitation of P reserves (*e.g.*, phosphate rock) that can be harvested for agricultural and industrial use (Cordell & White, 2011).

In the other hand, P also plays a significant role in freshwater ecosystems by influencing algal productivity as a crucial (co-)limiting nutrient (Conley et al., 2009; Howarth & Paerl, 2008; Schindler et al., 2016). Hence, the excessive loading of P to water bodies is a primary factor that drives eutrophication (Figure 1.1), a widespread global problem and major driver of water quality deterioration including the growth of harmful algal blooms (HAB) and oxygen depletion (Amirbahman et al., 2003; Carey et al., 2013; Carpenter, 2005; Carpenter et al., 1998; Diaz & Rosenberg, 2008; Jenny et al., 2016; Smil, 2000). Excessive P loadings to the lakes and reservoirs from surrounding landscapes have been identified as a major contributor to the increased occurrence of HAB over the past decades (Carey et al., 2013; Smith et al., 2016; Walsh et al., 2012). The increase in P loadings to freshwater systems is largely attributed to human activities, including excessive fertilizer usage, deforestation that leads to soil erosion, sewage discharges,

and etc. (Filippelli, 2008). Intensive usage and demand of P by human activities after the industrial revolution interrupted the natural P biogeochemical cycle and significantly increase the P content in freshwater systems all over the world, which raises the concern about eutrophication (Oliveira & Machado, 2013). For example, long-term fertilizer application and animal wastes associated with agricultural land has elevated the P loadings to water bodies across USA (Daniel et al., 1998).

Wide realization of the negative water quality impact of anthropogenic input of P to freshwater systems in the 1970s promoted the legislation to control the P discharge in North America (and later all over the world) (Ashley et al., 2011; Fletcher et al., 2015) and the efficient reduction of P loading was already evident in some cases (Schindler et al., 2016). However, various studies have demonstrated that despite efforts to reduce P input to the water bodies, eutrophication may persist due to internal nutrient cycling, wherein legacy P remains in the sediment or water column (i.e., internal loading) (Jenny et al., 2016; Tong et al., 2020). Thus, addressing the issue of overabundance of P in freshwater systems requires understanding and mitigating both external and internal P loadings. Effective management strategies should consider the anthropogenic drivers of increased P loadings, emphasizing the importance of sustainable practices to safeguard the health and integrity of freshwater ecosystems including lakes, ponds, rivers, and reservoirs worldwide.

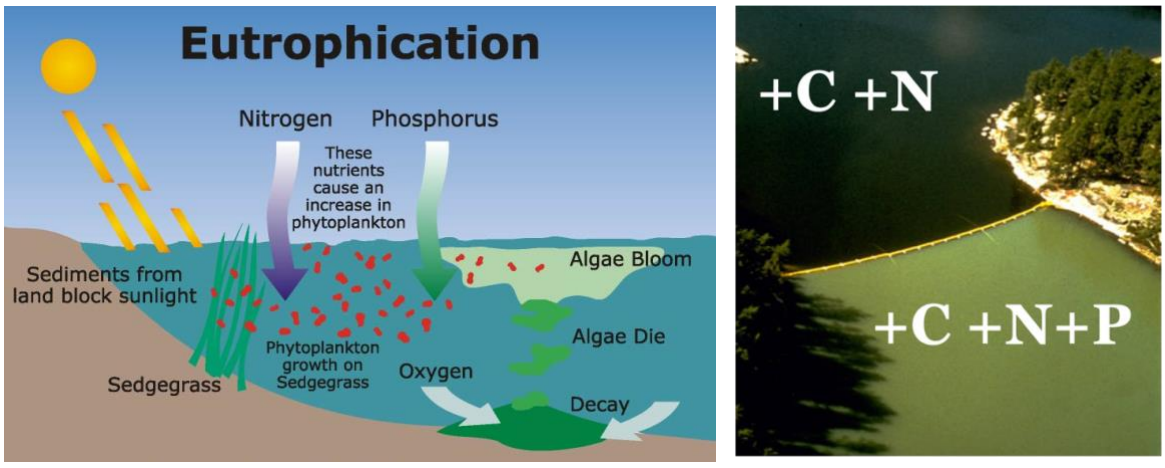

Figure 1.1: Left: diagram of eutrophication (adapted from City of Lincoln, Nerbraska); Right: Lake 226 whole-lake experiment which shows significant algal bloom under P addition (adapted from Fisheries and Oceans Canada).

1.2 Stormwater P export from urban landscapes: a growing concern

To control excessive human-caused input of P to freshwaters, agricultural watersheds have been the focus of most efforts, recognizing their significant contribution to anthropogenic P on a global scale (Engelbrecht & Morgan, 1961; Macintosh et al., 2018). However, it is important to acknowledge that urban watersheds have also become significant sources of P with the continued expansion of urban development worldwide (Duval, 2018). Urban land cover has increased rapidly in the past decades, converting natural or agricultural land to more impervious land cover (Stammler et al., 2017). The United Nations has projected a significant increase in the global population from 7.7 billion in 2020 to 9.7 billion in 2050, which is expected to result in a rise in urbanization in the near future (Cilluffo & Ruiz, 2019). Urban land cover introduces different sources/sinks and transport and emission pathways of P to the watersheds (Figure 1.2) (Duval, 2018; Yang & Toor, 2018). Generally, urban P export comprises discharge of P in both wastewater sewage (point source) and stormwater runoff (non-point source) (Carey et al., 2013). Followed by the concentration of population in urban areas promoted by industrial revolution, urban wastewater and stormwater infrastructures were developed with the mode to drainage the sewage and stormwater runoff, which carry the P-rich human waste, to the natural water bodies as quickly as possible, instead of disposing the human waste into agricultural lands surrounding the cities as it was in the ancient time (Ashley et al., 2011). This converted the modern civilization from P recycling to P one-way through-put dynamic, which ultimately enrich P in natural water bodies and bring widespread eutrophication issues (Ashley et al., 2011).

Given recent advances in the collection, treatment, and recovery of point-source P from wastewater, stormwater runoff is emerging as an increasingly important contributor to P export in urban areas (Desmidt et al., 2015; Liao et al., 2017; Oliveira & Machado, 2013). The percentage of impervious land cover, stormwater drainage infrastructures, climatic and hydrologic characteristics, hydrogeological conditions, soil and vegetation type, and land use type are among variables that make stormwater P export complex (Baek et al., 2020; Jacobson, 2011; Walsh et al., 2005). The increased imperviousness and the resulting changes in hydrology modify P build up and wash off processes. These effects cumulatively result in higher stormwater runoff P export in urban land covers compared to natural lands, especially under high precipitation and

snow melting events (Beck & Birch, 2012; Duan et al., 2012; Duval, 2018; Yang & Toor, 2018; Zeiger & Hubbart, 2017). Increase of salt input to receiving water bodies from impervious urban areas can further magnify the eutrophication risk associated with P enrichment by enhancing the stratification of water bodies and promoting the internal P loadings (Radosavljevic et al., 2022). As a result, it is crucial to understand the effects of urbanization on stormwater runoff P export to evaluate their negative effects on urban freshwater bodies and develop viable mitigation strategies. These include the strategies to reduce the P export loadings at both the source and the discharging point. Recovery of P from urban stormwater runoff, as what has been widely practiced in wastewater treatment (Desmidt et al., 2015), is also warranted due to the scarcity of P as resource for agricultural and industrial activities.

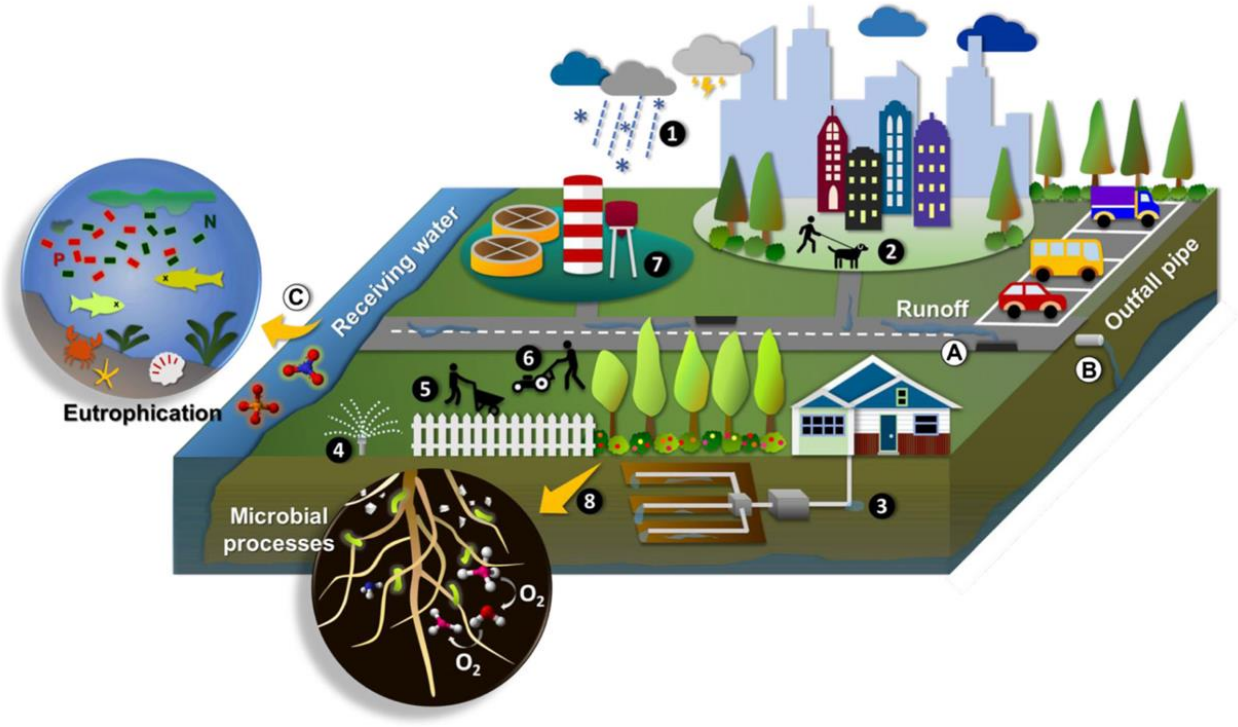

Figure 1.2: Sources and export pathways of nutrients (including P) in urban Environment (adapted from Yang & Lusk (2018)).

1.3 Stormwater best management practices (BMPs): potential to mitigate P export from urban stormwater runoff

Municipalities across the world are trying to adopt stormwater BMPs to deal with the negative impact of stormwater runoff on water quality and on urban flooding (Ashley et al., 2005, 2007; Jefferson et al., 2017). Early stormwater management aimed to reduce the export of particulate pollutants to receiving water bodies by attaching a stormwater pond (SWP) to the end of a conventional drainage network and using the storage volume and an outlet control structure to control the peak discharge to downstream water bodies (i.e., an 'end-of-pipe' solution, see Figure 1.3) (Bertrand-Krajewski, 2021; Persson & Wittgren, 2003). SWPs have been widely used for stormwater quality control for over 20 years and many municipalities regularly require inclusion of SWPs in subdivision drainage plans in southern Ontario (Drake & Guo, 2008). However, there has been an increasing recognition over time that negative trajectories are associated with urbanization at even low levels of imperviousness, and that the high connectivity of urban drainage systems has negative consequences for the ecology of surface water systems (Walsh et al., 2012). A range of approaches have now evolved to address additional concerns about water quality, erosion, and temperature (Fletcher et al., 2015). One example of this is the decentralized implementation of low impact development techniques (LID) BMPs such as bioretention cells (BRCs), which can be used to retain and treat urban runoff at the source with lower impact than SWPs on local aquatic ecology (Figure 1.3) (Chiandet & Xenopoulos, 2016; Gao et al., 2013; Hager et al., 2019). These technologies divert and filter the water before they get to the pipes of a conventional drainage system (Gao et al., 2018), and are aimed to restore pre-development hydrographs (Burns et al., 2012; Davis, 2008; Jefferson et al., 2017).

Stormwater BMPs can reduce urban runoff P loadings export via both hydrologic and biogeochemical processes, which can change the surface runoff quantity and P concentration, respectively. Many urban stormwater LID BMPs are efficient at reducing surface runoff quantity by enhancing infiltration of stormwater into underground, thus reduce the loadings of P export through surface runoff (Jefferson et al., 2017). Pollutants, including P, in stormwater runoff can be reduced by a variety of biogeochemical processes such as filtration, adsorption, sedimentation, nitrification/denitrification, and plant and microbial uptake (Beckingham et al., 2019; Hager et

al., 2019; Sharma et al., 2011, 2016; Song et al., 2015; Yang & Toor, 2018), etc. Appropriate non-structural stormwater BMP options such as sweeping and harvesting can also help reducing urban stormwater runoff P export at the source (Yang & Lusk, 2018) and should be thus incorporate with structural stormwater BMPs (Janke et al., 2017). However, the effects of many stormwater BMPs on urban P control remain mostly unexplored and highly uncertain (Hager et al., 2019). Understanding of the effects of stormwater BMPs on urban P export as well as the change of those effects under different environmental forcings is thus important for urban P management.

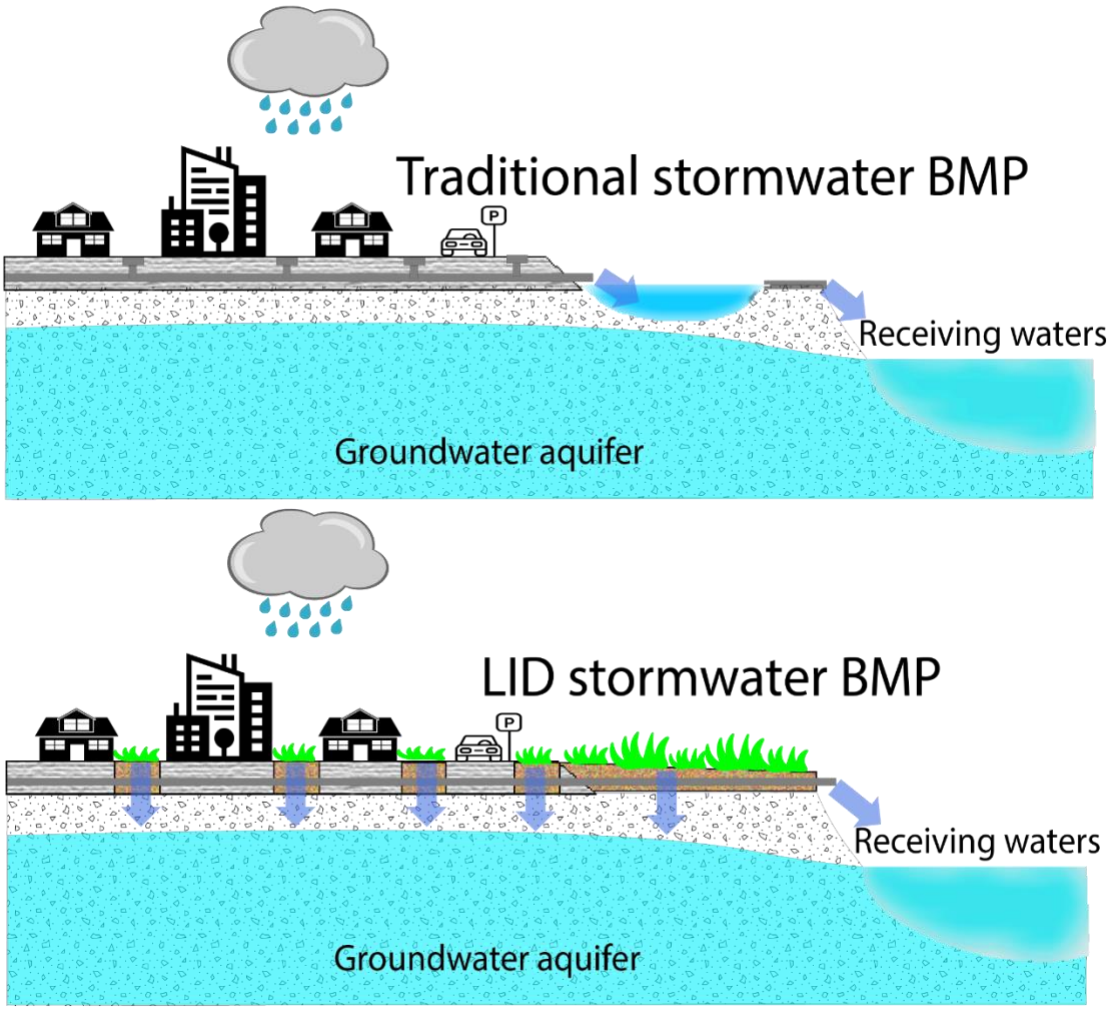

Figure 1.3: Diagram of traditional 'end of pipe' and innovative low-impact development (LID) stormwater best management practices (BMPs).

1.4 Key questions and thesis structure

The overarching objective of my PhD research is to assess the effects of stormwater best management practices (BMPs) on phosphorus (P) export from urban landscapes. The main questions I addressed in my research include:

(i) What are the knowns and unknowns about the stormwater runoff P sources and pathways, and the effects of stormwater BMPs on controlling P export in urban areas? (Chapter 2)

(ii) How to predict P reduction performance of bioretention cell (BRC) with process-based model? What are the dominant internal processes that control P reduction in this type of stormwater BMP? (Chapter 3)

(iii) What are the general effects of BRCs on urban stormwater runoff P? How are they different from that of nitrogen (N)? What are the potential factors that may affect these effects? (Chapter 4)

(iv) What are the general effects of other commonly used types of stormwater BMPs on urban stormwater runoff P? How different are they? What are the potential factors that may affect these effects and how to predict these effects with data-driven model? (Chapter 5)

I begin the research portion of this thesis (Chapter 2-5) with a review of existing literatures about the stormwater runoff P sources and pathways, and the effects of stormwater BMPs (with stormwater pond and BRC as representative systems for traditional and LID BMPs) on P loading in urban stormwater to address my first key research question. I also analyze the data in the International Stormwater BMP Database (ISBD) (Clary et al., 2020) to evaluate the typical urban stormwater runoff P concentration and speciation.

Following Chapter 2, I address my second research question with an individual system-scale field study of P dynamics in Elm Drive BRC facility located in Mississauga, ON. I develop a process-based model in Chapter 3 to simulate and analyze the multi-year P partitioning, accumulation and export in this BRC. I also conduct mass balance and sensitivity analysis to identify the fate of P and the key P retention process in this stormwater BMP system.

In Chapter 4 I evaluate the general effects of BRCs on urban P export by analyzing the data of multiple BRCs across North America in the ISBD. I compare these effects with the effects of BRCs on urban N export. I also introduce the data-driven approach in Chapter 4 by training a random forest model to predict the reduction and enrichment effects of BRCs on stormwater runoff P and N concentration. This model is then used to compare the importance of different explanatory variables and to identify the direction of influence by these variables.

Chapter 5 focuses on the same database as Chapter 4, but the analysis of effects on stormwater runoff P is expanded to 6 typical categories of BMPs, with the focus on comparing the difference of effects between traditional and LID stormwater BMPs. I compare the data-driven model for prediction of BMP P reduction and enrichment effects with different machine learning methods to address my fourth research question. The model with highest prediction accuracy is applied to compare the importance of different explanatory variables and to identify the direction of influence by these variables.

Chapter 6 summarizes the major conclusions to the four research questions and the main scientific contributions of this research. I also discuss about the potential future research directions following the work in this thesis. In particular, I discuss the need for further understanding about the internal P processes within the urban stormwater BMPs, and for applying the modelling tools developed in this thesis at upscaled studies to improve the understanding of effects of BMPs on urban P. I conclude with a brief discussion of the challenges and opportunities associated with urban P export control with stormwater BMPs.

Chapter 2

Contributions of sources, pathways and control solutions on phosphorus loading in urban stormwater: a review

This chapter is modified from:

Radosavljevic, J.[+], Zhou, B.[+], Slowinski, S., Rezanezhad, F., MacVicar, B., Kaykhosravi, S., Shafii, M., Parsons, C. T., & Van Cappellen, P. (2023) Contributions of sources, pathways and control solutions on phosphorus loading in urban stormwater: a review. *Under review* by coauthors.

[+]Authors contributed equally to this work

2.1 Summary

Phosphorus (P) is a key limiting nutrient for algal growth in freshwater ecosystems and contributes to cultural eutrophication and water quality impairment. Urban stormwater is a significant contributor of P transport to downstream ecosystems due to increasing point and non-point P sources and transport pathways in urban areas. As a result, urban stormwater best management practices (BMPs) such as stormwater ponds (SWPs) and bioretention cells (BRCs) are used to manage runoff from urban areas and attenuate P loadings in the watershed. In this review, we explore the state of knowledge about the sources and pathways of stormwater P loads, as well as impacts on P speciation. We also review the impact of BMPs with a focus on SWPs and BRCs. Finally, we identify research gaps and priorities with respect to the impacts of urban stormwater, and control solutions such as SWPs and BRCs, on P speciation and loading. Notable research gaps that we identify are the lack of understanding about internal P cycling processes within urban stormwater control solutions, as well as the impact of climate change on urban P speciation and loading.

2.2 Introduction and scope of literature review

Phosphorus (P) is one of the key limiting nutrients for algal growth and thus contributes to worsening eutrophication (Paerl et al., 2016; Schindler, 1974; Schindler et al., 2016). Urbanization can make significant change on the natural P dynamics by introducing various P sources and sinks (Nyenje et al., 2010; Riemersma et al., 2006) and by increasing imperviousness, which further modifies the hydrologic processes of stormwater (Jacobson, 2011; McGrane, 2016). This change can be even more complicated under the wide adoption of urban stormwater best management practices (BMPs) for runoff volume and water quality control (LeFevre et al., 2015; Troitsky et al., 2019). Climate change adds another layer of uncertainty to the influence of urbanization on P dynamics due to the potential change of urban P emissions, transport and the performance of stormwater BMPs under extreme events (Goh et al., 2019; Miller & Hutchins, 2017).

While several previous review articles have explored P dynamics in urban landscapes (Riemersma et al., 2006; Yang & Lusk, 2018), we argue that the scope of each review was limited. A systematic review and summary of stormwater runoff P sources, and transport and emissions pathways, and the effect of stormwater BMPs on urban P species and loading is lacking. Thus, a

comprehensive and holistic review that encompasses all the pathways, processes, and speciation is currently warranted. In this review, we explore the state of knowledge about multiple aspects of P in urban watersheds aiming to understand the impact of urban land cover on P speciation and loading. We first examined the typical urban stormwater runoff P concentration and speciation. We then assessed the state of knowledge about P sources and emission and transport pathways in urban areas and reviewed and evaluate the effect of stormwater BMPs on urban P speciation and loading. We also analyzed the data from the International Stormwater BMP Database (ISBD) (Clary et al., 2020) to figure out typical urban stormwater runoff P concentration and speciation, and the P control performance of urban stormwater BMPs. Research gaps and priorities are also highlighted for advancing the understanding of urban stormwater P dynamics.

2.3 Urban stormwater runoff P: speciation and concentration

2.3.1 P speciation

P occurs in many different chemical forms in urban stormwater runoff. The distribution of total P (TP) among these chemical forms of P in a water sample determines the relative reactivity to produce dissolved phosphate, the most bioavailable form of P, and therefore determines the potential bioavailability and eutrophication potential of all the P atoms in that sample. Although P does occur as different chemical species per se, the term speciation is often used to describe the distribution of P among its different operationally defined pools even when those pools are not actually different chemical species. The most common division for P speciation is dissolved versus particulate P (DP versus PP), and this division is operationally defined by filtration through a 0.45 μm filter. Among both the dissolved and particulate fractions, P can be found in either organic and inorganic forms, defined by whether the P is found in organic bonds (e.g., ester bonds) or not (Dunne & Reddy, 2005). Thus, urban stormwater P speciation can be further classified into particulate inorganic P (PIP), particulate organic P (POP), dissolved inorganic P (DIP) and dissolved organic P (DOP) (Figure 2.1).

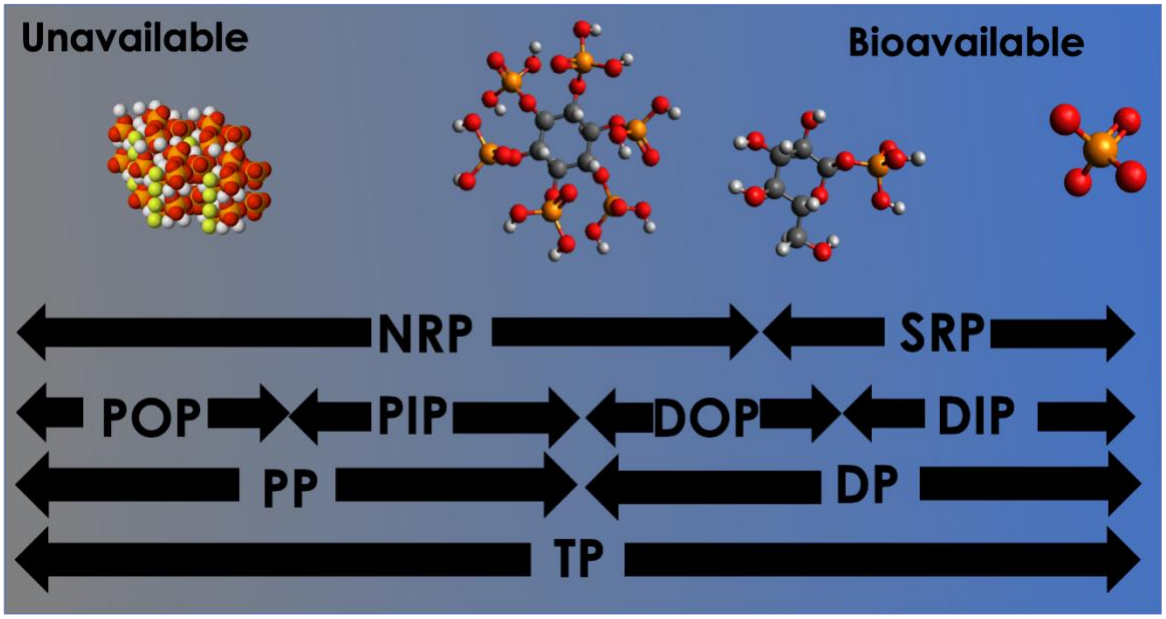

Figure 2.1: Phosphorus (P) speciation in urban stormwater runoff. TP – total P, PP – particulate P, DP – dissolved P, POP – particulate organic P, PIP – particulate inorganic P, DOP – dissolved organic P, DIP – dissolved inorganic P, NRP – non-reactive P, SRP – soluble reactive P.

The most common origin for organic P in the environment is nucleic acids (e.g., DNA and RNA), while the other major organic P species are other nucleotides, inositol phosphates, phospholipids, and phosphonates (Baldwin, 2013). Examples of POP, then, are particulate forms of P that contain nucleic acids such as algal cells and microbial cells, while good examples of DOP are molecules derived from plants, algae, or microbes such as phosphodiester, phosphomonoester, or pyrophosphate compounds (Frost et al., 2019; Song et al., 2015, 2017). Examples of PIP species are calcium and aluminum phosphate minerals and phosphate ions sorbed to mineral surfaces, while examples of DIP species are phosphates, either the orthophosphate ion or condensed phosphate molecules (McKelvie et al., 1995). Colloidal humic acid-bound phosphate is sometime considered as DOP species given its association with organic humic acid molecules, however, the P is technically not found in organic bonds in this species.

The most common way of determining P speciation within the dissolved and particulate fractions is using chemical extractions, that is, determining the reactivity of the P in a sample to a specific chemical extractant. In the case of dissolved orthophosphate, the most bioavailable and most abundant form of P in natural waters, the most common method for analyzing for it is

the molybdate blue reagent (Nagul et al., 2015). This reagent also reacts with and detects not only free orthophosphate, but also humic-bound colloidal orthophosphate and even potentially organic polyphosphates, however (Nagul et al., 2015; Tarapchak, 1983). For this reason, DP that is reactive to molybdate blue has been called soluble reactive P (SRP, or dissolved reactive P, DRP, or molybdate reactive P, MRP) to denote the fact that it is the dissolved (<0.45 μm) fraction of P that is reactive to molybdate blue (McKelvie et al., 1995; Nagul et al., 2015). Total DP can be determined in a <0.45 μm filtered sample directly by atomic emissions spectroscopy or persulfate digestion of a filtered (<0.45 μm) sample and molybdate blue analysis of the digest for the SRP produced by the oxidation of the dissolved unreactive P (DUP) (McKelvie et al., 1995). If total DP is determined, DUP can then be determined as the difference between SRP and DP. The DUP fraction represents more complex inorganic and organic P-containing molecules than orthophosphate such as polyphosphates, condensed phosphates, and the DOP molecules mentioned above (phosphodiester and phosphomonoester compounds). Although the SRP species is not necessarily just orthophosphate, because it is the fraction of P that is reactive to molybdate blue, which requires that the phosphate group in a molecule can be detached by the molybdate blue or are hydrolysable by the acidic molybdate solution (Nagul et al., 2015), it is often considered the fraction of P that is the most bioavailable for uptake by algae in water (Kao et al., 2022). And the other part of P (*i.e.,* non-reactive P (NRP), NRP = TP - SRP) is typically considered as unavailable for biological uptake (Figure 2.1).

2.3.2 Urban stormwater runoff P concentration and speciation

Urbanization typically results in high TP concentrations in stormwater runoff compared with TP concentrations in rainfall (0.0016 - 0.13 mg L^{-1}) (Migon & Sandroni, 1999) and natural land runoff (with typical TP concentration as 0.09 mg L^{-1}) (Minnesota Pollution Control Agency, 2008), with a median event mean concentration (EMC) of 0.22 mg L^{-1} (Table 2.1) for TP based on data from 397 sites in the ISBD. The EMC of urban stormwater runoff can vary significantly across different sites and events (Figure 2.2). For example, runoff from specific source areas such as surface parking lots with high levels of biogenic nutrients can have TP concentrations as high as 3.6 mg L^{-1} (Berretta & Sansalone, 2011b). In some regions, TP concentration of stormwater runoff from urbanized watersheds frequently exceeds the local water quality criteria. For example, TP

concentration of urban stormwater runoff in Ontario, Canada typically exceeds the Provincial Water Quality Guideline (0.03 mg L^{-1} for TP) (Tuppad et al., 2010).

In urban stormwater runoff, TP concentration is often strongly correlated with PP concentration (Czemiel Berndtsson, 2014; Dunne & Reddy, 2005; Uusitalo et al., 2000), and the fraction of PP in TP can be as high as 69% (Berretta & Sansalone, 2011a). The median EMC and fraction of PP in urban stormwater runoff are generally higher compared to DP levels (0.18 mg L^{-1} and 62% for PP versus 0.10 mg L^{-1} and 39% for DP, respectively) (Figures 2.2 and 2.3; Table 2.1). These patterns are attributive to the transportation of more sediment-bound particulate matter during the first flush (as observed in Yang et al. (2021)). Even though PP is typically not considered as a bioavailable P form, the hydrolysis of POP and the desorption of DIP from PIP could increase the bioavailable P species in natural streams because 40-50% of PP in urban runoff is associated with fine-grained sediments (11-150 μm), which makes PP transported in urban stormwater runoff prone to hydrolysis and desorption in receiving waterbodies (Perry et al., 2009; Yang & Lusk, 2018). SRP, known as the only bioavailable form of TP and the main contributor to eutrophication risks, typically accounts for 50-90% of DP (Berretta & Sansalone, 2011a; Goor et al., 2021; Liu & Davis, 2014). A median SRP fraction of 75% in DP has been reported based on data from 41 sites in the ISBD. As high as 96% of DP in urban stormwater runoff was found to be bioavailable in a study (Perry et al., 2009). In another study conducted in Florida, SRP was found to be the dominant P form, accounting for approximately 68% of TP in urban stormwater runoff (Yang & Toor, 2018). Previous studies suggest that DOP can also be an important contributor to the bioavailability of P in stormwater runoff other than DIP (Li & Brett, 2013; Li & Davis, 2016).

Table 2.1: Site median event mean concentration and fraction of different P species in TP in urban stormwater runoff calculated from the International Stormwater BMP Database (ISBD).

P species	Site average runoff EMC		Fraction in TP	
	Median ($mg\ L^{-1}$)	Data Number (sites, events)	Median (%)	Data Number (sites, events)
TP	0.23	397, 4836	-	-
PP	0.18	118, 1542	62	118, 1544
DP	0.10	116, 1519	39	118, 1560
SRP	0.07	204, 2437	32	199, 2544
DUP	0.05	39, 543	17	39, 518

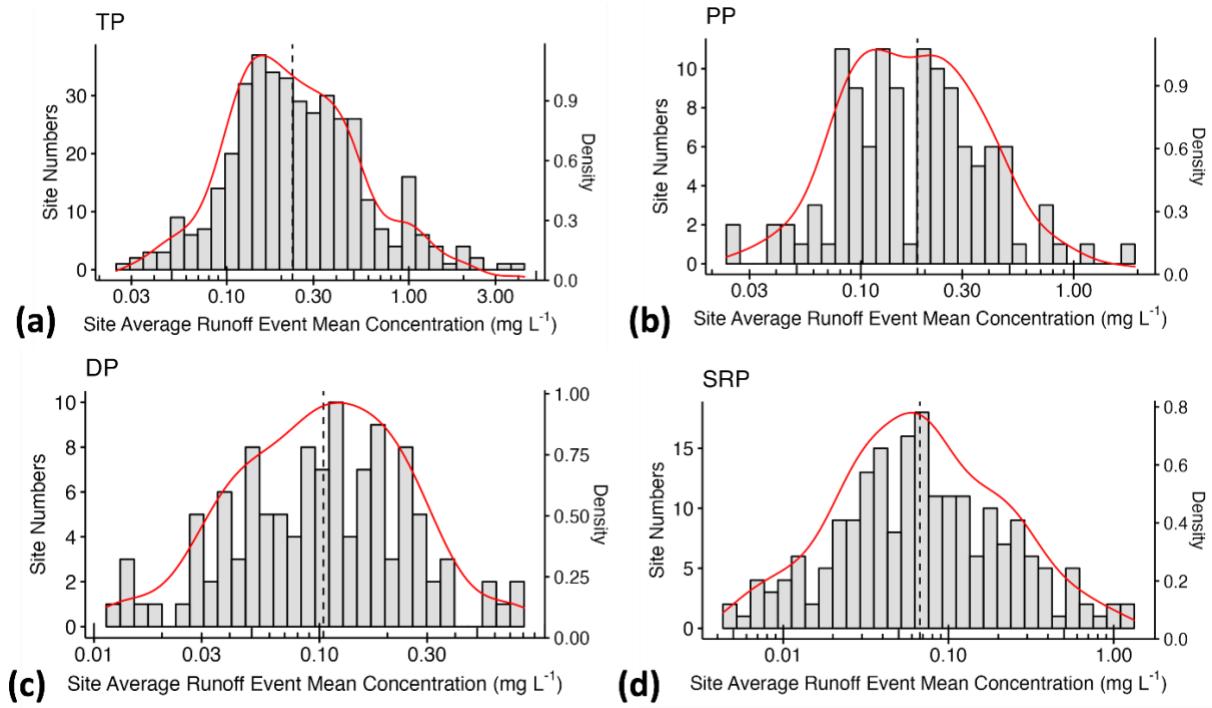

Figure 2.2: Distribution (histogram and density plot) of site average event mean concentration runoff (EMC) for TP (**a**), PP (**b**), DP (**c**), and SRP (**d**) obtained from the International Stormwater BMP Database (ISBD). Median values are shown as dashed line in each plot. Median, total site, and event numbers are summarized in Table 2.1.

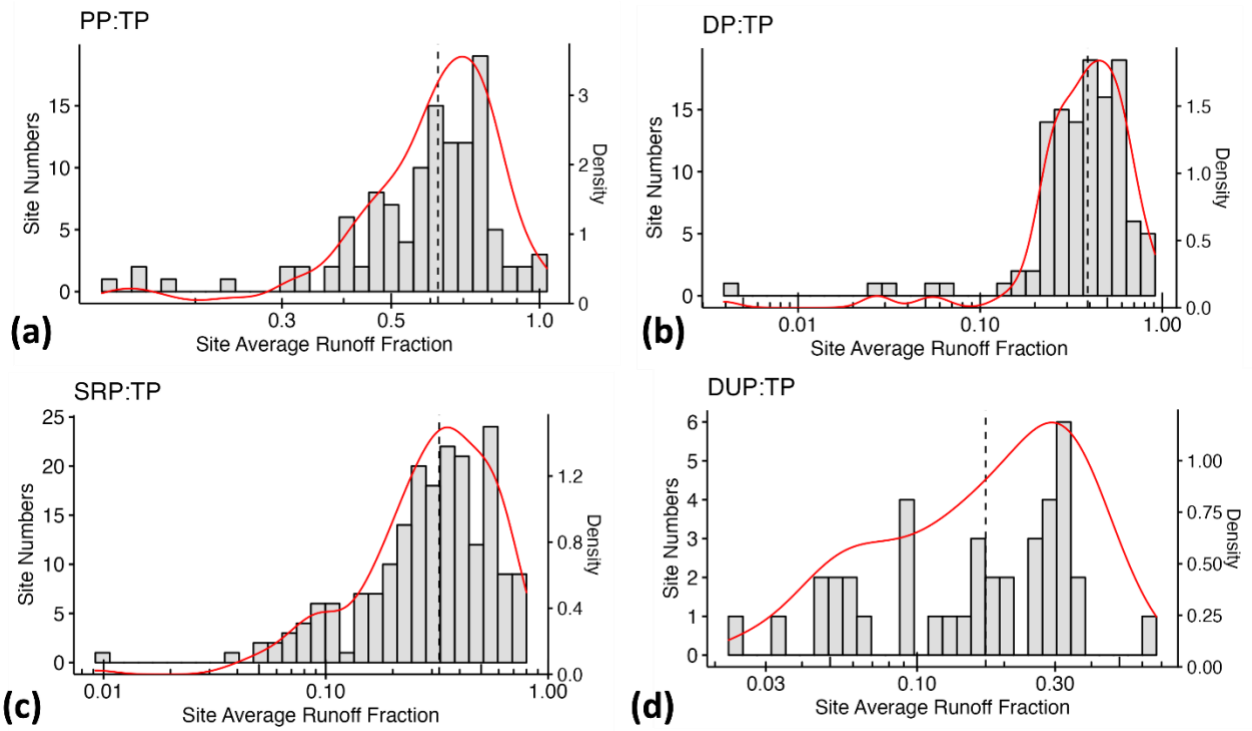

Figure 2.3: Distribution (histogram and density plot) of site average runoff fraction of PP (**a**), DP (**b**), SRP (**c**), and DUP (**d**) in TP obtained from the International Stormwater BMP Database. Median values are shown as dashed line in each plot. Median, total site, and event numbers are summarized in Table 2.1.

2.4 Urban P dynamics: sources and emission/transport pathways

The P cycle is impacted by a multitude of environmental sources and transport pathways (Figure 2.4). Synthetic fertilizer production and application are major contributors to global primary P flows and inputs. Although the fertilizers are mainly used in agriculture, about one-third of mined P has been utilized in urban areas (Cordell et al., 2009), potentially accumulated in urban landscapes, eventually leading to pollution in receiving water bodies (Kalmykova et al., 2012). Urban runoff, while representing only a small fraction of global TP inputs, can be a significant contributor to P export from urban areas (Macintosh et al., 2018) via storm drains, ponds, and other stormwater management infrastructure (Yang & Lusk, 2018). In urban watersheds, P inputs can be diverse and vary in their significance within the watershed. P sources include natural sources such as erosion and atmospheric deposition, anthropogenic sources such as synthetic

fertilizers, pet waste, automobile exhaust, detergents, leaking sanitary sewers, street solids, effluents from wastewater treatment plants (WWTP), and landfills, as well as biogenic sources such as leaf litter and grass clippings (Bratt et al., 2017). Among these sources, fertilizers, pet wastes, and atmospheric deposition are the most significant (non-point) sources of P to urban watersheds (Macintosh et al., 2018; Yang et al., 2021).

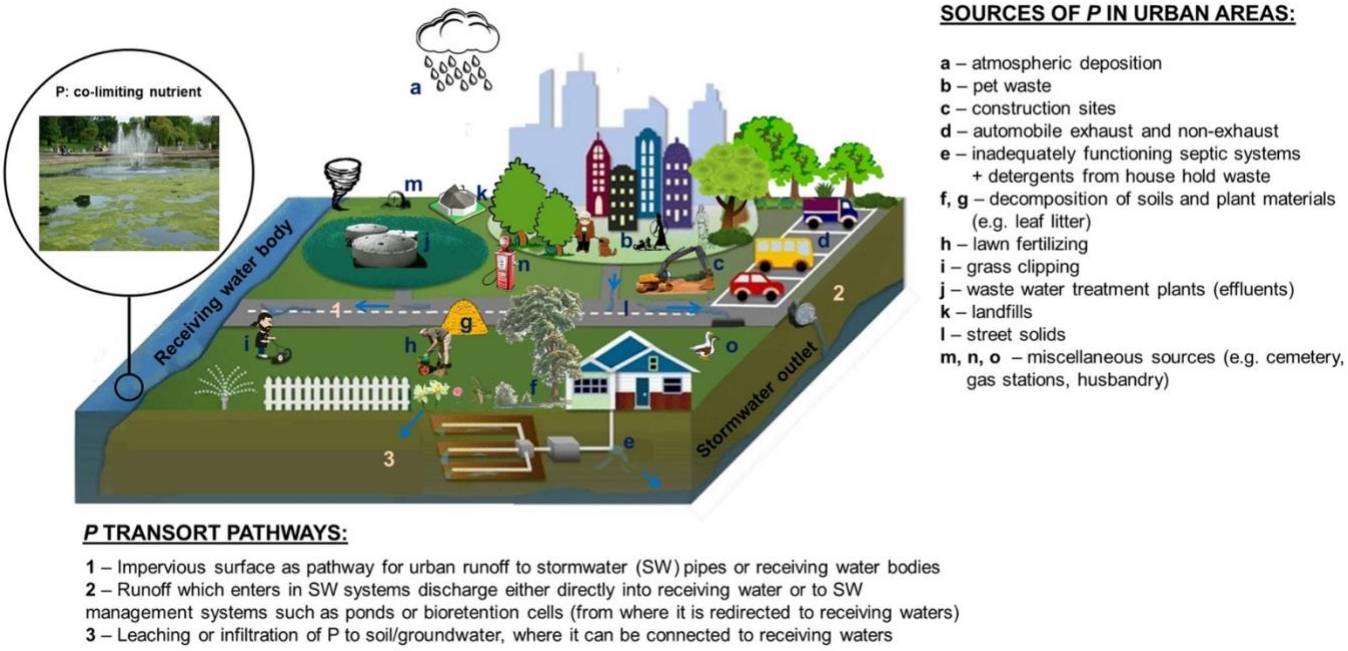

Figure 2.4: Major phosphorus (P) sources and transport pathways in urban area (adapted from Yang & Lusk (2018)).

In contrast to other land use systems such as agriculture, where P can be removed by plants and livestock, P removal pathways in urban watersheds are limited. Thus, relatively low P inputs may result in high runoff P concentrations and loadings during intense precipitation events (Kalmykova et al., 2012). Therefore, proper understanding of the diverse sources and transport pathways of P in urban watersheds is critical for managing urban runoff and minimizing the impact of urban environments on receiving water bodies.

2.4.1 Sources

2.4.1.1 Synthetic P fertilizers

Synthetic P fertilizers applied to urban lawns, parks, and golf courses accumulate in the soil and represent a primary source of PP runoff from vegetated urban areas (Soldat et al., 2009). This is concerning as soil P content is highly correlated with P runoff. Stormwater runoff exports from households' grass lawns and parks exhibit high variability, averaging 2.34 kg TP ha^{-1} (Toor et al., 2017). Meanwhile, golf courses contribute between 0.1-1 kg ha^{-1} yr^{-1} to DIP and 1.5-5 kg ha^{-1} yr^{-1} to TP (Bock & Easton, 2020). The variability in fertilizer inputs can be attributed to a range of factors, including the distribution of land cover within the watershed, type of fertilizers used, application timing, soil and plant type, and weather conditions. For instance, areas with a higher density of households with lawns may experience greater fertilizer inputs, which can lead to higher levels of P runoff. Similarly, areas with higher levels of rainfall may experience greater P runoff due to the greater volume of stormwater runoff (Bock & Easton, 2020; Soldat et al., 2009).

2.4.1.2 Pet waste

There has been limited research on the role of pet waste as a source of P in urban areas. Several studies have highlighted pet waste as a contributing factor of nutrients in watersheds (Baker et al., 2007; Bernhardt et al., 2008; Kalmykova et al., 2012; Macintosh et al., 2018; Morée et al., 2013), but few have emphasized its importance as a source of P (Hobbie et al., 2017; Macintosh et al., 2018). Macintosh et al. (2018) showed that in an urban watershed in Minneapolis, P inputs from pet waste were a significant contributor, with 0.82 kg ha^{-1} yr^{-1} (82 kg km^{-2} yr^{-1}) entering the watershed as either urine or feces that were not picked up. Similarly, Hobbie et al. (2017) found that pet waste contributed to 76% of the P input in seven developed watersheds, with P export from pet waste ranging from approximately 40 to 250 kg km^{-2} yr^{-1}.

Furthermore, Kalmaykova et al. (2012) reported P export fluxes of 10 t yr^{-1} for the city of Gothenburg, Sweden, which equates to 0.30 kg yr^{-1} per household with pets. Fissore et al. (2011) conducted a study on P export from 360 households in developed areas of Minnesota and found export fluxes of 0-0.53 kg yr^{-1} per household for dogs, while Baker et al. (2007) reported a value of 0.12 kg yr^{-1}. However, the speciation of P in pet waste as a source has received limited research attention. The majority of solid pet waste is in particulate form, specifically POP, the form that pet waste P enters stormwater runoff (Fissore et al., 2011). The variability in P inputs from pet

waste can be attributed to various factors, including the uneven distribution of pets, the type of breed, food intake, and the awareness of pet owners in properly disposing of pet waste in an environmentally friendly manner (Macintosh et al., 2018). Due to considerable magnitude of pet waste P in urban runoff, understanding its speciation will shed light on the development of effective management strategies to P mitigation in urban watersheds.

2.4.1.3 Atmospheric P deposition

Atmospheric deposition, comprising both wet and dry deposition, may play a substantial and variable role in the input of P in urban areas, primarily composed of DIP and TP. While a few studies have explored the impact of atmospheric deposition on P dynamics in urban settings, their focus has been on the overall P export rather than P speciation (Hobbie et al., 2017; Kalmykova et al., 2012; Redfield, 2002). Kalmykova et al. (2012) reported a total P mass of 3 t yr^{-1} from atmospheric deposition for the urban municipality of Gothenburg, Sweden, with surface area of 44,900 ha. This resulted in an areal P export of 6.7 kg km^{-2} yr^{-1}. Pandey et al., (2013) observed an increase in DIP loading by atmospheric deposition from 2007 to 2011 at eight sites within the Ganga River, ranging from 0.25-1.6 kg ha^{-1} yr^{-1} to 0.5-3.1 kg ha^{-1} yr^{-1}. Hobbie et al. (2017) found that P in atmospheric deposition contributed 13-33% of the overall P inputs to seven urbanized watersheds, with values ranging from around 40 kg km^{-2} yr^{-1} to 210 kg km^{-2} yr^{-1}. Hobbie et al. (2017) noted that P deposition in the Minneapolis area was influenced by wind erosion from construction sites. Nevertheless, it is difficult to discern P deposition originating within versus outside of the watershed transferred by wind via atmospheric deposition. Further research on atmospheric P deposition is needed to better understand its contribution and speciation in urban areas.

2.4.1.4 Erosional P sources

Erosional sources of P from sediment are thought to follow the general model of sediment production and yield through different phases of urbanization as proposed by Wolman and Schick (1967). Under this model, the phase of active construction is likely to increase the exposure of soils to erosion due to the removal of vegetation as part of construction. In general, urban areas and urban stormwater are associated with construction sites and yard work (Hobbie et al., 2017), but they are also dependent on geology and pedology of the area, as well as on weather

conditions (Hobbie et al., 2017). Sediment yield has been shown to be extremely high during the construction (12-200+ times background level) and moderately high (1.7-5 times background level) during active building (Chin, 2006). A comprehensive review by Russell et al. (2017) classified sites into forested, agricultural, and urban; and showed that urban sediment yield was much higher (even by the order of magnitude) than those in forested and agricultural sites. They also found that urban sediment yield was largely variable from site to site.

Sediment yield from a watershed can be sourced from the channel floodplain or the uplands (also known as the "hillslopes") of the watershed (Russell et al., 2019), and the balance of these two sources will have different implications for channel evolution and P export. In the first phase, the increase of surface erosion is thought to induce a phase of channel aggradation that can last just a few years or a couple of decades (Chin, 2006). In the second phase, the increasing power of the river and reduced inputs from upland sediment sources changes the balance so that the channels start to accelerate the transport of sediment (Papangelakis et al., 2019), beginning a phase of sediment export and channel enlargement that typically lasts multiple decades (Chin, 2006). Trimble (1997), for example, found the sediment storage loss from within the channel can be a major contributor to the watershed sediment yield. Channel enlargement in response to urbanization is well documented (Bevan et al., 2018; Hammer, 1972; Hawley et al., 2013; Pizzuto et al., 2000). It is therefore necessary to distinguish the source of sediment from previous studies such as those reviewed by Chin (2006) and Russell et al. (2017) to ascertain whether elevated sediment yield, once the initial phase of urbanization is complete is a function of hillslope or channel processes. Allmendinger et al. (2007), for example, found that upland erosion is an equal source to in-channel erosion over a 45-year period after watershed development. Fraley et al. (2009) emphasized the importance of floodplain sediments, which can store significant loadings of hillslope sediments and be readily mobilized by bank erosion during the channel enlargement phase of urban development. An urban hillslope sampling study by Russell et al. (2019) provided some of the best evidence to show that hillslope sources remain elevated, even for coarse sediments and even when the catchment is fully developed. Key sources were thought to gravel sources, construction activities, and residential areas.

To our knowledge, there is no research to date which reports specific P export coefficients or speciation information for erosional sources in urban areas. However, studies such as those of Carpenter et al. (1998), where erosion rates from watersheds under construction are as high as 0.05 kg km^{-2} yr^{-1}, must represent a significant source of P. The erosional sources of P mainly contain PP which is attributed to total suspended solids. We assume that P fluxes from erosion/construction sites in urban areas will be highly variable due to the geological and geotechnical conditions of the site, as well as which materials are used, and how waste of the site is managed and how is protected from different weather conditions (rainfall, wind). High importance of erosional sources in urban areas, thus P sources, lay in a huge sediment transport efficiency and increased runoff potential that could additionally lead to more eroding of available sedimentary sources (e.g., urban decay and renewal; construction sites and infill development; gravel surfaces in parks) (Russell et al., 2017).

2.4.1.5 Biomass (leaf litter, grass clipping, and street sweeping)

Biomass represents an important P source (Cowen & Lee, 1973; Wallace et al., 2008) that can increase the P content in urban stormwater runoff significantly (Hobbie et al., 2017; Wallace et al., 2008). A single grown tree can shed 15-25 kg of litterfall each fall (Novotny et al., 1985), and the P content of litterfall is typically between 0.1% and 0.3% of its mass (Heckman & Kluchinski, 2001; Hobbie et al., 2014). Most of the P released from the litterfall is in form of DOP and PP. Previous studies have also shown correlations between tree canopy cover and the P content of street solids (Kalinosky, 2015) and urban street runoff (Waschbusch et al., 1999). Hobbie et al. (2014) found that leaves sitting in water for 24 hours can leach up to 90% of their P, with 0.4-0.8 mg DP per gram of leaves leached over this time period.

Grass clippings are another source of biomass that can contribute to P inputs in urban areas. Barten and Johnson (2007) found that runoff from grass clippings has TP concentrations of 0.94-20.18 mg L^{-1} of P, based on an analysis of 26 households with lawns. Hobbie et al. (2017) showed that grass clippings contribute 15-30% of the total P budget (22-50 kg km^{-2} yr^{-1}), while leaf litter accounts for about 11-22% (16-37 kg km^{-2} yr^{-1}) of P inputs. Street sweeping accounts for 2-4% (3-7 kg km^{-2} yr^{-1}) of P inputs. However, reported data may vary depending on the timing of street debris removal following leaf litterfall in the watershed, overall management strategies

regarding leaf removal, and the type of vegetation present in the area. Understanding the dynamics of P inputs from biomass is crucial for effective urban nutrient management due to potential high contribution to overall P budget.

2.4.1.6 Street solids

Street solids represent a complex mixture of particulate matter which accumulates on roads and parking lots (Olsen et al., 2017). Street solids contribute to PP loading. The particle size of the street solids is an important control on the P speciation in the street solids. Often, due to the direct connectivity of impervious areas to stormwater management systems, it is important to understand the contribution of this source to control P discharge from urban landscapes. Street solids build up over time (Sorenson, 2013) and reach their peak buildup at one or two weeks of dryness (Sartor & Boyd, 1972; Sorenson, 2013). Although the P speciation in street solids have not been study well, the analyzed data showed that TP in street solids varied from 33.5 kg km^{-2} yr^{-1} to 370 kg km^{-2} yr^{-1} (DiBlasi et al., 2009). Drought followed by rainfall will be washed off the imperviousness, and the buildup process will restart (Olsen et al., 2017). Bioavailability of P increase along with the buildup time during period of dry days (Wang et al., 2020). The variability of street solids buildup mass is affected by traffic speed, traffic volume, curb height, wind speed and climate (Novotny, 2003). A common demonstration among a numerous study is that street solids loadings are higher in the fall season compared to other seasons (Olsen et al., 2017).

2.4.1.7 Automobile emissions

Automobile emissions (exhaust and non-exhaust), which are usually minor contributors to P sources in urban areas, could become important source of P in big cities (Amato et al., 2011; Farrauto et al., 2019; Parenago et al., 2020). Automobile exhaust represents motor emissions of matter which contain P, usually as additive to gasoline (Indris et al., 2020; Karjalainen et al., 2014); while automobile non-exhaust PP comes from wear of brakes, tires, and road pavement (Amato et al., 2011). Despite the importance of these sources in urban areas, data on P from automobile non-exhaust is scarce, while from exhaust are almost non-existing. Gasoline additive contains 900 mg kg^{-1} of P (Karjalainen et al., 2014), however, the amount of additive into gasoline is uncertain and it depends on manufacturer (Indris et al., 2014; Karjalainen et al., 2014). Consequently, it is difficult to evaluate the importance of automobile emissions overall on P

dynamics despite the traffic is huge component in urban areas. According to Amato et al. (2011) automobile non-exhaust source depends on climate, road surface characteristics and traffic conditions. More research is needed to evaluate this source in urban areas.

2.4.1.8 Urban wastewater

Urban wastewater discharged from residential/industrial areas via pipes contains high amounts of P that is coming from detergents together with excreta from human waste (Billen et al., 2021; Li et al., 2012; Quynh et al., 2005). Urban wastewater is rich in DP (both DIP and DOP) species. From 1950s, detergents significantly added to the urban P budget (Morée et al., 2013), and since 1990s they are recognizable sources of P in surface water (Powley et al., 2016). P contributions from detergents increased from 0 in 1950s to around 0.4 Tg P yr^{-1} in 2000s (Morée et al., 2013) due to production of P-based detergents. P in forms such as sodium tripolyphosphate are used as additives for increasing the effectiveness of the detergent (Yu et al., 2008). After use, P in detergents is often discharged with waste, and can become part of the stormwater especially during rainfall events (Chen et al., 2022).

The contribution of P through detergents differs from region to region. For example, after 1970 for North America, North Asia, and some European countries, total P loadings decreased due to wastewater treatment improvements and the use of P-free detergents (Morée et al., 2013). In countries where bans of P in laundry detergents were implemented (Hong et al., 2012), dishwasher detergent could also be the source of P (Han et al., 2011; Sabo et al., 2021), as well as P in deodorants, toothpaste and cosmetics (Sabo et al., 2021) and loading of P in those countries is estimated as 0.5 kg $person^{-1}$ yr^{-1} (Han et al., 2011), while Sabo et al. (2021) estimated 0.163 kg $person^{-1}$ yr^{-1} of P. Chen et al. (2022), in a study on few provinces in China (where detergent with and without P are sold), estimated P inputs from detergents below 30 kg km^{-2} yr^{-1}, except in highly populated areas such as Shanghai or Beijing, where P inputs from detergents vary between 35 and 148 kg km^{-2} yr^{-1}. In another study in UK, Comber et al. (2013) estimated P contribution of 0.175 g $person^{-1}$ day^{-1}.

Human waste (excreta) has a significant contribution to urban wastewater. Comber et al. (2013) reported 0.82 g P $person^{-1}$ day^{-1} that goes into the wastewater (from both urine and feces), while studies by Balmer et al. (1998) and Jönsson et al. (2004) for western populations reported

value of 1.4 g P person^{-1} day^{-1} for both types of excreta. Sabo et al. (2021) estimated daily P feces and urine values sum to the total of 0.51 kg P person^{-1} yr^{-1} (where range for urine was 0.45-1.3 g P person^{-1} day^{-1}, while for feces was 0.35-0.9 g P person^{-1} day^{-1}).

Although wastewater is typically discharged to receiving waters directly through separated sewage drainage systems, P can enter surface stormwater runoff discharge through leaks from sanitary sewer pipes (Sercu et al., 2011). Small leaks from sanitary sewers (of less than 10% of the total flow in the sewers) are common (Groffman et al., 2004), and they could easily increase P loadings in stormwater.

2.4.1.9 Wastewater treatment plant effluents

Wastewater treatment plants (WWTPs) can serve as potential sources of P for urban runoff due to the inherent nature of their treatment processes. In the context of urban environments, WWTPs play a pivotal role in treating domestic and industrial wastewater to reduce its pollutant content before discharge into receiving water bodies. However, during this treatment, phosphorus compounds can be inadvertently concentrated and subsequently released into the urban environment (Carey & Migliaccio, 2009). Although the processes in WWTP reduce phosphorus in the treated water, it can also result in the accumulation of phosphorus-rich sludge in WWTPs, which may, over time, be disposed of in landfills or used as agricultural fertilizers (De-Bashan & Bashan, 2004).

2.4.1.10 Landfills

Landfills serve as repositories of not only solid waste but also biochemically active agents, capable of generating leachate rich in various pollutants, including P. TP represents a critical component in the potential environmental impact of urban runoff stemming from landfills. The typical concentrations for TP of approximately 30 mg L^{-1}, is reported to be released into the surrounding environment warrant careful consideration (Papadopoulou et al., 2007). The percolation of leachate, containing this nutrient, through the landfill substrates can engender a substantial risk of introducing elevated P levels into adjacent groundwater resources. As runoff events occur, particularly during precipitation events, the leachate-enriched water can be mobilized and transported towards surface water bodies, exacerbating the potential for nutrient enrichment, and contributing to undesirable eutrophication phenomena (Papadopoulou et al., 2007).

Addressing the potential sources of total P in urban runoff from landfills necessitates a multifaceted approach that encompasses both improved leachate management strategies within landfills and effective urban planning measures to mitigate the downstream impacts on aquatic ecosystems.

2.4.1.11 Septic tanks and other subsurface sources

In addition to leaky sanitary sewers, underground septic tanks, whether decommissioned or still operating, can be sources of P (and other nutrients) (Robertson et al., 2019). Other potential subsurface sources of P include cemeteries and hydrocarbon-contaminated sites such as decommissioned gas stations. Cemeteries have also been shown to potentially cause elevated P concentrations in nearby groundwater (Franco et al., 2022; Żychowski, 2012). While the concentrations of P in petroleum hydrocarbons such as oil and gas are not well characterized, P-containing compounds used to be added to gasoline and other motor oils (Brooke et al., 2009; Indris et al., 2020; Totten, 2019). Given the large number of petroleum hydrocarbon-contaminated sites worldwide, many of them located in urban watersheds, it is likely that these contaminated soils could be a source of P in some watersheds.

2.4.1.12 Wild animals and husbandry

In urban environments, the influence of P sources from wild animals and husbandry on stormwater runoff presents a complex yet crucial research domain. Wild animals, through their natural activities and excreta deposition, can introduce P into urban landscapes (Dessborn et al., 2016; Metson et al., 2012; Scherer et al., 1995). Similarly, urban husbandry practices, including livestock keeping and poultry farming, contribute to P input through animal waste accumulation (Cooke & Williams, 1973). These sources possess the potential to elevate P concentrations in stormwater runoff, which, upon transport to urban water bodies, can foster nutrient enrichment and subsequently lead to adverse ecological consequences such as eutrophication. The estimated amount of P from that source is 0.25 kg P ha^{-1} (Cooke & Williams, 1973). Investigating the extent and impact of P contributions from wild animals and husbandry in urban stormwater runoff necessitates a comprehensive assessment of animal behavior, waste management practices, and hydrological dynamics within urban landscapes. Addressing these sources' implications not only enhances our understanding of urban nutrient dynamics but also informs

the development of sustainable urban planning strategies to mitigate P-related environmental challenges.

2.4.2 Transport pathways

P in urban areas could have various sources, as discussed earlier, and it can build-up over time (Yang et al., 2021). Once P has accumulated in the watershed, precipitation events can transport it through the drainage system (Figure 2.4). In conventional systems that are constructed of gutters, channels and pipes, the connectivity is high and travel times are low so that P is moved directly to receiving surface water bodies with little chance for filtration, adsorption, or deposition (Yang et al., 2021; Yang & Lusk, 2018).

For transportation of particles, together with P, seasonal first-flush is important, and it occurs when the initial storms of the have high pollutant/nutrient/particles concentrations or loadings than the storms later in the event. After a long dry period, first-flush could contribute significant P loading in stormwater runoff and, thus, receiving water bodies (Yang et al., 2021). The presence and strength of the first-flush depend on the species of P as influenced by multiple hydrologic and land use characteristics (Liu et al., 2019). For example, Lee et al. (2002) observed a strong first-flush effect of DIP in urban stormwater in watersheds of South Korea. Li et al. (2015) reported that in China, the first-flush strength of TP in stormwater associated with higher rainfall intensity.

2.4.3 Contribution of different urban land use types to P loadings

Ultimately, the P species and loadings originating from various sources in a catchment are combined together in stormwater. Within the urban land use type category, there are various land use types, such as: high density residential, medium density residential, low density residential, industrial, commercial, and parks and green spaces. Each of these urban land use types typically has a similar combination of different P sources, and as a result, the P concentration, loading and speciation from each of these land use types can be typified. For example, the EMCs for TP and SRP observed in the ISBD grouped by land use type (Figure 2.5) show that industrial land use has both the highest median TP and SRP EMCs, followed by residential, and then commercial land uses. It is not surprising that industrial land use contributes higher amounts of TP and SRP given that it is typically highly impervious, which, for transport-

limited contaminants, can drive high concentrations. Industrial land use may also represent a high concentration of vehicle (both exhaust and non-exhaust) emissions of P. Commercial land use likely has similar sources and transport pathways (high imperviousness) as industrial land use. Residential catchments contributing the next-highest TP and SRP EMCs is also not surprising, given the high population density in these catchments, and the human activities associated with residential areas that are potential sources of P such tending lawns and gardens and having pets (Kalmykova et al., 2012; Small et al., 2023). While residential catchments do have some pervious areas such as lawns and gardens, they also represent a concentrated area of imperviousness, depending on whether the residential area is high density, medium density, or low density (*e.g.,* depending on the extent of urban sprawl). Sources of imperviousness in residential catchments include roads, sidewalks, driveways, and roofs.

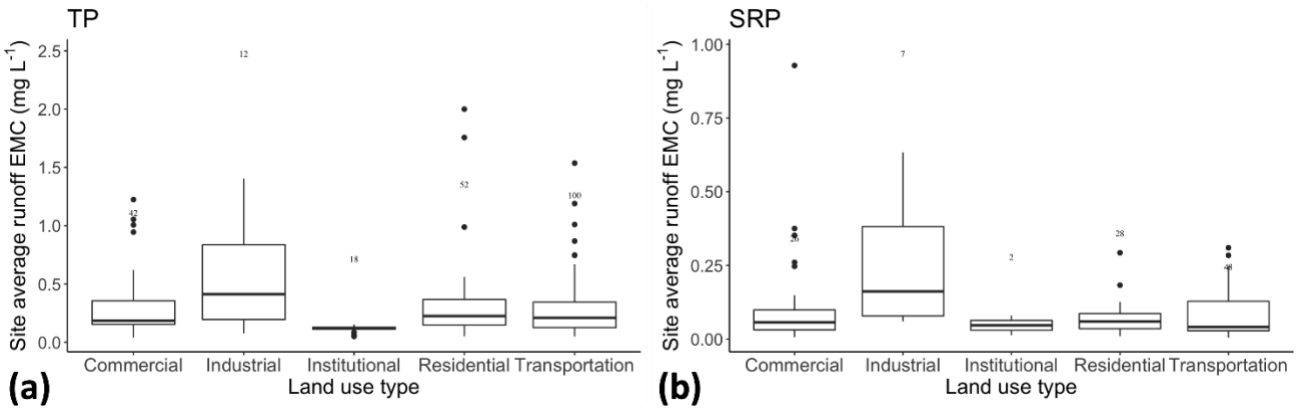

Figure 2.5: Boxplot of site average runoff EMC for TP (**a**) and SRP (**b**) under different land use types obtained from the International Stormwater BMP Database. Median values are shown as solid line in the boxplots.

2.5 Urban stormwater best management practices (BMP) systems as potential solutions for urban P control

Both traditional and LID stormwater BMPs can exert and influence on urban P dynamics by changing P loadings export through converting surface runoff to underground pathway (Goh et al., 2019; Kratky et al., 2017; Zahmatkesh et al., 2015), changing P concentration and modifying P speciation (Frost et al., 2019; Marvin et al., 2020; Song et al., 2017). Although many studies

show that the loadings of common pollutants such as TSS, nitrogen, pathogens and heavy metals in urban runoff can be reduced effectively by stormwater BMPs via various physical and biogeochemical processes (Beckingham et al., 2019; Hager et al., 2019; Sharma et al., 2011, 2016; Song et al., 2015; Yang & Toor, 2018), the effects of many stormwater BMPs on urban P control remains mostly unexplored and highly uncertain (Hager et al., 2019). For example, analysis of data from USA National Pollutant Performance Database shows that the P reduction performance of most BMP options cannot reach existing P removal targets, and all categories of BMPs excluding stormwater ponds (SWPs) have a high degree of uncertainty in their DP removal performance (Liu & Davis, 2014). Both BRCs and SWPs show highly variable P retention performance under different catchment characteristics and climatic conditions because of their complex internal biogeochemical P cycling processes and the sensitivities of these processes to environmental forcings (Marvin et al., 2020; Søberg et al., 2020; Troitsky et al., 2019).

Here we review the P cycling mechanisms of two stormwater BMPs, SWPs and bioretention cells (BRCs) (Figure 2.6), which are representative as traditional and LID stormwater BMPs. We also review their effects on P loading and speciation in the stormwater they discharge at their outlets. Except for SWPs and BRCs, other stormwater BMPs such as permeable pavement, infiltration trenches, and bioswales remain less studied and can have even higher P control performance uncertainties due to their variable design standards (Hager et al., 2019) and for this reason, they are not included in this review. In this review, we used the reduction efficiency as the metric to evaluate effects of SWPs and BRCs on runoff P since it is widely used in previous literatures (Duan et al., 2016; Janke et al., 2022; Marvin et al., 2020). Event scale reduction efficiency (RE) is calculated as below:

$$RE = \frac{\mathrm{IN}-\mathrm{OUT}}{\mathrm{IN}} \qquad \textbf{(Equation 2.1)}$$

where IN and OUT are the inflow and outflow values for EMC, event total flow volume, or event total loading. Further, we calculated the site average RE for BMPs in the ISBD. Site average concentration RE is calculated as the mean value of respective reduction efficiencies of all events monitored in a BMP. Site average flow or loading reduction efficiency is calculated by using Equation 2.1 with total inflow and outflow flow or loading summed up from all available events in a BMP.

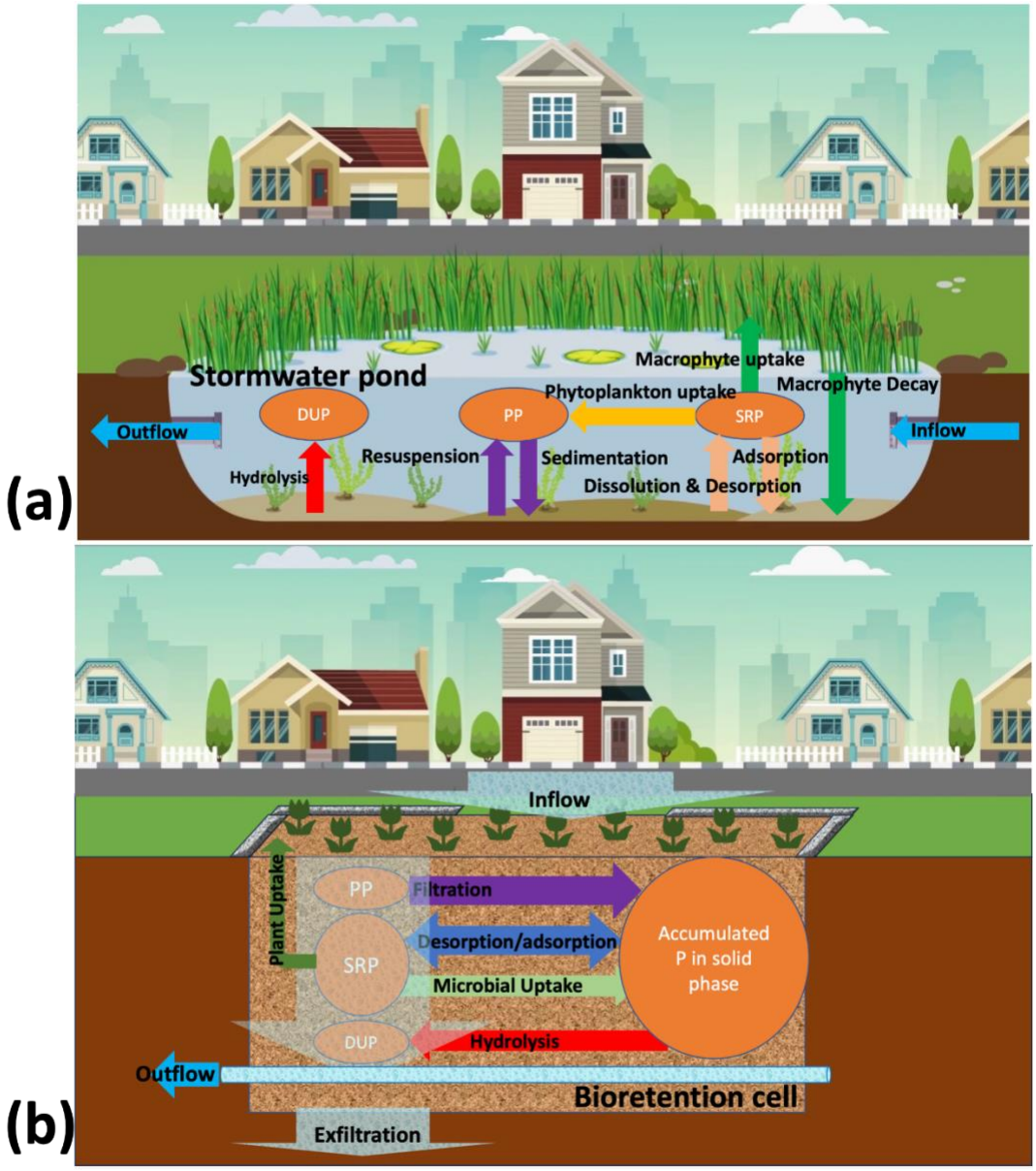

Figure 2.6: Typical internal P processes in stormwater pond (**a**) and bioretention cell (**b**). PP – particulate P, SRP – soluble reactive P, DUP – dissolved unreactive P.

2.5.1 Effects of stormwater ponds

For traditional urban stormwater BMPs such as SWPs, the median TP loading reduction efficiency calculated for SWPs in the ISBD is 62% (see Table 2.2), other studies show a wide range of P reduction efficiencies for SWPs, with TP loading reduction efficiency ranging from negative (Duan et al., 2016) to as high as 80% (Janke et al., 2022). Many studies show that the P reduction performance of SWPs is poorer than expected. For example, a study investigating the water quality of over 70 SWPs in Minnesota, USA found that the TP concentrations of pond water in most (73 %) of those SWPs are higher than US EPA Nationwide Urban Runoff Program criteria (0.15 mg L^{-1}) (Austin et al., 2021). Another study in Minnesota shows that over 40% of the 98 SWPs monitored have higher outflow than inflow TP concentrations and they are likely to export rather than retain P (Taguchi et al., 2020). Janke et al. (2022) recently reported the flow reduction by exfiltration and evapotranspiration, rather than P concentration reduction by internal biogeochemical processes, mainly account for the observed DP loading reduction in the SWPs they studied. The export of both DP and PP by SWPs have been found to be more common during dry periods (low-flow period) when internal processes contribute more than external input to outflow P loadings (Chiandet & Xenopoulos, 2011; Duan et al., 2016; Song et al., 2015; Williams et al., 2013).

P entering SWPs from urban stormwater runoff is eventually either flushed out at the pond outlet, taken up by macrophytes, or buried in the SWP's bottom sediments. Schroer et al. (2018) reported an average burial rate of 1.6 g P m^{-2} $year^{-1}$ according to data collected in 14 SWPs in South Carolina. PP is mainly retained by settlement, whose efficiency is expected to decrease as a given SWP ages because the accumulation of sediments decreases further accumulation capacity (Drake & Guo, 2008). There are multiple reduction processes of DP in SWPs, e.g., adsorption to suspended particles and pond sediment, and uptake by both phytoplankton and macrophytes (Troitsky et al., 2019). However, release of P from accumulated sediment at the bottom of SWPs (i.e., internal P loading) can result in P enrichment in water column.

Internal P loading in SWPs can result either from the desorption and dissolution of solid-bound P from pond sediments (Duan et al., 2016), similar to the P mobilization pathway widely observed in natural lakes (Orihel et al., 2017), or from the release of DOP via labile organic matter

decay in sediments (Song et al., 2017; Taguchi et al., 2020) (Figure 2.6a). Diurnal and seasonal thermal stratification of SWPs, which can be reinforced by both increasing salinization by high road salt inputs and reduced wind mixing by high vegetation cover (Janke et al., 2022; McEnroe et al., 2013), produces periodic or extensive anoxia zone at the sediment-water interface (He et al., 2015; Song et al., 2013). This stratification of redox condition in SWPs can stimulate different internal P loading mechanisms: Fe-bound P (or other redox-sensitive P phases) is more likely to be mobilized under anoxic conditions via the reductive dissolution of Fe (oxyhydr)oxides (Duan et al., 2016; Orihel et al., 2017) while microbial decay of labile organic P is more active under aerobic conditions (Taguchi et al., 2020). Recent studies have shown that redox-sensitive and labile organic P phases are the dominant contributors to internal P loading, with labile organic P often contributing more than redox-labile P due to its higher abundance in SWP sediments (Lusk & Chapman, 2021; Taguchi et al., 2020), which is similar to what has been observed for lake sediments by O'Connell et al. (2020). It has been shown that 75% of P in SWPs' sediment is in organic form and the seasonal mineralization of sediment organic matter, most of which have external origin (Schroer et al., 2018), may release significant amount of DOP and can contribute to a large portion of DP in pond water columns in summer due to more significant microbial activity (Frost et al., 2019; Song et al., 2017). Table 2.2 also shows that based on the data in the ISBD, SWPs have much lower concentration and loading reduction efficiencies for DUP compared with PP and SRP, indicating that DOP release from SWPs may be of greater concern.

Biological assimilation by phytoplankton in SWPs is intensive and is likely to transfer internal DP release from pond sediment to autochthonous suspended PP production in SWPs (Duan et al., 2016; Williams et al., 2013), and further decay of the PP in phytoplankton biomass can significantly increase SRP export from ponds (Palmer-Felgate et al., 2011). SRP uptake by macrophytes is not considered to contribute significantly to overall P reduction but macrophytes can reduce internal P release by both regulating pH to neutral state to prevent release of Fe-bound P and entrapping PP at the root zone (Borne, 2014). However, another study analyzed data of over 60 SWPs suggests that macrophytes are also likely to increase internal P loading in SWPs by providing organic carbon for Fe reduction in sediments (Austin et al., 2021).

Table 2.2: Median site-scale concentration, flow and loading reduction efficiency for different P species of stormwater pond and bioretention cell calculated from International Stormwater BMP Database.

BMP category	Site average reduction efficiency						
	Flow		Water quality parameter	Concentration		Loading	
	Median (%)	Data Number (sites, events)		Median (%)	Data Number (sites, events)	Median (%)	Data Number (sites, events)
Stormwater Pond	25	36, 228	TP	36	64, 673	62	35, 220
			PP	57	22, 278	79	11, 64
			DP	30	21, 320	38	10, 63
			SRP	35	37, 429	69	18, 149
			DUP	-11	10, 114	-37	3, 24
Bioretention Cell	61	27, 247	TP	-87	38, 457	60	25, 224
			PP	-4	5, 81	74	3, 52
			DP	-286	4, 80	20	3, 52
			SRP	-518	26, 275	33	18, 156
			DUP	14	2, 35	78	1, 32

2.5.2 Effects of bioretention cells

Urban LID stormwater BMPs such as BRCs are usually required to reduce between 35 and 85% of inflowing TP loads in regional stormwater BMP design manuals (Goh et al., 2019). However, Table 2.2 shows that although the median TP loading reduction efficiency of BRs can be as high as 60%, it is mainly achieved by flow reduction by groundwater recharge because of the negative (-87%) median TP concentration reduction efficiency, which means TP concentration is on average enriched. Both experimental and field studies in the literature show that BRCs have much higher P reduction performance variability compared to SWPs, with TP concentration and loading reduction efficiencies ranging from negative (that is, concentration increase or loading export) to 100% (all retained) (Marvin et al., 2020). This is likely attributed to the highly uncertain DP reduction performance of BRCs, with loading reduction efficiency ranges from -9.3 ~ 91% reported in literatures for field application (LeFevre et al., 2015), and PP reduction efficiency can be usually much higher (as high as over 90% based on Liu and Davis (2014)) due to the efficient filtration of particles by BRCs (Li & Davis, 2008). The much less efficient reduction of DP concentrations and loads compared to PP can be attributed to the high possibility of SRP concentration enrichment in BRs, with median concentration reduction efficiencies calculated as low as -538% in Table 2.2.

The P that loaded via surface runoff to BRCs can be accumulated in its filter media (filled with engineered soil), infiltrated into the native soil (and further recharged to the underlying groundwater aquifer) or lost via drainage at the outlet (Roy-Poirier et al., 2010a). There are different retention mechanisms by BRs for different forms of P: PP in runoff is mainly retained in BRC by filtration (Li & Davis, 2008) whereas DP is reduced by various processes such as adsorption (Erickson et al., 2007; Mei et al., 2012; Zhang et al., 2018), plant uptake (Fowdar et al., 2017; Rycewicz-Borecki et al., 2017) and microbial activity (Fraser et al., 2018; Poor et al., 2018) (Figure 2.6b). While highly reversible rapid electrostatic ion-exchange adsorption to filter media is considered as the dominant DP retention process in BRCs during storm events, irreversible slow sorption with inner sphere metal-hydroxyl complexes or coprecipitation with minerals can regenerate adsorption sites and can play more important role in the accumulation of stable P mineral phases in the long term (Hsieh et al., 2007; Liu & Davis, 2014; Lucas & Greenway, 2008;

Stumm, Werner, 2012). Most of the DP adsorbed by BRC filter media soil is available for plant uptake (Hsieh et al., 2007). While plant uptake is considered to play a minor role in BRC P reduction in many studies (Lucas & Greenway, 2008, 2011; Muerdter et al., 2020), other studies have shown that plants can accumulate up to 64% of the inflowing DP (Fowdar et al., 2017; Rycewicz-Borecki et al., 2017). The P reduction by plant uptake in BRC has been attributed to rhizosphere microbial activity (Lucas & Greenway, 2011) via rhizosphere microbes' degradation of organic associated P species to produce P species which are available for plant uptake. BRCs colonized with mycorrhizal fungi has been found to have 13~48% and 14~60% lower export for TP and SRP, respectively (Poor et al., 2018; Taylor et al., 2018).

However, BRCs filled with high P-index media is more likely to export rather than to retain SRP (Hunt et al., 2006; Shrestha et al., 2018). Compost mixed into BRC filter media to support plant growth is also likely to diminish P reduction efficiency by increasing DP leaching (Tirpak et al., 2021). Prolonged salt input, which is common in cold regions where road salt applied during winter, can even enhance release of SRP from BRC during snowmelt season (Goor et al., 2021). To enhance DP reduction, BRC filter media is usually amended with Fe or Al associated materials (e.g., water treatment residual) (Ament et al., 2021; Liu & Davis, 2014; Marvin et al., 2020).

2.6 Research gaps identified by literature review

2.6.1 Not all urban P sources and pathways are fully understood

As discussed in section *2.4.1*, the actual contributions of various potential P sources in urban landscapes to stormwater P are still not well understood. Examples of potential sources that are understudied for their contributions to P loading are: cemeteries, old subsurface stores of oil and gas, other underground storage sites, leaky sanitary sewers, groundwater, and vehicle emissions (both exhaust and non-exhaust). More work is needed to characterize the contributions of these potential sources, and to determine whether their contribution to the P loadings is considerable compared with other major P sources. While the contribution of some of these sources may be challenging to quantify, they may be crucial in understanding the P mass balance and metabolism of urban systems, and ultimately, the impact of urban catchments on P loading and speciation to downstream water bodies.

Given the significant contributions of P by human activities to the landscape in urban catchments, as outlined previously, a substantial amount of P is likely to be accumulated in the landscape and to have not been flushed out via stormwater runoff, which can function as P sources in the long run. This legacy P has been studied in agricultural catchments before, where it has been shown that up to 96% of the P added to the landscape can be retained in some landscape compartment such as soils, reservoir and riparian sediments, landfills or groundwater (Powers et al., 2016; Van Meter et al., 2021; Wironen et al., 2018). Van Meter et al. (2021) showed that P accumulated most in soils, followed by reservoir and riparian zone sediments, landfills, and finally followed by groundwater (i.e., soils > reservoir and riparian zone sediments > landfills > groundwater). In contrast, a similar study about legacy nitrogen accumulation showed that a larger fraction, comparable to the amount accumulated in soil, was accumulated in groundwater (Liu et al., 2021), reflecting the higher sorption and retention capacity of P by soils than of N.

In urban catchments, potential locations for accumulation and legacy storage are similar but slightly different than in agricultural catchments, with BMP sediments and filter media replacing reservoir sediments, giving potential landscape compartments of P accumulation of: soils, BMP sediments and filter media, stream riparian zones, landfills, and groundwater. It is expected that soils are the major accumulator of P like what has been observed in agricultural catchments. Interestingly, but also unsurprisingly, Yuan et al. (2007) found that urban and sub-urban soils were enriched in P relative to background levels in Nanjing (China) and Zhang (2004) found that P accumulation was higher in urban and sub-urban relative to rural soils in Hangzhou, China. Characterizing the legacy P accumulation in urban watersheds will enable us to better predict how and when the accumulated P could be released, where it will be released from, and therefore, the potential impacts of urban catchments on P loading and speciation (Haygarth et al., 2014; Sharpley et al., 2013).

2.6.2 P control performance of urban stormwater BMP systems is still not guaranteed

Based on sections 2.5.1 and 2.5.2, both SWPs and BRCs have highly uncertain effects on P, especially DP (for SWPs and BRCs it is more likely to be associated with DOP and DIP, respectively), due to their complicated internal biogeochemical processes that may remobilize previously

accumulated P within the system. Sensitivities of these internal processes to external environmental forcings related to watershed and climatic factors can further increase the uncertainty of stormwater BMPs' effects on urban P exports (Barbosa et al., 2012; Marvin et al., 2020; Søberg et al., 2020; Troitsky et al., 2019).

However, the internal P biogeochemical mechanisms within urban stormwater BMPs still remain poorly understood by both researchers and practitioners (Beckingham et al., 2019; Yang & Lusk, 2018). Most of previous studies have focused merely on quantifying the TP concentration or loading reduction efficiency of urban stormwater BMPs (Hager et al., 2019; Marvin et al., 2020; Troitsky et al., 2019), while just a few studies have tried to characterize the distribution of P species with time and/or depth inside these systems (Goor et al., 2021; Liu & Davis, 2014; Song et al., 2017; Taguchi et al., 2020; Zhou et al., 2023). There is also a lack of studies focusing on the impact of internal P loading from accumulated legacy P in BMPs on urban stormwater P export. Thus, more research that investigates the internal P cycling processes within different stormwater BMPs to better understand how these internal processes respond to external stressors and how these stormwater BMPs can be better designed to enhance reduction is needed. Quantification of P transformation kinetics of critical processes such as adsorption/desorption, plant and microbial uptake, filtration and hydrolysis in stormwater BMPs is highly recommended, which can help identify both critical P reduction and P leaching processes.

Reactive transport modelling is also proposed as a reliable tool for providing insight into internal P processes of stormwater BMPs. Although plenty of studies have focused on modelling the biogeochemical dynamics of other water quality parameters inside urban stormwater BMPs (Ahadi et al., 2020; German et al., 2003; Vezzaro et al., 2011, 2014, 2015; Vezzaro & Mikkelsen, 2012; Zhang et al., 2016; Zhang et al., 2004), there is a lack of modelling studies focused specifically on the P cycling dynamics within those systems. Stormwater modelling software such as SWMM and MUSIC has oversimplified water quality module, which only accounts for the simple first-order kinetic or the dilution effect by rainwater, to simulate P reduction by stormwater BMPs (Baek et al., 2020; Imteaz et al., 2013; Kaykhosravi et al., 2019; Wong et al., 2006). This is insufficient for not only the accurate estimation of TP loading reduction by stormwater BMPs, but also the simulation of transformation dynamics among various P species.

More intensive and rapid P transformation occurring in urban stormwater BMPs limits the application of existing model developed for natural systems (Troitsky et al., 2019). Thus, there is a need to translate the P cycling knowledge gained from previous and future field and experimental studies to develop comprehensive P reactive transport model for stormwater BMPs.

Overall, a better understanding of the P dynamics in urban stormwater BMPs can improve the design, deployment and maintenance of these systems, which can further improve their performance on controlling urban P export under current and future climate. Understanding the accumulation of P in BMPs will also potentially enable the recovery and recycling of P, like what is performed with urban wastewater (Metson et al., 2018).

2.6.3 Interactions of P with other urban contaminants

Urban watersheds are known to be important sources of other contaminants including salt ions (e.g., chloride, sodium, calcium), sulfate, dissolved nitrogen species (e.g., nitrate, ammonium, organic N), increased pH (e.g., increase in OH^- ions), heavy metals (e.g., lead, cadmium), pharmaceuticals, and other contaminants of emerging concern such as microplastics (Lapointe et al., 2022). These contaminants originate from the same sources as P (e.g., fertilizers) or from other sources that are more abundant in urban relative to non-urban areas, such as de-icing salts and construction materials. Due to the multitude of biogeochemical processes which contribute to P cycling in urban watersheds, these other chemical contaminants may have important interactions with P cycling that can modify P loadings and/or speciation.

For example, salt ions are known to compete for sorption sites with phosphate ions, mobilizing phosphate ions from soil surfaces and enhancing P concentrations and loadings in runoff (Kaushal et al., 2022). The competition between salt ions and phosphate ions (Kim & Koretsky, 2011) or the enhancement of stratification due to salinization may also enhance internal DP loading in BRCs and SWPs (McEnroe et al., 2013). High catchment sulfate loadings have been shown to drive sulfate reduction and sulfide formation in SWPs (Ku et al., 2016). Sulfate reduction can sequester iron into iron sulfides rather than iron oxides, reducing the capacity of sediments to retain P (Caraco et al., 1989; Gächter & Müller, 2003; Katsev et al., 2006). In contrast, enhanced dissolved calcium concentrations and increased pH may make calcium phosphate mineral precipitation favourable, contributing to a redox-stable sink for P in SWPs and

BRCs (Liu et al., 2021). Other nutrients (e.g., nitrate and ammonium) and pharmaceuticals may either reduce or enhance the uptake of P by algae and plants (Carter et al., 2015; Carvalho et al., 2014).

In addition to the impact of these contaminants on within watershed processes and urban stormwater P loading and speciation to downstream water bodies, there are also interactions that can affect the eutrophication potential of P once it reaches the water bodies. For example, the ratio between dissolved (bioavailable) nitrogen species, and dissolved bioavailable P species can impact whether N or P is the limiting nutrient for algal growth (Dodds & Smith, 2016; Ryther & Dunstan, 1971). Another macronutrient for certain algal species (diatoms) whose ratio with DP can impact algal community composition is dissolved silicon (Maavara et al., 2018). The presence of dissolved iron, and likely its ratio with DP, can also determine the favourability for nitrogen-fixing cyanobacteria (Molot et al., 2014; Verschoor et al., 2017). Salinization of downstream receiving bodies due to high external salt loadings originating from road salts or other urban sources can also enhance internal P recycling and other eutrophication symptoms (Radosavljevic et al., 2022) and mobilize heavy metals in sediments (Kaushal et al., 2019, 2022). Hence, urban contaminant loading evaluations should not focus only on P, urban water quality assessments also require taking into account the interactions of P with other urban contaminants in soils, stormwater runoff, BMPs, and in downstream water bodies to assess the cumulative impacts of urban land use on the water quality.

2.6.4 Impact of climate change on urban P cycling

2.6.4.1 Climate change impacts on urban P export and eutrophication potential

Climate change is attributed to increasing anthropogenic emission of greenhouse gases, which causes global warming due to increasing solar radiation being trapped within the atmosphere (Solomon et al., 2009). Along with temperature and precipitation being impacted by climate change (Kaushal et al., 2014; Withers & Jarvie, 2008), extreme events such as heavy rain; windstorms; extreme heat and cold temperature; and droughts are forecasted to occur more frequently in the coming decades (Forzieri et al., 2018; Kaushal et al., 2014). For example, in Canada, climate projections predict that the winters will be wetter and warmer, while summer temperatures will be systematically higher with significant potential for prolonged periods of

drought (Zhang et al., 2008; Zhang et al., 2004). Globally, an increase in both average air temperatures and extreme periods of drought followed by extreme precipitation events (in terms of both intensity and depth) are projected (Romero-Lankao et al., 2014). At the same time, the climate is considered the main natural stressor of change in stormwater runoff water quality and quantity (Kaushal et al., 2014; Kim & Newman, 2019; Semadeni-Davies et al., 2008; Sohn et al., 2019). Climate change can also increase the seasonal variability of stormwater runoff characteristics (Schindler, 2009; Wilby et al., 2006; Withers & Jarvie, 2008), in which, can affect water quality in receiving freshwater bodies due to increased export of suspended sediments, organic matter, and nutrients from watersheds (Withers & Jarvie, 2008).

A few previous studies have highlighted how the cumulative effects of climate change and might be expected to modify P speciation and loading in watersheds, with an increase in P loads being expected (Chen et al., 2015; Yindong et al., 2022; Zango et al., 2022). For example, Zango et al. (2022) predicted that P loads from urban watersheds will increase by 19 to 24% due to climate change. Chen et al. (2014) also forecasted an increase in anthropogenic P loads to receiving waterbody due to both urbanization and climate change. Yingdong et al. (2022) showed that the terrestrial P retention capacities of watersheds will decrease under future climate scenarios, and the duration and frequency of extreme precipitation events associated with climate change could increase the export of accumulated P. Under climate change, increasing level of CO2 is likely to decrease plant uptake of P (Maharajan et al., 2021) and this may also weaken the P retention capacity of urban watersheds.

Additionally, climate change is expected to exacerbate the eutrophication risk introduced by elevated urban P export to receiving water bodies. This impact takes place in many ways that include, but are not limited to: (1) increasing P accumulation in receiving waterbodies during summer because of increases in water residence times and the duration of the anoxia during longer periods of drought (Van Vliet & Zwolsman, 2008), (2) enhancing internal biological growth and production under elevated average air temperatures (Withers & Jarvie, 2008), and (3) increasing internal P loading in receiving water bodies due to the more stable stratification caused by increasing road salt application under more extreme cold seasons in urban areas

and/or due to the increased duration of anoxia associated with longer durations of drought periods (Ladwig et al., 2023; Radosavljevic et al., 2022).

2.6.4.2 Impact of stormwater BMP systems on urban P loading control under future climate

The water quality improvement effects by stormwater BMs can be affected by multiple geophysical factors such as climate, hydrology, land, soil, and topographical conditions (Barbosa et al., 2012). An important question is thus to what extent their P reduction performance changes under different climatic conditions. Increased frequency of occurrence of extreme hydrologic events under climate change brings larger uncertainties for urban P cycling by modifying the patterns of runoff hydrograph, pollutants buildup and snow accumulation/snowmelt processes (Aygün et al., 2020; German et al., 2003; Romero-Lankao et al., 2014; Sharma et al., 2011, 2016; Trenberth, 2011). This can bring uncertainties to the hydrologic and P reduction performance of existing stormwater BMPs by both changing the magnitude and temporal distribution of P input loading to the systems and modifying the internal biogeochemical processes within them. It has been found that the disproportionately high export of pollutants during just a few extreme events can account for a large portion of P export from stormwater BMP systems such as BRCs (Goor et al., 2021; Jefferson et al., 2017). P loading reduction efficiency of BRCs is likely to be decreased due to the significant deterioration of runoff reduction performance under changing inflow regimes driven by climate change (Chowdhury & Chakraborty, 2016; Daly et al., 2012; Hathaway et al., 2014; Metson et al., 2018). For SWPs, decreased settlement efficiency for TSS due to less water residence time under increasingly intensive inflow regime (Beckingham et al., 2019; Chiandet & Xenopoulos, 2016; Drake & Guo, 2008; Persson & Wittgren, 2003; Sharma et al., 2016) may decrease PP reduction efficiency. Whereas water quantity reduction performance of existing stormwater BMP systems is more likely to be affected by changing rainfall volume, water quality (e.g., P) control performance is expected to be significantly influenced by changing temporal distribution of rainfall (Baek et al., 2020).

Despite the expectation that the functioning of stormwater BMP systems can be affected under future climate, previous studies showed stormwater BMP systems such as BRCs and SWPs are still likely to attenuate the climate change impact on urban runoff quantity and quality (Cording et al., 2018; Sharma et al., 2011, 2016). Stormwater BMP systems are believed to

provide climate impact mitigation benefits for urban P loading control by increasing resiliency of urban hydrologic cycling (Dudula & Randhir, 2016; Gill et al., 2007; Pyke et al., 2011; Zahmatkesh et al., 2015), even though these benefits can be diminished under increasing extreme events (Kratky et al., 2017; Wang et al., 2019; Wang et al., 2019). To enhance the adaptability of stormwater BMP systems under increasing extreme events brought by climate change, redundant application of stormwater BMP systems is suggested because treating a small portion of impervious area has little change on urban water and P cycling due to the hysteresis effect of those systems (Jefferson et al., 2017). Although there are studies investigate the effectiveness of stormwater BMP systems on control of other water quality parameters under various climatic condition (Baek et al., 2020; Dudula & Randhir, 2016; Sharma et al., 2016; Zahmatkesh et al., 2015), few of previous studies focused directly on impact of climate change on P reduction effect of stormwater BMP systems. Previous models developed for system-scale stormwater BMP P cycling analysis (Li & Davis, 2016; Liu & Davis, 2014; Roy-Poirier et al., 2010b) have not been coupled with watershed-scale P model and climate change projections to simulate urban P cycling under climate change condition. More upscaling research with specific focus on investigating the impacts of the interactions between urbanization, climate change and stormwater BMP systems on P speciation and loading is recommended, which requires advanced understanding on the impact of climate change on internal P biogeochemical processes of urban stormwater BMP systems.

2.7 Conclusions

Urban stormwater runoff can contribute substantial loads of phosphorus, a nutrient that can contribute to water pollution and eutrophication in receiving water bodies. The uncertainties surrounding P sources in urban stormwater arise from a complex interplay of hydrological, climatic, land use, human activity, and other factors. Runoff from impervious surfaces such as roads, rooftops, and parking lots can contain that originates from a variety of sources in urban lanscapes, including sediment-bound P from eroded soil, residual fertilizers from lawns and gardens, and organic matter from decaying plant material or pet waste. The exact composition and proportion of these sources can vary greatly depending on factors like land use patterns, weather conditions, and maintenance practices within the area. The speciation and loading of the P originating from urban landscapes can be variable due to the different combinations of sources. The dynamic nature of urban environments makes it challenging to precisely quantify the contributions of each source, leading to uncertainties in predicting P loadings accurately.

In spite of the wide adoption of stormwater best management practices (BMPs) in urban area, both traditional (e.g., stormwater pond) and innovative (e.g., bioretention cell) BMPs have highly uncertain performance in P export control. Various stormwater BMPs have different effects on changing the concentration, loadings, and species of P export from urban areas. The inefficient control of P (especially for dissolved P) by many stormwater BMPs can be largely attributed to their complex internal biogeochemical mechanisms that can cause significant release of legacy P, which is typically enriched due to prolonged accumulation of P from the catchment and inappropriate maintenance activities. The increased uncertainty of the internal P mechanisms within urban stormwater BMPs under changing climate conditions further questions their efficacy on controlling urban P export under future climate.

To effectively manage P pollution in urban stormwater, it will be essential to enhance the understanding of the biogeochemical mechanisms of P and its interaction with other pollutants at sources, transport pathways, and stormwater BMPs in urban area so as to optimize the management strategy. This can be achieved by employing a combination of field monitoring and modelling to analyze and predict the P speciation and loadings in exported urban stormwater, and the resulting impacts on water quality, under current and future climates.

Chapter 3

Modeling multi-year phosphorus dynamics in a bioretention cell: phosphorus partitioning, accumulation, and export

This chapter is modified from:

Zhou, B., Shafii, M., Parsons, C. T., Passeport, E., Rezanezhad, F., Lisogorsky, A., & Van Cappellen, P. (2023) Modeling multi-year phosphorus dynamics in a bioretention cell: Phosphorus partitioning, accumulation, and export. Science of The Total Environment, 876, 162749. https://doi.org/10.1016/j.scitotenv.2023.162749

3.1 Summary

Phosphorus (P) export from urban areas via stormwater runoff contributes to eutrophication of downstream aquatic ecosystems. Bioretention cells (BRCs) are a Low Impact Development (LID) technology promoted as a green solution to attenuate urban peak flow discharge, as well as the export of excess nutrients and other contaminants. Despite their rapidly growing implementation worldwide, a predictive understanding of the efficiency of BRCs in reducing urban P loadings remains limited. Here, we present a reaction-transport model to simulate the fate and transport of P in a BRC facility in the greater Toronto metropolitan area. The model incorporates a representation of the biogeochemical reaction network that controls P cycling within the BRC. We used the model as a diagnostic tool to determine the relative importance of processes immobilizing P in the BRC. The model predictions were compared to multi-year observational data on 1) the outflow loads of total P (TP) and soluble reactive P (SRP) during the 2012-2017 period, 2) TP depth profiles collected at 4 time points during the 2012-2019 period, and 3) sequential chemical P extractions performed on core samples from the filter media layer obtained in 2019. Results indicate that exfiltration to underlying native soil was principally responsible for decreasing the surface water discharge from the BRC (63% runoff reduction). From 2012 to 2017, the cumulative outflow export loads of TP and SRP only accounted for 1% and 2% of the corresponding inflow loads, respectively, hence demonstrating the extremely high P reduction efficiency of this BRC. Accumulation in the filter media layer was the predominant mechanism responsible for the reduction in P outflow loading (57% retention of TP inflow load) followed by plant uptake (21% TP retention). Of the P retained within the filter media layer, 48% occurred in stable, 41% in potentially mobilizable, and 11% in easily mobilizable forms. There were no signs that the P retention capacity of the BRC was approaching saturation after 7 years of operation. The reactive transport modeling approach developed here can in principle be transferred and adapted to fit other BRC designs and hydrological regimes to estimate P surface loading reductions at a range of temporal scales, from a single precipitation event to long-term (*i.e.,* multi-year) operation.

3.2 Introduction

Urban runoff is a major source of surface water and groundwater pollution (Arnold & Gibbons, 1996). In particular, urban runoff can carry excess phosphorus (P) to receiving surface freshwater bodies (Perry et al., 2009; Valtanen et al., 2014; Yang & Lusk, 2018) where it contributes to worsening eutrophication (Schindler, 1974; Schindler et al., 2016). To alleviate urban peak runoff flows and contaminant export, stormwater best management practices (BMPs) are being implemented, including decentralized low impact development (LID) technologies. Bioretention cells (BRCs) are a common LID approach; they consist of a depression in the ground where the natural soil has been replaced by an engineered filter media often covered with vegetation. BRCs can potentially reduce runoff P loading by (i) facilitating groundwater recharge and, hence, reducing surface runoff, and (ii) retaining P in the filter media through physical and biogeochemical processes, and through removal via plant uptake (Barber et al., 2003; Hager et al., 2019; Li & Davis, 2008b; Spraakman et al., 2020).

P in stormwater runoff is usually partitioned into four operationally-defined pools: dissolved inorganic P (DIP), dissolved organic P (DOP), particulate organic P (POP) and particulate inorganic P (PIP) (Dunne & Reddy, 2005). In most instances, particulate P (PP = POP + PIP) dominates the total P (TP) load (Vaze & Chiew, 2004). The soluble reactive P (SRP) pool is largely comprised of DIP (*e.g.,* phosphate) and is of most direct concern because it is readily assimilated by plants, including aquatic algae (Orihe et al., 2017). Nonetheless, a fraction of dissolved organic P (DOP) and even some forms of PP may also be bioavailable (Li & Brett, 2013; Young et al., 1985). Moreover, biogeochemical processes such as enzymatic hydrolysis of organic-P and desorption of PIP may generate additional SRP while, conversely, the formation of mineral precipitates may transform SRP into stable and less mobile PIP phases (Orihe et al., 2017).

A growing number of studies have assessed the performance of BRCs in reducing PP and total suspended solids (TSS) loads (*e.g.*, Li & Davis, 2008b; Liu & Davis, 2014; Teng et al., 2004). Significant variation in the removal of dissolved P (DP = DIP + DOP) has been reported, with reductions in DP concentrations between inflow and outflow ranging from -9.3 to +91% (LeFevre et al., 2015; Marvin et al., 2020; Perry et al., 2009). Some authors attribute observed reductions in DP surface loads by BRCs entirely to a reduction in the surface runoff flow, rather than in-cell

biogeochemical processes immobilizing DP (Jefferson et al., 2017). This explanation may apply to BRCs whose filter media have a high background P content or older cells that have reached P saturation because of the excessive application of compost and fertilizers to promote vegetation growth (Hurley et al., 2017; Mullane et al., 2015; Tirpak et al., 2021). Yet, overall, our predictive understanding of the internal processes that affect the fate of P in BRCs remains rather limited.

Existing stormwater management and reactive transport models, *e.g.*, SWMM, COMSOL, HYDRUS, and DRAINMOD, have been applied to BRCs (Abi Aad et al., 2010; Brown et al., 2013b; He & Davis, 2011; Stewart et al., 2017). Modeling studies have also focused on better understanding the hydrology of BRCs (*e.g.,* Daly et al., 2012; Dussaillant et al., 2003, 2004; Roy-Poirier et al., 2015) and assessing the reactive transport of various contaminants (Kabir et al., 2017; Li & Davis, 2008; Quinn & Dussaillant, 2014; Randelovic et al., 2016). However, few studies have specifically addressed the fate of P in BRCs (Li & Davis, 2016; Roy Poirer et al., 2010). There is also a lack of data on the efficiency of BRCs to reduce surface runoff P over a multi-year time window.

Key processes that control P dynamics in BRCs include filtration, (fast) adsorption, slow sorption (which includes processes such as absorption and mineral (co-)precipitation), organic P hydrolysis, and plant uptake. By representing these processes in a mass balance model, it becomes possible to analyze their relative contributions to the performance of a BRC in reducing P outflow loading. Such knowledge, in turn, may help inform the design and implementation of BRCs in urban P abatement strategies designed to combat eutrophication of downstream streams, lakes and wetlands. To our knowledge, the BRC P model presented here is the first to incorporate all the main P transformation processes within the cell system. The model is calibrated using multi-year data series on meteorology, cell outflow discharge and water chemistry, in addition to P accumulation and chemical fractionation for a BRC located in Ontario, Canada.

3.3 Material and Methods

3.3.1 Study site, field monitoring and lab analyses

The study BRC facility is located in the City of Mississauga within the greater Toronto metropolitan region (Ontario, Canada), and monitored by the Credit Valley Conservation authority (CVC) since the facility was built in 2011. The facility, hereafter referred to as the Elm Drive bioretention system, comprises a sequence of six hydraulically connected cells with a total surface area of 145 m^2 (Figure AA1 in Supplementary Materials) receiving drainage from a 6,456 m^2 residential catchment and discharging into Cooksville Creek, a tributary of Lake Ontario (Sakshi & Singh, 2016). Each cell consists, from top to bottom, of: 1) a 15-cm ponding area to accommodate ponded water, which is equipped with an overflow outlet directly draining into the underdrain pipe when the maximum storage capacity is exceeded; 2) a 45-cm filter media layer filled with fine sand augmented with 3-5 % dry weight leaf compost and covered by an additional thin (1 ~ 5 cm) shredded hardwood bark mulch layer, in accordance to the Low Impact Development Stormwater Management Planning and Design guide of Credit Valley Conservation (CVC, 2010); 3) a 1.15-m bedding storage layer that includes a thin (0.15 m) coarse sand layer and a 1 m thick gravel layer. The six cells are connected via elevated perforated underdrain pipes in the bedding storage layer, which drains excess water when water level in the bedding storage rises above the bottom elevation of the pipe.

Between 2012 and 2017, CVC monitored on-site precipitation (rain and snow), air temperature, outflow discharge, outflow water chemistry, water level in the bedding storage layer (multiple piezometers) and soil chemistry (CVC, 2018). An area velocity flowmeter connected to an automated water sampler recorded the outflow discharge and triggered water sample collection in a maintenance hole at the downstream outlet of the BRC facility. For each precipitation event, a flow-weighted composite sample was collected and analyzed in an accredited laboratory for TP and SRP concentrations using the Standard Method 4500-P (Rice et al., 2012). Due to difficulties associated with collecting sheet flow water samples in the study drainage area, inflow water discharge and chemistry were not directly monitored (Sakshi & Singh, 2016), and rather approximated using rainfall-runoff modeling and existing water quality data in this study.

In 2013, 2014 and 2016, samples from two depth intervals (0-5 cm and 25-30 cm) of the filter media layer were collected from three cells and analyzed for acid extractable TP by EPA Method 6010C (Symbol, 2007). In 2019, we collected 2 to 3 cores in each of the six cells, with sampling locations distributed between the upstream and downstream edges of a cell. Details on the 14 cores, including their locations and the analyses performed, can be found in Lisogorsky (2022). The vertical TP distributions in the filter media were measured using the magnesium nitrate digestion method of (Aspila et al., 1976)) on core slices from 2 cm depth intervals. In addition, we determined the distribution of the solid-bound P among different operationally defined pools using a modification of SEDEX sequential extraction method detailed in (O'Connell et al., 2020; Parsons et al., 2017; Ruttenberg, 1992)). As shown in Figure AB2 in the Supplementary Materials, SEDEX-extracted P pools include reactive P, mineral P, recalcitrant inorganic P and unreactive organic P pools. The chemical extraction results reported for depth intervals 2-4 cm were composites from 4 different filter media samples, and for depth interval 12-14 cm from 5 samples. Results from the other depth intervals were from replicate analyses on a single core sample.

3.3.2 Phosphorus reactive-transport modeling

3.3.2.1 Conceptual framework

The six cells of the Elm Drive bioretention system all have the same structural configuration. When a hydrological event (rainfall or snowmelt) occurs, the inflow water is distributed over all the cells. We therefore modeled the bioretention system as one single (average) cell consisting of the 3 layers illustrated in Figure 3.1. Figures 3.1 and 3.2 further identify the hydrological and P transformation and exchange processes considered within each layer; Table 3.1 provides the terminology and Table 3.2 the notations used throughout the text. In agreement with the monitoring data, the hydrological model assumed that drainage from the bedding storage layer only proceeded when the stored water level exceeded the elevation of the bottom of the underdrain pipe. Similar model structures have been considered in previous studies of BRCs but without the granular representation of the physical and biogeochemical processes affecting P cycling inside the cell (Daly et al., 2012; Randelovic et al., 2016).

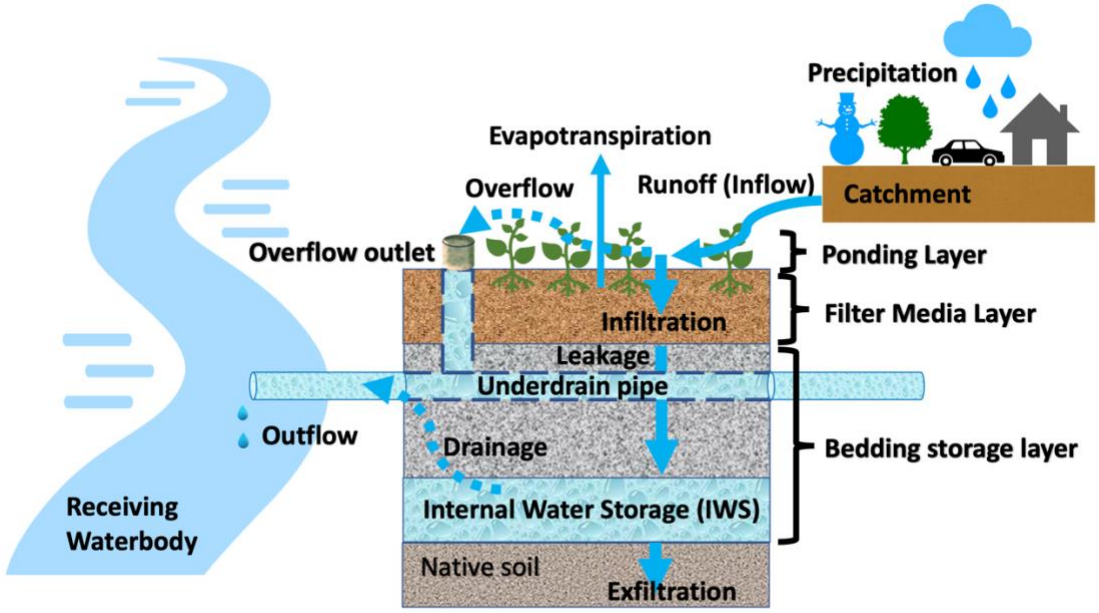

Figure 3.1: Conceptual diagram of the vertical structure and hydrology of the bioretention cell.

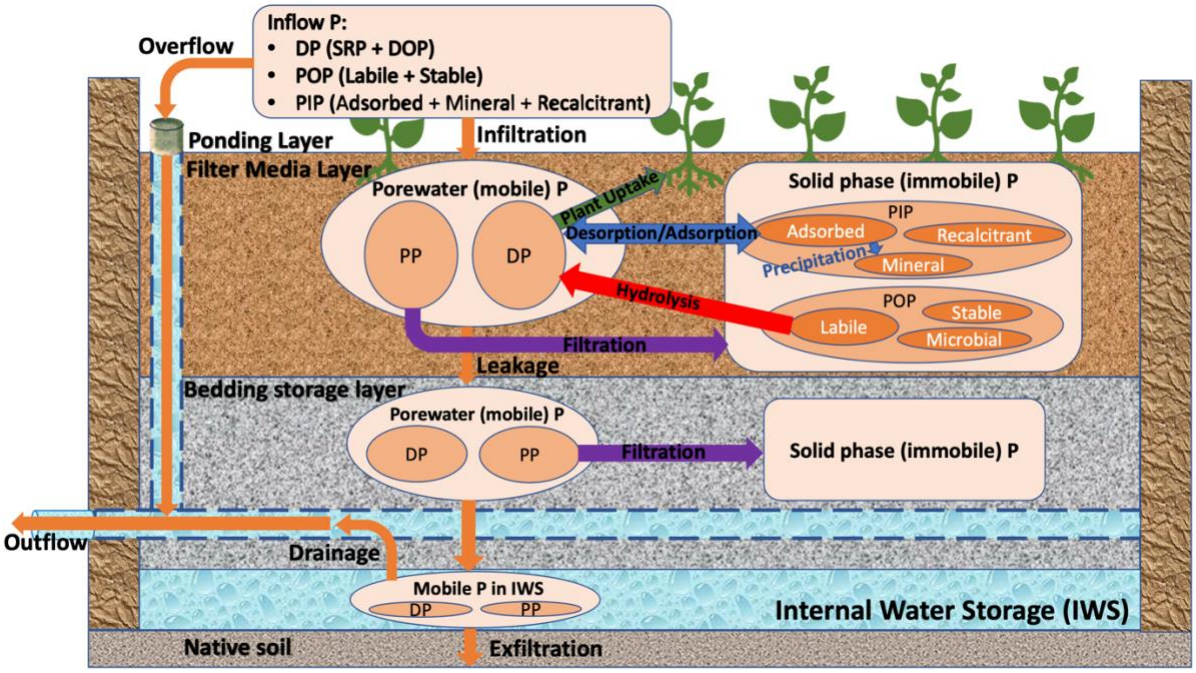

Figure 3.2: Conceptual diagram of the biogeochemical phosphorus model for the bioretention cell.

Table 3.1: Terminology used in Chapter 3.

Bioretention cell	
Ponding layer	depressed zone on top of the cell that accommodates excess inflow during heavy rainfall
Filter media layer	layer above the underdrain pipe, also referred to as the soil layer
Bedding storage layer	combination of layers just above and below the underdrain and including a thin (15 cm) sand layer and a deep (1 m) coarse (stone) layer
Hydrology	
Inflow	runoff flowing into the cell via the ponding layer
Infiltration	fraction of the inflow that percolates through the filter media layer
Overflow	water draining directly from the ponding layer into the underdrain (and then discharged via the outflow) when the maximum ponded water storage is exceeded
Leakage	water draining from the filter media layer into the bedding storage layer
Internal water storage (IWS)	water stored in the submerged zone of bedding storage layer
Drainage	excess water draining into the underdrain pipe when the IWS water level rises above the underdrain level
Outflow	water leaving the cell via the underdrain pipe.
Exfiltration	water leaving the cell by percolating into the surrounding soil
Evapotranspiration	water leaving the bioretention system via evapotranspiration
P biogeochemical processes	
Filter media layer accumulation	total P (TP) accumulating in filter media layer
Plant uptake	dissolved P (DP) taken up from the filter media layer by plants and removed when the plants are harvested
Filter media retention efficiency	fraction of inflow TP accumulating in the filter media layer or being extracted by plants
Bedding storage layer accumulation	fraction of inflow TP accumulating in the bedding storage layer
Adsorption	fast transfer of dissolved P (DP) into the adsorbed P pool
Desorption	fast desorption of adsorbed PIP to porewater DP
Precipitation	combination of all slow chemical sorption processes, including mineral (co-)precipitation, that lead to stable soil mineral P
Filtration	combination of all the physical processes that retain colloidal P by interception, sedimentation, and particle diffusion
Hydrolysis	hydrolysis of labile organic P compounds releasing soluble reactive P (SRP) to the pore water solution

Table 3.2: Notations used in bioretention cell P model.

Abbrev.	Explanation	Abbrev.	Explanation
For inflow water quantity and quality estimation			
A_{BC}	Area of bioretention cells	S_s	Snowpack, units: m
A_{PP}	Area of permeable pavement	S_c	Water storage in catchment repression zone, unit: m
DA	Drainage area	Ep	Evaporation, units: m
la	Impervious fraction of drainage area	CR	Available water storage space in catchment repression zone, unit: m
A_{BMP}	Area of BMP system	P	Precipitation, unit: m
f	Fraction of rainfall events that produce runoff	T	Air temperature, °C
R_v	Runoff coefficient of drainage area	PET	Potential evapotranspiration, unit: m. Estimated by Thornswaite method (J. H. Chang, 1959).
T_t	Threshold temperature for occurrence of snowmelt	Q_{in_c}	Runoff generated in catchment, unit: m
DD	Degree-time factor	C_{TP_in}	Inflow TP concentration
$S_{c,max}$	Maximum repression zone water storage space in catchment	α_{TDP} , α_{PIP} , α_{POP}	Fraction of DP, PIP and POP in inflow TP
n_{PET}	Coefficient for evaporation estimation in catchment repression zone	β_{Labile}, β_{Stable}	Labile and stable fraction of inflow POP
Q_{in}	Inflow water quantity, units: m	$\beta_{Adsorbed}$, $\beta_{Mineral}$, β_{Recal}	Adsorbed, mineral and recalcitrant fraction of inflow PIP
Q_m	Snowmelt, units: m	β_{SRP}	SRP fraction of inflow DP
For ponding layer			
$S_{P,max}$	Maximum ponding storage	Q_O	Overflow water, units: m
S_P	Ponded water, units: m	C_{o_i}	Overflow concentration of species i (DP or PP)
For filter media layer			
d_{fm}	Thickness of filter media layer	I_{max}	Maximum plant P uptake rate
K_S	Hydraulic conductivity of filter media soil	$K_{m,\,PU}$	Michaelis constant for plant P uptake
n_{fm}	Porosity of filter media soil	$C_{PU,min}$	Minimum DP concentration for the occurrence of plant uptake
s_h	Saturation at hygroscopic point	k_{precip}	Precipitation (slow sorption) rate constant
β	Leakage coefficient	k_{Hy}	Hydrolysis rate constant
s_{fc}	Field capacity of filter media	x	Transport distance along soil depth
s	Soil moisture	C_{DP}, C_{PP}	Porewater concentration of DP and PP
I	Infiltration, units: m	R_{DP}, R_{PP}	Reactive rate of DP and PP in porewater
ET	Evapotranspiration, unit: m	D_x	Dispersion
L	Leakage from filter media to bedding storage layer, units: m	V_x	Advection rate in porewater
α_L	Dispersity	R_{Filt}, R_{Ad}, R_{PU}, R_{precip}, R_{Hy}	Reaction rate of filtration, adsorption, plant uptake, precipitation and hydrolysis
λ	Kinetic filtration coefficient	C_{eq}	Equilibrium DP concentration in porewater

Q_{max}	Maximum adsorption capacity	$M_{Adsorbed,PIP}$, $M_{Mineral,PIP}$, $M_{Recalcitrant,PIP}$, $M_{Labile,POP}$, $M_{Stable,POP}$	Soil concentration (unit: mg/kg soil) of adsorbed PIP, mineral PIP, recalcitrant PIP, labile POP and stable POP
K_L	Thermodynamic parameter of adsorption	C_{i_FM}	Outflow concentration of species i (DP or PP) from filter media layer
k_{ad}	Adsorption (fast sorption) kinetic parameter		
For bedding storage layer			
u	Bottom elevation of the bottom of underdrain	λ_s	Filtration coefficient for PP in internal layers except filter media
k_e	Exfiltration rate constant	h_{fm_u}	Elevation of top of filter media
b_{Sr}	Base level of internal water storage (IWS)	d_s	Depth of internal layers except filter media that is effective for PP removal
$S_{r,crit}$	Threshold IWS water storage for drainage	b_{bs}	Elevation of bottom of bedding storage zone
n_{bs}	Porosity of bedding storage zone	B_s	Base level of water in IWS zone
R_{ex}	Exfiltration rate	C_{PP_s}	PP concentration of water enters IWS zone
S_r	Water storage in bedding storage layer, units: m	C_{r_i}	Concentration of species i in water in submerged zone of bedding storage layer
Q_d	Drainage water from bedding storage layer, units: m	M_i	Outflow loading of species i (DP or PP)
Q_{out}	Outflow water from bioretention cell, units: m	f_N	Trained neural network model for drainage rate

3.3.2.2 Hydrological processes

The equations representing hydrological processes are given in Table 3.3. We used mass balance equations to identify water level in various compartments of the BRC. Similar to a previous study (Sakshi & Singh, 2016), we calculated inflow to the BRC based on precipitation data, a simple rainfall-runoff model given in (Schueler, 1987)), and a fixed runoff coefficient. Snow accumulation and snowmelt were derived from the precipitation and air temperature data following (SINGH & KUMAR, 1996). We estimated evaporation with the Thornthwaite method (Chang, 1959). Water ponding occurs when inflow rate exceeds infiltration rate where the latter is assumed to follow Darcy's law. Model diverts inflow directly to the outlet of the cell when the amount of ponded water exceeds the maximum storage capacity of 0.15 m. We split the bedding storage (with coarse grain size) into unsaturated and saturated zones (i.e., internal water storage (IWS)) as shown in Figure 3.1. Variations of water level in this layer are calculated from the net difference between leakage from the filter media layer and the exfiltration plus drainage from the bedding storage layer.

When water in the bedding storage layer rises above the drainage pipe, model calculates the drainage rate proportional to the hydraulic head, that is, the difference between the IWS level and the underdrain bottom elevation (Abi Aad et al., 2010). Available data from piezometers indeed revealed a strong correlation between drainage flow and the hydraulic head. We used the data to train a neural network regression model to derive the functional dependence (f_N) between the drainage outflow and the hydraulic head. This approach yielded a better model performance than a traditional fitted nonlinear regression model. Full details are provided in the Supplementary Materials (section Method AA1). Moreover, between inflow events, when the water level of the bedding storage layer dropped below the drainage pipe, the piezometric data showed an exponential deepening of the water level due to exfiltration of water into the underlying native soil (Brown et al., 2013b; He & Davis, 2011). Hence, the exfiltration flow was modeled assuming a linear dependence on the water mass in the bedding storage layer. The entire set of equations describing the hydrological model was solved numerically using the forward Euler method.

Table 3.3: Equations of the hydrologic model.

No.	Process Name (references of model equation included in brackets)	Mathematical Equation
Inflow water quantity estimation		
T3.3.1	Inflow* (Schueler, 1987)	$Q_{in} = \begin{cases} \frac{(DA \cdot R_v + A_{BMP}) \cdot (Q_m + P)}{A_{BC}} - CR, when\ T > T_t \\ \frac{(DA \cdot R_v + A_{BMP}) \cdot Q_m}{A_{BC}} - CR, when\ T \le T_t \end{cases}$
T3.3.2	Snowmelt (SINGH & KUMAR, 1996)	$Q_m = \begin{cases} \min\{S_s, DD \cdot (T - T_t)\}, when\ T > T_t \\ 0, when\ T \le T_t \end{cases}$
T3.3.3	Snowpack mass balance	$\frac{dS_s}{dt} = \begin{cases} -Q_m, when\ T > T_t \\ \mathrm{P}, when\ T \le T_t \end{cases}$
T3.3.4	Catchment repression storage water balance	$\frac{dS_c}{dt} = \mathrm{CR} - \max\{S_c, \mathrm{Ep}\}$
T3.3.5	Evaporation in catchment repression zone	$\mathrm{Ep} = n_{PET} \cdot PET$
T3.3.6	Catchment retention	$CR = \max\{0, \min\{S_{c,max} - S_c, Q_{in\_c}\}\}$
Water in ponding layer		
T3.3.7	Ponded water mass balance	$\frac{dS_P}{dt} = min\{S_{P,max}, max\{S_P + Q_{in}, Q_{in} - I\}\}$
T3.3.8	Overflow	$Q_O = \max\{0, S_P + Q_{\mathrm{in}} - I - S_{P,max}\}$
Water in filter media layer		
T3.3.9	Soil moisture mass balance (Laio et al., 2001)	$n_{fm} \cdot d_{fm} \cdot \frac{ds}{dt} = I - ET - L$
T3.3.10	Infiltration	$I = \begin{cases} \min\{Q_{in} + S_P, n_{fm} \cdot d_{fm} \cdot (1 - s)\}, when\ s \ne 1 \\ K_S \cdot (Q_{in} + S_P), when\ s = 1\ (Darcy's\ law) \end{cases}$
T3.3.11	Evapotranspiration (Laio et al., 2001)	$ET = \begin{cases} (\mathrm{s} - s_h) \cdot PET, when\ T > 0 \\ 0, \quad when\ T < 0 \end{cases}$
T3.3.12	Leakage (Laio et al., 2001)	$\mathrm{L} = \begin{cases} \max\left\{0, \frac{K_s}{e^{\beta(1 - s_{fc})} - 1} \cdot \left(e^{\beta(\mathrm{s} - s_{fc})} - 1\right)\right\}, when\ \mathrm{s} \ne 1 \\ I, \quad when\ s = 1 \end{cases}$
Water in bedding storage layer		
T3.3.13	Bedding storage water balance	$\frac{dS_r}{dt} = \frac{L - Q_d}{n_{bs}} + R_{exfiltration}$
T3.3.14	Exfiltration	$R_{exfiltration} = -\frac{1}{k_e} \cdot S_r$
T3.3.15	Drainage	$Q_d = \begin{cases} f_N(S_r - S_{r,crit}), \quad when\ S_r > S_{r,crit} \\ 0, \quad when\ S_r \le S_{r,crit} \end{cases}$
T3.3.16	Outflow	$Q_{out} = Q_d + Q_O$

*Assume all the precipitation on the permeable pavement and bioretention cell will go into the bioretention cell and can be counted within 'inflow'.

3.3.2.3 Phosphorus fate and transport

The conceptual structure and mathematical formulation of the P model are presented in Figure 3.2 and Table 3.4. Because no direct data on P concentrations and chemical speciation of the inflow were collected at the study site, we used literature values for P in urban runoff in temperate climate zones. We assumed an average 40% of the inflowing TP to be under dissolved forms (Berretta & Sansalone, 2011b; Goor et al., 2021; Liu & Davis, 2014), and equal distribution of dissolved P (DP) between SRP (here we assume it is equivalent as DIP) and DOP (Goor et al., 2021; Liu & Davis, 2014). As an initial guess, we assumed the partitioning of inflowing particulate P (PP, including colloidal material) over various operational pools (labile POP, stable POP, and adsorbed, mineral and recalcitrant PIP) to resemble that obtained with the chemical extractions of the core-top samples collected in 2019. Moreover, we further adjusted the partitioning of inflowing PP to yield the best model fit to the depth distributions of various pools observed in 2019. In multi-year model simulations, the inflow TP concentration, DP and PP fractions (40 and 60%), and the partitioning of DP and PP over their different fractions were assumed to be time-invariant. Clearly, this is a simplifying approximation that cannot be assessed independently with the available data.

The representation of the fate and transport of P inside the filter media layer builds on previous studies (Li & Davis, 2016; Liu & Davis, 2014; Marvin et al., 2020; Roy-Poirier et al., 2010b). The DP and mobile (i.e., colloidal) PP distributions were calculated by solving one-dimensional advection-dispersion equations for saturated/unsaturated soils with terms accounting for P biogeochemical transformations and exchanges between the mobile pore water and the immobile solid matrix. We used modified versions of equations given in Randelovic et al. (2016), Zhang et al. (2016), and Zhang et al. (2016) to assess the performance of BRCs in treating micro-pollutants and retaining nanoparticles, respectively. The advection rate (v_x) is equal to the pore velocity and derived at each time step from the infiltration rate simulated by the hydrologic model. Within the typical range of dispersivity values for soil environments, the transport of DP and mobile PP was advection-dominated, and therefore the model results were not very sensitive to the actual value assigned to the dispersivity.

In the filter media layer, P was transferred from the mobile phase to the immobile matrix by fast, reversible adsorption of DP and by filtration of colloidal PP. Porewater DP was further taken up by plant roots and the assimilated P was subsequently permanently removed from the BRC when vegetation was pruned or replaced during the regular maintenance at the site. While adsorbed P could return to the pore water by desorption, a fraction of the adsorbed P was permanently immobilized in the solid phase by various slow, irreversible sorption processes, including the (co-)precipitation of phosphate-containing mineral phases (Lucas & Greenway, 2008). For the P transformation processes considered, we opted for simple yet robust model representations reported in the literature, such as linear rate expressions or Monod-type expressions.

Porewater and solid-phase P in the filter media layer are partitioned into the same pools as in the inflow TP (*i.e.,* SRP, DOP, POP and PIP). For the solid-phase P, an additional pool of microbial POP was included. Although microbial growth and decay can result in short-term changes to the mass of P stored in microbial biomass as well as to the SRP concentration in porewater (Lucas & Greenway, 2011; Zinger et al., 2021), we assumed that their net effect on the long-term P distribution pattern was negligible (Fowdar et al., 2017; Lucas & Greenway, 2011). Stated otherwise, the soil microbial POP pool was treated as being at steady state. The POP and recalcitrant PIP pools could thus only increase upon P removal from the pore water via filtration, while DP could be produced by hydrolysis of labile POP.

The partial differential equations (PDEs) describing the mobile DP and PP mass balances in the filter media layer were solved numerically by the Crank-Nicolson method. The time-dependent upper boundary conditions were the DP and PP inflow concentrations during periods of infiltration (that is, when the water level in the ponding layer was positive); they were set equal to 0 during periods when there was no ponding water and, hence, no infiltration. No-diffusion Neumann lower boundary conditions were imposed at the bottom of the filter media layer.

The model treats the water-saturated portion of the bedding storage zone as a well-mixed reservoir. P mass balance equations were therefore ordinary differential equations that were solved numerically by the forward Euler method. The leakage P flux from the overlying filter

media layer was imposed as input to the bedding storage layer. Filtration of colloidal PP in the unsaturated bedding storage zone was assumed to be at steady-state and was simulated by a simple depth filtration model. The concentrations of the different P pools in the water carried by the underdrain pipe to the outflow were assumed to be the same as those in the water of the bedding storage zone. We calculated the outflow P loading by summing the loads from the underdrain pipe and the overflow. The overflow TP concentration was treated as a calibration parameter based on the measured outflow data. Note that overflow rarely occurred at the study site during the observation period and, hence, most outflow P was associated with water from the bedding storage layer leaving the cell via the underdrain.

Table 3.4: Equations of P model

No.	Process Name (references of model equation included in brackets)	Mathematical Equation
P in filter media layer		
T3.4.1	DP transport in porewater (Randelovic et al., 2016)	$\frac{\partial(C_{DP})}{\partial t} = D_x \cdot \frac{\partial^2 C_{DP}}{\partial x^2} - v_x \cdot \frac{\partial C_{DP}}{\partial x} + R_{DP}$
T3.4.2	PP transport in porewater (Zhang et al., 2016)	$\frac{\partial(C_{PP})}{\partial t} = D_x \cdot \frac{\partial^2 C_{PP}}{\partial x^2} - v_x \cdot \frac{\partial C_{PP}}{\partial x} + R_{PP}$
T3.4.3	Adsorbed PIP mass balance	$\frac{d(M_{Adsorbed,PIP})}{dt} = R_{Filt} \cdot \alpha_{PIP} \cdot \beta_{Adsorbed} + R_{Ad} \cdot \frac{n_{fm} \cdot s}{\rho_{fm}} - R_{precip}$
T3.4.4	Mineral PIP mass balance	$\frac{d(M_{Mineral,PIP})}{dt} = R_{precip} + R_{Filt} \cdot \alpha_{PIP} \cdot \beta_{Mineral}$
T3.4.5	Recalcitrant PIP mass balance	$\frac{d(M_{Recalcitrant,PIP})}{dt} = R_{Filt} \cdot \alpha_{PIP} \cdot \beta_{Recalcitrant}$
T3.4.6	Labile POP mass balance	$\frac{d(M_{Labile,POP})}{dt} = R_{Filt} \cdot \alpha_{POP} \cdot \beta_{Labile} - R_{Hy}$
T3.4.7	Stable POP mass balance	$\frac{d(M_{Stable,POP})}{dt} = R_{Filt} \cdot \alpha_{POP} \cdot \beta_{Stable}$
T3.4.8	DP Reactive Rate in porewater	$R_{DP} = R_{Hy} - R_{Ad} - R_{PU}$
T3.4.9	PP Reactive Rate in porewater	$R_{PP} = -R_{Filt}$
T3.4.10	Dispersion	$D_x = \alpha_L \cdot v_x$
T3.4.11	Advection	$v_x = \frac{I}{n_{fm} \cdot s}$
T3.4.12	PP kinetic filtration (Tufenkji & Elimelech, 2004; Zhang et al., 2016)	$R_{Filt} = \lambda \cdot v_x \cdot C_{PP}$
T3.4.13	DP adsorption & desorption (Limousin et al., 2007; McGechan & Lewis, 2002; Mei, Yang, Guo, et al., 2012)	$M_{Adsorbed,PIP} = \frac{Q_{max} \cdot K_L \cdot C_{eq}}{1 + K_L \cdot C_{eq}}$ $R_{Ad} = k_{ad} \cdot (C_{DP} - C_{eq})$
T3.4.14	Plant Uptake (Barber, 1995)	$R_{PU} = \frac{I_{max} \cdot (C_{SRP} - C_{PU,min})}{K_{m,PU} + C_{SRP} - C_{PU,min}}$
T3.4.15	Hydrolysis (Olson, 1963; Müller & Bünemann, 2014)	$R_{Hy} = k_{Hy} \cdot M_{Labile,POP}$
P in bedding storage layer		
T3.4.16	PP depth filtration (Tiveron et al., 2018)	$C_{PP\_s} = C_{PP\_FM} \cdot e^{(-\lambda_s \cdot d_s)}$
T3.4.17	DP and PP concentration in IWS	$\frac{dC_{r\_i}}{dt} = \frac{L \cdot C_{i\_FM} + n_{bs} \cdot (S_r + B_s) \cdot C_{r\_i}}{L + n_{bs} \cdot (S_r + B_s)}$
T3.4.18	Outflow P loading	$M_i = C_{r\_i} \cdot Q_d + C_{o\_i} \cdot Q_o$

3.3.3 Model parameterization, calibration and evaluation

The earliest TP data measurements of the filter media in 2013 indicated that the original media material was already relatively rich in TP. The chemical extractions performed on deeper sections of the 2019 cores (below 20 cm) further suggested that this initial P was largely in the mineral and recalcitrant pools. Based on the final model calibration, the initial mineral and recalcitrant PIP pools in the filter media layer were fixed at 90 and 190 mg kg^{-1}, respectively. The initial pore water TP concentrations in both layers were set to 0. The initial concentrations of the other solid-phase P pools in both the filter media and bedding storage layers were also set to 0, with the exception of the microbial POP pool in the filter media, which was fixed at 10 mg kg^{-1} based on literature values (Lucas & Greenway, 2011). Note that the microbial POP pool remained constant during the simulations.

Similar to the time scale of the climate data series, our model also runs at the 10-minute time scale covering the period from November 2012 to December 2019. To evaluate model performance, we considered multiple quantities and compared the simulated and measured values. These quantities include water outflow volumes as well as SRP and TP outflow loads from 2012 to 2017 (calculation details are in Supplementary Materials, section Method AA2), TP concentrations in the filter media measured in 2013, 2014, 2016, and 2019, and vertical (along depth) distributions of P pools extracted from 2019 cores (Table 3.5). We used the Nash-Sutcliffe efficiency (NSE) metric to evaluate the goodness of fit between simulated results and observed concentrations/loads (Legates & McCabe, 1999). Regarding TP profile in depth of the soil media compartment, we compared model-simulated time-dependent profiles with median values of TP concentrations measured on all the filter media samples available for a given time point and depth interval. For P pools within PP, as shown in Table 3.5, we assessed the correspondence between model-simulated P pools and measured SEDEX extraction data. The sum of loosely-adsorbed and humic-associated P extracted in steps 1 and 2 of the SEDEX protocol was compared to the sum of the model-calculated labile fractions of PIP and POP, plus 90% of the microbial POP (based on Parsons et al. (2017) and Ruttenberg (1992)).

We used the dynamically-dimensioned search algorithm of Tolson & Shoemaker (2007) to conduct automatic model calibration and find optimum values of model parameters. First, we

started with the hydrology model, found the best hydrology model parameters, and then followed with the identification of best values for P model parameters. Permissible ranges for the adjustable parameters in the two models were compiled from information contained in technical reports for the study site (*e.g.*, soil hydraulic conductivity, exfiltration rate constant), as well as values reported in the literature (*e.g.*, hydrolysis rate constant). The resulting information is summarized in Table 3.6.

The calibration of the hydrology model involved optimizing 13 parameters to maximize the NSE for the monthly outflow volumes. By contrast, the calibration of the P model had multiple outcome targets, namely, matching TP accumulation in the filter media layer, the 2019 TP partitioning over the different P pools, plus the outflow TP and SRP loadings. Therefore, the P model parameters were adjusted in two steps. First, 10 parameters related to P fate and transport processes in the filter media layer (*i.e.*, dispersion, adsorption, filtration, precipitation, plant uptake, and hydrolysis) and the 3 parameters describing the relative contributions of DP, PIP, and POP to the inflow TP were tuned to best reproduce the results of the SEDEX sequential extraction results for 2019. Second, the filtration coefficient of the bedding storage layer and the overflow TP concentration were calibrated to match the cumulative outflow TP loading between 2012 and 2017, that is the period over which CVC did monitor the outflow volumes. The final calibrated parameter values are given in Table 3.6.

3.3.4 Sensitivity analyses

We conducted global sensitivity analyses to assess (1) the sensitivity of the model-predicted runoff flow reduction on the 13 calibrated parameters of the hydrology model, and (2) the sensitivity of the modeled P accumulation in the bioretention cell on the 14 calibrated parameters of the P model. We applied the elementary effects (EEs) method (Morris et al., 2014) using the Matlab SAFE (Sensitivity Analysis for Everyone) toolbox (Pianosi et al., 2015). For the P model, we conducted two rounds of sensitivity analyses. In the first round, the objective function was the cumulative filter media TP accumulation from 2012 to 2019. In the second round, we focused on the accumulation of reactive forms of P by defining the objective function as the average fraction of the accumulated TP in the filter media layer that was present as reactive P at

the end of 2019. For more details on the sensitivity analyses, see Supplementary Materials (section Method AA3).

Table 3.5: Matched observed and simulated data for model simulation evaluation

Simulated Data	Observed Data (n: data number)	Lab Analysis Method to Obtain Observed Data	Lab Analysis Method References	Period of Available Observed Data
For Hydrologic Model				
Simulated outflow flowrate	Outflow flowrate (measured in 10-minute interval)	-	-	Nov 2012 ~ Dec 2017
For P Model				
Simulated TP concentration for outflow composite samples*	Measured TP concentration for outflow composite samples (n = 44)	Standard Method 4500-P	(APHA, 2018)	Nov 2012 ~ Dec 2017
Simulated SRP concentration for outflow composite samples*	Measured SRP concentration for outflow composite samples (n = 43)	Standard Method 4500-P	(APHA, 2018)	Nov 2012 ~ Dec 2017
Simulated TP loading for monitored events with composite samples*	Calculated TP loading for monitored events with composite samples (n = 44)	Calculated*	-	Nov 2012 ~ Dec 2017
Simulated SRP loading for monitored events with composite samples*	Calculated SRP loading for monitored events with composite samples (n = 43)	Calculated*	-	Nov 2012 ~ Dec 2017
Simulated soil TP	Measured soil TP (n = 133)	EPA Method 6010C (for 2013, 2014 and 2016); Magnesium nitrate digestion method (for 2019)	(Aspila et al., 1976; Symbol, 2007)	2013, 2014, 2016, 2019
90% microbial POP + labile POP + Adsorbed PIP	Reactive P (Loosely adsorbed P + Organic associated P, n = 15)	SEDEX** (extraction step 1 and 2)	(Parsons et al., 2017; Ruttenberg, 1992)	2019
Mineral PIP	Mineral P (Fe-bound P + Ca bound P, n = 15)	SEDEX** (extraction step 3 and 4)	(Parsons et al., 2017; Ruttenberg, 1992)	2019
Recalcitrant PIP	Recalcitrant inorganic P (n = 15)	SEDEX** (extraction step 5)	(Parsons et al., 2017; Ruttenberg, 1992)	2019
10% microbial POP + Stable organic P	Unreactive organic P (n = 15)	SEDEX** (extraction step 6)	(Parsons et al., 2017; Ruttenberg, 1992)	2019

* Calculated by the method specified in Supplementary Materials (Method AB2).

**Details about SEDEX method can be seen in Supplementary Materials (Figure AB2).

Table 3.6: Parameters of hydrologic (**A**) and P (**B**) model

Abbrev.	Adopted value*	Reported/ Selected/ Calculated values**	Units	A
For inflow water quantity estimation				
A_{BC}	*145*	145 [a]	m^2	
A_{PP}	*530*	530 [a]	m^2	
DA	*5781*	5781 [a]	m^2	
la	*0.446*	0.446 [a]	-	
A_{BMP}	*675*	$A_{BMP} = A_{BC} + A_{PP}$	m^2	
f	0.62	0.35 ~ 1	-	
R_v	0.33	$R_v = 0.05 + f * la$	-	
T_t	-0.23	-0.3 ~ 0.3	℃	
DD	0.57 ×10^{-5}	(0.49~6.25) × 10^{-5} [b]	$m \cdot (℃ \cdot 10min)^{-1}$	
$S_{c,max}$	0.09	0.02~0.09	m	
n_{PET}	10	2~10	-	
For ponding layer				
$S_{P,max}$	*0.15*	0.15 [a]	m	
For filter media layer				
d_{fm}	*0.45*	0.45 [a]	m	
K_S	0.0213	0.0208~0.0233 [a]	$m \cdot (10\ min)^{-1}$	
n_{fm}	0.4	0.35 ~ 0.45 [c]	-	
s_h	0.083	0.08~0.19 [c]	-	
β	12.5	12.1 ~ 14.8 [c]	-	
s_{fc}	0.35	0.35~0.65 [c]	-	
For bedding storage layer				
u	*-1.216*	-1.216 [a]	m	
k_e	189	170~200 [d]	$(10\ min)^{-1}$	
b_{Sr}	-1.45	-1.45 ~ -1.35 [d]	m	
$S_{r,crit}$	0.21	$S_{r,crit} = u - b_{Sr}$	m	
n_{bs}	0.48	0.35 ~ 0.5 [c]	-	

Abbrev.	Adopted value*	Reported/ Selected/ Calculated values**	Units	B
For inflow P concentration and partitions				
C_{TP_in}	4.3	0.37~6.5 [e]	mg/L	
α_{TDP}	*0.4*	0.3~0.53 [e, f]	-	
α_{PIP}	0.18	-	-	
α_{POP}	0.42	-	-	
β_{Labile}	0.27	-	-	
β_{Stable}	0.73	-	-	
$\beta_{Adsorbed}$	0.36	-	-	
$\beta_{Mineral}$	0.02	-	-	
β_{Recal}	*0.62*	-	-	
β_{SRP}	*0.5*	0.4~0.58 [f]	-	
For ponding layer				
C_{TP_over}	0.33	-	mg/L	
For filter media layer				
α_L	1	0.01~1 [g]	cm	
λ	0.025	0.01 ~ 0.06 (median: 0.02) [h]	cm^{-1}	
Q_{max}	683.5	275.1 ~ 843.5 [i, j]	mg P kg^{-1}	
K_L	0.2	0.02 ~ 0.22 [i]	-	
k_{ad}	0.15	0.1 ~ 0.41 [i]	(10 min)$^{-1}$	
I_{max}	3.33 ×10^{-7}	2.68 ~ 9.79 × 10^{-7} [k]	μmol (cm^2)$^{-1}$ s^{-1}	
$K_{m,PU}$	12.7	0.4 ~ 16 [k]	μmol L^{-1}	
$C_{PU,min}$	0.25	0.1 ~ 0.6 [k]	μmol L^{-1}	
R_{precip}	0.052	0.03 ~ 0.42 [l]	mg P kg^{-1} day^{-1}	
k_{Hy}	5.0 × 10^{-4}	3.1 ~ 5 × 10^{-4} [m]	day^{-1}	
For bedding storage layer				
λ_s	0.06	-	cm^{-1}	
h_{fm_u}	*-0.271*	-0.271 [a]	m	
d_s	72.9	$d_s = h_{fm\_u} - b_{Sr} - d_{fm}$	cm	
b_{bs}	*-1.871*	-1.871 [a]	m	
B_s	0.42	$B_s = b_{Sr} - b_{bs}$	m	

***** Values obtained by calibration (in non-italic) or selected based on references (in italic).

** Sources of selected data:

a. (CVC, 2016);

b. (Kuusisto, 1980; SINGH & KUMAR, 1996);

c. (Laio et al., 2001);

d. Observed from monitoring data.

e. (Berretta & Sansalone, 2011; Yang & Lusk, 2018);

f. (Berretta & Sansalone, 2011; Goor et al., 2021; Liu & Davis, 2014);

g. *https://www.enviro.wiki/*;

h. (Li & Davis, 2008c);

i. (Mei, Yang, Guo, et al., 2012)*;*

j. (Mei et al., 2012; Zhang et al., 2018)*;*

k. (Barber, 1995; Föhse et al., 1991; Kelly et al., 1992)*;*

l. (Müller & Bünemann, 2014)*;*

m. (Jones et al., 1984)*;*

3.4 Results

3.4.1 Outflow water quantity

Simulated outflow water quantity from November 2012 to December 2017 agreed well with the observed values with an NSE of 0.79 and 0.77 at the monthly and daily scales (see Figure 3.3 for the results at monthly scale). Model results imply that, over the 5-year simulation time frame during which outflow was monitored, the bioretention facility reduced the cumulative runoff by 64%, which is close to the runoff reduction efficiency (65%) estimated from monitored outflow data.

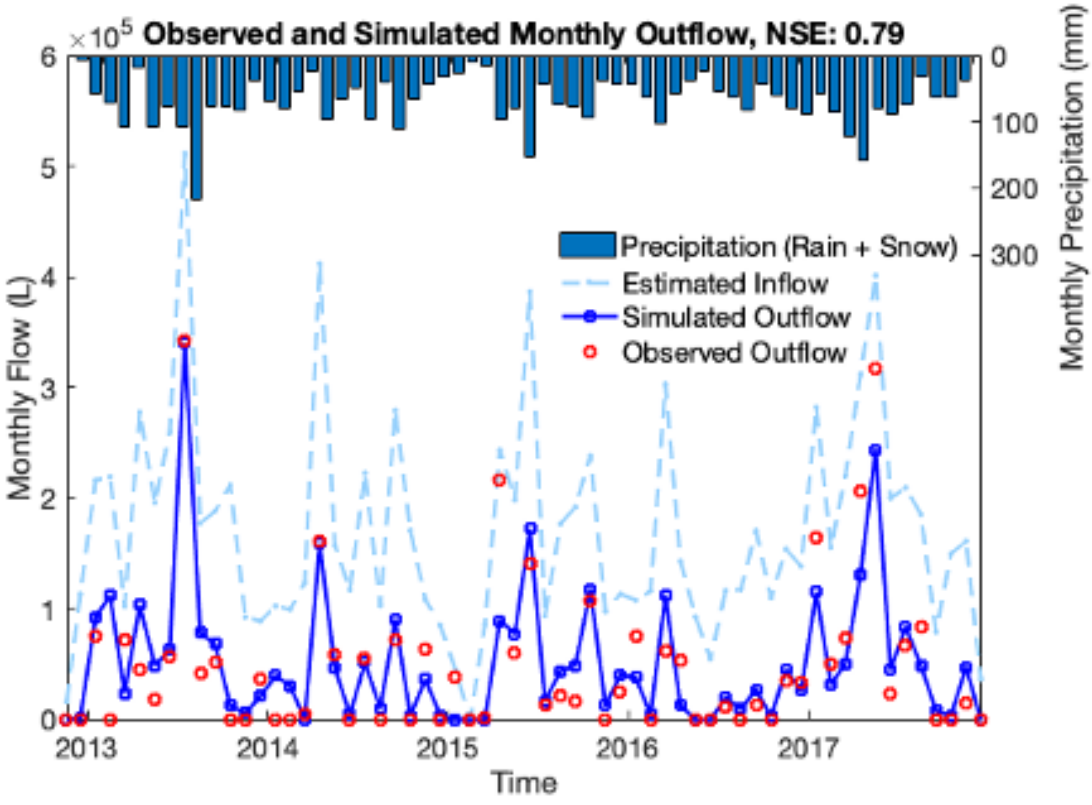

Figure 3.3: Monthly precipitation, inflow, and outflow for the period during which outflow volumes were monitored (November 7, 2012, to December 30, 2017). The modeled monthly inflow and outflow volumes were estimated using the equations in Table 3.3. The offset between inflow and outflow is due to evapotranspiration and exfiltration.

3.4.2 Outflow TP and SRP loads

Simulated cumulative TP and SRP outflow loadings of all monitored events from November 2012 to December 2017 agreed well with the observed values with an NSE of 0.79 and 0.76 (Figure 3.4). Note that, as no inflow TP data were available, we ran the model using a range of values for P in the inlet, and realized that an inflow TP concentration of 4.3 mg L^{-1} best explained the observed cumulative TP outflow loads (Figure 3.4) and the observed TP accumulation in the BRC (Figure 3.5). With significantly lower (higher) TP inflow concentration, the model underpredicted (overpredicted) both the outflow and accumulation of P (Figure AA3 in Supplementary Materials). Mean, median and standard deviation values of modelled TP and SRP outflow loadings also agreed well with those of the observed data (Figure AA4 in Supplementary Materials). Most inflow events resulted in small outflow P loads: < 10 g per event for TP and < 6 g per event for SRP. The few large events recorded over the 5-year period contributed over 50% of the TP and SRP outflow loads. For example, a single high-flow event in July 2013, accounted for about 36% of the observed cumulative export of TP and 27% of that of SRP between 2012 and 2017.

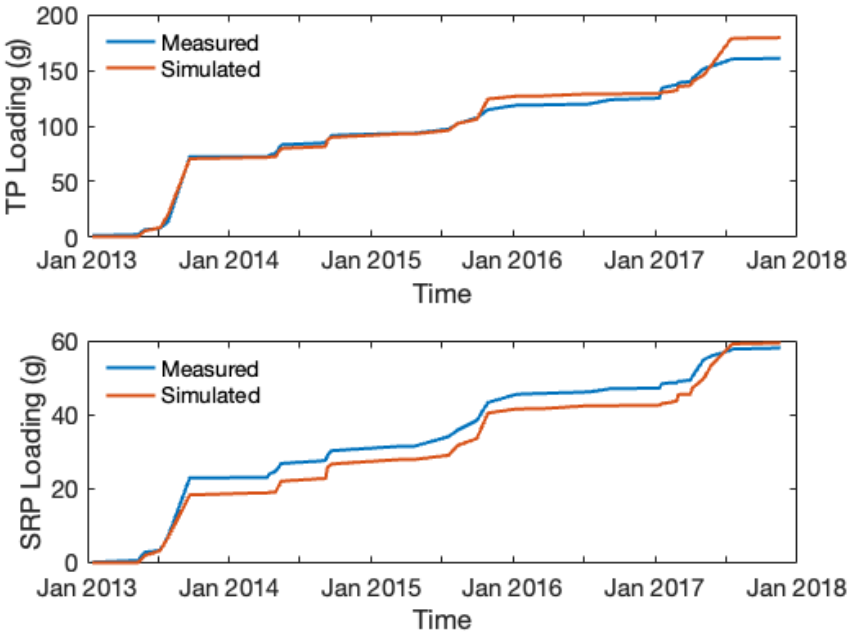

Figure 3.4: Observed and modeled cumulative TP and SRP outflow loads for the period during which the outflow volumes plus the concentrations of TP and SRP were measured (November 7, 2012, to December 30, 2017). Nash-Sutcliffe efficiency (NSE) values for the simulated cumulative TP and SRP loads are 0.79 and 0.76, respectively.

3.4.3 P accumulation in the filter media layer

Model properly reproduced vertical profile of TP concentrations in soil media (see Figure 3.5) with NSE of 0.82. Moreover, model reproduced the patterns that we had observed in our data. Among these patterns are that TP concentrations measured in the filter media layer increased with time and decreased with depth with pronounced gradient down the soil media as time passed. However, there was significant variability in TP concentrations in a given depth interval and at a given time point, as shown in Figure 3.5. This variability illustrates the large horizontal heterogeneity in P distributions within and between the six cells of the bioretention system. The larger TP concentration ranges for the year 2019 reflect the greater number of core locations we sampled in 2019 compared to the far fewer locations sampled in previous years by CVC. Despite the relatively large concentration ranges in Figure 3.5, a clear long-term P accumulation trend can be observed. It was this multi-year temporal trend, and those shown in Figure 3.4, that the 1D reaction-transport model was designed to capture.

Notable discrepancies between measured and modelled TP concentrations occurred in 2014 at 5 cm depth and those near and below 20 cm in 2019. Between sample collection in 2013 and 2014, maintenance work was conducted to replace the vegetation in the BRC. This may have disturbed the topmost filter media and reset the TP concentration in the top layer to the observed lower value.

Both the measured and modelled TP depth profiles imply that P actively accumulated in the filter media between October 2013 and November 2019. According to model results, average TP concentration in the filter media layer (*i.e.,* integrated from 0 to 45 cm depth) increased from 331 mg kg^{-1} in 2013 to 534 mg kg^{-1} in 2019. Per unit mass filter media, the accumulation was equivalent to 35 mg P kg^{-1} yr^{-1}; per unit cell surface area, to 25 g P m^{-2} yr^{-1}. For the entire BRC facility, this translates to about 3.6 kg yr^{-1}, monotonically increasing since the facility was built. Results further showed that the accumulation of TP mostly took place in the upper part of the filter media layer. For instance, 63% of all the TP that had accumulated by 2019 was stored in the top 22 cm. As seen in Figure 3.6, the model also reproduced the observed decreasing trends with depth of the proportions of reactive solid-bound P and unreactive POP pools (defined in Table 3.5). These trends were balanced by increases in the relative contributions of mineral and

recalcitrant PIP with depth. (Note that depth profiles of absolute concentrations of P pools are plotted in Figure AA6 in Supplementary Materials).

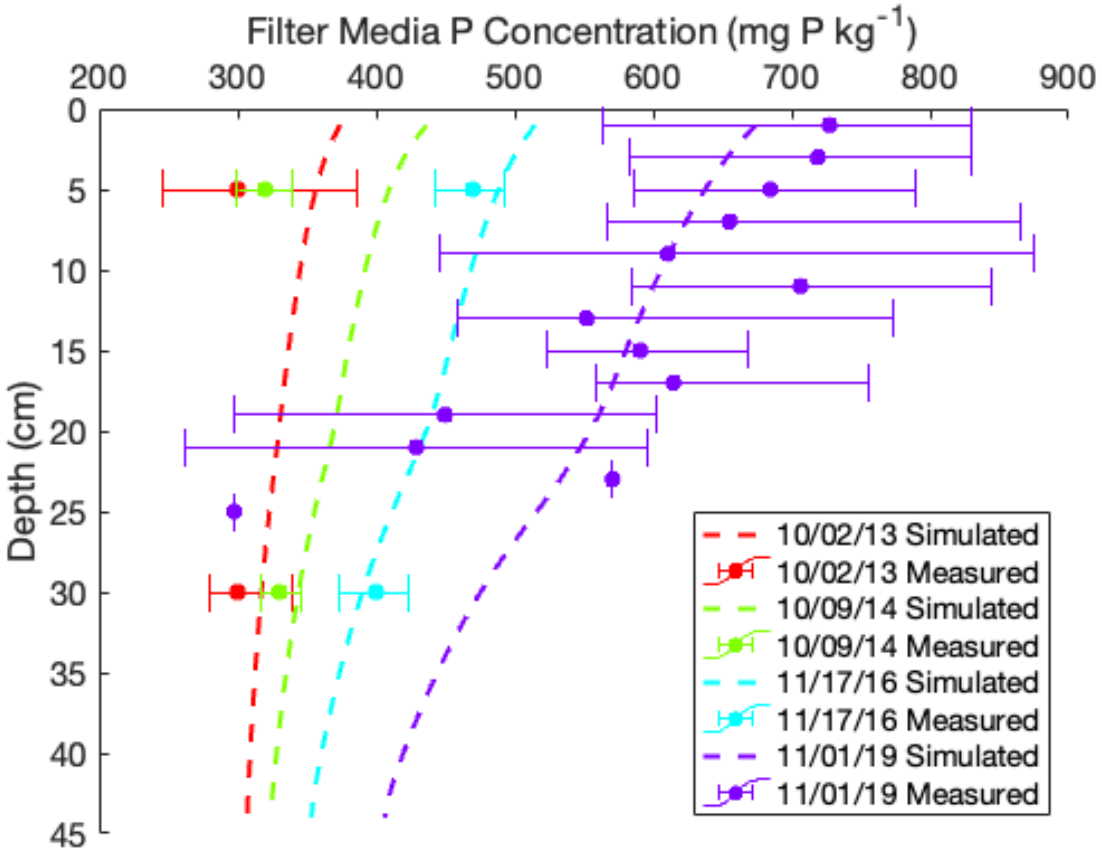

Figure 3.5: Measured and modeled concentration depth profiles of TP in the filter media layer as a function of time. Dots represent median values and error bars indicate maximum and minimum values of the TP concentrations measured at a given depth in the cores collected at the times indicated on the graph. The Nash-Sutcliffe efficiency (NSE) for the ensemble of modeled concentration profiles is 0.82.

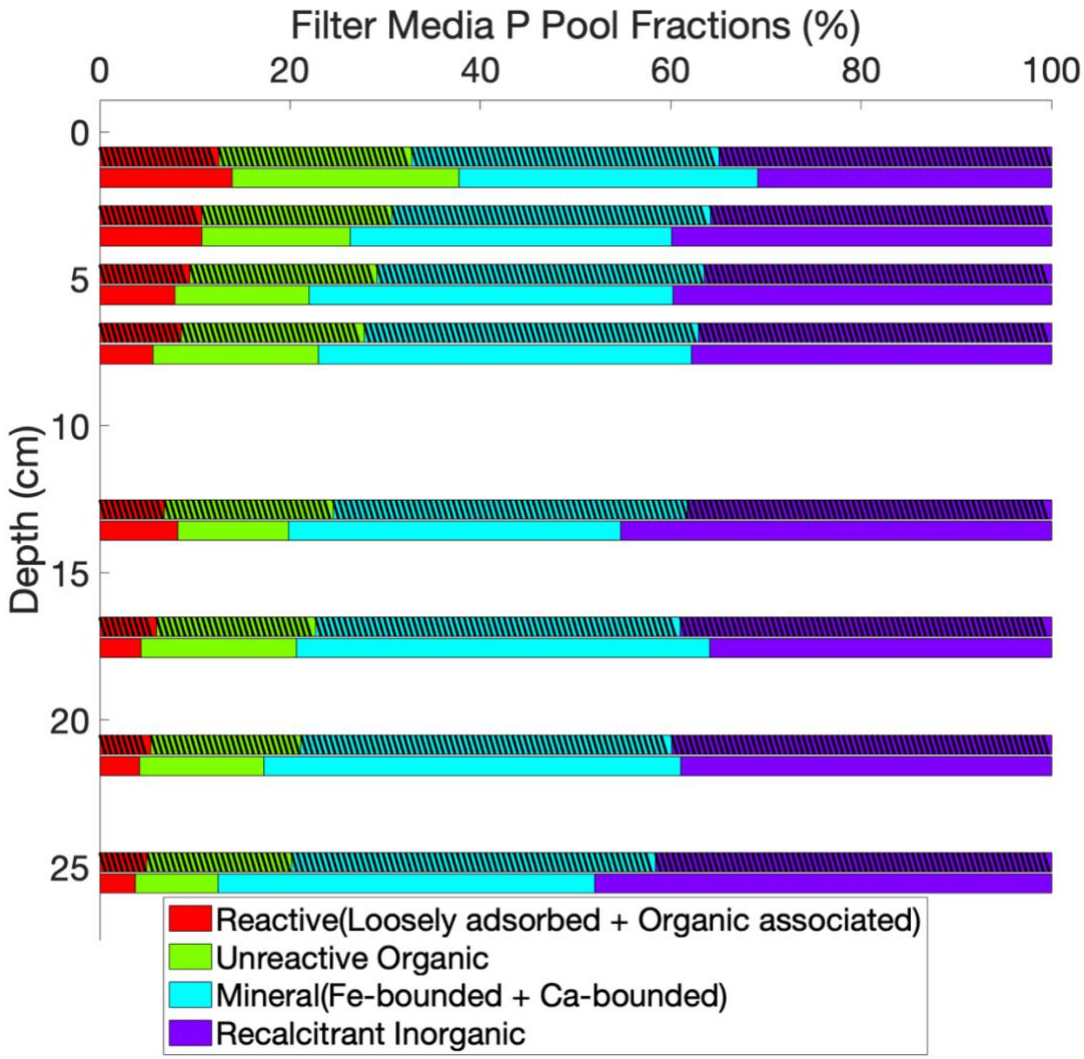

Figure 3.6: Measured (bottom, unshaded bars) and modeled (top, shaded bars) distributions of TP over the different pools in the filter media layer as a function of depth. The measured results were obtained from the SEDEX extractions on core samples collected on November 1, 2019 (see text for details). Nash-Sutcliffe efficiency (NSE) values for the simulated fractions of reactive P, unreactive organic P, mineral P, and recalcitrant inorganic P are 0.73, -0.16, 0.35, and 0.11, respectively.

3.4.4 Mass balances and plants

According to the water balance, exfiltration into the underlying native soil was the dominant surface runoff reduction (63% of inflow) mechanism (Figure 3.7a). Most outflow exited the cell via the underdrain (32% of inflow) with overflow only accounting on average for 3.5% of the inflow. Evapotranspiration plus internal storage had the smallest contributions to the water balance (1.5% of inflow). The interannual water balance varied depending on the climate conditions. For example, runoff reduction via exfiltration increased to 73% in the dry year of 2016, while overflow increased to 13% in the wet year of 2013 (Figure AA7 in Supplementary Materials).

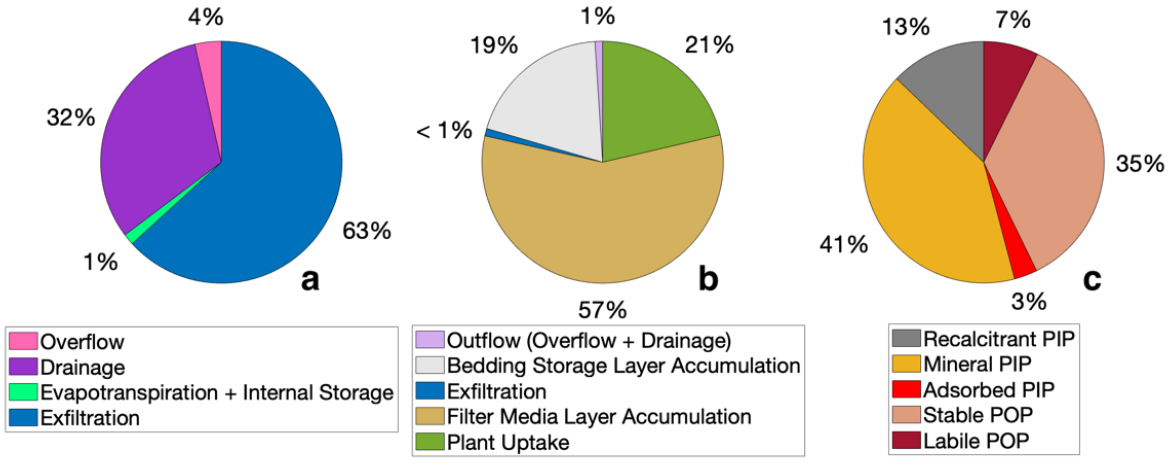

Figure 3.7: Fate of water inflow to the bioretention cell system (**a**), retention and export of P entering the bioretention cell (**b**), and (**c**) partitioning of P accumulated in the filter media layer over the different extracted pools. The percentages are model-calculated cumulative values for the period 2013-2019.

The P mass balance modeling results in Figure 3.7b implied that the filter media layer retained the most P entering the facility (57%), followed by plant uptake (21%) and accumulation in the bedding storage layer (19%). Plant uptake retained the most SRP (51%) entering the facility, while accumulation in the filter media accounted for 45% of SRP retention (Figure AB8 in Supplementary Materials). Export through outflow and exfiltration was estimated to only represent about 3 and 4% of the TP and SRP influx, respectively. The distribution of P retained in the filter media layer between the different pools is shown in Figure 3.7c. The largest P sink in the BRC was mineral PIP. It accounted for 41% of all P accumulated in the filter media layer,

compared to just 3% for the adsorbed PIP pool. Together, the stable (*i.e.*, unreactive) POP and recalcitrant PIP pools represented 48% of the P accumulated in the filter media layer.

Because of the lack of quantitative data on vegetation growth and removal, we also ran the model without plant P uptake. The total TP retention by the filter media layer did not change much, from 77% to 79% without and with plants, respectively (Figure AA9a in Supplementary Materials). The partitioning of P in the filter media layer changed significantly, however. In particular, the adsorbed PIP pool increased from 3.1% in the presence of plants to 22% in their absence (Figure AA9b in Supplementary Materials).

3.4.5 Sensitivity analyses

The sensitivity analysis of the hydrologic model identified f, the climatic parameter representing the fraction of rainfall events producing runoff, as having the most significant impact on the runoff reduction efficiency of the BRC (mean elementary effect or EE of 0.2; Figure AA10a in Supplementary Materials). Other sensitive parameters were, in descending order: b_{Sr} and n_{bs}, which are related to water storage in the bedding layer (EE values of 0.13 and 0.09, respectively), and the exfiltration rate constant, k_e (EE value of 0.023). Parameters with the lowest sensitivities were those related to filter media characteristics and evapotranspiration (i.e., β, s_{fc}, s_h, n_{fm}, K_S), which had mean EE values < 0.01.

For the P model, the kinetic filtration coefficient, λ, exerted the most influence on TP retention (mean EE value of 31.5, Figure AA10b in Supplementary Materials). Furthermore, the model was less sensitive to the parameters describing the equilibrium adsorption isotherm, K_L and Q_{max} (mean EE of 0.12 and 0.05, respectively), compared to kinetic parameters including the adsorption coefficient (k_{ad}, mean EE: 2.70), plant uptake parameters ($K_{m,\,PU}$, I_{max} and $C_{PU,min}$, with mean EE values of 0.50, 0.32 and 0.10, respectively), and the mineral precipitation rate constant (k_{Precip}, mean EE value of 0.16). Parameters with relatively low sensitivity were those describing the partitioning of inflow TP over the different pools (α_{POP}, β_{Labile} and $\beta_{Adsorbed}$, with mean EE values of 0.04, 0.04 and 0.03, respectively), the hydrolysis rate constant (k_{Hy}, with a mean EE value of 0.02), as well as most hydrological model parameters, with the notable exception of the fraction of rainfall events that produce runoff (f, with mean EE value of 0.18) (Figure AA10c in Supplementary Materials).

3.5 Discussion

3.5.1 Phosphorus runoff reduction

3.5.1.1 Hydrological impacts

According to the modeling results, exfiltration plays a dominant role in reducing the surface runoff volume, yet it accounts for less than 1% of the reduction in the P input flux. The reason is that most P entering the system is immobilized within the topmost part of the filter media layer (Figure 3.5) and, therefore, never makes it to the bottom of the bedding storage layer. The sensitivity analyses of the hydrologic parameters further imply that it is not only the cell's hydrology but also its P runoff reduction performance that are mainly sensitive to the fraction of rainfall events that produce runoff (f). This is not entirely surprising as a BRC only functions when it receives inflow and the associated P.

Climate studies show increasing trends in precipitation extremes for Southern Ontario that will likely continue in the coming decades (Deen et al., 2016, 2021). With the rising frequency of high-intensity precipitation events, more rainfall is converted into runoff. In turn, this decreases the surface flow reduction efficiency of the BRC since less water can be exfiltrated into native soil under wetter year (see Figure AA7 in Supplementary Materials). The greater outflow and decreased contact time of porewater P with the filter media can potentially cause a greater fraction of the P input to be exported with the outflow and this can be further verified by future scenarios analysis with the model developed in this study. Previous research has similarly highlighted that changes in the inflow regime driven by climate change will impact BRCs' performance in terms of surface runoff reduction (Beecham & Chowdhury, 2012; Daly et al., 2012; Hathaway et al., 2014) and runoff P reduction (Shrestha et al., 2018).

3.5.1.2 Role of P immobilization processes

Our modeling results indicate that the majority of P is retained in the filter media layer (57%) followed by the bedding storage layer (20%). Earlier work has shown comparably high retention efficiencies of P loading by BRC filter media (*e.g.*, 47–59% in Geronimo et al. (2015)). Previous studies have shown continuous P retention in BRC filter media under long-term ($\geq$ 7 years) operation (Johnson & Hunt, 2016; Komlos & Traver, 2012; Muerdter et al., 2016). Similar to our results, these studies show preferential P accumulation within the uppermost portion of the filter

media compared to lower depths (section *3.4.3*). Nonetheless, our model estimates show that the deeper zone (23-45 cm) of the filter media still trapped a significant fraction of the incoming P (37% of all P accumulated P in the filter media). This contrasts with the work of Komlos & Traver (2012) and Muerdter et al. (2016) who suggested a near-complete retention within the top 10 cm of filter media (Komlos & Traver, 2012; Muerdter et al., 2016). In our model simulations, 41% of the P accumulation in the filter media is due to adsorption of DP followed by stabilization by slower sorption processes (see Figure 3.7c). The latter may include (co-)precipitation of phosphate ions with Ca, Al, and Fe minerals such as hydroxyapatite, variscite, strengite, and ferric iron (hydr)oxides (Hussain et al., 2015; Robertson et al., 2019; Sabur et al., 2022). Other studies support the prevalence of this P retention mechanism in soil-type media. For example, precipitation of mineral coatings containing phosphate has been found to be the dominant long-term P retention mechanism in soils of drainfields and septic systems (Robertson et al., 2019). Irreversible P sorption in bioretention filter media has also been shown to be enhanced by amendments of fly-ash or water treatment residue that contains high contents of Ca, Al, and Fe (Liu & Davis, 2014; Marvin et al., 2020; Zhang et al., 2018; Zhang et al., 2008).

Hydrolysis of organic P is a potential source of DP exported from bioretention cells (Hurley et al., 2017). However, for the Elm Drive bioretention system, the results do not support a major role for this process (Figure AA10b in Supplementary Materials). Any DOP released to the pore solution is rapidly sequestered by adsorption and subsequently immobilized by slow sorption mechanisms. However, the model simulations suggest that hydrolysis of organic P affects the lability of the accumulated POP and, therefore, the fraction of retained P that is under reactive forms (Figure AA10d in Supplementary Materials). Our findings agree with those of the recent study of Liu et al. (2021) who also report that irreversible sorption is the major SRP retention mechanism in a BRC, while the hydrolysis of organic P is negligible (Liu et al., 2021).

3.5.1.3 Importance of plant uptake

Comparison of model runs with and without plant P uptake illustrates the importance of a vegetative layer as a design component of bioretention cells. Our analyses imply that plant uptake accounts for 21% decrease in the inflowing P load in our study site (Figure 3.7b). Previous laboratory experiments presented in Geronimo et al. (2015) indicated that plants removed

between 2 and 21% of the P input. Our results further show that plant uptake removes 51% of the inflowing SRP (Figure AB8a in Supplementary Materials), that is, somewhat lower than Fowdar et al. (2017) who reported a 64% removal of the SRP inflow by plants. In the latter study, the inflow SRP concentration (~ 3 mg L^{-1}) was significantly higher than the average SRP concentration estimated for the inflow to the Elm Drive bioretention system (0.86 mg L^{-1}). When we ran the model with a 3 mg L^{-1} inflow SRP concentration, the fraction of inflow SRP removed by plants increases to 58%, which is close to that found by Fowdar et al. (2017).

The P removal performance by plants can be expected to vary significantly from one bioretention system to another. First, the uptake is not constant through time but varies with the season and may even be mostly dominated by bursts of activity of mycorrhizal fungi during storm events (Lucas & Greenway, 2011). Second, the importance of plant P uptake likely depends on the plant species selected (Henderson et al., 2007), as well as the maintenance regime (*e.g.*, frequency of pruning and biomass removal). Because detailed information on the vegetation cover in our study case was not available, we opted for a simple mathematical representation (Table 3.4) with the model parameter calibration constrained by values reported in the literature (Barber, 1995; Föhse et al., 1991; Kelly et al., 1992).

According to model results, average annual plant P uptake was 1.4 kg P, or 9.6 g P per m^2. From year to year, the uptake ranges between 1.0 and 1.6 kg yr^{-1}, that is, 6.9 and 11 g m^{-2} yr^{-1}. These values fall towards the high end of the range of annual plant P uptake rates in BRCs found in the literature: 0.02 to 11 g m^{-2} yr^{-1} (Lucas & Greenway, 2008; Turk et al., 2017) because of the relatively high P inflow loading indicated by our model. The typical P content in macrophyte plants in BRCs further ranges from 0.85 to 2.5 mg g^{-1} (Lucas & Greenway, 2008; Rycewicz-Borecki et al., 2017; Schachtman et al., 1998), which yields an annual production between 3.8 and 11.1 kg of plant biomass per m^2 for the Elm Drive bioretention system. For comparison, macrophyte biomass production rates of 0.5 to 10.8 kg m^{-2} yr^{-1} have been reported for treatment wetlands that tend to receive higher P loads (Kadlec & Wallace, 2008). To avoid P stored in plant biomass to be returned to the filter media with litterfall, the vegetation needs to be removed regularly from the bioretention system. Considering typical harvestable amounts of P of standing crops (1

to 5 g P m^{-2}; (Dagenais et al., 2018; Kadlec & Wallace, 2008), biannual plant removal is recommended to delay the saturation of the filter media layer.

3.5.1.4 Inflow TP concentration

Average TP concentrations reported for urban runoff are typically much smaller than the TP inflow concentration of 4.3 mg L^{-1} we obtained from the model calibration (Yang & Lusk, 2018). To verify the credibility of such a high concentration, we decided to collect water samples near the inlet to the bioretention system, as well as ponded water and water extracted from the mulch layer on top of the filter media during a rain event in October 2021 (details on sampling and analytical protocols are given in Method AA5 in Supplementary Materials). The TP concentrations measured near the inlet showed high variability between the first flush (5.4 mg L^{-1} measured on one water sample) and 0.1 mg L^{-1} measured subsequently on two water samples. The ponded water sample exhibited a relatively high TP concentration (2.8 mg L^{-1}), while the SRP concentrations measured on ten water samples extracted from the mulch layer (which can be considered closest to the water entering the filter media layer) were as high as 8.1 mg L^{-1} with a mean concentration of 2.5 mg L^{-1}. Together with the observed TP mass accumulation in the filter media (see Method AA4 in the Supplementary Materials), the measured TP and SRP concentrations are consistent with a high average inflow TP concentration (i.e., 4.3 mg L^{-1}) inferred from fitting the model to the available data. However, further monitoring will be needed to fully characterize the inflow P speciation and concentrations during precipitation events.

A possible reason for the high inflow P concentration is the location of the bioretention system in a fairly dense subdivision and adjacent to a parking lot (Figure AB1). Surface runoff from parking areas can be enriched in P, as shown by Berretta & Sansalone (2011) who reported TP concentrations as high as 6.5 mg L^{-1} and a mean value of 3.5 mg L^{-1}. In addition, our filter media core analyses and model simulations excluded the mulch layer. Thus, the 'TP inflow concentration' in our model corresponds to the influent TP concentration entering the filter media layer, that is, after the inflow water has passed through the mulch layer. Mulch used in BRCs to attenuate soil erosion can exhibit a much higher P sorption capacity than the underlying filter media (Mei et al., 2012a). Our limited event-based field sampling in October 2021 suggests that both high initial runoff P concentrations and P leaching from the mulch layer could

contribute to the elevated TP input concentration inferred for this bioretention system. Thus, attention should be given to the potential impact of P release from the mulch layer on the long-term P retention performance in this and other BRCs. The use of low-P mulch and the regular removal of plant litter are recommended as part of the maintenance plans of bioretention systems.

Even when a much lower inflow TP concentration of 0.37 mg L^{-1} is imposed, the model still predicts a very high removal of the inflow P. The retention of P in the filter media plus plant P uptake then account for 77% of the P input, compared to 79% in the simulations with 4.3 mg L^{-1} TP inflow. The relative importance of plant uptake in the 0.37 mg L^{-1} simulations is much reduced, however (Figure AA9, panels c and d). This is because the much lower porewater DP that often becomes limiting for plant uptake (see Eq T3.4.14). Under the low inflow TP conditions, mineral PIP and stable POP represent 85% of the P accumulation in the filter media. In other words, more of the accumulated P is present in stable (or unreactive) forms.

3.5.2 Bioretention systems: design considerations

The fate and transport model presented here provides a tool to assess the roles of various design components of BRCs in controlling the P runoff reduction performance. As shown here for the Elm Drive bioretention system, the efficient reduction of the P outflow flux is predominantly due to the filter media layer that provides a high capacity for filtration of incoming PP, as well as sufficient sorption sites for DP. To avoid a premature saturation of sorption sites (Qiu et al., 2019), one approach is to add to the filter media Al- and Fe-rich materials that have a high affinity for phosphate ions and can promote transformation of loosely adsorbed P to more stable forms of P (Marvin et al., 2020). However, these amendments can decrease the hydraulic conductivity of the filter media layer (Ament et al., 2021), in turn increasing the risk of overflow during precipitation events. In a similar vein, a fine-grained filter media that increases the filtration capacity (Sansalone & Ma, 2009), may cause clogging and formation of cake layer on top of the filter media layer also resulting in a drop in the hydraulic conductivity (Li & Davis, 2008a, 2008b). The model simulations presented here indicate that the high P runoff reduction capacity of the Elm Drive BRC system reflects a good balance between maintaining a sufficiently high hydraulic conductivity of the filter media layer, and efficient filtration and sorption that immobilizes the

incoming P plus plant uptake. It is worth noting that in addition to the importance of vegetation as P accumulators inferred from the modeling results, plant roots can help to counteract clogging in bioretention cells (Skorobogatov et al., 2020).

A key question regarding the use of BRCs for urban P abatement is how long the filter media can continue to accumulate P, that is, how long before the medium gets "saturated" (Hager et al., 2019; Marvin et al., 2020). Our core data and model results show no evidence that the Elm Drive BRC is approaching saturation after 7 years of operation. They further suggest that most of the dissolved P input to the cell is retained as condensed mineral phases, rather than simply partitioning onto a limited number of sorption sites of the filter medium, as is often assumed in P retention models (Komlos & Traver, 2012; Muerdter et al., 2016). The formation of these mineral phases may confer a very large capacity to accumulate P in the BRC. The long-term P retention performance may therefore be more controlled by processes such as clogging of the filter medium by the particulate load of urban runoff entering the cell than by an actual saturation of the P accumulation capacity (Li & Davis, 2008a). More research on the actual forms under which P is retained in BRCs is recommended, given the importance for implementing effective maintenance practices that extend the life-span of the P retention benefits of BRCs.

The model simulations also highlight the importance of the bedding storage layer in reducing surface runoff (Brown et al., 2013b), which results from the effective exfiltration of water to the underlying native soil. In addition, the modeling suggests that further removal of PP occurs in the bedding storage layer itself. The P immobilization in the filter media layer plus that in the bedding storage layer limits the amount of P that is exfiltrated and, hence, potentially transported by groundwater flow to a downstream water body.

3.5.3 Model limitations

The model reproduces the main features of the observed multi-year P accumulation and the 2019 depth distribution of the P pools in the filter media layer, as well as the event-based outflow P loadings (Figures 3.4, 3.5, 3.6). Nonetheless, further model developments and data acquisition should help resolve uncertainties associated with the assumptions, approximations, and oversimplifications that underpin the current results. One obvious approximation is the time-invariant inflow TP concentration and its fractionation among the different pools. The simulations

also ran with all model parameters remaining constant over time, including reaction and physiological parameters that are known to be temperature dependent. As a result, in its current form, the model does not account for seasonal patterns in P cycling and removal processes, such as plant uptake or POP hydrolysis. One example of model-data discrepancy is the underpredicted outflow under the high-flow conditions of spring snowmelt (such as in April 2015). This likely reflects the simplistic method used to estimate inflow based on a single runoff coefficient (see Table 3.3, Eqs. T3.3.1 to T3.3.6). During the snowmelt period, the lower actual rates of evapotranspiration result in higher runoff than simulated. More sophisticated and accurate rainfall-runoff calculations that more realistically simulate the runoff generation during snowmelt season would help improve the performance of the hydrology and, therefore, the P fate and transport model for the bioretention systems.

The model further does not account for the high variability in TP and SRP concentrations of composite samples observed during low-flow events (see Figure AA5 in Supplementary Materials). Low-flow events showed variable outflow TP and SRP concentrations, including some of the highest values measured, while the higher flow events were associated with relatively low outflow TP and SRP concentrations (Figure AA5). The model simulations most closely reproduced the flow-weighted outflow concentrations for events with TP ≤ 0.1 mg L^{-1} (which represents 70% of the outflow samples) and SRP ≤ 0.07 mg L^{-1} (which represent 80% of the outflow samples), most of which occurred when the total event outflow was larger than 30,000 L. The reason why the model does not capture the high variability in the TP and SRP outflow concentrations during low-flow events could indicate an aspect of the P dynamics in the BRC system that is not represented in the model and will require further investigation. This reduced performance at the lower outflow volumes only had a minor impact on the long-term model-predicted cumulative TP and SRP loads, however. Besides, not all the deviations between measured and modelled P concentrations are necessarily due to the model. Errors associated with sample collection, storage and analysis could also contribute to variations in observed concentrations (Jarvie et al., 2002).

3.5.4 Model future applications

The modeling results highlight the processes and chemical speciation that control the long-term P retention efficiency of the BRC. As such, the results provide new insights into the cell's functioning and generate recommendations for maintenance and monitoring practices. By contrast, many P retention studies rely on concentrations measured in the inflow and outflow. Although these studies quantify the instantaneous P concentration reduction in surface runoff, they yield little information on the fate of the incoming P because the cell is treated as a black box. For the BRC considered here, we conclude that the surface P load reduction is truly due to retention of P in the system and not P leaching to the underlying native soil. Should the latter be the case, the BRC could potentially act as a long-term pathway of P pollution to the regional groundwater system. It is important to note that the efficient trapping of P in the filter media also reflects the cell's raised underdrain and storage bedding layer that prevent the development of anoxic conditions that could cause a release of P from the filter medium back to the pore water, followed by P export from the system.

The P reactive transport modeling approach outlined in our study can be transferred and adapted to fit other bioretention system configurations and hydrological regimes. With appropriate field monitoring data, ideally including in-system P speciation data, the parameters for the hydrologic and P partitioning process calculations could be recalibrated. In the absence of sufficient data, the parameter values and ranges reported here could be used as initial guesses. Model simulations similar to those performed here could then estimate the P loading reduction performance of a given BRC at a range of temporal scales, from a single precipitation event to long-term (i.e., multiple years) operation.

The model also provides a baseline for further model developments and adaptation to other urban settings that, in turn, can enable future data interpretation applications and scenario testing. This latter could include assessing the impacts of hydrological changes accompanying climate warming on the performance of P runoff reduction of BRCs, both at the individual system scale and watershed scale. The detailed, process-based model could also be used to derive simple relationships between the P runoff reduction efficiency and design characteristics of BRCs and

biophysical conditions that could be used to scale up the effects of BRCs on the export of P from entire urban watersheds.

3.6 Conclusions

This study presents a numerical model that simulates the fate and transport of P in a bioretention system located in Ontario, Canada. Unlike existing models, we incorporated a detailed representation of the biogeochemical and exchange processes that control P cycling in various compartments of the system. We further compared model-predicted depth distributions of different P forms (that are, reactive, unreactive organic, mineral and recalcitrant inorganic form) in the filter media layer (i.e., within the particulate P pool) with data obtained from detailed sequential chemical extractions of P. Overall, the results indicate that, over the 7-year study period, the study bioretention system decreased 64% of surface water runoff, principally through groundwater recharge. Moreover, almost all (~98%) of the P input to the system was prevented from entering the outlet, mostly retained in the filter media layer, some in the bedding storage layer, and some within plant biomass. The modeling and sequential extraction data point to mineral (inorganic) P as the largest sink for incoming P. The latter accumulates as a result of filtration of colloidal P and fast adsorption of dissolved P followed by (co-)precipitation of phosphate-containing mineral phases. Extremely high attenuation of P loadings in the system exhibits excellent performance in controlling stormwater runoff and P wash-off from the urban drainage area upstream of our study site.

To a large extent, the system's performance reflects an opportune balance between the filter media layer's P immobilization capacity (via filtration and sorption) and the continuation of favorable hydraulic conductivity that avoids excessive overflow. In addition, sufficient space in the bedding storage layer and regular pruning and harvesting of the vegetative cover are important design and upkeep considerations for the long-term runoff P reduction performance of the system. The model presented in this work is thus potential to be a predictive tool for bioretention cells system design and performance evaluation under certain P reduction targets. The mass balance calculations and sensitivity analyses further imply that the system's runoff and P reduction efficiencies are lower during wet years or when more of the yearly precipitation occurs as intensive events. Because the latter are becoming more frequent with ongoing climate

change, future applications of the modeling approach presented here could include simulations of surface flow and P runoff reduction under regional climate projections.

Chapter 4

How efficient are bioretention cells in controlling phosphorus and nitrogen enrichment of urban stormwater? Insights from the International Stormwater Best Management Practice Database

This chapter is modified from:

Zhou, B., Parsons, C. T., Shafii, M., Rezanezhad, F., Passeport, E., & Van Cappellen, P. (2023) How efficient are bioretention cells in controlling phosphorus and nitrogen enrichment of urban stormwater? Insights from the International Stormwater Best Management Practice Database. Under review.

4.1 Summary

Bioretention cells (BRCs) are a common technology to reduce stormwater runoff volumes and peak flows. They have also been proposed as a best management practice (BMP) to control the export of contaminants from urban landscapes, including the macronutrients phosphorus (P) and nitrogen (N). We extracted hydrologic and nutrient concentration data for over 400 precipitation events across more than 30 BRCs from the International Stormwater BMP Database. The concentration data included total P (TP), soluble reactive P (SRP), total N (TN), and dissolved inorganic N (DIN). The concentrations of TP and SRP were on average higher in the surface outflows compared to the inflows. However, the corresponding outflow loads of TP and SRP, were generally lower, mainly because of reductions to surface runoff volumes. By contrast, on average BRCs exhibited slightly lower outflow TN concentrations while DIN concentrations were similar between outflow and inflow. Hence, because they are generally more efficient in reducing N than P loads, BRCs tended to decrease the TN:TP and DIN:SRP ratios of stormwater runoff, potentially altering nutrient limitation patterns in receiving aquatic ecosystems. Changes to P and N speciation were also prevalent, with BRCs typically increasing the SRP:TP and (NO_3^-+NO_2^-):NH_4^+ ratios. Random forest modeling identified inflow concentrations and BRC age as key variables modulating the changes in TP, SRP, and TN concentrations between inflow and outflow. For DIN, the BRC's storage volume and drainage area also emerged as an important explanatory variable. Overall, our findings imply that the impacts of BRCs on the P and N concentrations, speciation, and loads of urban runoff are highly variable. Although the P and N loads in surface runoff are usually reduced by BRCs, the implications for downstream nutrient limitation and potential groundwater quality deterioration deserve further attention.

4.2 Introduction

Urbanization increases the imperviousness of land cover which, in turn, may enhance efflux of suspended solids, heavy metals, organic contaminants, and nutrients to receiving water bodies (Valtanen et al., 2014). Conveyance of phosphorus (P) and nitrogen (N) by urban stormwater can exacerbate eutrophication of aquatic ecosystems (Schindler, 1974; Schindler et al., 2016). The export of soluble reactive P (SRP) and that of dissolved inorganic N (DIN = nitrate-N + nitrite-N + ammonium-N) are of particular concern because these are the chemical forms of P and N that

are most readily utilised by algae and aquatic plants (Camargo & Alonso, 2006; Orihel et al., 2017). Therefore, interest in implementing stormwater best management practices (BMPs) to control P and N release from urban landscapes is growing.

Bioretention cells (BRCs) are a common BMP that not only helps attenuate stormwater runoff through subsurface infiltration but may also protect receiving surface water bodies against excess nutrient loading. For instance, BRCs have been reported to remove P associated with suspended matter by filtration (Berretta & Sansalone, 2012; Liu & Davis, 2014) and to reduce dissolved P loads by sorption to the filter medium (Hsieh et al., 2007; Sansalone & Ma, 2009), microbial activity (Poor et al., 2018; Taylor et al., 2018), and root uptake (Fowdar et al., 2017; Lucas & Greenway, 2008). Similarly, BRCs may reduce N loading through filtration, nitrification, and denitrification (Geronimo et al., 2015; Goh et al., 2019; Luo et al., 2020).

Nonetheless, the performance of BRCs as a P and N control BMP is highly variable, especially when considering the most bioavailable nutrient fractions (Ding et al., 2019; Goh et al., 2019; Marvin et al., 2020). Among stormwater BMPs, BRCs exhibit the most widely ranging differences in P concentration between inflow and surface outflow (Jefferson et al., 2017). Additionally, the effects of BRCs on P and N concentrations and loads tend to show significant seasonal trends (Brown et al., 2013a; Goor et al., 2021; Passeport et al., 2009). While BRCs are often assumed to remove P and N from stormwater runoff, several studies have reported increased P and N outflow concentrations, in particular for SRP and DIN (Brown et al., 2013a; Hager et al., 2019; Jefferson et al., 2017; Shrestha et al., 2018; Tirpak et al., 2021; Valenca et al., 2021). Factors purportedly contributing to nutrient enrichment of the outflow include: (i) surface application of fertilizers and compost (Hurley et al., 2017; Mullane et al., 2015; Tirpak et al., 2021), (ii) saturation of sorption sites of the filter media (or soil) as the BRC ages (Hsieh et al., 2007; Koch et al., 2014), and (iii) variations in external factors, such as watershed (*e.g.,* imperviousness) and climatic characteristics (*e.g.,* precipitation) that influence P and N fate and transport in BRCs (Goh et al., 2019; Kratky et al., 2017; Schroer et al., 2018; Shrestha et al., 2018).

In this study, multi-year monitoring data on BRCs were extracted from the International Stormwater BMP Database (ISBD), an open-access online database (Clary et al., 2020). In contrast to previous work, we assessed the effects of BRCs on P and N loads in addition to concentrations.

We aimed to answer the following questions: 1) Are BRCs an effective BMP to reduce eutrophication risks caused by excess of P and N concentrations and loads in urban stormwater runoff? and 2) Which factors affect the changes in P and N concentrations between inflow and outflow of BRCs?

4.3 Methodology

4.3.1 Data extraction and treatment

The ISBD comprises precipitation, discharge, and water quality data (recorded as event mean concentrations, or EMCs) collected from 1999 to 2021 for BRCs (labelled as 'bioretention' for BMP categories) located primarily in the continental USA. The dataset further provides information on the upstream watersheds of the BRCs, including the drainage area (Clary et al., 2011) and the average climate conditions based on long-term (> 50 years) historical records (Driscoll et al., 1989). We extracted discharge data plus EMCs of total P (TP), total N (TN), soluble reactive P (SRP), ammonium-N (NH_4^+-N), nitrate-N (NO_3^--N), and nitrite-N (NO_2^--N). The analytical methods are summarized in Table AB1 of the Supplementary Materials. For concentrations below the detection limit (approximately 6% of the data), we assigned a value equal to the detection limit. The inflow and outflow concentrations were then paired with discharge data to estimate event-integrated (*i.e.,* total mass) loads. We further calculated the DIN (NH_4^+-N + NO_3^--N + NO_2^--N), non-reactive P (NRP = TP – SRP), and non-reactive N (NRN = TN – DIN) EMCs, as well as the event mean SRP:TP, DIN:TN, (NO_3^- + NO_2^-):NH_4^+, TN:TP, and DIN:SRP molar ratios. In addition to long-term (average) climate conditions at each site, we included the mean monthly temperatures to assess seasonal trends.

4.3.2 Reduction and enrichments factors

Because of high variability in the relative effects among BRCs and flow events on the various water quality and flow parameters considered, reduction and enrichment factors (*REFs*) were calculated for each event, as:

$$REF = \begin{cases} \frac{\mathrm{IN}-\mathrm{OUT}}{\mathrm{IN}}, & if\ \mathrm{IN} > \mathrm{OUT} \\ \frac{\mathrm{OUT}-\mathrm{IN}}{\mathrm{OUT}}, & if\ \mathrm{OUT} > \mathrm{IN} \end{cases} \qquad \textbf{(Equation 4.1)}$$

where IN and OUT apply to the inflow and outflow values for any given EMC, total event flow volume, event-integrated load, or event mean molar ratio. Events for which IN > OUT imply a reduction of the parameter value considered while, conversely, when OUT > IN the parameter is higher or "enriched" in the surface outflow of the BRC. The *REF* values range between 0 and 1 for both reduction and enrichment. To minimize the impact of outliers, the Wilcoxon signed-rank analysis (Walpole et al., 1993) was used to test for differences between inflow and outflow parameter values.

We also report the percentages of BRCs that, on average, exhibit a reduction or enrichment of the water quality variables considered. For a concentration or molar ratio, a BRC's average REF value was calculated as the arithmetic mean of all event *REFs* for that site, while a BRC's average load *REF* was calculated with Equation 4.1 using the total inflow and outflow loads summed over all the events. For sites with data for more than 5 events, the Mann-Kendall test (Helsel & Hirsch, 1992) was used to evaluate temporal changes to P and N concentration and loading *REFs*. However, because most BRCs were monitored for less than 2 years (Figure AB1 in supplementary materials) very few significant temporal trends were detected (Table AB2) and, hence, not further considered here.

4.3.3 Machine learning

Random forest regressions were used to determine to what extent the potential explanatory variables listed in Table 4.1 can account for the observed variability in the *REF* values of TP, TN, SRP, and DIN concentrations. We used the 'randomForest' package in *R* (RColorBrewer & Liaw, 2018). The algorithms were trained on 80% of the data and three separate 10-fold validations were carried out to identify the best model. The remaining 20% of data were used to evaluate predictive accuracy. Goodness of fit between predicted and observed *REFs* was evaluated with the Nash-Sutcliffe efficiency (NSE) (Legates & McCabe, 1999). The importance of each explanatory variable was quantified by the permutation feature importance method using the 'permimp' package in R (Debeer et al., 2021) and expressed as a percentage. Partial dependence analyses were carried out with the 'pdp' package in *R* (Greenwell, 2017) to analyze the impact of each explanatory variable on the *REFs* except land use (because it is a categorical variable).

Table 4.1: Explanatory variables included in the random forest regression analysis of the concentration reduction and enrichment factors (*REFs*).

Abbreviation	Description
Bioretention cell characteristics	
V_BMP:DA	Ratio of the bioretention cell (BRC) storage volume (filter media volume + ponding volume) to the drainage area of the BRC (units: m)
Age	BRC age at a given inflow event (units: years), calculated as the difference between event record date and the BRC's start of service date
Watershed characteristics	
IN_Conc	Influent concentration for a given event (units: mg L^{-1})
Imperv	Imperviousness of watershed (units: %)
LandUse	Land use type of watershed; categories included are "Institutional", "Residential", "Transportation", "Industrial", "Commercial", "Undeveloped", plus the mix of any two of aforementioned types, e.g., "Commercial & Undeveloped"
Site-specific average climate conditions	
P_Depth_SA	Average annual total precipitation depth (units: cm)
P_Intensity_SA	Average precipitation intensity (units: cm hr^{-1})
ADP_SA	Average inter-event dry duration (units: hour)
Event-specific climate characteristics	
Month	Month of event date
Temp	Monthly average air temperature for the month during which the event occurred (units: °C)

4.4 Results

4.4.1 Nutrient concentrations, ratios, and loads

The event-based inflow and outflow concentrations and loads of the different P and N chemical pools extracted from ISBD are compared in Figure 4.1; the molar ratios are shown in Figure 4.2. While the mean outflow concentrations of TN and DIN usually remained close to their respective mean inflow values, the mean concentrations of TP and SRP concentrations were markedly higher in the outflow than the inflow (Figure 4.1a). Only 40% and 18% of the individual events recorded showed a reduction in the outflow TP and SRP concentrations, respectively (Figure 4.3a and Table 4.2). On average, 73% and 89% of the BRC sites were found to enrich the TP and SRP outflow concentrations (Figure 4.3c and Table 4.2). By contrast, on average 60% and 48% of BRCs reduced the outflow TN and DIN concentrations, respectively (Figure 4.3c and Table 4.2).

The above concentration changes translated into a generally higher contribution of SRP to TP in the outflow (mean SRP:TP of 0.65) relative to the inflow (mean SRP:TP of 0.27). By contrast, although most events (79%) and BRCs (88%) exhibited an enrichment of the (NO_3^-+ NO_2^-):NH_4^+ ratio (Figures 4.3b, 4.3c and AB2 and Table 4.2), the mean DIN:TN ratios of inflow and outflow were similar (0.45 and 0.46, Figure 4.2). As a result, for most events the TN:TP and DIN:SRP ratios decreased between inflow and outflow.

The P and N loads showed distinctly different trends than the corresponding concentrations (Figures 4.1 and 4.3). Overall, most BRCs experienced reductions in their outflow SRP, TP, DIN, and TN loads (67% for SRP, 72% for TP, 83% for DIN, 95% for TN; Table 4.3). This was mainly due to the general decrease in the outflow volumetric flow relative to the inflow (Figure AB3).

4.4.2 Seasonality

The seasonality of TP and TN EMCs and the corresponding *REFs* are shown in Figure 4.4. Both TP and TN EMCs tended to be the highest in the summer. Enrichment of outflow TP was also more likely in the summer and extending into fall (June to October). The seasonal trends of the DIN concentration and *REF* were similar to those of TN (Figure AB4). For SRP, the seasonal patterns were more complicated than for TP (Figure AB4), with enrichment dominating across the entire year, including during the winter (December to March).

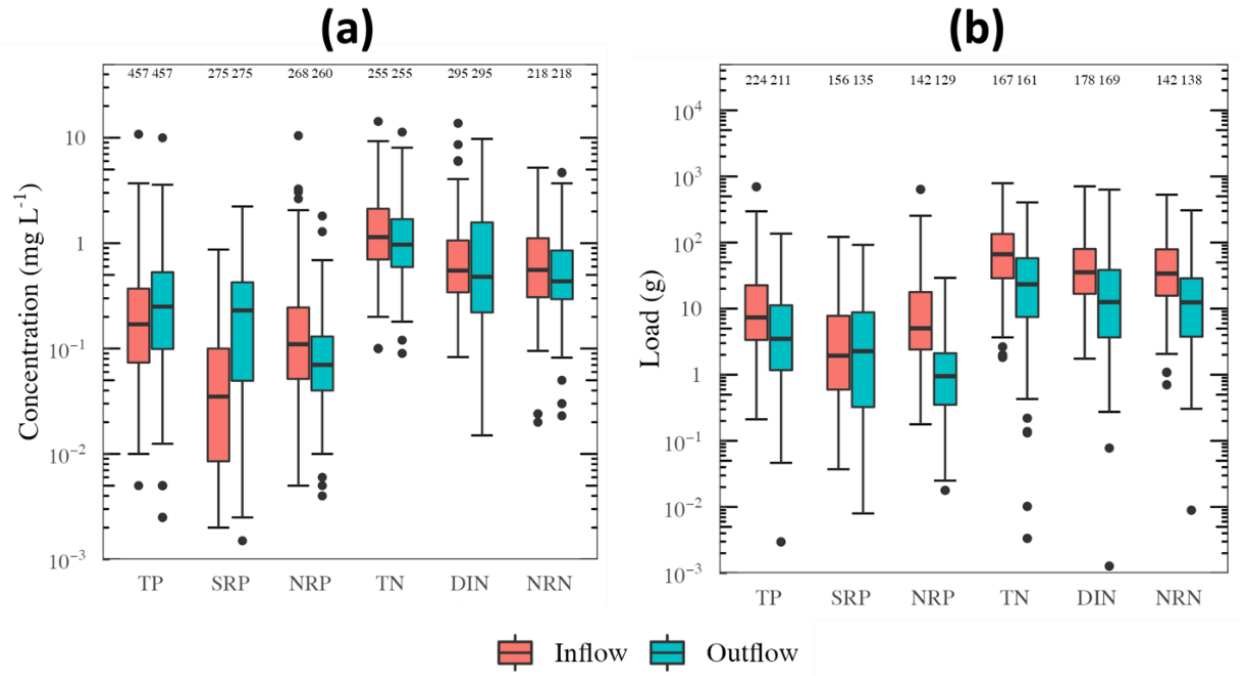

Figure 4.1: Boxplots of inflow and outflow concentrations (**a**) and loads (**b**) of TP, SRP, NRP, TN, DIN, and NRN. The number of data points included for each variable is shown on top of the plot. Note that some events did not generate any outflow; in these cases, the outflow loads were 0. Because we used a logarithmic scale, zero values were excluded from plot (**b**).

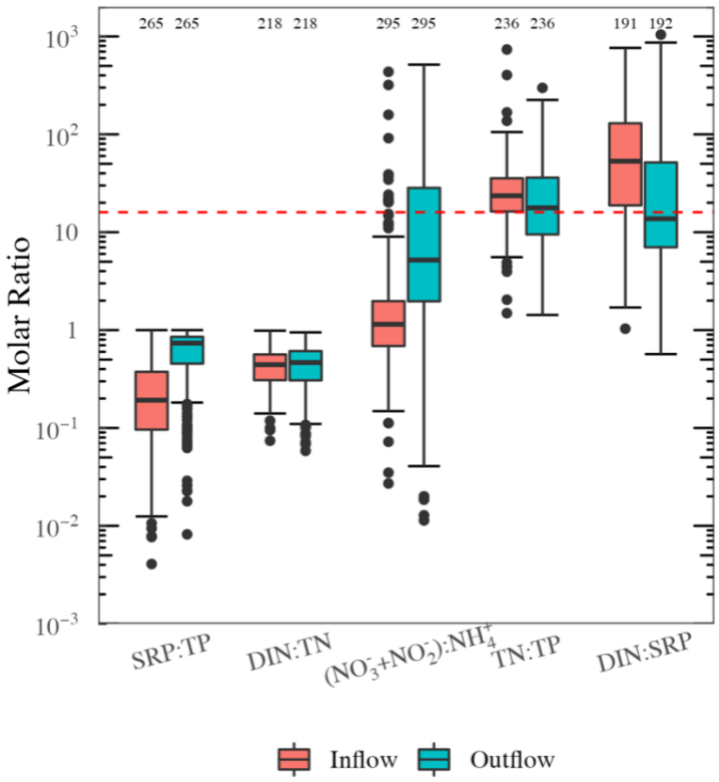

Figure 4.2: Boxplot of inflow and outflow molar ratios for SRP:TP, DIN:TN, $(NO_3^-+ NO_2^-):NH_4^+$, TN:TP, and DIN:SRP. The dashed horizontal line corresponds to the average N:P molar ratio of 16 in algal biomass (the so-called Redfield ratio). The number of data points included for each ratio is shown on top of the plot.

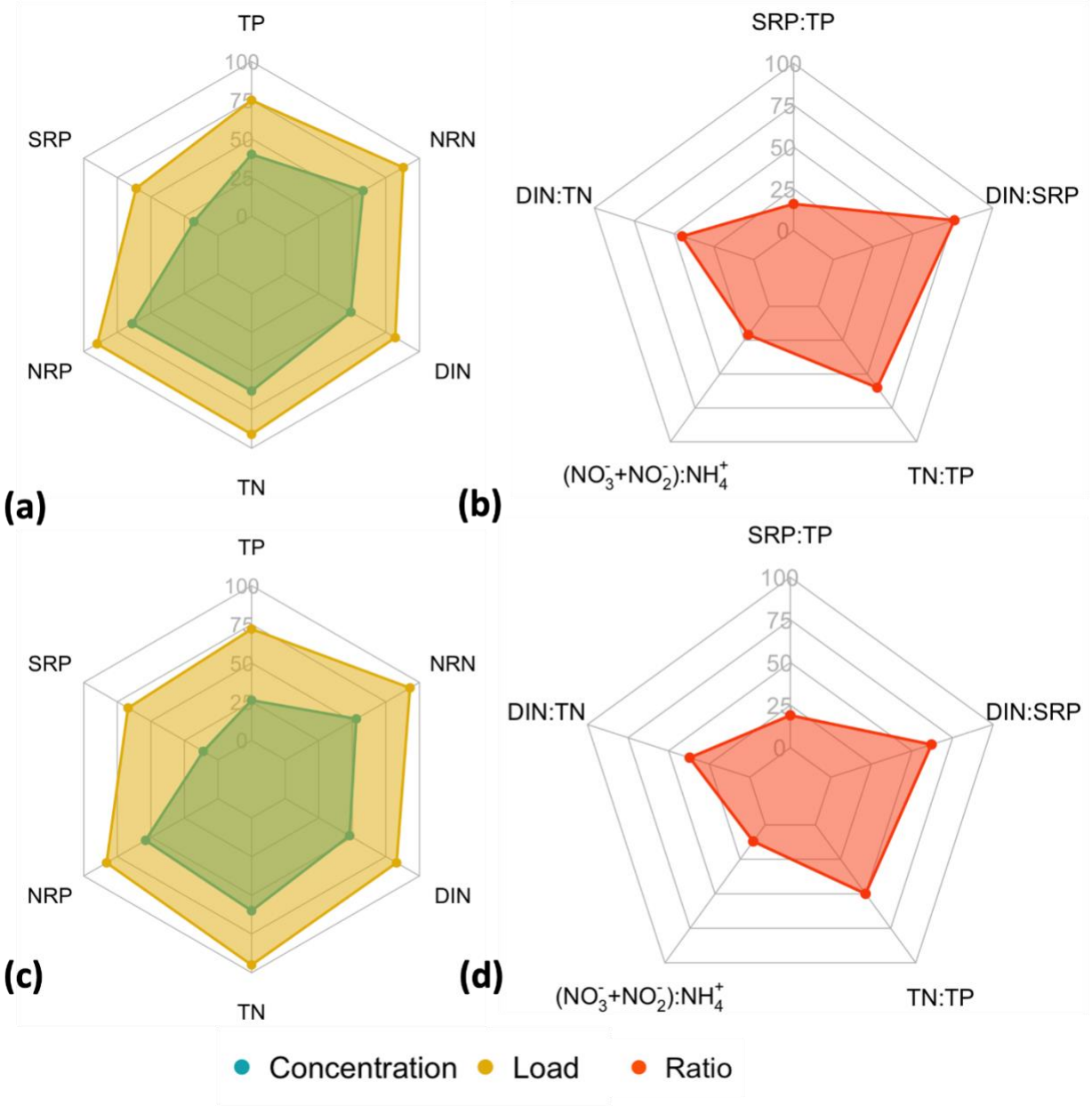

Figure 4.3: Radar charts for the percentages of inflow events (**a** and **b**) and bioretention cells (BRCs, **c** and **d**) that exhibit reduction in concentrations (blue) and loads (yellow) for TP, SRP, NRP, TN, DIN, and NRN (**a** and **c**) and in molar ratios (red) for SRP:TP, DIN:TN, $(NO_3^- + NO_2^-):NH_4^+$, TN:TP, and DIN:SRP (**b** and **d**). Percentage ranges from 0 to 100%. Note that when the percentage is less than 50% for events or BRCs then, on average, the corresponding concentration or load increases between inflow and surface outflow (*i.e.*, enrichment).

Table 4.2: Statistics for inflow and outflow concentrations and molar ratios. *REF* = reduction or enrichment factor.

Water Quality Parameter	Event-scale results			Total site number and % of sites that exhibit reduction
	Total event number and % of events that exhibit reduction	Wilcoxon p-value*	Median REF	
TP	467 (40%)	2.2×10^{-9}	0.25 (Enrichment)	39 (26%)
SRP	286 (18%)	1.5×10^{-29}	0.77 (Enrichment)	27 (11%)
NRP	276 (64%)	1.6×10^{-6}	0.33 (Reduction)	26 (54%)
TN	261 (63%)	1.2×10^{-3}	0.21 (Reduction)	25 (60%)
DIN	306 (49%)	**0.10**	0.04 (Reduction)	25 (48%)
NRN	229 (58%)	0.013	0.17 (Reduction)	19 (53%)
SRP:TP	275 (16%)	6.0×10^{-36}	0.67 (Enrichment)	26 (19%)
DIN:TN	229 (45%)	**0.28**	0.06 (Enrichment)	19 (37%)
$(NO_3^-+NO_2^-):NH_4^+$	306 (21%)	1.3×10^{-25}	0.75 (Enrichment)	25 (12%)
TN:TP	246 (60%)	0.042	0.17 (Reduction)	26 (50%)
DIN:SRP	204 (76%)	7.6×10^{-14}	0.57 (Reduction)	21 (62%)

p* value of Wilcoxon Signed-Rank test by comparing inflow and outflow values. Difference between inflow and outflow values can be considered as statistically significant if *p* value is smaller than 0.05. *p* values that are higher than 0.05 are highlighted in **bold.

Table 4.3: Statistics for inflow and outflow loads.

Water Quality Parameter	Event-scale results			Total site number and % of sites that exhibit reduction
	Total event number and % of events that exhibit reduction	Wilcoxon *p*-value*	Median REF	
TP	225 (75%)	3.0×10^{-14}	0.63 (Reduction)	25 (72%)
SRP	163 (61%)	**0.057**	0.42 (Reduction)	18 (67%)
NRP	146 (90%)	7.4×10^{-20}	0.85 (Reduction)	17 (83%)
TN	160 (91%)	2.6×10^{-22}	0.68 (Reduction)	19 (95%)
DIN	175 (82%)	3.4×10^{-15}	0.67 (Reduction)	18 (83%)
NRN	139 (88%)	6.0×10^{-19}	0.70 (Reduction)	14 (93%)

p* value of Wilcoxon Signed-Rank test by comparing inflow and outflow values. Difference between inflow and outflow values can be considered as statistically significant if *p* value is smaller than 0.05. *p* values that are higher than 0.05 are highlighted in **bold.

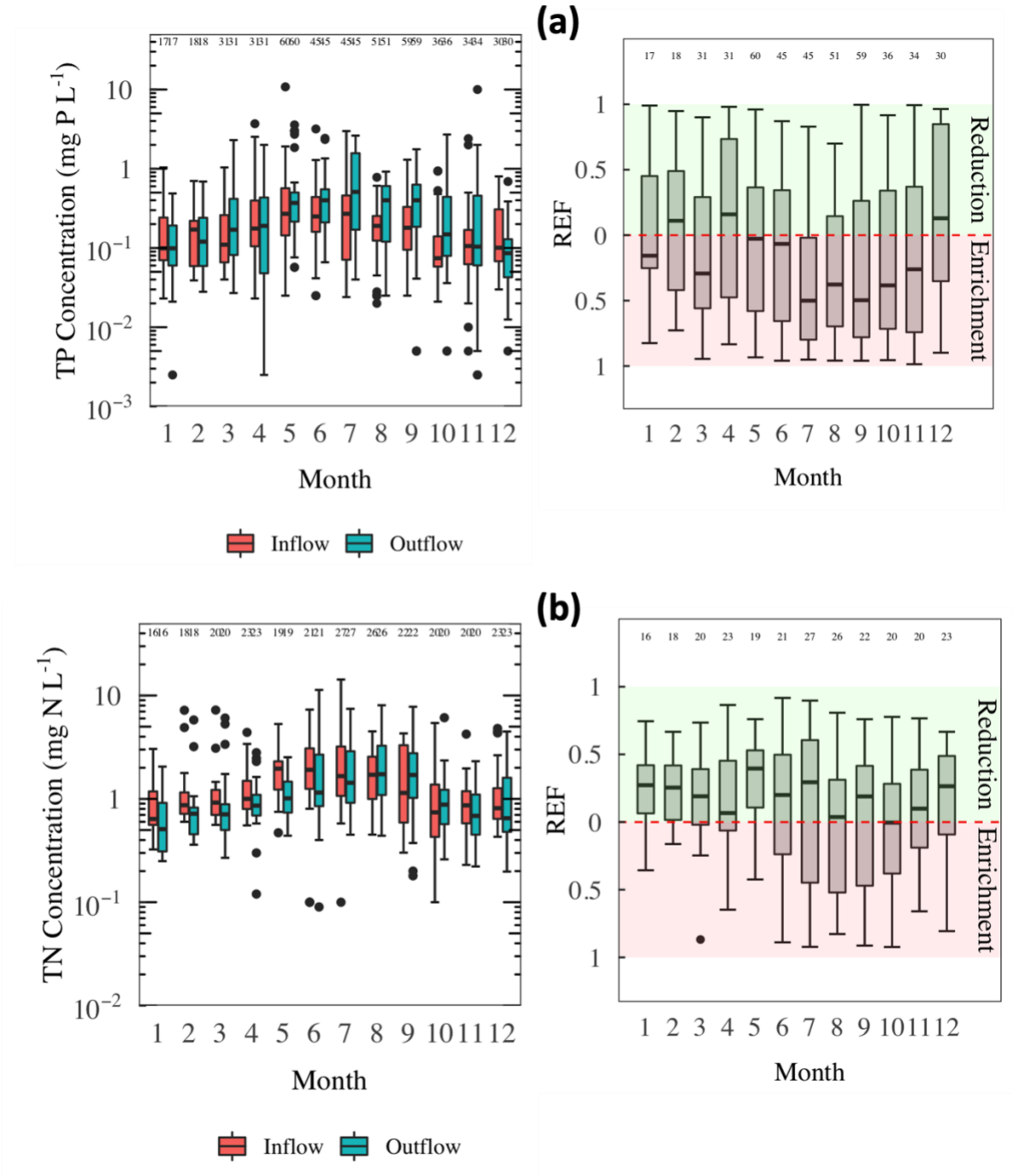

Figure 4.4: Boxplot of inflow and outflow concentrations of TP and TN (data from all available sites) in different months (left panels of **a** and **b**), and the corresponding reduction or enrichment factors (REFs) for the same parameters (right panels of **a** and **b**). Month 1 is January and Month 12 is December. Dashed line in the right panels shows the zero value, that is, no reduction or enrichment. The number of data points included for each variable is shown on top of the plot.

4.4.3 Random forest regressions

The random forest predictions yielded the highest simulation accuracy for SRP (NSE = 0.71) and the lowest accuracy for DIN (NSE = 0.45) (Figure 4.5). The inflow concentrations emerged as the most important predictive variable for the *REFs* of TP, TN, SRP, and DIN concentrations (Figure 4.6), followed by the age of the BRC, except for DIN where the ratio between the BRC storage volume and drainage area played a slightly more important role than age. Variables related to annually averaged climate characteristics (see Table 4.1) were less important than those related to seasonal climate variability (*i.e.*, month of the year and monthly average temperature), except for the TP concentrations whose *REF* appeared to be more sensitive to the average annual precipitation depth and intensity. Factors related to climate conditions played relatively more important roles for the EMCs of TP and TN than for their most bioavailable fractions, that is, SRP and DIN.

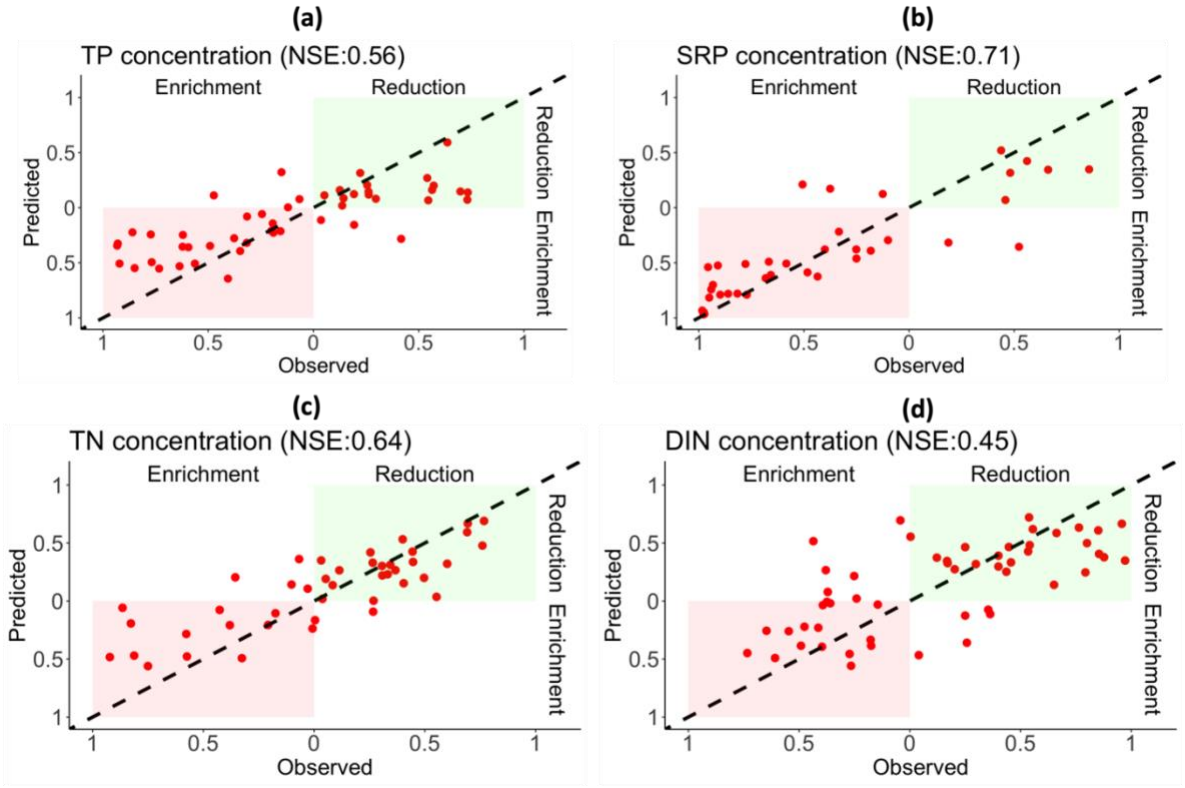

Figure 4.5: Random forest regressions. Event-based predicted vs. observed reduction and enrichment factors (REF) for TP (**a**), SRP (**b**), TN (**c**), and DIN (**d**). Green shading corresponds to reduction of the corresponding concentration, red shading to enrichment. NSE stands for the Nash-Sutcliffe efficiency.

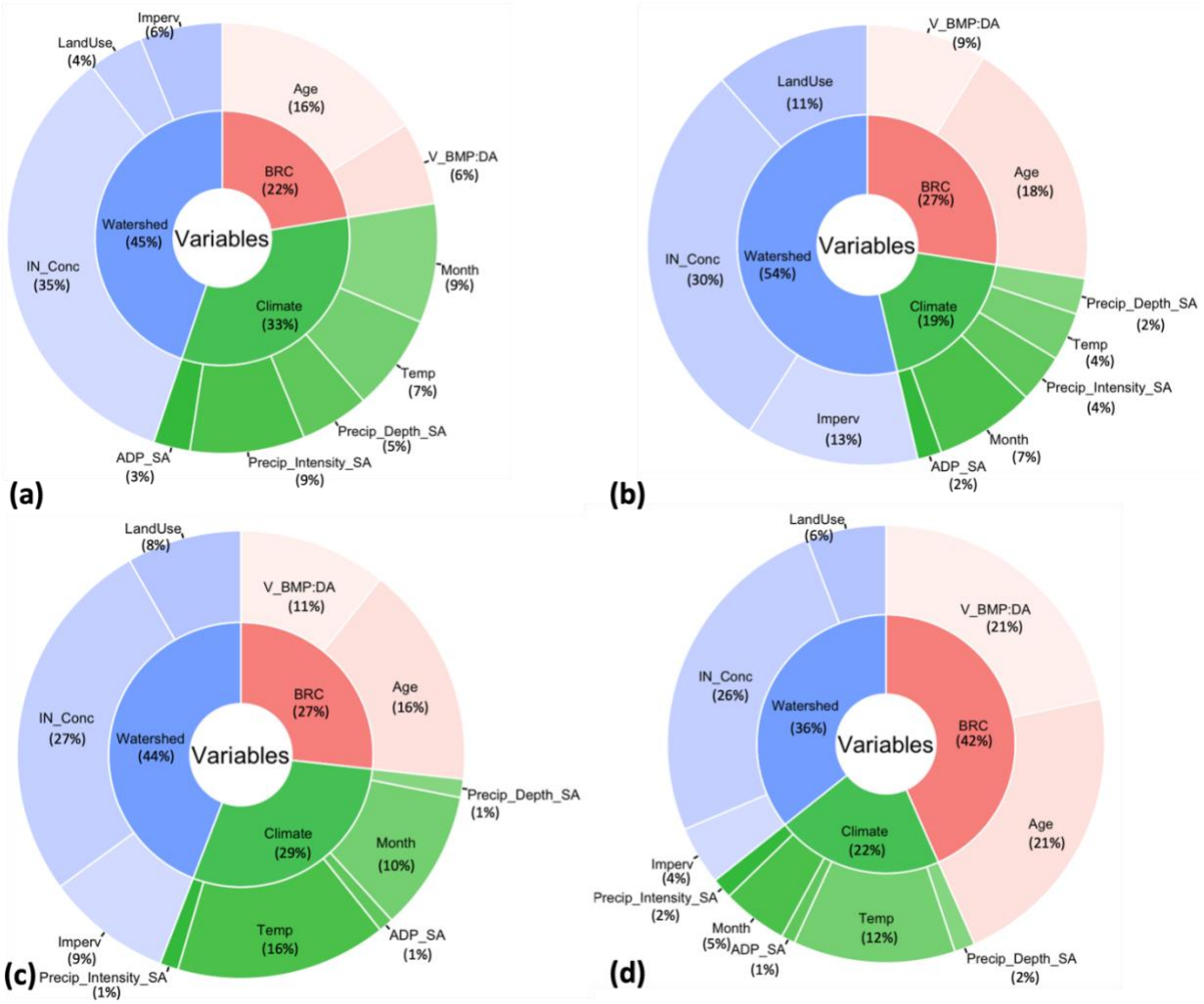

Figure 4.6: Relative importance of the explanatory variables included in the random forest regressions of the concentration reduction and enrichment factors ($REFs$) of TP (**a**), SRP (**b**), TN (**c**) and DIN (**d**). Table 4.1 identifies the variables and their categories (blue = watershed, green = climate, red = bioretention cell (BRC)).

4.4.4 Partial dependence plots

Partial dependence plots (PDPs) for the *REFs* of TP, SRP, TN, and DIN EMCs are shown in Figure 4.7 and Figures AB5 to AB7 in supplementary materials. In the PDPs, positive and negative values indicate reduction and enrichment of the corresponding EMCs, respectively. The PDPs for TP, TN, and DIN exhibited minimal values during the summer months and negative trends with temperature. By contrast, SRP enrichment appeared to be enhanced at lower temperatures. Wetter conditions (*i.e.,* higher precipitation depth and intensity plus shorter inter-event dry periods) favored the reduction of the TN and DIN concentrations while also lowering the enrichment of TP and SRP. Lower (higher) inflow concentrations generally promoted enrichment (reduction) of the outflow concentrations. Aging of BRCs enhanced the reduction performance for TN but had the opposite effect for DIN. The PDPs all showed a sharp drop when imperviousness of the watershed crossed a threshold, with the lowest threshold of around 50% observed for the TP concentrations.

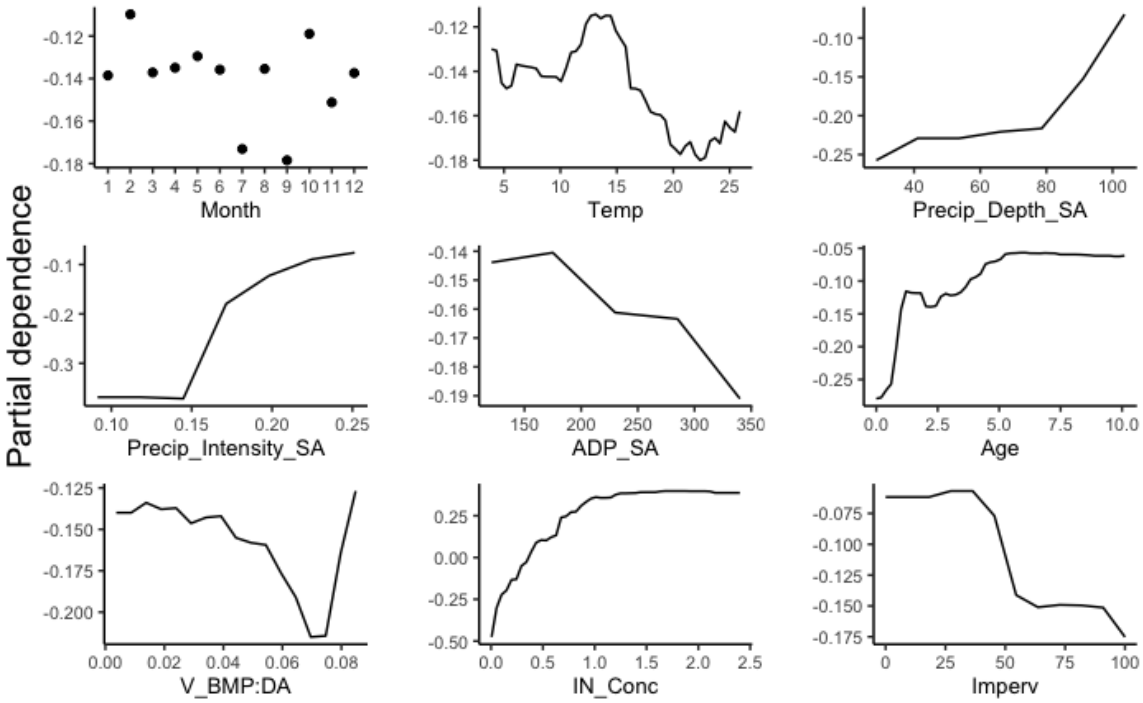

Figure 4.7: Partial dependence plots for the explanatory variables included in the random forest modeling for the TP concentration reduction and enrichment factors (REFs) – see Table 4.1 for the identification of the variables and their categories. Note that positive values on the panels correspond to TP outflow concentration reduction while negative values represent TP outflow concentration enrichment.

4.5 Discussion

Do BRCs reduce P and N in urban runoff? Answers to this question depend on which nutrient element (P or N), what chemical forms (speciation), and whether concentrations or loadings are considered. The data extracted from the ISBD further indicate that the effects of BRCs on the EMCs and runoff loads of P and N are highly variable. The following sections therefore focus on the general trends emerging from our data analyses.

4.5.1 SRP and DIN concentrations and loads

The majority of BRCs included in our analyses exhibited enrichment of the TP and SRP concentrations in their outflow (see section *4.4.1*). By contrast, enrichment of the outflow DIN EMC occurred almost as frequently as reduction. Increases in the concentrations of SRP and DIN have previously been attributed to leaching from fertilizer or mulch applied to BRCs to support vegetation growth (Hurley et al., 2017; Mullane et al., 2015; Tirpak et al., 2021). Enhanced leaching of dissolved P and N, as well as export of particulate-associated P and N, has also been observed immediately after construction of a BRC (Dietz & Clausen, 2005). This may reflect leaching from materials used in the construction of a BRC, especially when plants and their root systems have not fully matured. One would then expect the occurrence and magnitude of SRP and DIN enrichment to diminish over time as the sources in the filter medium and mulch layer are gradually depleted and uptake by plant roots gains in importance (Dietz & Clausen, 2005).

Biogeochemical transformations within BRCs can also cause changes in the SRP and DIN EMCs between inflow and outflow (Ding et al., 2019; Zhou et al., 2023). For instance, SRP and DIN can be generated by the decomposition of dissolved and particulate organic matter entering the BRC. Desorption of phosphate from inorganic particulate matter can also be a source of SRP, while denitrification can have the opposite effect on DIN. Further process-based studies are recommended to fully unravel the biogeochemical reaction networks within BRCs and their role in modulating the *REF* values of SRP and DIN concentrations.

Based on the comparison of inflow and outflow P and N concentrations, some authors have argued that BRCs generally act as nutrient sources (Tirpak et al., 2021; Valenca et al., 2021; Weiss et al., 2008). Such a view, however, ignores the impact of BRCs on P and N loads. Because

BRCs usually efficiently reduce surface runoff volumes (Figure AB3) they can offset concentration enrichments. As a result, BRCs on average reduce surface runoff loads of TP, NP, TN, NRN and DIN (Figure 4.1b). Nonetheless, a relatively large proportion of BRC sites (33%) still shows enrichment of both SRP concentrations and SRP loads. This is concerning given the role of SRP as the primary driver of algal blooms in many freshwater bodies (Baker et al., 2014; Mohamed et al., 2019; Schindler, 1974; Schindler et al., 2016).

Phosphorus load reduction is a common approach to protect receiving lakes from the impacts of eutrophication (Bocaniov et al., 2023; Environment and Climate Change Canada & Ontario Ministry of the Environment and Climate Change, 2018). For example, designating total maximum daily loads (TMDL) that a water body can receive is a federally mandated nutrient control criterium for impaired waters in the United States (Jarvie et al., 2013). In severely impacted aquatic ecosystems, however, controlling nutrient concentrations may be critical for the protection of aquatic life (Canadian Council of Ministers of the Environment, 2007). Therefore, given that BRCs typically increase SRP concentrations they may not be suitable in locations where abatement of P concentrations in receiving water courses is the primary goal.

4.5.2 Potential impacts on groundwater quality

Perhaps the largest knowledge gap identified through our analyses is the ultimate fate of P and N removed from surface flows. While BRCs overall tend to reduce the surface runoff loads of TP and TN, the extents to which P and N are retained within the cells, emitted to the atmosphere (for N), or exported to the underlying native soil and shallow groundwater remains largely undetermined. In other words, few complete P and N mass balances have been developed for BRCs. Such mass balances are best informed by time series data on P and N concentrations and speciation for inflow, outflow, atmospheric deposition, and filter media, plus estimates of mass removal with harvested vegetation and soil-atmosphere exchanges (for N). Such data sets, however, are currently very scarce (for an exception, see Zhou et al. (2023)).

Exfiltration from BRCs is rarely directly measured but can be deduced from the system's water balance based on known or estimated inflow, outflow, and evapotranspiration (Zhou et al., 2023). Except in arid climates, evapotranspiration is typically a small component of the water budget and, hence, surface flow reductions are mostly due to exfiltration to the underlying soil.

It is also reasonable to assume, based on most BRC designs, that the nutrient concentrations in exfiltrating water are close to those measured in the outflowing surface water (Zhou et al., 2023). Thus, in most cases for TP and SRP, and half the cases for DIN, the exfiltrating concentrations would be higher than the inflow concentrations.

Nitrate is a pollutant of concern in groundwater due to its high solubility and negative impact on public health (World Health Organization, 2008), while SRP in discharging groundwater can impact the water quality of connected surface water bodies (Roy & Bickerton, 2014). Thus, given the growing implementation of BRCs in urban areas, research into the possible nutrient enrichment of shallow aquifers and downstream surface water bodies caused by enhanced groundwater recharge via BRCs should be prioritized (Jefferson et al., 2017). This is especially true at locations with shallow water tables and permeable soils where the transfer of solutes from BRCs to groundwater is facilitated (Zhang & Chui, 2017).

4.5.3 Potential impacts on nutrient limitation

Our results clearly show that BRCs have divergent impacts on surface runoff P and N concentrations, speciation, and loads. On average, the outflow TN:TP and DIN:SRP ratios are lower than their inflow counterparts. Thus, BRCs promote the transition of urban runoff from P to N stoichiometric limitation of algal growth. The shift is more pronounced for DIN:SRP than TN:TP because of the greater increase in the SRP:TP ratio compared to the DIN:TN ratio (Figure 4.2). That is, BRCs tend to increase the more bioavailable fraction of TP to a greater extent than that of TN. While the importance of controlling N loads compared to P loads to mitigate eutrophication of freshwater ecosystems remains contentious (Hellweger et al., 2022; Paerl et al., 2016, 2020; Schindler et al., 2016), decreases in molar N:P ratios below the canonical Redfield value of 16 have been associated with undesirable ecological consequences, including the emergence cyanobacterial dominance (Schindler et al. (2016) and references therein) and toxin production (Orihel et al., 2012).

Several factors may contribute to the dissimilar effects of BRCs on the DIN:TN and SRP:TP ratios. These include differences in the nature of inflowing N and P in urban stormwater runoff. A large fraction of P carried by urban storm water runoff typically occurs in the NRP fraction that, in turn, is mostly associated with suspended matter (Yang & Toor, 2018). Filtration of the latter

then effectively retains NRP in the BRC where it accumulates (Li & Davis, 2008; Zhou et al., 2023). By contrast, a large fraction of TN in stormwater runoff is usually under the form of DIN (Figure 4.2). Furthermore, much of inflowing non-reactive (NRN) tends to occur in dissolved form, such as dissolved organic-N (Lusk et al., 2020; Troitsky et al., 2019). Hence, filtration is not as effective for N as for P (Li & Davis, 2014).

Various geochemical and biological processes within BRCs can eliminate SRP and DIN from inflowing surface runoff, including ion exchange reactions, mineral precipitation, plus assimilation by plants, fungi, and bacteria (Hsieh et al., 2007; Poor et al., 2018; Sansalone & Ma, 2009; Skorobogatov et al., 2020; Taylor et al., 2018). From the information available in ISBD, it is not possible to evaluate the relative importance of these removal mechanisms. However, one critical difference between P and N is the importance of gaseous species in the biogeochemical cycling of N, but not of P (Wang et al., 2015). Denitrification and, to a lesser extent, nitrification may cause the permanent removal of DIN to the atmosphere (Austin et al., 2004; Li & Davis, 2014). In summary, the observed changes in N:P ratios imparted by BRCs carry the signatures of the large differences in the biogeochemistry of the two nutrient elements.

Also noteworthy is the observation that BRCs typically reduce the NH_4^+ concentration but enrich the NO_3^-+NO_2^- concentration (Figure AB2), hence increasing the (NO_3^-+NO_2^-):NH_4^+ ratio (section *4.4.1*). This finding is consistent with previous studies where BRCs were found to efficiently remove ammonium via sorption and nitrification but were inefficient at nitrate removal via denitrification, hence increasing the risk of nitrate leaching (Li & Davis, 2014). A simple mass balance calculation shows that the observed average reduction of the NH_4^+-N concentration at most accounts for 52% of the mean increase in the NO_3^--N+NO_2^--N concentration. In other words, nitrification of inflowing NH_4^+ alone cannot explain the NO_3^-+NO_2^- enrichment in the outflow. Other N sources must therefore play a role such as the oxidative degradation of organic-N.

The changes in DIN speciation caused by BRCs may impact the algal community structure and toxin production in receiving water bodies (Monchamp et al., 2014; Trommer et al., 2020). Moreover, many aquatic species are sensitive to elevated levels of ammonium and nitrite and, less so, nitrate (Canadian Council of Ministers of the Environment, 2007). Overall, our data

analysis therefore highlights the multiple effects BRCs can have on the P and N concentrations, speciation, and loads of urban runoff. When advocating BRCs as a eutrophication risk reduction strategy, the potential consequences for the ecology of receiving water bodies and groundwater quality should therefore be carefully evaluated.

4.5.4 Insights from random forest modeling

The discussion so far has emphasized the importance of inflow speciation and in-system biogeochemical processes in modulating the changes in P and N concentrations between inflow and surface outflow. The random forest modeling provides complementary information on the roles of watershed and climate drivers, as well as the age and storage volume of BRCs. Together, these additional variables contribute significantly to explaining the observed variations in the concentration REFs of TP, SRP, TN, and DIN, as shown by the fair agreement between the observed and predicted REFs in Figure 4.5. In particular, the random forest regressions are reasonably successful in separating the events resulting in enrichment versus reduction of the TP, SRP, TN, and DIN EMCs.

4.5.4.1 Watershed characteristics

The inflow concentrations are identified as the most important variables affecting the corresponding *REF* values (Figure 4.6). Enrichment of TP, SRP, TN and DIN concentrations is predicted to be more likely during events with lower influent concentrations (section *4.4.4*). This finding is both conceptually intuitive and consistent with previous observations that show leaching of P and N from BRCs experiencing dilute inflow events (e.g., Li & Davis, 2016; McGechan & Lewis, 2002). This raises the possibility of a release of legacy P and N accumulated in BRCs following improved nutrient management in watersheds that lowers the input concentrations reaching the BRCs.

Relative to the inflow concentrations, watershed imperviousness and land use seem to carry less explanatory importance for the TP, SRP, TN, and DIN concentration changes. Nonetheless, the true importance of imperviousness and land use effects may be under-represented because these watershed characteristics also influence inflow nutrient concentrations and speciation (Slowinski et al., 2023). Schroer et al. (2018), for example, showed how imperviousness affects pollutant and nutrient buildup and wash off, as well as their

accumulation rates within stormwater BMP systems. The PDPs in Figures 4.7 and AB5 to AB7 in supplementary materials imply a highly non-linear response of the concentration *REFs* to increasing impervious land cover, with abrupt increases in TP and SRP enrichment and decreases in TN and DIN reduction. This would imply that, in densely built urban areas, BRCs may be less effective as a nutrient control practice.

4.5.4.2 Climate and seasonality

Previous studies have linked variations in P and N concentration enrichments and reductions to differences in local climatic conditions (Goh et al., 2019; Kratky et al., 2017). Our finding that wetter climate conditions tend to dampen P concentration enrichment and promote N concentration reduction by BRCs is in line with the study of Horvath et al. (2023). Our work further shows that P and N concentration *REFs* are more sensitive to seasonal climate cycles than long-term climatic averages (Figures 4.4, 4.6, and AB4). For example, the TP concentration shows the highest mean *REF* values during summer to late fall (July-November, Figure 4.4a). A somewhat similar pattern is observed for the DIN concentration (Figure AB4b) with, on average, enrichment during the months of June to September and reduction for most of the rest of the year. Whereas the mean TN concentration *REFs* show only a weak seasonal trend (Figure 4.4b), the SRP concentrations exhibit their highest enrichment during the winter months (January to March, Figure AB4a) and the lowest enrichment in spring (April-May).

The contrasting seasonal trends of the *REFs* of the TP, TN, SRP, and DIN concentrations arise from the interplay between multiple season-dependent drivers, including temperature, the frequency and intensity of inflow events (Figure AB9), the inflow concentrations (Figures 4.4 and AB4), as well as biological and biogeochemical activities (nutrient uptake by roots, microbial heterotrophic activity, etc.) not explicitly represented in our random forest modeling. The seasonal trends highlight the differences between P and N, as well as the importance of speciation. For example, the dissimilar seasonal trends of the concentration *REFs* of TP and SRP may in part be the outcome of their opposite dependencies on temperature (compare Figure 4.7 and Figure AB5). A deeper understanding of the seasonal and inter-annual trends in P and N *REFs* will be needed to predict how changing weather conditions projected under climate warming, including increased frequency of high-intensity rainfall and extended dry periods between rainfall

events (Pörtner et al., 2022; Tebaldi et al., 2006), may alter the effects of BRCs on P and N speciation, concentrations and loads of urban surface runoff.

4.5.4.3 BRC age and design characteristics

The anticipated life cycle of most BRCs falls within 8-25 years (Komlos & Traver, 2012). Up to 5 years, BRC age should generally have little effect on SRP enrichment (Figure AB5), while over the same time span BRCs may switch from reducing to enriching outflow DIN (Figure AB7). Furthermore, the prediction for SRP appears to contradict results of some previous studies, such as Lucas & Greenway (2011) who proposed that, with the exhaustion of sorption sites, BRCs tend to progressively become less efficient at retaining SRP. These predictions, however, should be considered with caution because most BRCs included in the random forest regressions were less than 5 years old (Figure AB8).

Cell storage volume to watershed area ratio was identified to be a more important predictor variable for DIN than BRC age (Figure 4.6). The role of this factor may be due to its relationships to water saturation and residence time in the filter medium that, in turn, control the relative impacts of ammonification, nitrification, and denitrification, with the latter typically favored by longer water residence times (Seitzinger et al., 2006; Zarnetske et al., 2011). Other design factors, such as the presence of an internal submerged zone and vegetation, are known to be important in modulating concentration changes of P and N by BRCs (Boehm et al., 2020; Wang et al., 2019; Zhang et al., 2021). Longer monitoring data series, in concert with more detailed information on the design and maintenance regime of BRCs, will be needed to fully delineate the complex effects of BRCs on P and N in urban runoff.

4.6 Conclusions

The synthesis and analysis of the data extracted from the ISBD offer insights into the range of impacts of BRCs on the speciation, concentrations, and loads of P and N in urban surface runoff. The major findings and trends emerging from our work are the following.

1. On average, BRCs enrich the surface outflow concentration of TP and even more that of SRP; they reduce the outflow concentration of TN and impart little change to that of DIN.
2. The outflow loads of TP and DIN typically decrease due to the reduction of surface flows by BRCs. However, because of the compensating effects of flow reduction and concentration increase, the mean SRP inflow and outflow loads are not significantly different. However, BRCs exhibit a markedly greater likelihood of enriching the SRP concentration in urban runoff than that of DIN.
3. Because of the different impacts on P and N, BRCs are more likely to decrease the N:TP and DIN:SRP ratios, hence causing urban runoff to become more N limiting relative to P.
4. Outflow from BRCs generally carry higher SRP:TP and $(NO_3^-+NO_2^-):NH_4^+$ ratios than the inflow. Thus, when proposing BRCs as a potential eutrophication control strategy, the multiple effects on P and N speciation, concentrations, and loads should be taken into consideration.
5. Random forest regressions identify inflowing concentrations and BRC age as major variables affecting the enrichment or reduction factors of the concentrations of TP, SRP, TN, and DIN.
6. Wetter climate conditions tend to weaken P enrichment and enhance N reduction by BRCs, while very high watershed imperviousness may have opposite effects.
7. The impacts of BRCs exhibit strong seasonal variability because of the large seasonal cyclicity of temperature, precipitation patterns, inflow concentrations and speciation, and in situ biogeochemical activity.
8. The consequences of exfiltration from BRCs for groundwater nutrient enrichment and subsurface transport require further research.

Chapter 5

Phosphorus control by stormwater infrastructure: modelling with data-driven approach and exploring the importance of BMP, climate and watershed characteristics

This chapter is modified from:

Zhou, B., Parsons, C. T., & Van Cappellen, P. (2023) Phosphorus control by stormwater infrastructure: modelling with data-driven approach and exploring the importance of BMP, climate and watershed characteristics. Under review by coauthors.

5.1 Summary

A variety of best management practices (BMPs) have been employed to attenuate phosphorus (P) export in urban stormwater and mitigate the eutrophication of receiving waterbodies. However, P control performance varies considerably depending on the BMP, climate, and watershed conditions. Many BMPs are reported to enrich P concentrations, which questions their efficiency to control P export from urban watersheds. In this study, we evaluated the effects of BMPs on total P (TP) and soluble reactive P (SRP) in urban runoff using hydrologic and concentration data for six categories of stormwater BMPs. These included traditional systems (retention pond, wetland basin and detention basin) and low-impact development (LID) systems (bioretention cell, grass swale and grass strip), from the International Stormwater BMP Database. Further, we developed machine learning (ML) models to predict P reduction or enrichment effects for specific BMP systems under different watershed and climatic conditions. We found that although LID BMPs more efficiently reduce runoff volume, they are generally more likely to enrich TP and SRP concentrations compared to traditional BMPs. These combined effects lead to poorer P load reduction performance for LID BMPs. Both traditional and LID BMPs are more likely to enrich SRP concentration in drier climates, when influent SRP concentrations are low and when watershed imperviousness is high. The SRP concentration reduction and enrichment performance of LID BMPs is also generally more sensitive to the BMP, climate, and watershed factors, than traditional BMPs. We found that the random forest model presented herein provided the most accurate estimation of BMPs effects on P concentrations compared to other ML methods. This study suggests that switching to LID BMPs from more traditional approaches has the potential to exacerbate P driven eutrophication in receiving water bodies. Our results also show that ML methods, especially the random forest model, can more robustly estimate the effects of stormwater BMPs on urban runoff P compared to the traditional reduction efficiency method by accounting for both P reduction and enrichment effects.

5.2 Introduction

Urbanization increases impervious land cover and concentrates human-related activity, which has elevated and intensified pollutant export to receiving water bodies via surface stormwater runoff (Valtanen et al., 2014; Yang et al., 2021; Yang & Lusk, 2018). Among exported pollutants from urban areas, phosphorus (P), especially in bioavailable forms (e.g., soluble reactive P (SRP)), is of great concern due to its role as the nutrient limiting eutrophication in many water bodies (Schindler, 1974; Schindler et al., 2016).

In response to this challenge, policies promoting urban stormwater management have been implemented all over the world in the past 40 years (Chang et al., 2018). A variety of structural stormwater best management practices (BMPs) have been applied to limit the ecological impact of urban stormwater runoff on receiving waterbodies, including traditional options such as end-of-pipe stormwater ponds (SWPs) and more innovative low-impact development (LID) options such as bioretention cells (BRCs) (Hager et al., 2019; Jefferson et al., 2017). As shown in Figure 1.3 in Chapter 1, while traditional BMPs reduce runoff pollutant load via centralized retention-based treatments, LID BMPs were designed to reduce surface runoff pollutant load by promotion of decentralized infiltration, which diverts surface runoff to the subsurface (Gao et al., 2013; Hager et al., 2019; Sample et al., 2012).

Many urban stormwater BMPs systems have proven efficient for control of flooding as well as certain pollutants such as TSS and heavy metals. However, the efficacy of these systems with respect to the control of P export is more variable (Jefferson et al., 2017; Li & Davis, 2008; Teng et al., 2004). While some studies show that BMPs are efficient at reducing P loads in urban stormwater runoff (Liu & Davis, 2014; Zhou et al., 2023), others found that they can enrich P concentration due to leaching of legacy P, originating either from fertilizer inappropriately applied directly to the BMP, or accumulated from the watershed (Hurley et al., 2017; Taguchi et al., 2020). It is recognized that different categories of BMPs can have different effects on P concentrations and loads (Hager et al., 2019) and it has also been shown that the efficacy of BMPs within the same category can also vary considerably depending on individual BMP, climate, and watershed conditions (Barbosa et al., 2012; German et al., 2003; Liu et al., 2018).

Although complex mechanistic models have been developed for a few individual BMP systems (Li & Davis, 2016; Zhou et al., 2023), most modelling tools used to estimate the effects of BMPs on P export at the watershed scale are oversimplified. Typically, such models assign either a fixed reduction efficiency or a single first-order P reaction coefficient based on the average value from a few previous studies (Baek et al., 2020; Hanief & Laursen, 2019). These methods, lack the complexity needed to account for different BMP, watershed or climatic characteristics in any particular location which diminishes their accuracy. Further, they are unable to forecast BMP performance based on climate or land use change scenarios, limiting their utility for watershed planning. A few recent modelling studies have tried to account for variations in BMP P control performance through the use of innovative methods such as Bayesian method, frequency analysis and Monte Carlo analysis to simulate the distribution of P reduction efficiency (Liu et al., 2018; Park et al., 2015; Sparkman et al., 2017). However, most still make the optimistic assumption that BMPs reduce P concentration throughout their lifespan with few considering the possibility of P concentration enrichment (Lintern et al., 2020).

In recent years, machine learning (ML) methods have emerged as powerful tools with applications across many domains, including the prediction of BMP hydrological and pollutant reduction performance (Fang et al., 2021; Khan et al., 2013; Wang et al., 2019; Zhang et al., 2021). The use of ML methods has resulted in higher prediction accuracy but has also highlighted the need for consistent monitoring and effective consolidation of the resulting data, as ML methods typically perform better when trained on large datasets. The International Stormwater BMP Database (ISBD) (Clary et al., 2020) is an excellent example of consolidated high quality monitoring data, which can facilitate the use of ML models. In this study, we examined the concentration and load reduction and enrichment effects of six typical categories of traditional and LID BMPs (three for each) from the ISBD. We then trained ML models to estimate their reduction and enrichment effects on P concentration given BMP, watershed and climatic conditions.

5.3 Methodology

5.3.1 Data acquisition, selection, and synthesis

Influent and effluent water quality data, recorded as event-mean concentrations (EMC) of total phosphorus (TP) and SRP, were retrieved from version 02-08-2021 of the ISBD (https://bmpdatabase.org/). The data were selected to include six typical urban stormwater BMP categories (Table 5.1) located primarily within the continental United States (see spatial distribution of BMPs in Figure AC1 in supplementary materials). These include three traditional centralized BMP categories (stormwater pond (SWP), detention basin (DB) and wetland basin (WB)), and three decentralized LID BMP categories (bioretention cell (BRC), grass swale (BS) and grass strip (BI)). We matched water quality data with flow (inflow and outflow), precipitation (event mean precipitation intensity), watershed characteristics (drainage area, imperviousness and land use types), and local climatic conditions obtained from historical climate records (site average annual precipitation depth, precipitation intensity and inter-event dry duration) for analysis. TP and SRP event loads were estimated from EMC data from the inflow and outflow and corresponding flow data.

To include factors related to the BMP system characteristics, we calculated the ratio between BMP surface area and drainage area, as well as the BMP system age at the time each event occurred. The air temperature for each event was assigned based on the monthly local average air temperature obtained from the United States Geological Survey (USGS) Science Database (https://www.sciencebase.gov/catalog/item/4fb5528ee4b04cb937751d9e). Land use types within the watersheds were split between six categories (institutional, residential, transportation, industrial, commercial and undeveloped) plus mixed land use types, based on key words associated with each BMP in the ISBD (see Table AC1 in supplementary materials for details).

Table 5.1: Definition of BMP category*

Category	Description
Detention Basin (DB)	Dry extended detention grass-lined and concrete lined basins that empty out after a storm.
Stormwater Pond (SWP)	Surface wet pond with a permanent pool of water, may include underground wet vaults.
Wetland Basin (WB)	Similar to a retention pond (with a permanent pool of water), typically with more than 50 of its surface covered by emergent wetland vegetation.
Grass Swale (BS)	Shallow, vegetated channel, also called bioswale or vegetated swale.
Grass Strip (BI)	Vegetated areas designed to accept laterally distributed sheet flow from adjacent impervious areas, also called buffer strips or vegetated buffers.
Bioretention Cell (BRC)	Shallow, vegetated basins with a variety of planting/filtration media and often including underdrains. Also called rain gardens and biofiltration.

*Adapted from Clary et al. (2020)

5.3.2 Metrics of BMP effects on P runoff

BMP's effect on runoff TP and SRP are evaluated and quantified by calculating the event-scale and site/scale reduction/enrichment factors (REFs) in this study, as elaborated in section *4.3.2*.

5.3.3 BMP performance predictions using machine learning methods

To predict BMP P reduction performance given BMP, climate and watershed characteristics, we trained 6 models using common ML methods (Table 5.3). Factors listed in Table 5.2 were used as predictors. The dataset was split with 80% used for model training and 20% for validation. We conducted 3 separate 10-fold cross-validations for each model and recorded the average Nash-Sutcliffe efficiency (NSE) (Legates & McCabe, 1999) to compare model accuracy. The method which provided the highest average simulation accuracy was subsequently used to evaluate the importance of predictors by quantifying their effects on model prediction accuracy. We used the 'pdp' package in R to conduct partial dependence analysis for each numerical predictor to identify the direction of influence on REFs (Greenwell, 2017). Land use and BMP category predictors were excluded from this analysis as the only categorical predictors in the dataset.

Table 5.2: Explanatory variables included in the machine learning prediction of the concentration reduction and enrichment factors (*REFs*) of urban stormwater best management practices (BMPs).

Abbreviation	Description
BMP characteristics	
A_BMP:DA	Ratio between BMP surface area to the drainage area of the BMP
BMP_Category	Category of BMP (see Table 1)
Age*	BMP age at a given inflow event (units: years), calculated as the difference between event record date and the BMP's start of service date
Watershed characteristics	
IN_Conc	Influent concentration for a given event (units: mg L^{-1})
Imperv	Imperviousness of watershed (units: %)
LandUse	Land use type of watershed; categories included are "Institutional", "Residential", "Transportation", "Industrial", "Commercial", "Undeveloped", plus the mix of any two of aforementioned types, e.g., "Commercial & Undeveloped"
Site-specific average climate conditions	
Precip_Depth_SA	Average annual total precipitation depth (units: cm)
Precip_Intensity_SA	Average precipitation intensity (units: cm hr^{-1})
ADP_SA	Average inter-event dry duration (units: hour)
Event-specific climate characteristics	
Month**	Month of event date
Temp*	The monthly local average air temperature at the month when the event occurred (unit: °C)
Precip_Intensity_E**	Event mean precipitation intensity (unit: cm hr^{-1})

*Calculate average values for all available events of each site for site-scale analysis

**Not included in site-scale analysis

Table 5.3: Machine learning methods tried in the study.

Method	R function	Reference
Generalized linear model (GLM)	glm	(Chambers & Hastie, 1992)
Nearest neighbour clustering (kNN)	knn	(Torgo, 2016)
Neural network (NN)	nnet	(Torgo, 2016)
Linear support vector machines (SVM)	svmLinear	(Karatzoglou et al., 2019)
Decision tree (DT)	rpart	(Therneau & Atkinson, 1997)
Random forest (RF)	rf	(Breiman, 2001)

5.4 Results

5.4.1 P reduction performance by BMPs

Figure 5.1 shows that the number of traditional BMPs monitored increased dramatically in the late 1970s, whereas LID BMPs did not become prevalent until the late 1990s. Most (62.5%) traditional BMPs (*i.e.*, DB, SWP and WB) reduced SRP concentrations whereas most (92.5%) LID BMPs (*i.e.*, BS, BI and BRC) enriched SRP concentrations (Figures 5.1b and 5.2a). Similar patterns are present for TP (Figure 5.1a). On average SWPs exhibited the strongest reduction effect for SRP concentration, whereas BRCs showed strongest enrichment effect (Figure 5.2a). Compared to traditional BMPs, LID BMPs generally exhibited lower REFs for SRP concentration and higher REFs for flow, which, although exerting opposing effects on loads, cumulatively result in lower SRP REFs for loads.

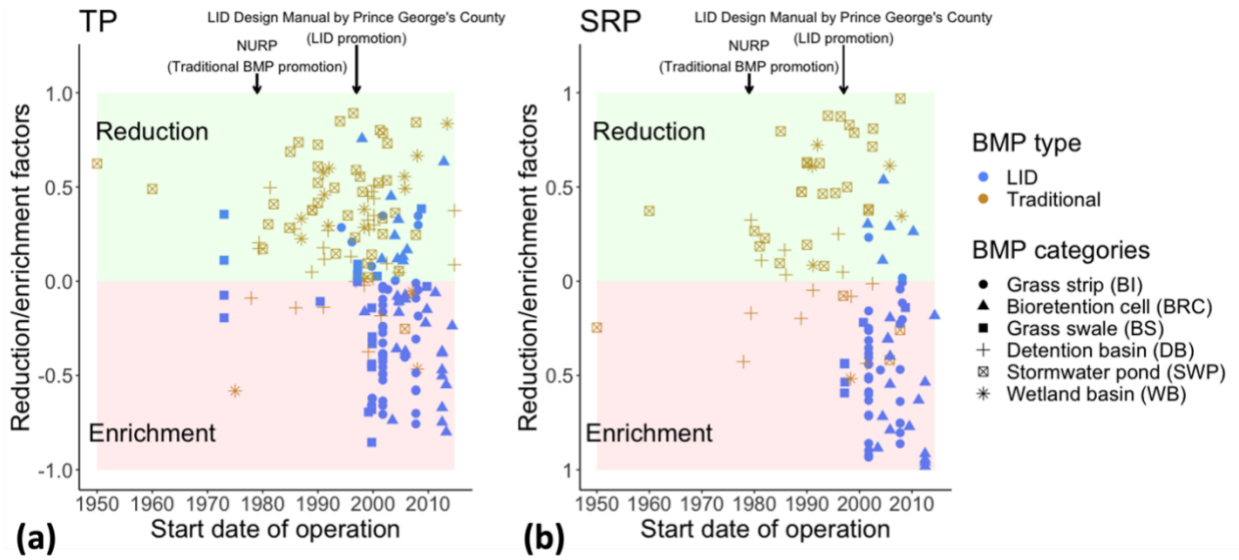

Figure 5.1: Site-scale TP (**a**) and SRP (**b**) concentration reduction/enrichment factors of traditional and low-impact development (LID) stormwater best management practices (BMPs) along their start dates of operation. The arrows mark the time when the application of traditional and LID stormwater BMPs were promoted in the USA (though the implementation of US EPA National Urban Runoff Program (NURP) and the publication of LID Design Manual by Prince George's County, respectively).

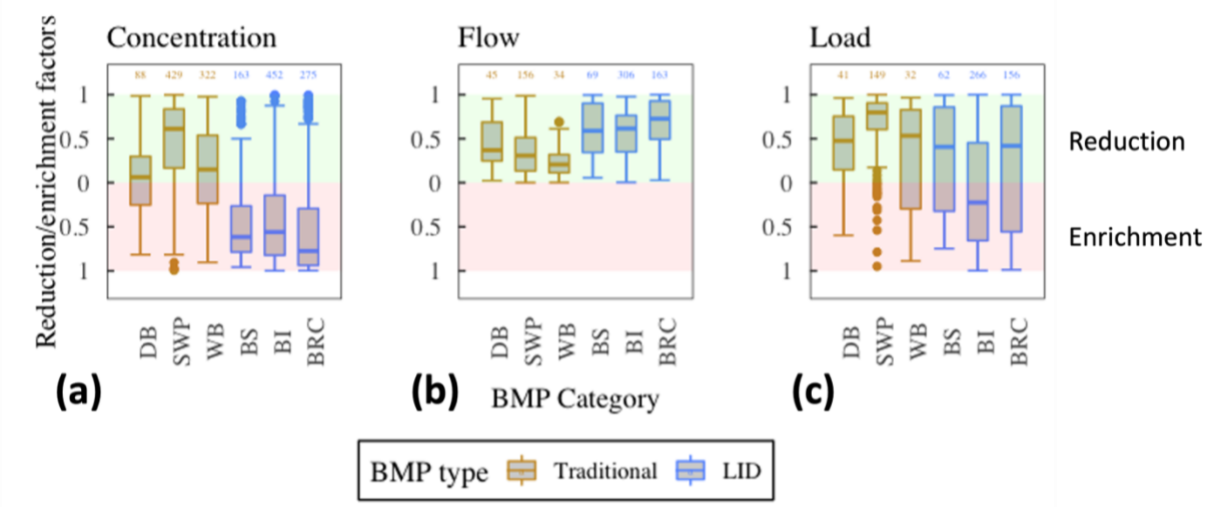

Figure 5.2. Event-scale SRP concentration, flow and load reduction/enrichment factors of different categories of BMPs. See Table 5.1 for the definition of BMP categories.

5.4.2 Comparison of Machine Learning models

Of the six ML models evaluated herein, the Random Forest (RF) model consistently provided the most accurate predictions of SRP and TP concentration REFs (Figure AC2). Figure 5.3 shows an example of validation results, from one fold, for prediction of SRP concentration REFs per event (Figure 5.3a) and per site (Figure 5.3b) using the RF model. This example provided NSE values of 0.67 and 0.76, respectively, similar to the average values provided by the triplicate 10-fold cross validation of X and Y (Figure AC2 and Table AC3).

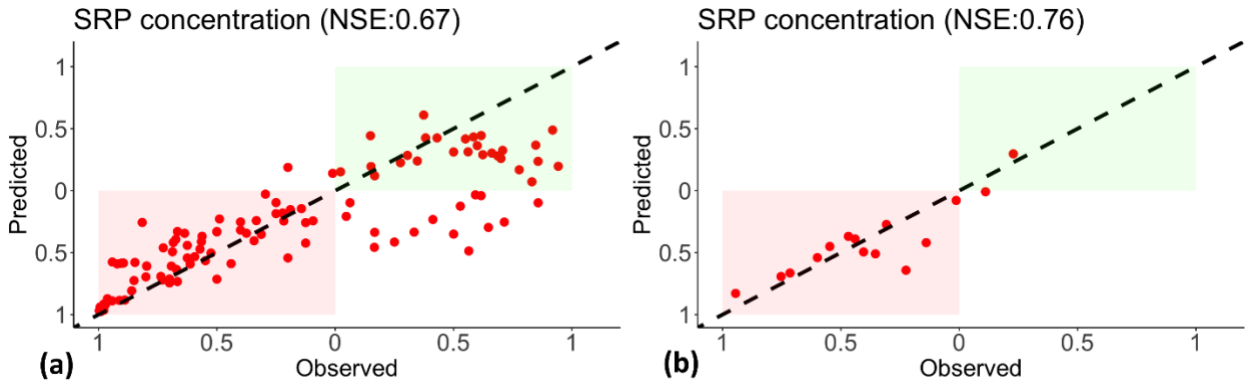

Figure 5.3. Event (**a**) and site (**b**) scale observed vs. simulated SRP concentration elimination/enrichment factors (REF s) by random forest model. Zones where observed reduction cases are also predicted correctly as reduction are colored as green, while zones where observed enrichment cases are also predicted correctly as enrichment are colored as red.

5.4.3 Factors influencing BMP P reduction performance

The relative importance of factors contributing to the RF model for the prediction of SRP concentration REF per site are shown in Figure 5.4a. BMP system characteristics are identified as the most important category, followed by watershed and climatic factors. Partial dependence plots, shown in Figure 5b, indicate that SRP concentrations tend to be enriched at sites where influent SRP concentrations (IN_Conc), annual total precipitation depth (Precip_Depth_SA) and average precipitation intensity (Precip_Intensity_SA) are lower and when the average inter event dry period (ADP_SA), temperature (Temp) and watershed imperviousness (Imperv) are higher.

The partial dependence analysis (Figure 5.4b) and factor value plot (Figure AC3) are in good general agreement with two exceptions. Partial dependence plots show that BMPs tend to reduce SRP more efficiently as they age, whereas Figure AC3 shows that BMPs which enrich SRP concentration are on average older than those which reduce SRP. Similarly, partial dependence analysis indicates the absence of a monotonic influence of temperature on SRP concentration control performance, whereas factor value box plots (Figure AC3) show that BMPs at lower temperatures tend to enrich SRP more than those at higher temperatures. Comparison of the Box plots of factor values also shows that differences between sites which enriched SRP concentrations and those that reduced SRP concentrations are more significant among LID BMPs compared to traditional BMPs, as indicated by p-values.

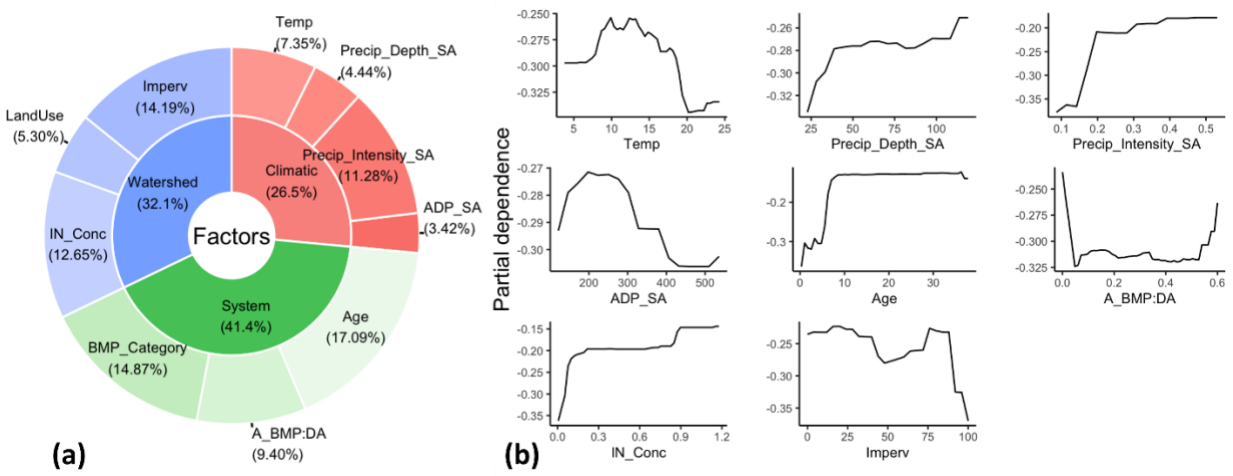

Figure 5.4: (a) Relative importance of factors under different categories (see Table 5.2 for definition for factors and their categories) quantified by random forest model for prediction of per site SRP reduction/enrichment factors (REFs). **(b)** Partial dependence plot for factors included in random forest model for prediction of per site SRP reduction/enrichment factors (REFs). BMP category and land use predictors are excluded as categorical variables (see Table 5.2 for definition for factors). Partial dependence with positive values represent reduction effects while negative values represent enrichment effects.

5.5 Discussion

5.5.1 Adoption of LID BMPs may increase P export

Changes to urban stormwater BMP implementation over time, reflected in the ISBD, are closely correlated with the promotion of urban stormwater BMPs in the United States (Figure 5.1). Subsequent to The Clean Water Act (US Congress, 1972), enacted in 1972, and the National Urban Runoff Program (NURP) (US EPA, 1982), conducted between 1979 and 1983, the implementation and monitoring of traditional BMPs increased markedly (Figure 5.1). These regulatory and policy implements both emphasized the importance of controlling pollutant loads in urban stormwater runoff (Fletcher et al., 2015).

Similarly, following the publication and distribution of the LID Design Manual by Prince George's County in 1999 (Prince George's County, 1999), many public authorities in the US shifted to the preferential adoption of LID BMPs over traditional options. This abrupt shift in stormwater management strategy, evident in Figure 5.1, was due in part to a desire to restore predevelopment hydrographs in urban areas (Fletcher et al., 2015; Gao et al., 2013). Although the punctuated timing of changes to stormwater management strategies discussed herein are likely specific to the US, the general trend away from traditional and toward LID BMPs over the last two decades is exhibited in many other countries (Chang et al., 2018).

Surprisingly, although LID BMPs are commonly assumed to be more environmentally friendly (Gao et al., 2013), our analysis indicates that they typically enrich stormwater runoff P concentration more frequently and to a greater extent than traditional BMPs (Figures 5.1 and 5.2a). This finding is consistent with several previous studies which report enrichment of P within urban stormwater by some LID BMPs (Hurley et al., 2017; Mullane et al., 2015; Tirpak et al., 2021). However, our findings, based on an extensive dataset, indicate that enrichment of P concentration by LID BMPs is not limited to a few isolated systems but is prevalent across the continental United States (Figures 5.1 and 5.2a). This unintended effect merits increased recognition and should be considered by authorities tasked with stormwater management prior to the replacement of centralized traditional stormwater BMPs with decentralized LID BMPs in urban areas.

The top considerations for LID BMP design and maintenance are often the promotion of stormwater infiltration, to reduce flood risk, and increasing urban green spaces, to foster local community acceptance. Therefore, the ability of BMPs to reduce P export may be diminished in deference to these primary goals of the BMP design. For example, vegetation is considered important in LID BMPs for soil porosity regulation, pollutant uptake and ecological aesthetics (Fowdar et al., 2017; Skorobogatov et al., 2020). However, addition of compost and fertilizers to promote vegetation increases P stored in LID BMPs, which can enrich P concentrations in runoff (Hurley et al., 2017; Mullane et al., 2015; Tirpak et al., 2021). P saturation of soil within LID BMPs can also be caused by continuous inputs of P from the upstream drainage area. While this accumulation does remove P exported from the drainage area, it can also diminish the capability of the BMP to reduce P concentration in P runoff over time and lead to desorption of SRP (Lucas & Greenway, 2011). Evidence for this effect within this study is mixed as partial dependence plots and factor analyses provide conflicting evidence on the effect of BMP age (Figures 5.4b and AC3). Further, P saturation of soil is rarely observed in LID BMP field studies due to the typically high P adsorption capacity of engineering soil applied in those systems (Johnson & Hunt, 2016; Komlos & Traver, 2012; Zhou et al., 2023).

Traditional BMPs can also enrich stormwater runoff P concentration in their outflow due to internal P loading which recycles legacy P from sediments back to the water column (Orihel et al., 2017; Song et al., 2017; Taguchi et al., 2020). However, our results suggest that enrichment of stormwater P concentrations by LID BMPs, likely caused by leaching of P from soil media, is much more prevalent than P enrichment from traditional BMPs caused by internal P loading. Although LID BMPs exhibit better surface runoff flow reduction performance than traditional options, their SRP loading reduction efficiencies are lower compared to traditional BMPs due to concentration enrichment (Figure 5.2b and c). Further, the quality of infiltrating water is also largely unknown. If SRP concentration increases are present in infiltrating water, similar to those exhibited in the surface outflows, the quality of shallow aquifers can be jeopardized in addition to the quality of nearby surface waterbodies due to subsurface flow paths (Jefferson et al., 2017; Zhang & Chui, 2017).

5.5.2 Machine learning model as a practical predictive tool for BMP P reduction performance estimation

The fact that many BMPs, especially those designed as LID, failed to reduce P concentration questions the typical method to estimate urban BMP P reduction performance at watershed scale by assigning these systems a fixed P removal efficiency, which always assume that BMP systems can reduce P concentration (Baek et al., 2020; Hanief & Laursen, 2019). A more practical and accurate method to predict and evaluate urban BMP applications should consider their failure to reduce surface runoff P, or further, account for their potential enrichment effects on surface runoff P under certain design, watershed and climatic context. In this study, the data-driven ML methods can predict both P reduction and enrichment cases, thus provide significantly higher prediction accuracy than traditional methods. As shown in this study, ML method can also shed light on the rank of importance of different variables on affecting the P reduction performance of BMPs by quantifying the importance of variables (predictors) based on their influence on prediction accuracy (Dinov, 2018). Our results show that RF model outperforms other ML options in case of prediction accuracy. Another study also found RF method provides higher accuracy for bioretention cell's heavy metal reduction performance compared to GLM and NN method (Fang et al., 2021). However, some other ML options can generate the model under more explicit mathematical format. For example, GLM can generate mathematical equations while DT can provide explicit tree-based rule for prediction (Dinov, 2018).

Compared to mechanistic model, ML model can not incorporate internal biogeochemical processes. This thus limits its prediction accuracy if the BMP system, watershed and climatic conditions differ significantly from existing data. Besides, some potential important variables, including the initial legacy P accumulated and the plant density and species in BMP systems, can not be included in this study due to lack of information available. Future data collection for urban stormwater BMPs should not only increase the number of sites under different design, watershed and climatic context monitored, but also increase the dimensions of data (i.e., variables recorded) to improve the prediction performance of ML model. In spite of its limitation, ML model can still be a more accurate method to estimate BMP P reduction performance especially at watershed scale, where the simulation of internal processes within BMP is not the main focus.

5.5.3 A bunch of factors contribute to uncertainty of BMP P reduction performance

Our study shows that a bunch of factors, related to BMP system, watershed and climatic characteristics, are potential to make urban stormwater BMP more likely to reduce or enrich P concentration. Generally, the influence of these factors seems more significant for LID compared to traditional BMPs because of the more significant variation of the factors' values under reduction and enrichment cases (see section *5.4.3*). The RF model developed in our study indicates that watershed characteristics plays more important role on affecting P reduction and enrichment effects of BMPs compared to climatic and BMP system characteristics.

5.5.3.1 BMP system characteristics

The RF model developed in our study indicates that system characteristics play a more important role compared to climatic and watershed characteristics on affecting SRP concentration reduction and enrichment effects of BMPs at site-scale. As discussed in *5.4.1*, BMP categories play an important role here because LID BMPs are much more likely to enrich SRP concentration compared to traditional BMPs. However, the actual direction of the influence of BMP age (Age) and area ratio (A_BMP:DA) are not clear as the contradictory results we got from partial dependence plots and boxplots (see Figure 5.4 and Figure AC3).

5.5.3.2 Watershed characteristics

It is not surprising that sites with larger imperviousness are more likely to enrich P concentration in our results (Figure 5.4). This can be attributed to excessive external P loading to BMPs from stormwater runoff at urban watersheds with low BMP coverage and high imperviousness (Valtanen et al., 2014; Yang & Lusk, 2018), which speed up the legacy P accumulation in BMPs and deteriorate their P reduction performance. It is noteworthy that compared to traditional BMPs, LID BMPs are more frequently applied in watersheds with higher imperviousness, which may be another reason why LID BMPs are more prone to enrich P. Influent concentration is a factor that can indirectly reflect the watershed characteristics. Our results show that LID BMPs are significantly more likely to enrich P when the influent concentration is lower. This can be attributed to the fact that the soil media of LID BMPs are more likely to release SRP when the water phase concentration is lower than the equilibrium concentration (Li & Davis, 2016; McGechan & Lewis, 2002).

5.5.3.3 Climatic characteristics

Our results suggest that both traditional and LID BMPs are more likely to enrich P under dryer (i.e., lower site annual precipitation and intensity, higher interevent dry period) climate (section *3.3*). A previous study focused on ISBD also found that LID BMPs are more likely to leach SRP under dryer climate (Horvath et al., 2023). One possible explanation for more significant P enrichment effects by BMPs at dryer places is that the internal P release affects outflow P concentration more significantly during low-flow events, which has already observed in many traditional BMPs (Chiandet & Xenopoulos, 2011; Duan et al., 2016; Song et al., 2015; Williams et al., 2013). Prolonged anoxia in BMPs at dryer places due to less oxygen fed by stormwater runoff can also promote internal P release, especially in traditional BMPs (Duan et al., 2016). Soil media of LID BMPs typically have higher P availability (i.e., higher possibility to leach P) at sites with higher aridity (Ippolito et al., 2010).

Internal P loading from sediments in traditional BMPs due to either desorption or organic matter decay is typically thought to be positively correlated with temperature due to prolonged stratification-related anoxia at water-sediment interface and enhanced microbial activities under warmer climate (McEnroe et al., 2013; Song et al., 2017; Taguchi et al., 2020). P availability in the high-sand (>50%) soil, typically used as the media materials of LID BMPs, is also found to be higher under warmer climate (Hou et al., 2018). The finding that both traditional and LID BMPs are more likely to enrich P concentration at lower temperature in this study may thus suggest that other temperature-related factors were playing major effect in here. One possible factor is the excessive road salt application in cold region, which can promote the immobilization of adsorbed P in soil media of LID BMPs (Goor et al., 2021) and enhance the internal P loading due to prolonged stratification of traditional BMPs (Radosavljevic et al., 2022).

5.6 Conclusion

We evaluated the P concentration and load reduction and enrichment performance of 6 categories of urban stormwater BMPs (3 as traditional systems and 3 as LID systems). We further developed machine learning models to predict the reduction and enrichment effects of stormwater BMPs on stormwater runoff P concentration under specific BMP systems, watershed and climatic conditions. We conclude that although LID BMPs are more efficient at reducing runoff quantity, they are generally more likely to enrich TP and SRP concentrations compared to traditional BMPs, which further leads to the poorer P load reduction performance of LID BMPs. Both traditional and LID BMPs are more likely to enrich SRP concentration under higher BMP system age, higher watershed imperviousness and dryer and colder climates. While SRP concentration reduction and enrichment performance of LID BMPs is also more sensitive to BMP system, watershed and climatic factors compared to traditional BMPs. We found that random forest model provides more accurate estimation for BMPs' effects on urban stormwater P concentrations compared to other machine learning methods.

Our findings indicate that switching from traditional to LID BMPs may actually increase the eutrophication risks of receiving waterbodies due to elevated P concentration in both outflow and infiltrated water from LID BMPs. More studies focus on understanding the mechanisms of enrichment effects by BMPs are needed. We also recommend amendments of design and maintenance guidelines for BMPs, especially those LID systems, to improve their P reduction performance and to avoid P enrichment effects. The machine learning model developed in this study can provide more accurate and reliable estimation for BMPs' effects on urban stormwater P export compared to traditional methods due to its ability to predict both P reduction and enrichment cases. Further collection and integration of urban stormwater monitoring data can improve the predictive accuracy of this model.

Chapter 6

Conclusions

6.1 Summary of major findings

In this thesis, I reviewed the knowns and unknowns about sources and pathways of stormwater phosphorus (P) export, and the effects of stormwater best management practices (BMPs) on P control in urban areas. By analyzing data from the inflow, outflow and soil cores collected from Elm Drive BRC and stormwater BMPs in the International Stormwater BMP Database (ISBD), I evaluated the effects of several typical categories of stormwater BMPs (with specific focus on bioretention cell (BRC)) on urban stormwater runoff P export and the implications of these effects on receiving surface water bodies and groundwater quality. Both process-based and data-driven modelling tools were developed to predict these effects, which advances the understanding of the impact of internal processes and external factors on the efficacy of stormwater BMPs for attenuation of urban P export.

By reviewing the sources and pathways of urban stormwater P export, I found that a variety of sources can contribute to elevating the P content in urban stormwater runoff, which makes urban stormwater runoff a substantial P export pathway that needs to be controlled (Chapter 2). The diversity of P sources and pathways under different land uses makes the loading and speciation of P in exported urban stormwater runoff highly variable, and this complexity can be further increased due to interactions with other pollutants and climate change (Chapter 2). Although I found that the Elm Drive bioretention facility is efficient at reducing urban stormwater P export by accumulating P in relatively stable forms within filter media over multiple years (Chapter 3), my review of case studies in the literature (Chapter 2) and analysis of data in the ISBD (Chapters 4 and 5) indicate that BRCs and other stormwater BMPs have highly variable effects on urban P export, with many BMPs typically enriching P concentration instead of reducing it. My results show that compared to traditional BMPs, low-impact development (LID) BMPs (*e.g.*, BRCs) are more likely to enrich P concentration (Chapter 5), which indicates excessive legacy P accumulated within these systems during operation. Although this P concentration enrichment can be partially offset by the more efficient flow reduction by LID BMPs, the P loading

reduction performance of LID BMPs is still worse than traditional BMPs typically (Chapter 5). My work also highlights that enriched P concentration by some LID BMPs such as BRCs may increase the P loading diverted to subsurface pathways and decrease the N to P ratio in stormwater that is discharged to receiving waterbodies, which implicate further P enrichment in groundwater and changes to nutrient limitation in surface waterbodies (Chapters 4 and 5).

By reviewing the literature, analyzing the modelling results of the Elm Drive bioretention facility, and checking the importance of variables in the machine learning model developed using data from the ISBD, I found that the highly variable P control effects exhibited by urban stormwater BMPs can be attributed to both complicated internal processes within the BMPs that promote the retention or release of P (Chapters 2 and 3) and the impact of explanatory variables related to climate, watershed and BMP characteristics (Chapters 4 and 5). Through development of a process-based model for Elm Drive bioretention facility, I found that the efficient P loading reduction provided by this BRC is largely attributable to filtration of particulate P and transformation of loosely adsorbed P to stable mineral P inside the system, which increases the accumulation capacity for P (Chapter 3). On the other hand, by developing data-driven models with machine learning methods (*e.g.,* random forest), I found that LID BMPs are generally more sensitive to explanatory variables related to climate, watershed and BMP characteristics than traditional BMPs. Furthermore, LID BMPs are more likely to enrich P under specific conditions, such as when the influent P concentration is low, in drier climates, and when watershed imperviousness is high (Chapters 4 and 5).

Both the process-based and data-driven model developed in this thesis represent novel tools to estimate the P control performance of urban stormwater BMPs. Compared to the most traditional estimation method, which uses a single reduction efficiency coefficient, the process-based model developed in Chapter 3 represents a more robust modelling framework to estimate the long-term accumulation of P and other pollutants in an individual stormwater BMP by accounting for complex internal physical and biogeochemical processes. The data-driven model developed in Chapters 4 and 5 constitutes a more accurate modelling tool which can be applied directly at larger scales where data on P contents within BMPs are hard to obtain. This model can be used to estimate the effects of stormwater BMPs on urban P export under different climate

and watershed contexts. However, the limitations of data-driven models compared to process-based models, such as the lack of strength to explain internal mechanisms, should be recognized.

Considering the global environmental policy trend to promote replacing traditional stormwater BMPs with LID BMPs, the findings of this thesis should serve as a caution that the effects of stormwater BMPs on urban P export require careful investigation, and potentially, further regulation. Systematic P reduction should not be assumed for urban stormwater BMPs. Current design and maintenance of urban stormwater LID BMPs, which typically try to enhance plant growth via application of fertilizers, may exacerbate the P enrichment effects of infiltration-based systems observed herein and increase downstream eutrophication risks. From the perspective of policy making, clear BMP P control regulation may be warranted. Potential previously unrecognized side effects of stormwater BMPs, such as nutrient enrichment and changes to nutrient limitation in groundwater and surface waters should also be considered. Variability of the P control performance of these systems under different watershed and climatic conditions need to be considered for more robust stormwater management. Appropriate design and maintenance regimes for urban stormwater BMPs is needed to avoid excessive legacy P accumulation and to enhance the retention of P in more stable forms. Overall, more efforts are needed to enhance the capacity of urban stormwater BMPs to reduce P export and related eutrophication risks.

6.2 Future perspectives

6.2.1 Improve process-based models for urban stormwater BMPs

My results in Chapter 3 indicate that transformation of loosely adsorbed P to mineral P largely accounts for the efficient P retention observed in the Elm Drive bioretention facility. Thus, the adsorption capacity of BRC filter media for loosely adsorbed P alone does not adequately represent the retention capacity for dissolved P. However, the process-based BRC P model developed in Chapter 3 simulates the slow sorption rate with a constant transformation rate, without considering the capacity of BRC filter media to transform loosely adsorbed P into mineral P. The capacity of soil to retain P via 'slow sorption' can be estimated based on the concentration of Al and Fe oxides in the soil (McGechan & Lewis, 2002). This could be included in the process-based model to provide a more accurate estimation on the lifespan of BRC filter media for efficient P retention prior to saturation. More field monitoring studies are also needed to characterize the typical concentration of Al and Fe in bioretention filter media so as to estimate its maximum capacity for P retention.

Besides, the process-based BRC P model developed in Chapter 3 relies on the assumption that there is no leaching of P from the mineral P pool. This is likely not valid in reality under certain redox conditions. Although the presence of underdrain in some BRCs can help maintain oxic conditions in the system, anoxic environments in BRC filter media under prolonged saturation caused by stormwater events can enhance the dissolution of P from Fe bound mineral P pool (Hurley et al., 2017). Redox conditions can also increase the release of P in other BMP systems. For example, as shown in Chapter 2, anoxic conditions at the sediment-water-interface can also increase P leaching from sediment. Thus, future research can focus more on investigating the redox conditions inside the urban stormwater BMPs and on understanding the impact of redox conditions on internal P release from urban stormwater BMPs.

Another aspect which requires further investigation is the P contents accumulated in urban stormwater BMPs due to the addition of fertilizer or other anthropogenic products, which are rarely recorded. This can help to accomplish the mass balance analysis for urban stormwater BMPs and to explain the P concentration enrichment effects by many urban stormwater BMPs shown in Chapter 4 and 5. By improving the understanding of the transformation mechanisms of

P within the urban stormwater BMPs and the quantification of the P input to these BMPs, the process-based model developed in this thesis can be further improved and will be more robust to estimate the P reduction or enrichment effects of urban stormwater BMPs.

6.2.2 Application of process-based and data-driven urban stormwater BMP P models for upscaled studies

Both process-based and data-driven modelling tools I developed in this thesis were applied to estimate the effects of urban stormwater BMPs at individual system scale. One future potential application of these modelling tools is to apply them at larger scales to estimate the effects of urban stormwater BMPs on P export at watershed, regional or continental scale. This will be important for evaluation of the influence of urban stormwater BMPs on both surface and ground water quality, as discussed in Chapters 4 and 5. The upscaled modelling of effects of urban stormwater BMPs on P export can be done by connecting the process-based and data-driven modelling tools developed in this thesis with existing modelling tools for urban stormwater runoff quantity and quality simulation. Furthermore, the integrated watershed-BMP model can improve our understanding of the impact of climate change on urban stormwater P export by running under different climatic scenarios.

For the process-based P model for BRCs developed in this thesis, further simplification is needed for upscaled studies due to the complexity of the model. This can be achieved by assuming steady state and neglecting unimportant processes identified by sensitivity and mass balance analysis in the model, which can simplify the complicated process-based model to a parsimonious model. However, as discussed in section *6.2.1*, further understanding of the internal processes for P transformation (especially the dynamic for P enrichment) within urban stormwater BMPs is required to increase the applicability of process-based model (and associated parsimonious model) to upscaled studies.

On the other hand, because the data-driven modelling tools developed in this thesis are trained by field monitoring data from BMPs across different watershed, climate and BMP characteristics, they can be used directly for upscaled studies without the intensive demand of field monitoring data for each BMP site. However, the accuracy of data-driven models can be improved with training the model with extensive data that covers BMPs under diverse watershed,

climate and BMP characteristics. Extended collection and aggregation of field monitoring BMP performance data in databases such as the ISBD is essential in the future to improve the prediction performance. Information about the P contents within existing urban stormwater BMPs is warranted.

6.2.3 Explore the impact of P exported from urban stormwater BMPs on receiving water bodies and groundwater

As discussed in Chapters 4 and 5 in this thesis, enrichment of P concentration and decrease of N to P ratios caused by some BMPs, such as BRCs, requires more attention due to its potential to alter the nutrient limitation in receiving water bodies. A further research direction is to explore to what extent nutrient limitation in natural water bodies can be influenced. Another interesting direction is to quantify to what extent the groundwater quality may be impacted by urban stormwater BMPs since the exfiltration of stormwater from BMPs (especially LID BMPs) diverts P into the subsurface (Chapters 4 and 5). Almost all previous studies focused on analyzing the P contents inside the stormwater BMPs and at inflow and outflow, while few studies studied the fate of P after it is exfiltrated to the subsurface. Analysis of the exfiltrated water quality and changes to groundwater quality underneath BMPs is warranted. To improve stormwater management strategies using LIDs both their advantages (*e.g.*, save of spaces, efficient runoff quantity reduction) and the aforementioned potential disadvantages should be considered.

6.2.4 Extend analysis and modelling to other chemical constituents

In this thesis, I compared the effects of BRCs on P and N export and found that there is significant decoupling of these elements within BRCs. This analysis can be further expanded in the future to understand the trade-off between the control of P and other chemical constituents by urban stormwater BMPs. For example, although in this thesis I showed that BRCs are not as efficient as we expected to control SRP export, they have been shown to be efficient at reducing the loads of heavy metals and TSS in many studies (Lange et al., 2020; Li & Davis, 2008b, 2008a). It is also important to understand to what extent the removal of other pollutants might be affected my implantation of measures to enhance P removal. The urban stormwater BMP model developed in this thesis can be further extended to other chemical constituents. It can also be extended to quantify this trade-off by coupling the reactive transport processes of P and other constituents.

In this thesis I focused on exploring the influence of factors related to climate, watershed and BMP characteristics on P control performance within urban stormwater BMPs. Another potential future research direction is thus to understand the impact of other chemical constituents on BMP P control performance. As Chapter 2 of this thesis already showed, other chemical constituents such as chloride can compete with the adsorption sites and deteriorate the P control performance of bioretention cells (Goor et al., 2021). The complicated composition of urban stormwater runoff may indicate that P control performance cannot be separated from the interaction from other chemical constituents. Further characterization of the effects and mechanisms of the interaction between P and other chemical constituents within urban stormwater BMPs can enhance our qualitative and predictive understanding on the effects of urban stormwater BMPs on P control.

Code and Data Availability Statement

The model and data analysis code used for this thesis will be available online after the work is published. For Chapter 3, the model code and simulated data used are made available on the Federated Research Data Repository (FRDR; https://doi.org/10.20383/103.0640). Field monitoring data used was provided by Credit Valley Conservation (CVC) authority and is available on their open data portal (https://cvc-camaps.opendata.arcgis.com/). Lab analysis data of soil cores collected in 2019 in Elm Drive bioretention cell (see section *3.3.1*) is available on the Federated Research Data Repository (FRDR; https://doi.org/10.20383/103.0643). Data used in Chapter 2, 4 and 5 was extracted from the open access International Stormwater BMP Database (http://www.bmpdatabase.org/, accessed January 2022) and related data analysis and model code will be shared through the GitHub repository.

References

Abi Aad, M. P., Suidan, M. T., & Shuster, W. D. (2010) Modeling techniques of best management practices: Rain barrels and rain gardens using EPA SWMM-5. Journal of Hydrologic Engineering, 15, 434-443. https://doi.org/10.1061/(ASCE)HE.1943-5584.0000136

Ahadi, N., Sharifi, Z., Hossaini, S. M., Rostami, A., & Renella, G. (2020) Remediation of heavy metals and enhancement of fertilizing potential of a sewage sludge by the synergistic interaction of woodlice and earthworms. Journal of hazardous materials, 385, 121573. https://doi.org/10.1016/j.jhazmat.2019.121573

Allmendinger, N. E., Pizzuto, J. E., Moglen, G. E., & Lewicki, M. (2007) A sediment budget for an urbanizing watershed, 1951-1996, Montgomery County, Maryland, USA 1. JAWRA Journal of the American Water Resources Association, 43, 1483-1498. https://doi.org/10.1111/j.1752-1688.2007.00122.x

Amato, F., Pandolfi, M., Moreno, T., Furger, M., Pey, J., Alastuey, A., ... & Querol, X. (2011) Sources and variability of inhalable road dust particles in three European cities. Atmospheric Environment, 45, 6777-6787. https://doi.org/10.1016/j.atmosenv.2011.06.003

Ament, M. R., Hurley, S. E., Voorhees, M., Perkins, E., Yuan, Y., Faulkner, J. W., & Roy, E. D. (2021) Balancing hydraulic control and phosphorus removal in bioretention media amended with drinking water treatment residuals. ACS ES&T Water, 1, 688-697. https://doi.org/10.1021/acsestwater.0c00178

American Public Health Association, & American Water Works Association. (1995) Standard methods for the examination of water and wastewater. In Standard methods for the examination of water and wastewater (pp. 1000-1000).

Amirbahman, A., Pearce, A. R., Bouchard, R. J., Norton, S. A., & Steven Kahl, J. (2003) Relationship between hypolimnetic phosphorus and iron release from eleven lakes in Maine, USA. Biogeochemistry, 65, 369-386. https://doi.org/10.1023/A:1026245914721

APHA. (2018) Standard methods for the examination of water and wastewater. American Public Health Association (APHA).

Arnold Jr, C. L., & Gibbons, C. J. (1996) Impervious surface coverage: the emergence of a key environmental indicator. Journal of the American planning Association, 62, 243-258. https://doi.org/10.1080/01944369608975688

Ashley, K., Cordell, D., & Mavinic, D. (2011) A brief history of phosphorus: from the philosopher's stone to nutrient recovery and reuse. Chemosphere, 84, 737-746. https://doi.org/10.1016/j.chemosphere.2011.03.001

Ashley, R., Bertrand-Krajewski, J. L., & Hvitved-Jacobsen, T. (2005) Sewer solids—20 years of investigation. Water Science and Technology, 52, 73-84. https://doi.org/10.2166/wst.2005.0063

Ashley, R., Blanksby, J., Cashman, A., Jack, L., Wright, G., Packman, J., ... & Maksimovic, C. (2007) Adaptable urban drainage: addressing change in intensity, occurrence and uncertainty of stormwater (AUDACIOUS). Built Environment, 33, 70-84. https://doi.org/10.2148/benv.33.1.70

Aspila, K. I., Agemian, H., & Chau, A. S. Y. (1976) A semi-automated method for the determination of inorganic, organic and total phosphate in sediments. Analyst, 101, 187-197. https://doi.org/10.1039/AN9760100187

Austin, A. T., Yahdjian, L., Stark, J. M., Belnap, J., Porporato, A., Norton, U., U., Ravetta, D. A., & Schaeffer, S. M. (2004) Water pulses and biogeochemical cycles in arid and semiarid ecosystems. Oecologia, 141, 221-235. https://doi.org/10.1007/s00442-004-1519-1

Aygün, O., Kinnard, C., & Campeau, S. (2020) Impacts of climate change on the hydrology of northern midlatitude cold regions. Progress in Physical Geography: Earth and Environment, 44, 338-375. https://doi.org/10.1177/0309133319878123

Baek, S. S., Ligaray, M., Pyo, J., Park, J. P., Kang, J. H., Pachepsky, Y., ... & Cho, K. H. (2020) A novel water quality module of the SWMM model for assessing low impact development (LID) in urban watersheds. Journal of Hydrology, 586, 124886. https://doi.org/10.1016/j.jhydrol.2020.124886

Baker, D. B., Confesor, R., Ewing, D. E., Johnson, L. T., Kramer, J. W., & Merryfield, B. J. (2014) Phosphorus loading to Lake Erie from the Maumee, Sandusky and Cuyahoga rivers: The importance of bioavailability. Journal of Great Lakes Research, 40, 502-517. https://doi.org/10.1016/j.jglr.2014.05.001

Baker, L. A., Hartzheim, P. M., Hobbie, S. E., King, J. Y., & Nelson, K. C. (2007) Effect of consumption choices on fluxes of carbon, nitrogen and phosphorus through households. Urban Ecosystems, 10, 97-117. https://doi.org/10.1007/s11252-006-0014-3

Baldwin, D. S. (2013) Organic phosphorus in the aquatic environment. Environmental Chemistry, 10, 439-454. https://doi.org/10.1071/EN13151

Balmer, P., Ekfjorden, L., Lumley, D., & Mattsson, A. (1998) Upgrading for nitrogen removal under severe site restrictions. Water science and technology, 37, 185-192. https://doi.org/10.1016/S0273-1223(98)00287-X

Barber, M. E., King, S. G., Yonge, D. R., & Hathhorn, W. E. (2003) Ecology ditch: A best management practice for storm water runoff mitigation. Journal of Hydrologic Engineering, 8, 111-122. https://doi.org/10.1061/(ASCE)1084-0699(2003)8:3(111)

Barber, S. A. (1995) Soil nutrient bioavailability: a mechanistic approach. John Wiley & Sons. https://doi.org/10.1017/S0021859600073238

Barbosa, A. E., Fernandes, J. N., & David, L. M. (2012) Key issues for sustainable urban stormwater management. Water research, 46, 6787-6798. https://doi.org/10.1016/j.watres.2012.05.029

Barten, J. M., & Johnson, J. (2007) Minnesota Phosphorus Fertilizer Law. LakeLine, 27, 23-28. http://lindenhurstlakes.com/Images/No_P/27-02-07%5B1%5D.pdf

Beck, H. J., & Birch, G. F. (2012) Metals, nutrients and total suspended solids discharged during different flow conditions in highly urbanised catchments. Environmental monitoring and assessment, 184, 637-653. https://doi.org/10.1007/s10661-011-1992-z

Beckingham, B., Callahan, T., & Vulava, V. (2019) Stormwater ponds in the southeastern US coastal plain: hydrogeology, contaminant fate, and the need for a social-ecological framework. Frontiers in Environmental Science, 7, 117. https://doi.org/10.3389/fenvs.2019.00117

Beecham, S., & Chowdhury, R. (2012) Effects of changing rainfall patterns on WSUD in Australia. In Proceedings of the Institution of Civil Engineers-Water Management (Vol. 165, No. 5, pp. 285-298). Thomas Telford Ltd. https://doi.org/10.1680/wama.10.00115

Bernhardt, E. S., Band, L. E., Walsh, C. J., & Berke, P. E. (2008) Understanding, managing, and minimizing urban impacts on surface water nitrogen loading. Annals of the New York Academy of Sciences, 1134, 61-96. https://doi.org/10.1196/annals.1439.014

Berretta, C., & Sansalone, J. (2011a) Hydrologic transport and partitioning of phosphorus fractions. Journal of Hydrology, 403, 25-36. https://doi.org/10.1016/j.jhydrol.2011.03.035

Berretta, C., & Sansalone, J. (2011b) Speciation and transport of phosphorus in source area rainfall–runoff. Water, Air, & Soil Pollution, 222, 351-365. https://doi.org/10.1007/s11270-011-0829-2

Berretta, C., & Sansalone, J. (2012) Fate of phosphorus fractions in an adsorptive-filter subject to intra-and inter-event runoff phenomena. Journal of environmental management, 103, 83-94. https://doi.org/10.1016/j.jenvman.2012.02.028

Bertrand-Krajewski, J. L. (2021) Integrated urban stormwater management: Evolution and multidisciplinary perspective. Journal of Hydro-Environment Research, 38, 72-83. https://doi.org/10.1016/j.jher.2020.11.003

Bevan, V., MacVicar, B., Chapuis, M., Ghunowa, K., Papangelakis, E., Parish, J., & Snodgrass, W. (2018) Enlargement and evolution of a semi-alluvial creek in response to urbanization. Earth Surface Processes and Landforms, 43, 2295-2312. https://doi.org/10.1002/esp.4391

Billen, G., Aguilera, E., Einarsson, R., Garnier, J., Gingrich, S., Grizzetti, B., ... & Sanz-Cobena, A. (2021) Reshaping the European agro-food system and closing its nitrogen cycle: The potential of combining dietary change, agroecology, and circularity. One Earth, 4, 839-850. https://doi.org/10.1016/j.oneear.2021.05.008

Bocaniov, S. A., Scavia, D., & Van Cappellen, P. (2023) Long-term phosphorus mass-balance of Lake Erie (Canada-USA) reveals a major contribution of in-lake phosphorus loading. Ecological Informatics, 102131. https://doi.org/10.1016/j.ecoinf.2023.102131

Bock, E. M., & Easton, Z. M. (2020) Export of nitrogen and phosphorus from golf courses: A review. Journal of environmental management, 255, 109817. https://doi.org/10.1016/j.jenvman.2019.109817

Boehm, A. B., Bell, C. D., Fitzgerald, N. J., Gallo, E., Higgins, C. P., Hogue, T. S., ... & Wolfand, J. M. (2020) Biochar-augmented biofilters to improve pollutant removal from stormwater–can they improve receiving water quality?. Environmental Science: Water Research & Technology, 6, 1520-1537. https://doi.org/10.1039/D0EW00027B

Borne, K. E. (2014) Floating treatment wetland influences on the fate and removal performance of phosphorus in stormwater retention ponds. Ecological engineering, 69, 76-82. https://doi.org/10.1016/j.ecoleng.2014.03.062

Bratt, A. R., Finlay, J. C., Hobbie, S. E., Janke, B. D., Worm, A. C., & Kemmitt, K. L. (2017) Contribution of leaf litter to nutrient export during winter months in an urban residential watershed. Environmental Science & Technology, 51, 3138-3147. https://doi.org/10.1021/acs.est.6b06299

Breiman, L. (2001) Random forests. Machine learning, 45, 5-32. https://doi.org/10.1023/A:1010933404324

Brooke, D., Crookes, M., Quarterman, P., & Burns, J. (2009) Environmental risk evaluation report: Triphenyl phosphate (CAS no. 115-86-6). Environment Agency, Bristol, UK, 140.

Brown, R. A., Birgand, F., & Hunt, W. F. (2013a) Analysis of consecutive events for nutrient and sediment treatment in field-monitored bioretention cells. Water, Air, & Soil Pollution, 224, 1-14. https://doi.org/10.1007/s11270-013-1581-6

Brown, R. A., Skaggs, R. W., & Hunt Iii, W. F. (2013b) Calibration and validation of DRAINMOD to model bioretention hydrology. Journal of hydrology, 486, 430-442. https://doi.org/10.1016/j.jhydrol.2013.02.017

Burns, M. J., Fletcher, T. D., Walsh, C. J., Ladson, A. R., & Hatt, B. E. (2012) Hydrologic shortcomings of conventional urban stormwater management and opportunities for reform. Landscape and urban planning, 105, 230-240. https://doi.org/10.1016/j.landurbplan.2011.12.012

Cabrera, F., Diaz, E., Toca, C. G., & De Arambarri, P. (1982) A modification of the hydrogen peroxide method of determination of total phosphorus in natural waters. Water Research, 16, 1061-1064. https://doi.org/10.1016/0043-1354(82)90042-2

Camargo, J. A., & Alonso, Á. (2006) Ecological and toxicological effects of inorganic nitrogen pollution in aquatic ecosystems: a global assessment. Environment international, 32, 831-849. https://doi.org/10.1016/j.envint.2006.05.002

Canadian Council of Ministers of the Environment. (2007) Canadian Water Quality Guidelines for the Protection of Aquatic Life. ISBN: 1-896997-34-1. https://ccme.ca/en/res/nutrients-en-canadian-water-quality-guidelines-for-the-protection-of-aquatic-life.pdf

Caraco, N. F., Cole, J. J., & Likens, G. E. (1989) Evidence for sulphate-controlled phosphorus release from sediments of aquatic systems. Nature, 341, 316-318. https://doi.org/10.1038/341316a0

Carey, R. O., Hochmuth, G. J., Martinez, C. J., Boyer, T. H., Dukes, M. D., Toor, G. S., & Cisar, J. L. (2013) Evaluating nutrient impacts in urban watersheds: Challenges and research opportunities. Environmental Pollution, 173, 138-149. https://doi.org/10.1016/j.envpol.2012.10.004

Carey, R. O., & Migliaccio, K. W. (2009) Contribution of wastewater treatment plant effluents to nutrient dynamics in aquatic systems: a review. Environmental management, 44, 205-217. https://doi.org/10.1007/s00267-009-9309-5

Carpenter, S. R. (2005) Eutrophication of aquatic ecosystems: bistability and soil phosphorus. Proceedings of the National Academy of Sciences, 102, 10002-10005. https://doi.org/10.1073/pnas.0503959102

Carpenter, S. R., Caraco, N. F., Correll, D. L., Howarth, R. W., Sharpley, A. N., & Smith, V. H. (1998) Nonpoint pollution of surface waters with phosphorus and nitrogen. Ecological applications, 8, 559-568. https://doi.org/10.1890/1051-0761(1998)008[0559:NPOSWW]2.0.CO;2

Carter, L. J., Williams, M., Böttcher, C., & Kookana, R. S. (2015) Uptake of pharmaceuticals influences plant development and affects nutrient and hormone homeostases. Environmental science & technology, 49, 12509-12518. https://doi.org/10.1021/acs.est.5b03468

Carvalho, P. N., Basto, M. C. P., Almeida, C. M. R., & Brix, H. (2014) A review of plant–pharmaceutical interactions: from uptake and effects in crop plants to phytoremediation in constructed wetlands. Environmental Science and Pollution Research, 21, 11729-11763. https://doi.org/10.1007/s11356-014-2550-3

Chambers, J. M., & Hastie, T. J. (1992) Linear models. Chapter 4 of statistical models in S. Wadsworth & Brooks/Cole, 1992.

Chang, N. B., Lu, J. W., Chui, T. F. M., & Hartshorn, N. (2018) Global policy analysis of low impact development for stormwater management in urban regions. Land use policy, 70, 368-383. https://doi.org/10.1016/j.landusepol.2017.11.024

Chang, J. H. (1959) An evaluation of the 1948 Thornthwaite classification. Annals of the Association of American Geographers, 49, 24-30. https://doi.org/10.1111/j.1467-8306.1959.tb01594.x

Chen, D., Hu, M., Guo, Y., & Dahlgren, R. A. (2015) Influence of legacy phosphorus, land use, and climate change on anthropogenic phosphorus inputs and riverine export dynamics. Biogeochemistry, 123, 99-116. https://doi.org/10.1007/s10533-014-0055-2

Chen, X., Wang, Y., Bai, Z., Ma, L., Strokal, M., Kroeze, C., ... & Shi, X. (2022) Mitigating phosphorus pollution from detergents in the surface waters of China. Science of The Total Environment, 804, 150125. https://doi.org/10.1016/j.scitotenv.2021.150125

Chiandet, A. S., & Xenopoulos, M. A. (2011) Landscape controls on seston stoichiometry in urban stormwater management ponds. Freshwater Biology, 56, 519-529. https://doi.org/10.1111/j.1365-2427.2010.02519.x

Chiandet, A. S., & Xenopoulos, M. A. (2016) Landscape and morphometric controls on water quality in stormwater management ponds. Urban Ecosystems, 19, 1645-1663. https://doi.org/10.1007/s11252-016-0559-8

Chin, A. (2006) Urban transformation of river landscapes in a global context. Geomorphology, 79, 460-487. https://doi.org/10.1016/j.geomorph.2006.06.033

Chin, D. A. (2012) Water-quality engineering in natural systems: fate and transport processes in the water environment. John Wiley & Sons.

Chowdhury, R. B., & Chakraborty, P. (2016) Magnitude of anthropogenic phosphorus storage in the agricultural production and the waste management systems at the regional and country scales. Environmental Science and Pollution Research, 23, 15929-15940. https://doi.org/10.1007/s11356-016-6930-8

Clary, J., Jones, J., Leisenring, M., Hobson, P., & Strecker, E. (2020) International stormwater BMP database: 2020 summary statistics. The Water Research Foundation: Alexandria, VA, USA. https://www.waterrf.org/resource/international-stormwater-bmp-database-2020-summary-statistics

Clary, J., Quigley, M., Poresky, A., Earles, A., Strecker, E., Leisenring, M., & Jones, J. (2011) Integration of low-impact development into the international stormwater BMP database. Journal of Irrigation and Drainage Engineering, 137, 190-198. https://doi.org/10.1061/(asce)ir.1943-4774.0000182

Comber, S., Gardner, M., Georges, K., Blackwood, D., & Gilmour, D. (2013) Domestic source of phosphorus to sewage treatment works. Environmental Technology, 34, 1349-1358. https://doi.org/10.1080/09593330.2012.747003

Conley, D. J., Paerl, H. W., Howarth, R. W., Boesch, D. F., Seitzinger, S. P., Havens, K. E., ... & Likens, G. E. (2009) Controlling eutrophication: nitrogen and phosphorus. Science, 323, 1014-1015. https://doi.org/10.1126/science.1167755

Cooke, G. W., & Williams, R. J. B. (1973) SIGNIFICANCE OF MAN-MADE SOURCES OF PHOSPHORUS: FERTILIZERS AND FARMING: THE PHOSPHORUS INVOLVED IN AGRICULTURAL SYSTEMS AND POSSIBILITIES OF ITS MOVEMENT INTO NATURAL WATER. In Phosphorus in fresh water and the marine environment (pp. 19-33). Pergamon. https://doi.org/10.1016/B978-0-08-017697-0.50007-9

Cordell, D., Drangert, J. O., & White, S. (2009) The story of phosphorus: global food security and food for thought. Global environmental change, 19, 292-305. https://doi.org/10.1016/j.gloenvcha.2008.10.009

Cordell, D., & White, S. (2011) Peak phosphorus: clarifying the key issues of a vigorous debate about long-term phosphorus security. Sustainability, 3, 2027-2049. https://doi.org/10.3390/SU3102027

Cording, A., Hurley, S., & Adair, C. (2018) Influence of critical bioretention design factors and projected increases in precipitation due to climate change on roadside bioretention performance. Journal of Environmental Engineering, 144, 04018082. https://doi.org/10.1061/(asce)ee.1943-7870.0001411

CVC (2010) Low Impact Development Stormwater Management Planning and Design Guide. Credit Valley Conservation (CVC), downloaded on December 1, 2022 at: https://cvc.ca/wp-content/uploads/2014/04/LID-SWM-Guide-v1.0_2010_1_no-appendices.pdf

CVC (2016) Elm Drive Low Impact Development Infrastructure Performance and Assessment Technical Report (Issue May). Credit Valley Conservation (CVC) Water and Climate Change Science Division. https://files.cvc.ca/cvc/uploads/2016/06/TechReport_Elm_Drive_Final.pdf

CVC (2018) Case Study: Monitoring low impact development at the Elm Drive demonstration site. Credit Valley Conservation (CVC). https://cvc.ca/wp-content/uploads/2018/05/Elm-Drive-Low-Impact-Development-Monitoring-Case-Study_Mar-22.pdf

Czemiel Berndtsson, J. (2014) Storm water quality of first flush urban runoff in relation to different traffic characteristics. Urban Water Journal, 11, 284-296. https://doi.org/10.1080/1573062X.2013.795236

Dagenais, D., Brisson, J., & Fletcher, T. D. (2018) The role of plants in bioretention systems; does the science underpin current guidance?. Ecological Engineering, 120, 532-545. https://doi.org/10.1016/j.ecoleng.2018.07.007

Daly, E., Deletic, A., Hatt, B. E., & Fletcher, T. D. (2012) Modelling of stormwater biofilters under random hydrologic variability: a case study of a car park at Monash University, Victoria (Australia). Hydrological Processes, 26, 3416-3424. https://doi.org/10.1002/hyp.8397

Daniel, T. C., Sharpley, A. N., & Lemunyon, J. L. (1998) Agricultural phosphorus and eutrophication: A symposium overview. Journal of environmental quality, 27, 251-257. https://doi.org/10.2134/JEQ1998.00472425002700020002X

Davis, A. P. (2008) Field performance of bioretention: Hydrology impacts. Journal of hydrologic engineering, 13, 90-95. https://doi.org/10.1061/(ASCE)1084-0699(2008)13:2(90)

De-Bashan, L. E., & Bashan, Y. (2004) Recent advances in removing phosphorus from wastewater and its future use as fertilizer (1997–2003). Water research, 38, 4222-4246. https://doi.org/10.1016/j.watres.2004.07.014

Debeer, D., Hothorn, T., & Strobl, C. (2021) Package 'permimp'. http://www.maths.bristol.ac.uk/R/web/packages/permimp/permimp.pdf

Deen, T. A., Arain, M. A., Champagne, O., Chow-Fraser, P., Nagabhatla, N., & Martin-Hill, D. (2021) Evaluation of observed and projected extreme climate trends for decision making in Six Nations of the Grand River, Canada. Climate Services, 24, 100263. https://doi.org/10.1016/j.cliser.2021.100263

Deng, Z., Qiu, X., Liu, J., Madras, N., Wang, X., & Zhu, H. (2016) Trend in frequency of extreme precipitation events over Ontario from ensembles of multiple GCMs. Climate dynamics, 46, 2909-2921. https://doi.org/10.1007/s00382-015-2740-9

Desmidt, E., Ghyselbrecht, K., Zhang, Y., Pinoy, L., Van Der Bruggen, B., Verstraete, W., Rabaey, K., & Meesschaert, B. (2015) Global Phosphorus Scarcity and Full-Scale P-Recovery Techniques: A Review. Critical Reviews in Environmental Science and Technology, 45, 336–384. https://doi.org/10.1080/10643389.2013.866531

Dessborn, L., Hessel, R., & Elmberg, J. (2016) Geese as vectors of nitrogen and phosphorus to freshwater systems. Inland Waters, 6, 111–122. https://doi.org/10.5268/IW-6.1.897

Diaz, R. J., & Rosenberg, R. (2008) Spreading dead zones and consequences for marine ecosystems. Science, 321, 926–929. https://doi.org/10.1126/science.1156401

DiBlasi, C. J., Li, H., Davis, A. P., & Ghosh, U. (2009) Removal and fate of polycyclic aromatic hydrocarbon pollutants in an urban stormwater bioretention facility. Environmental Science & Technology, 43, 494–502. https://doi.org/10.1021/es802090g

Dietz, M. E., & Clausen, J. C. (2005) A field evaluation of rain garden flow and pollutant treatment. Water, Air, and Soil Pollution, 167, 123-138. https://doi.org/10.1007/s11270-005-8266-8

Ding, B., Rezanezhad, F., Gharedaghloo, B., Van Cappellen, P., & Passeport, E. (2019) Bioretention cells under cold climate conditions: Effects of freezing and thawing on water infiltration, soil structure, and nutrient removal. Science of the Total Environment, 649, 749-759. https://doi.org/10.1016/j.scitotenv.2018.08.366

Dinov, I. D. (2018) Data science and predictive analytics. Cham, Switzerland: Springer. https://doi.org/10.1007/978-3-319-72347-1

Dodds, W. K., & Smith, V. H. (2016) Nitrogen, phosphorus, and eutrophication in streams. Inland Waters, 6, 155-164. https://doi.org/10.5268/IW-6.2.909

Drake, J., & Guo, Y. (2008) Maintenance of Wet Stormwater Ponds in Ontario. Canadian Water Resources Journal, 33, 351–368. https://doi.org/10.4296/cwrj3304351

Driscoll, E. D., Palhegyi, G. E., Strecker, E. W., & Shelley, P. E. (1989) Analysis of storm events characteristics for selected rainfall gauges throughout the United States. US Environmental Protection Agency, Washington, DC. https://www.nrc.gov/docs/ML1232/ML12320A112.pdf

Duan, S., Kaushal, S. S., Groffman, P. M., Band, L. E., & Belt, K. T. (2012) Phosphorus export across an urban to rural gradient in the Chesapeake Bay watershed. Journal of Geophysical Research: Biogeosciences, 117(G1). https://doi.org/10.1029/2011JG001782

Duan, S., Newcomer-Johnson, T., Mayer, P., & Kaushal, S. (2016) Phosphorus Retention in Stormwater Control Structures across Streamflow in Urban and Suburban Watersheds. Water, 8, 390. https://doi.org/10.3390/w8090390

Dudula, J., & Randhir, T. O. (2016) Modeling the influence of climate change on watershed systems: Adaptation through targeted practices. Journal of Hydrology, 541, 703–713. https://doi.org/10.1016/j.jhydrol.2016.07.020

Dunne, E. J., & Reddy, K. R. (2005) Phosphorus biogeochemistry of wetlands in agricultural watersheds. Nutrient management in agricultural watersheds: a wetland solution. Wageningen, The Netherlands: Wageningen Academic Publishers, 105-119. https://doi.org/10.3920/978-90-8686-558-1

Dussaillant, A., Cozzetto, K., Brander, K., & Potter, K. (2003) Green-Ampt model of a rain garden and comparison to Richards equation model. WIT Transactions on Ecology and the Environment, 67. https://doi.org/10.2495/SPD030841

Dussaillant, A. R., Wu, C. H., & Potter, K. W. (2004) Richards equation model of a rain garden. Journal of Hydrologic Engineering, 9, 219-225. https://doi.org/10.1061/(ASCE)1084-0699(2004)9:3(219)

Duval, T. P. (2018) Effect of residential development on stream phosphorus dynamics in headwater suburbanizing watersheds of southern Ontario, Canada. Science of the Total Environment, 637, 1241–1251. https://doi.org/10.1016/j.scitotenv.2018.04.437

Engelbrecht, R. S., & Morgan, J. J. (1961) Land drainage as a source of phosphorus in Illinois surface waters. Trans. Semin. Algae & Metro. Wastes, 1960, 74–79.

Environment and Climate Change Canada, & Ontario Ministry of the Environment and Climate Change. (2018) Canada-Ontario Lake Erie Action Plan: Partnering on Achieving Phosphorus Loading Reductions to Lake Erie from Canadian Sources. Queen's Printer for Ontario. ISBN: 978-0-660-25269-8. https://www.canada.ca/content/dam/eccc/documents/pdf/great-lakes-protection/dap/action_plan.pdf

Erickson, A. J., Gulliver, J. S., & Weiss, P. T. (2007) Enhanced Sand Filtration for Storm Water Phosphorus Removal. Journal of Environmental Engineering, 133, 485–497. https://doi.org/10.1061/(ASCE)0733-9372(2007)133:5(485)

Fang, H., Jamali, B., Deletic, A., & Zhang, K. (2021) Machine learning approaches for predicting the performance of stormwater biofilters in heavy metal removal and risk mitigation. Water Research, 200, 117273. https://doi.org/10.1016/j.watres.2021.117273

Farrauto, R. J., Deeba, M., & Alerasool, S. (2019) Gasoline automobile catalysis and its historical journey to cleaner air. Nature Catalysis, 2, 603–613. https://doi.org/10.1038/s41929-019-0312-9

Filippelli, G. M. (2008) The global phosphorus cycle: past, present, and future. Elements, 4, 89–95. https://doi.org/10.2113/GSELEMENTS.4.2.89

Fissore, C., Baker, L. A., Hobbie, S. E., King, J. Y., McFadden, J. P., Nelson, K. C., & Jakobsdottir, I. (2011) Carbon, nitrogen, and phosphorus fluxes in household ecosystems in the Minneapolis-Saint Paul, Minnesota, urban region. Ecological Applications, 21, 619–639. https://doi.org/10.1890/10-0386.1

Fletcher, T. D., Shuster, W., Hunt, W. F., Ashley, R., Butler, D., Arthur, S., Trowsdale, S., Barraud, S., Semadeni-Davies, A., Bertrand-Krajewski, J. L., Mikkelsen, P. S., Rivard, G., Uhl, M., Dagenais, D., & Viklander, M. (2015) SUDS, LID, BMPs, WSUD and more – The evolution and application of terminology surrounding urban drainage. Urban Water Journal, 12, 525–542. https://doi.org/10.1080/1573062X.2014.916314

Föhse, D., Claassen, N., & Jungk, A. (1991) Phosphorus efficiency of plants. Plant and Soil, 132, 261-272. https://doi.org/10.1007/BF00010407

Forzieri, G., Bianchi, A., e Silva, F. B., Herrera, M. A. M., Leblois, A., Lavalle, C., Aerts, J. C. J. H., & Feyen, L. (2018) Escalating impacts of climate extremes on critical infrastructures in Europe. Global Environmental Change, 48, 97–107. https://doi.org/10.1016/j.gloenvcha.2017.11.007

Fowdar, H. S., Hatt, B. E., Cresswell, T., Harrison, J. J., Cook, P. L., & Deletic, A. (2017) Phosphorus fate and dynamics in greywater biofiltration systems. Environmental Science & Technology, 51, 2280-2287. https://doi.org/10.1021/acs.est.6b04181

Fraley, L. M., Miller, A. J., & Welty, C. (2009) Contribution of In-Channel Processes to Sediment Yield of an Urbanizing Watershed 1. JAWRA Journal of the American Water Resources Association, 45, 748–766. https://doi.org/10.1111/j.1752-1688.2009.00320.x

Franco, D. S. P., Georgin, J., Campo, L. A. V., Mayoral, M. A., Goenaga, J. O., Fruto, C. M., Neckel, A., Oliveira, M. L., & Ramos, C. G. (2022) The environmental pollution caused by cemeteries and cremations: A review. Chemosphere, 136025. https://doi.org/10.1016/j.chemosphere.2022.136025

Fraser, A. N., Zhang, Y., Sakowski, E. G., & Preheim, S. P. (2018) Dynamics and functional potential of stormwater microorganisms colonizing sand filters. Water (Switzerland), 10. https://doi.org/10.3390/w10081065

Frost, P. C., Prater, C., Scott, A. B., Song, K., & Xenopoulos, M. A. (2019) Mobility and Bioavailability of Sediment Phosphorus in Urban Stormwater Ponds. Water Resources Research, 55, 3680–3688. https://doi.org/10.1029/2018WR023419

Gächter, R., & Müller, B. (2003). Why the phosphorus retention of lakes does not necessarily depend on the oxygen supply to their sediment surface. Limnology and Oceanography, 48(2), 929-933. https://doi.org/10.4319/lo.2003.48.2.0929

Gao, C., Liu, J., Zhu, J., & Wang, Z. W. (2013) Review of Current Research on Urban Low-impact Development Practices. Research Journal of Chemistry and Environment, 17, 209–214.

Gao, Y., Church, S. P., Peel, S., & Prokopy, L. S. (2018) Public perception towards river and water conservation practices: Opportunities for implementing urban stormwater management practices. Journal of Environmental Management, 223, 478–488. https://doi.org/10.1016/j.jenvman.2018.06.059

German, J., Svensson, G., Gustafsson, L. G., & Vikström, M. (2003) Modelling of temperature effects on removal efficiency and dissolved oxygen concentrations in stormwater ponds. Water Science and Technology, 48, 145–154. https://doi.org/10.2166/wst.2003.0513

Geronimo, F. K. F., Maniquiz-Redillas, M. C., & Kim, L. H. (2015) Fate and removal of nutrients in bioretention systems. *Desalination and Water Treatment*, *53*, 3072-3079. https://doi.org/10.1080/19443994.2014.922308

Gill, S. E., Handley, J. F., Ennos, A. R., & Pauleit, S. (2007) Adapting Cities for Climate Change: The Role of the Green Infrastructure. Built Env., 33. https://doi.org/10.2148/benv.33.1.115

Glorot, X., & Bengio, Y. (2010) Understanding the difficulty of training deep feedforward neural networks. Proceedings of the Thirteenth International Conference on Artificial Intelligence and Statistics, 249–256. Available from https://proceedings.mlr.press/v9/glorot10a.html.

Goh, H. W., Lem, K. S., Azizan, N. A., Chang, C. K., Talei, A., Leow, C. S., & Zakaria, N. A. (2019) A review of bioretention components and nutrient removal under different climates—future directions for tropics. Environmental Science and Pollution Research, 26, 14904-14919. https://doi.org/10.1007/s11356-019-05041-0

Goor, J., Cantelon, J., Smart, C. C., & Robinson, C. E. (2021) Seasonal performance of field bioretention systems in retaining phosphorus in a cold climate: Influence of prolonged road salt application. Science of The Total Environment, 778, 146069. https://doi.org/10.1016/j.scitotenv.2021.146069

Greenwell, B. M. (2017) pdp: An R package for constructing partial dependence plots. R J., 9, 421. https://journal.r-project.org/articles/RJ-2017-016/RJ-2017-016.pdf

Groffman, P. M., Law, N. L., Belt, K. T., Band, L. E., & Fisher, G. T. (2004) Nitrogen fluxes and retention in urban watershed ecosystems. Ecosystems, 7, 393–403. https://doi.org/10.1007/s10021-003-0039-x

Hager, J., Hu, G., Hewage, K., & Sadiq, R. (2019) Performance of low-impact development best management practices: a critical review. Environmental Reviews, 27, 17-42. https://doi.org/10.1139/er-2018-0048

Hammer, T. R. (1972) Stream channel enlargement due to urbanization. Water Resources Research, 8, 1530–1540. https://doi.org/10.1029/WR008i006p01530

Han, H., Bosch, N., & Allan, J. D. (2011) Spatial and temporal variation in phosphorus budgets for 24 watersheds in the Lake Erie and Lake Michigan basins. Biogeochemistry, 102, 45–58. https://doi.org/10.1007/s10533-010-9420-y

Hanief, A., & Laursen, A. E. (2019) Meeting updated phosphorus reduction goals by applying best management practices in the Grand River watershed, southern Ontario. Ecological Engineering, 130, 169–175. https://doi.org/10.1016/j.ecoleng.2019.02.007

Hathaway, J. M., Brown, R. A., Fu, J. S., & Hunt, W. F. (2014) Bioretention function under climate change scenarios in North Carolina, USA. Journal of Hydrology, 519, 503-511. https://doi.org/10.1016/j.jhydrol.2014.07.037

Hawley, R. J., MacMannis, K. R., & Wooten, M. S. (2013) Bed coarsening, riffle shortening, and channel enlargement in urbanizing watersheds, northern Kentucky, USA. Geomorphology, 201, 111–126. https://doi.org/10.1016/j.geomorph.2013.06.013

Haygarth, P. M., Jarvie, H. P., Powers, S. M., Sharpley, A. N., Elser, J. J., Shen, J., Peterson, H. M., Chan, N.-I., Howden, N. J. K., & Burt, T. (2014) Sustainable phosphorus management and the need for a long-term perspective: The legacy hypothesis. ACS Publications.

https://doi.org/10.1021/es502852s

He, J., Vale, C., & Chu, A. (2015) Variation in Water Quality of a Stormwater Pond from Diurnal Thermal Stratification. Journal of Water Resource and Hydraulic Engineering, 4, 181–190. https://doi.org/10.5963/jwrhe0402008

He, Z., & Davis, A. P. (2011) Process modeling of storm-water flow in a bioretention cell. Journal of Irrigation and Drainage Engineering, 137, 121-131. https://doi.org/10.1061/(ASCE)IR.1943-4774.0000166

Heckman, J. R., & Kluchinski, D. (2001) Agronomics of land application of municipal collected shade tree leaves: I. Soil properties. Journal of Sustainable Agriculture, 17, 33–40. https://doi.org/10.1300/J064v17n02_05

Hellweger, F. L., Martin, R. M., Eigemann, F., Smith, D. J., Dick, G. J., & Wilhelm, S. W. (2022) Models predict planned phosphorus load reduction will make Lake Erie more toxic. Science, 376, 1001-1005. https://doi.org/10.1126/science.abm6791

Helsel, D. R., & Hirsch, R. M. (1992) Statistical methods in water resources (Vol. 49). Elsevier. https://pubs.usgs.gov/tm/04/a03/tm4a3.pdf

Henderson, C., Greenway, M., & Phillips, I. (2007) Removal of dissolved nitrogen, phosphorus and carbon from stormwater by biofiltration mesocosms. Water Science and Technology, 55, 183-191. https://doi.org/10.2166/wst.2007.108

Hobbie, S. E., Baker, L. A., Buyarski, C., Nidzgorski, D., & Finlay, J. C. (2014) Decomposition of tree leaf litter on pavement: implications for urban water quality. Urban Ecosystems, 17, 369–385. https://doi.org/10.1007/s11252-013-0329-9

Hobbie, S. E., Finlay, J. C., Janke, B. D., Nidzgorski, D. A., Millet, D. B., & Baker, L. A. (2017) Contrasting nitrogen and phosphorus budgets in urban watersheds and implications for managing urban water pollution. Proceedings of the National Academy of Sciences, 114, 4177–4182. https://doi.org/10.1073/pnas.1618536114

Hong, B., Swaney, D. P., Mörth, C.-M., Smedberg, E., Hägg, H. E., Humborg, C., Howarth, R. W., & Bouraoui, F. (2012) Evaluating regional variation of net anthropogenic nitrogen and phosphorus inputs (NANI/NAPI), major drivers, nutrient retention pattern and management implications in the multinational areas of Baltic Sea basin. Ecological Modelling, 227, 117–135. https://doi.org/10.1016/j.ecolmodel.2011.12.002

Horvath, I. R., Zhang, K., Mayer, B. K., & Parolari, A. J. (2023) Effects of Regional Climate and BMP Type on Stormwater Nutrient Concentrations in BMPs: A Meta-Analysis. Environmental Science & Technology, 57, 5079-5088.

https://doi.org/10.1021/acs.est.2c05942

Hou, E., Chen, C., Luo, Y., Zhou, G., Kuang, Y., Zhang, Y., Heenan, M., Lu, X., & Wen, D. (2018) Effects of climate on soil phosphorus cycle and availability in natural terrestrial ecosystems. Global Change Biology, 24, 3344–3356. https://doi.org/10.1111/gcb.14093

Howarth, R., & Paerl, H. W. (2008) Coastal marine eutrophication: Control of both nitrogen and phosphorus is necessary. Proceedings of the National Academy of Sciences, 105, E103–E103. https://doi.org/10.1073/pnas.0807266106

Hsieh, C. H., Davis, A. P., & Needelman, B. A. (2007) Bioretention column studies of phosphorus removal from urban stormwater runoff. Water Environment Research, 79, 177-184. https://doi.org/10.2175/106143006X111745

Hunt, W. F., Jarrett, A. R., Smith, J. T., & Sharkey, L. J. (2006) Evaluating Bioretention Hydrology and Nutrient Removal at Three Field Sites in North Carolina. Journal of Irrigation and Drainage Engineering, 132, 600–608. https://doi.org/10.1061/(asce)0733-9437(2006)132:6(600)

Hurley, S., Shrestha, P., & Cording, A. (2017) Nutrient leaching from compost: Implications for bioretention and other green stormwater infrastructure. Journal of Sustainable Water in the Built Environment, 3, 04017006. https://doi.org/10.1061/JSWBAY.0000821

Hussain, S. I., Blowes, D. W., Ptacek, C. J., Jamieson-Hanes, J. H., Wootton, B., Balch, G., & Higgins, J. (2015) Mechanisms of phosphorus removal in a pilot-scale constructed wetland/BOF slag wastewater treatment system. Environmental Engineering Science, 32, 340-352. https://doi.org/10.1089/ees.2014.0376

Imteaz, M. A., Ahsan, A., Rahman, A., & Mekanik, F. (2013) Modelling stormwater treatment systems using MUSIC: Accuracy. Resources, Conservation and Recycling, 71, 15–21. https://doi.org/10.1016/j.resconrec.2012.11.007

Indris, S. N., Rudolph, D. L., Glass, B. K., & Cappellen, P. Van. (2020) Evaluating phosphorous from vehicular emissions as a potential source of contamination to ground and surface water. Cogent Environmental Science, 6, 1794702. https://doi.org/10.1080/23311843.2020.1794702

Ippolito, J. A., Blecker, S. W., Freeman, C. L., McCulley, R. L., Blair, J. M., & Kelly, E. F. (2010) Phosphorus biogeochemistry across a precipitation gradient in grasslands of central North America. Journal of Arid Environments, 74, 954–961. https://doi.org/10.1016/j.jaridenv.2010.01.003

Jacobson, C. R. (2011) Identification and quantification of the hydrological impacts of

imperviousness in urban catchments: A review. Journal of Environmental Management, 92, 1438–1448. https://doi.org/10.1016/j.jenvman.2011.01.018

Janke, B. D., Finlay, J. C., & Hobbie, S. E. (2017) Trees and Streets as Drivers of Urban Stormwater Nutrient Pollution. Environmental Science and Technology, 51, 9569–9579. https://doi.org/10.1021/acs.est.7b02225

Janke, B. D., Finlay, J. C., Taguchi, V. J., & Gulliver, J. S. (2022) Hydrologic processes regulate nutrient retention in stormwater detention ponds. Science of the Total Environment, 823, 153722. https://doi.org/10.1016/j.scitotenv.2022.153722

Jarvie, H. P., Sharpley, A. N., Withers, P. J., Scott, J. T., Haggard, B. E., & Neal, C. (2013) Phosphorus mitigation to control river eutrophication: murky waters, inconvenient truths, and "postnormal" science. Journal of Environmental Quality, 42, 295-304. https://doi.org/10.2134/jeq2012.0085

Jarvie, H. P., Withers, J. A., & Neal, C. (2002) Review of robust measurement of phosphorus in river water: sampling, storage, fractionation and sensitivity. Hydrology and Earth System Sciences, 6, 113-131. https://doi.org/10.5194/hess-6-113-2002

Jefferson, A. J., Bhaskar, A. S., Hopkins, K. G., Fanelli, R., Avellaneda, P. M., & McMillan, S. K. (2017) Stormwater management network effectiveness and implications for urban watershed function: A critical review. Hydrological Processes, 31, 4056-4080. https://doi.org/10.1002/hyp.11347

Jenny, J.-P., Normandeau, A., Francus, P., Taranu, Z. E., Gregory-Eaves, I., Lapointe, F., Jautzy, J., Ojala, A. E. K., Dorioz, J.-M., & Schimmelmann, A. (2016) Urban point sources of nutrients were the leading cause for the historical spread of hypoxia across European lakes. Proceedings of the National Academy of Sciences, 113, 12655–12660. https://doi.org/10.1073/pnas.1605480113

Jerry S. Olson. (1963) Energy Storage and the Balance of Producers and Decomposers in Ecological Systems. Ecology, 44, 322–331. https://doi.org/10.2307/1932179

Johnson, J. P., & Hunt, W. F. (2016) Evaluating the spatial distribution of pollutants and associated maintenance requirements in an 11 year-old bioretention cell in urban Charlotte, NC. Journal of Environmental Management, 184, 363–370. https://doi.org/10.1016/j.jenvman.2016.10.009

Jones, C. A., Cole, C. V., Sharpley, A. N., & Williams, J. R. (1984) A Simplified Soil and Plant Phosphorus Model: I. Documentation. Soil Science Society of America Journal, 48, 800–805. https://doi.org/10.2136/sssaj1984.03615995004800040020x

Jönsson, H., Stintzing, A. R., Vinnerås, B., & Salomon, E. (2004) Guidelines on the use of urine and faeces in crop production. EcoSanRes Programme.

Kabir, M. I., Daly, E., & Maggi, F. (2017) Geochemical modelling of heavy metals in urban stormwater biofilters. Ecological Engineering, 102, 565-576. https://doi.org/10.1016/j.ecoleng.2017.02.064

Kadlec, R. H., & Wallace, S. (2008) Treatment wetlands. CRC press. https://doi.org/10.1201/9781420012514

Kalinosky, P. M. (2015) Quantifying solids and nutrient recovered through street sweeping in a suburban watershed. University of Minnesota. https://www.proquest.com/docview/1696068860?pq-origsite=gscholar&fromopenview=true

Kalmykova, Y., Harder, R., Borgestedt, H., & Svanäng, I. (2012) Pathways and management of phosphorus in urban areas. Journal of Industrial Ecology, 16, 928–939. https://doi.org/10.1111/j.1530-9290.2012.00541.x

Kao, N., Mohamed, M., Sorichetti, R. J., Niederkorn, A., Van Cappellen, P., & Parsons, C. T. (2022) Phosphorus retention and transformation in a dammed reservoir of the Thames River, Ontario: Impacts on phosphorus load and speciation. Journal of Great Lakes Research, 48, 84–96. https://doi.org/10.1016/j.jglr.2021.11.008

Karatzoglou, A., Smola, A., Hornik, K., & Karatzoglou, M. A. (2019) Package 'kernlab.' CRAN R Project. http://cran.rediris.es/web/packages/kernlab/kernlab.pdf

Karjalainen, P., Pirjola, L., Heikkilä, J., Lähde, T., Tzamkiozis, T., Ntziachristos, L., Keskinen, J., & Rönkkö, T. (2014) Exhaust particles of modern gasoline vehicles: A laboratory and an on-road study. Atmospheric Environment, 97, 262–270. https://doi.org/10.1016/j.atmosenv.2014.08.025

Katsev, S., Tsandev, I., L'Heureux, I., & Rancourt, D. G. (2006) Factors controlling long-term phosphorus efflux from lake sediments: Exploratory reactive-transport modeling. Chemical Geology, 234, 127–147. https://doi.org/10.1016/j.chemgeo.2006.05.001

Kaushal, S. S., Likens, G. E., Pace, M. L., Haq, S., Wood, K. L., Galella, J. G., Morel, C., Doody, T. R., Wessel, B., & Kortelainen, P. (2019) Novel 'chemical cocktails'' in inland waters are a consequence of the freshwater salinization syndrome.' Philosophical Transactions of the Royal Society B, 374, 20180017. https://doi.org/10.1098/rstb.2018.0017

Kaushal, S. S., Mayer, P. M., Vidon, P. G., Smith, R. M., Pennino, M. J., Newcomer, T. A., Duan, S., Welty, C., & Belt, K. T. (2014) Land use and climate variability amplify carbon, nutrient,

and contaminant pulses: a review with management implications. JAWRA Journal of the American Water Resources Association, 50, 585–614. https://doi.org/10.1111/jawr.12204

Kaushal, S. S., Reimer, J. E., Mayer, P. M., Shatkay, R. R., Maas, C. M., Nguyen, W. D., Boger, W. L., Yaculak, A. M., Doody, T. R., & Pennino, M. J. (2022) Freshwater salinization syndrome alters retention and release of chemical cocktails along flowpaths: From stormwater management to urban streams. Freshwater Science, 41, 420–441. https://doi.org/10.1086/721469

Kaykhosravi, S., Abogadil, K., Khan, U. T., & Jadidi, M. A. (2019) The low-impact Development Demand Index: A new approach to identifying locations for LID. Water (Switzerland), 11. https://doi.org/10.3390/w11112341

Kelly, J. M., Barber, S. A., & Edwards, G. S. (1992) Modeling magnesium, phosphorus and potassium uptake by loblolly pine seedlings using a Barber-Cushman approach. Plant and Soil, 139, 209-218. https://doi.org/10.1007/BF00009312

Khan, U. T., Valeo, C., Chu, A., & He, J. (2013) A data driven approach to bioretention cell performance: prediction and design. Water, 5, 13-28. https://doi.org/10.3390/w5010013

Kim, S. Y., & Koretsky, C. (2011) Influence of NaCl and CaCl2 on lake sediment biogeochemistry. Applied Geochemistry, 26, S198-S201. https://doi.org/10.1016/j.apgeochem.2011.03.103

Kim, Y., & Newman, G. (2019) Climate change preparedness: Comparing future urban growth and flood risk in Amsterdam and Houston. Sustainability, 11, 1048. https://doi.org/10.3390/su11041048

Koch, B. J., Febria, C. M., Gevrey, M., Wainger, L. A., & Palmer, M. A. (2014) Nitrogen removal by stormwater management structures: A data synthesis. JAWRA Journal of the American Water Resources Association, 50, 1594-1607. https://doi.org/10.1111/jawr.12223

Komlos, J., & Traver, R. G. (2012) Long-term orthophosphate removal in a field-scale storm-water bioinfiltration rain garden. Journal of Environmental Engineering, 138, 991-998. https://doi.org/10.1061/(asce)ee.1943-7870.0000566

Kratky, H., Li, Z., Chen, Y., Wang, C., Li, X., & Yu, T. (2017) A critical literature review of bioretention research for stormwater management in cold climate and future research recommendations. Frontiers of Environmental Science & Engineering, 11, 1-15. https://doi.org/10.1007/s11783-017-0982-y

Ku, J., Liang, J., Ulrich, A., & Liu, Y. (2016) Sulfide production and management in municipal stormwater retention ponds. Journal of Environmental Engineering, 142, 04015071.

https://doi.org/10.1061/(ASCE)EE.1943-7870.0001026

Kuusisto, E. (1980) On the values and variability of degree-day melting factor in Finland. Hydrology Research, 11, 235-242. https://doi.org/10.2166/nh.1980.0011

Ladwig, R., Rock, L. A., & Dugan, H. A. (2023) Impact of salinization on lake stratification and spring mixing. Limnology and Oceanography Letters, 8, 93-102. https://doi.org/10.1002/lol2.10215

Laio, F., Porporato, A., Fernandez-Illescas, C. P., & Rodriguez-Iturbe, I. (2001) Plants in water-controlled ecosystems: active role in hydrologic processes and response to water stress: IV. Discussion of real cases. Advances in Water Resources, 24, 745-762. https://doi.org/10.1016/S0309-1708(01)00007-0

Lange, K., Österlund, H., Viklander, M., & Blecken, G. T. (2020) Metal speciation in stormwater bioretention: Removal of particulate, colloidal and truly dissolved metals. Science of the Total Environment, 724, 138121. https://doi.org/10.1016/j.scitotenv.2020.138121

Lapointe, M., Rochman, C. M., & Tufenkji, N. (2022) Sustainable strategies to treat urban runoff needed. Nature Sustainability, 5, 366-369. https://doi.org/10.1038/s41893-022-00853-4

Lee, J. H., Bang, K. W., Ketchum Jr, L. H., Choe, J. S., & Yu, M. J. (2002) First flush analysis of urban storm runoff. Science of the total environment, 293, 163-175. https://doi.org/10.1016/S0048-9697(02)00006-2

LeFevre, G. H., Paus, K. H., Natarajan, P., Gulliver, J. S., Novak, P. J., & Hozalski, R. M. (2015) Review of dissolved pollutants in urban storm water and their removal and fate in bioretention cells. Journal of Environmental Engineering, 141, 04014050. https://doi.org/10.1061/(ASCE)EE.1943-7870.0000876

Legates, D. R., & McCabe Jr, G. J. (1999) Evaluating the use of “goodness-of-fit” measures in hydrologic and hydroclimatic model validation. Water Resources Research, 35, 233-241. https://doi.org/10.1029/1998WR900018

Li, B., & Brett, M. T. (2013) The influence of dissolved phosphorus molecular form on recalcitrance and bioavailability. Environmental Pollution, 182, 37-44. https://doi.org/10.1016/j.envpol.2013.06.024

Li, D., Wan, J., Ma, Y., Wang, Y., Huang, M., & Chen, Y. (2015) Stormwater runoff pollutant loading distributions and their correlation with rainfall and catchment characteristics in a rapidly industrialized city. PloS one, 10, e0118776. https://doi.org/10.1371/JOURNAL.PONE.0118776

Li, G. L., Bai, X., Yu, S., Zhang, H., & Zhu, Y. G. (2012) Urban phosphorus metabolism through

food consumption: The case of China. Journal of Industrial Ecology, 16, 588-599. https://doi.org/10.1111/j.1530-9290.2011.00402.x

Li, H., & Davis, A. P. (2008a) Heavy Metal Capture and Accumulation in Bioretention Media. Environmental Science & Technology, 42, 5247–5253. https://doi.org/10.1021/es702681j

Li, H., & Davis, A. P. (2008b) Urban Particle Capture in Bioretention Media. I: Laboratory and Field Studies. Journal of Environmental Engineering, 134, 409–418. https://doi.org/10.1061/(ASCE)0733-9372(2008)134:6(409)

Li, H., & Davis, A. P. (2008c). Urban Particle Capture in Bioretention Media. II: Theory and Model Development. Journal of Environmental Engineering, 134, 419–432. https://doi.org/10.1061/(ASCE)0733-9372(2008)134:6(419)

Li, J., & Davis, A. P. (2016) A unified look at phosphorus treatment using bioretention. Water Research, 90, 141-155. https://doi.org/10.1016/j.watres.2015.12.015

Li, L., & Davis, A. P. (2014) Urban stormwater runoff nitrogen composition and fate in bioretention systems. Environmental Science & Technology, 48, 3403-3410. https://doi.org/10.1021/es4055302

Liao, K. H., Deng, S., & Tan, P. Y. (2017) Blue-green infrastructure: new frontier for sustainable urban stormwater management. In Greening cities: Forms and functions (pp. 203-226). Singapore: Springer Singapore. https://doi.org/10.1007/978-981-10-4113-6_10

Limousin, G., Gaudet, J. P., Charlet, L., Szenknect, S., Barthes, V., & Krimissa, M. (2007) Sorption isotherms: A review on physical bases, modeling and measurement. Applied geochemistry, 22, 249-275. https://doi.org/10.1016/j.apgeochem.2006.09.010

Lintern, A., McPhillips, L., Winfrey, B., Duncan, J., & Grady, C. (2020) Best management practices for diffuse nutrient pollution: Wicked problems across urban and agricultural watersheds. Environmental Science & Technology, 54, 9159-9174. https://doi.org/10.1021/acs.est.9b07511

Lisogorsky, A. (2022) Field derived phosphorus accumulation rates and fractionation in bioretention cells (Master's thesis, University of Waterloo). https://uwspace.uwaterloo.ca/handle/10012/18784

Liu, J., & Davis, A. P. (2014) Phosphorus speciation and treatment using enhanced phosphorus removal bioretention. Environmental Science & Technology, 48, 607-614. https://doi.org/10.1021/es404022b

Liu, J., Van Meter, K. J., McLeod, M. M., & Basu, N. B. (2021) Checkered landscapes: hydrologic and biogeochemical nitrogen legacies along the river continuum. Environmental Research

Letters, 16, 115006. https://doi.org/10.1088/1748-9326/ac243c

Liu, Y., Engel, B. A., Flanagan, D. C., Gitau, M. W., McMillan, S. K., Chaubey, I., & Singh, S. (2018) Modeling framework for representing long-term effectiveness of best management practices in addressing hydrology and water quality problems: Framework development and demonstration using a Bayesian method. Journal of hydrology, 560, 530-545. https://doi.org/10.1016/j.jhydrol.2018.03.053

Liu, Y., Goor, J., & Robinson, C. E. (2021) Behaviour of soluble reactive phosphorus within field-scale bioretention systems. Journal of Hydrology, 601, 126597. https://doi.org/10.1016/j.jhydrol.2021.126597

Liu, Y., Wang, C., Yu, Y., Chen, Y., Du, L., Qu, X., ... & Gui, C. (2019) Effect of urban stormwater road runoff of different land use types on an urban river in Shenzhen, China. Water, 11, 2545. https://doi.org/10.3390/W11122545

Lucas, W. C., & Greenway, M. (2008) Nutrient retention in vegetated and nonvegetated bioretention mesocosms. Journal of Irrigation and Drainage Engineering, 134, 613-623. https://doi.org/10.1061/(ASCE)0733-9437(2008)134:5(613)

Lucas, W. C., & Greenway, M. (2011) Phosphorus retention by bioretention mesocosms using media formulated for phosphorus sorption: Response to accelerated loads. Journal of Irrigation and Drainage Engineering, 137, 144-153. https://doi.org/10.1061/(ASCE)IR.1943-4774.0000243

Luo, H., Guan, L., Jing, Z., He, B., Cao, X., Zhang, Z., & Tao, M. (2020) Performance evaluation of enhanced bioretention systems in removing dissolved nutrients in stormwater runoff. Applied Sciences, 10, 3148. https://doi.org/10.3390/app10093148

Lusk, M. G., & Chapman, K. (2021) Chemical fractionation of sediment phosphorus in residential urban stormwater ponds in Florida, USA. Urban Science, 5, 81. https://doi.org/10.3390/urbansci5040081

Lusk, M. G., Toor, G. S., & Inglett, P. W. (2020) Organic nitrogen in residential stormwater runoff: Implications for stormwater management in urban watersheds. Science of the Total Environment, 707, 135962. https://doi.org/10.1016/j.scitotenv.2019.135962

Maavara, T., Slowinski, S., Rezanezhad, F., Van Meter, K., & Van Cappellen, P. (2018) The role of groundwater discharge fluxes on Si: P ratios in a major tributary to Lake Erie. Science of the Total Environment, 622, 814-824. https://doi.org/10.1016/j.scitotenv.2017.12.024

Macintosh, K. A., Mayer, B. K., McDowell, R. W., Powers, S. M., Baker, L. A., Boyer, T. H., & Rittmann, B. E. (2018) Managing diffuse phosphorus at the source versus at the

sink. Environmental Science & Technology, 52, 11995-12009. https://doi.org/10.1021/acs.est.8b01143

Maharajan, T., Ceasar, S. A., Krishna, T. P. A., & Ignacimuthu, S. (2021) Management of phosphorus nutrient amid climate change for sustainable agriculture. Journal of Environmental Quality, 50, 1303-1324. https://doi.org/10.1002/jeq2.20292

Marvin, J. T., Passeport, E., & Drake, J. (2020) State-of-the-art review of phosphorus sorption amendments in bioretention media: A systematic literature review. American Society of Civil Engineers. https://doi.org/10.1061/JSWBAY.0000893

McEnroe, N. A., Buttle, J. M., Marsalek, J., Pick, F. R., Xenopoulos, M. A., & Frost, P. C. (2013) Thermal and chemical stratification of urban ponds: Are they 'completely mixed reactors'?. Urban Ecosystems, 16, 327-339. https://doi.org/10.1007/s11252-012-0258-z

McGechan, M. B., & Lewis, D. R. (2002) SW—soil and water: sorption of phosphorus by soil, part 1: principles, equations and models. Biosystems Engineering, 82, 1-24. https://doi.org/10.1006/bioe.2002.0054

McGrane, S. J. (2016) Impacts of urbanisation on hydrological and water quality dynamics, and urban water management: a review. Hydrological Sciences Journal, 61, 2295-2311. https://doi.org/10.1080/02626667.2015.1128084

McKelvie, I. D., Peat, D. M., & Worsfold, P. J. (1995) Analytical perspective. Techniques for the quantification and speciation of phosphorus in natural waters. In Analytical Proceedings Including Analytical Communications (Vol. 32, No. 10, pp. 437-445). Royal Society of Chemistry. https://doi.org/10.1039/AI9953200437

Mei, Y., Yang, X. H., Guo, Y. N., He, J., Jiang, R., Li, Y. Q., & Li, J. Q. (2012) Thermodynamic and kinetics studies of the adsorption of phosphorus by bioretention media. Thermal Science, 16, 1506-1509. https://doi.org/10.2298/TSCI1205506M

Mei, Y., Yang, X. H., Jiang, R., Di, C. L., & Zhang, X. J. (2012) Phosphorus isothermal adsorption characteristics of mulch of bioretention. Thermal Science, 16, 1358-1361. https://doi.org/10.2298/TSCI1205358M

Metson, G. S., Hale, R. L., Iwaniec, D. M., Cook, E. M., Corman, J. R., Galletti, C. S., & Childers, D. L. (2012) Phosphorus in Phoenix: a budget and spatial representation of phosphorus in an urban ecosystem. Ecological Applications, 22, 705-721. https://doi.org/10.1890/11-0865.1

Metson, G. S., Powers, S. M., Hale, R. L., Sayles, J. S., Öberg, G., MacDonald, G. K., ... & Bouwman, A. F. (2018) Socio-environmental consideration of phosphorus flows in the urban sanitation chain of contrasting cities. Regional environmental change, 18, 1387-

1401. https://doi.org/10.1007/s10113-017-1257-7

Migon, C., & Sandroni, V. (1999) Phosphorus in rainwater: Partitioning inputs and impact on the surface coastal ocean. Limnology and Oceanography, 44, 1160-1165. https://doi.org/10.4319/lo.1999.44.4.1160

Miller, J. D., & Hutchins, M. (2017) The impacts of urbanisation and climate change on urban flooding and urban water quality: A review of the evidence concerning the United Kingdom. Journal of Hydrology: Regional Studies, 12, 345-362. https://doi.org/10.1016/j.ejrh.2017.06.006

Minnesota Pollution Control Agency. (2008) Minnesota Stormwater Manual. https://stormwater.pca.state.mn.us/images/b/b8/Minnesota_Stormwater_Manual.pdf

Mohamed, M. N., Wellen, C., Parsons, C. T., Taylor, W. D., Arhonditsis, G., Chomicki, K. M., ... & Haffner, D. G. (2019) Understanding and managing the re-eutrophication of Lake Erie: Knowledge gaps and research priorities. Freshwater Science, 38, 675-691. https://doi.org/10.1086/705915

Molot, L. A., Watson, S. B., Creed, I. F., Trick, C. G., McCabe, S. K., Verschoor, M. J., ... & Schiff, S. L. (2014) A novel model for cyanobacteria bloom formation: the critical role of anoxia and ferrous iron. Freshwater Biology, 59(6), 1323-1340. https://doi.org/10.1111/fwb.12334

Monchamp, M. E., Pick, F. R., Beisner, B. E., & Maranger, R. (2014) Nitrogen forms influence microcystin concentration and composition via changes in cyanobacterial community structure. PloS One, 9, e85573. https://doi.org/10.1371/journal.pone.0085573

Morée, A. L., Beusen, A. H. W., Bouwman, A. F., & Willems, W. J. (2013) Exploring global nitrogen and phosphorus flows in urban wastes during the twentieth century. Global biogeochemical cycles, 27, 836-846. https://doi.org/10.1002/gbc.20072

Morris, D. J., Speirs, D. C., Cameron, A. I., & Heath, M. R. (2014) Global sensitivity analysis of an end-to-end marine ecosystem model of the North Sea: Factors affecting the biomass of fish and benthos. *Ecological Modelling*, *273*, 251-263. https://doi.org/10.1016/j.ecolmodel.2013.11.019

Muerdter, C. P., Smith, D. J., & Davis, A. P. (2020) Impact of vegetation selection on nitrogen and phosphorus processing in bioretention containers. Water Environment Research, 92, 236-244. https://doi.org/10.1002/wer.1195

Mullane, J. M., Flury, M., Iqbal, H., Freeze, P. M., Hinman, C., Cogger, C. G., & Shi, Z. (2015) Intermittent rainstorms cause pulses of nitrogen, phosphorus, and copper in leachate from

compost in bioretention systems. Science of the Total Environment, 537, 294–303. https://doi.org/10.1016/j.scitotenv.2015.07.157

Müller, C., & Bünemann, E. K. (2014) A 33P tracing model for quantifying gross P transformation rates in soil. Soil Biology and Biochemistry, 76, 218-226. https://doi.org/10.1016/j.soilbio.2014.05.013

Nagul, E. A., McKelvie, I. D., & Kolev, S. D. (2015) The nature of the salt error in the Sn (II)-reduced molybdenum blue reaction for determination of dissolved reactive phosphorus in saline waters. Analytica Chimica Acta, 896, 120-127. https://doi.org/10.1016/j.aca.2015.09.021

Novotny, V. (2003) Incorporating diffuse pollution abatement into watershed management–watershed vulnerability. In Diffuse Pollution Conference, Dublin.

Novotny, V., Sung, H. M., Bannerman, R., & Baum, K. (1985) Estimating nonpoint pollution from small urban watersheds. Journal (Water Pollution Control Federation), 339-348. https://doi.org/10.2307/25042596

Nyenje, P. M., Foppen, J. W., Uhlenbrook, S., Kulabako, R., & Muwanga, A. (2010) Eutrophication and nutrient release in urban areas of sub-Saharan Africa—a review. Science of the total environment, 408, 447-455. https://doi.org/10.1016/j.scitotenv.2009.10.020

O'Connell, D. W., Ansems, N., Kukkadapu, R. K., Jaisi, D., Orihel, D. M., Cade-Menun, B. J., Hu, Y., Wiklund, J., Hall, R. I., Chessell, H., Behrends, T., & Van Cappellen, P. (2020) Changes in sedimentary phosphorus burial following artificial eutrophication of Lake 227, Experimental Lakes Area, Ontario, Canada. *Journal of Geophysical Research: Biogeosciences*, *125*(8), e2020JG005713. https://doi.org/10.1029/2020JG005713

O'dell, J. (1993) Environmental Protection Agency Method 350.1: Determination of Ammonia Nitrogen by Semi-Automated Colorimetry. United States Environmental Protection Agency: Washington, DC, USA, 45268.

O'Dell, J. (1993) Method 353.2, Revision 2.0: Determination of nitrate-nitrite nitrogen by automated colorimetry. Environmental Monitoring Systems Laboratory, US Environmental Protection Agency, Cincinnati, Ohio.

Oliveira, M., & Machado, A. V. (2013) The role of phosphorus on eutrophication: a historical review and future perspectives. Environmental Technology Reviews, 2, 117-127. https://doi.org/10.1080/21622515.2013.861877

Olsen, C., Dell, T., & Brim, J. (2017). Nutrient Sources in Urban Areas – A Literature Review.

https://erams.com/co-stormwater-center/wp-content/uploads/2017/09/Nutrient_Sources_Literature_Review-2017-6-5RefUpdate.pdf

Orihel, D. M., Baulch, H. M., Casson, N. J., North, R. L., Parsons, C. T., Seckar, D. C., & Venkiteswaran, J. J. (2017) Internal phosphorus loading in Canadian fresh waters: a critical review and data analysis. *Canadian Journal of Fisheries and Aquatic Sciences*, *74*, 2005-2029. https://doi.org/10.1139/cjfas-2016-0500

Orihel, D. M., Bird, D. F., Brylinsky, M., Chen, H., Donald, D. B., Huang, D. Y., Giani, A., Kinniburgh, D., Kling, H., & Kotak, B. G. (2012) High microcystin concentrations occur only at low nitrogen-to-phosphorus ratios in nutrient-rich Canadian lakes. Canadian Journal of Fisheries and Aquatic Sciences, 69, 1457-1462. https://doi.org/10.1139/f2012-088

Paerl, H. W., Havens, K. E., Xu, H., Zhu, G., McCarthy, M. J., Newell, S. E., Scott, J. T., Hall, N. S., Otten, T. G., & Qin, B. (2020) Mitigating eutrophication and toxic cyanobacterial blooms in large lakes: The evolution of a dual nutrient (N and P) reduction paradigm. Hydrobiologia, 847, 4359-4375. https://doi.org/10.1007/s10750-019-04087-y

Paerl, H. W., Scott, J. T., McCarthy, M. J., Newell, S. E., Gardner, W. S., Havens, K. E., Hoffman, D. K., Wilhelm, S. W., & Wurtsbaugh, W. A. (2016) It takes two to tango: when and where dual nutrient (N & P) reductions are needed to protect lakes and downstream ecosystems. Environmental science & technology, 50, 10805-10813. https://doi.org/10.1021/acs.est.6b02575

Palmer-Felgate, E. J., Mortimer, R. J., Krom, M. D., Jarvie, H. P., Williams, R. J., Spraggs, R. E., & Stratford, C. J. (2011) Internal loading of phosphorus in a sedimentation pond of a treatment wetland: Effect of a phytoplankton crash. Science of the total environment, 409, 2222-2232. https://doi.org/10.1016/j.scitotenv.2011.02.034

Pandey, J., Singh, A. V., Singh, A., & Singh, R. (2013) Impacts of changing atmospheric deposition chemistry on nitrogen and phosphorus loading to Ganga River (India). Bulletin of environmental contamination and toxicology, 91, 184-190. https://doi.org/10.1007/s00128-013-1016-5

Papadopoulou, M. P., Karatzas, G. P., & Bougioukou, G. G. (2007) Numerical modelling of the environmental impact of landfill leachate leakage on groundwater quality–a field application. Environmental Modeling & Assessment, 12, 43-54. https://doi.org/10.1007/s10666-006-9050-x

Papangelakis, E., MacVicar, B., & Ashmore, P. (2019) Bedload sediment transport regimes of semi-alluvial rivers conditioned by urbanization and stormwater management. Water Resources Research, 55, 10565-10587. https://doi.org/10.1029/2019WR025126

Parenago, O. P., Oganesova, E. Y., Lyadov, A. S., & Sharaeva, A. A. (2020) Synthesis of environmentally safe antiwear additives to lubricating materials: State of the art and prospects. Russian Journal of Applied Chemistry, 93, 1629-1637. https://doi.org/10.1134/S1070427220110014

Park, D., Kang, H., Jung, S. H., & Roesner, L. A. (2015) Reliability analysis for evaluation of factors affecting pollutant load reduction in urban stormwater BMP systems. Environmental Modelling & Software, 74, 130-139. https://doi.org/10.1016/j.envsoft.2015.08.010

Parsons, C. T., Rezanezhad, F., O'Connell, D. W., & Van Cappellen, P. (2017) Sediment phosphorus speciation and mobility under dynamic redox conditions. Biogeosciences, 14, 3585-3602. https://doi.org/10.5194/bg-14-3585-2017

Passeport, E., Hunt, W. F., Line, D. E., Smith, R. A., & Brown, R. A. (2009) Field study of the ability of two grassed bioretention cells to reduce storm-water runoff pollution. Journal of Irrigation and Drainage Engineering, 135, 505-510. https://doi.org/10.1061/(ASCE)IR.1943-4774.0000006

Perry, S., Garbon, J., & Lee, B. (2009) Urban Stormwater Runoff Phosphorus Loading and BMP Treatment Capabilities. Imbrium Systems. https://www.imbriumsystems.com/Portals/0/documents/sm/technical_docs/Urban%20Stormwater%20Runoff%20Phosphorus%20Loading%20and%20BMP%20Treatment%20Capabilities.pdf

Persson, J., & Wittgren, H. B. (2003) How hydrological and hydraulic conditions affect performance of ponds. Ecological Engineering, 21(4-5), 259-269. https://doi.org/10.1016/j.ecoleng.2003.12.004

Pfaff, J. D. (1993) Method 300.0 Determination of inorganic anions by ion chromatography. US Environmental Protection Agency, Office of Research and Development, Environmental Monitoring Systems Laboratory, 28.

Pianosi, F., Sarrazin, F., & Wagener, T. (2015) A Matlab toolbox for global sensitivity analysis. Environmental Modelling & Software, 70, 80-85. https://doi.org/10.1016/j.envsoft.2015.04.009

Pizzuto, J. E., Hession, W. C., & McBride, M. (2000) Comparing gravel-bed rivers in paired urban and rural catchments of southeastern Pennsylvania. Geology, 28, 79-82. https://doi.org/10.1130/0091-7613(2000)028<0079:CGRIPU>2.0.CO;2

Poor, C., Balmes, C., Freudenthaler, M., & Martinez, A. (2018) Role of mycelium in bioretention systems: Evaluation of nutrient and metal retention in mycorrhizae-inoculated mesocosms. Journal of Environmental Engineering, 144, 04018034.

https://doi.org/10.1061/(ASCE)EE.1943-7870.0001373

Pörtner, H. O., Roberts, D. C., Adams, H., Adler, C., Aldunce, P., Ali, E., Ara Begum, R., Betts, R., Bezner Kerr, R., Biesbroek, R., Birkmann, J., Bowen, K., Castellanos, E., Cissé, G., Constable, A., Cramer, W., Dodman, D., Eriksen, S. H., Fischlin, A., ... Zaiton Ibrahim, Z. (2022) Climate change 2022: impacts, adaptation and vulnerability. IPCC. https://edepot.wur.nl/565644

Powers, S. M., Bruulsema, T. W., Burt, T. P., Chan, N. I., Elser, J. J., Haygarth, P. M., ... & Zhang, F. (2016) Long-term accumulation and transport of anthropogenic phosphorus in three river basins. Nature Geoscience, 9, 353-356. https://doi.org/10.1038/ngeo2693

Powley, H. R., Durr, H. H., Lima, A. T., Krom, M. D., & Van Cappellen, P. (2016) Direct discharges of domestic wastewater are a major source of phosphorus and nitrogen to the Mediterranean Sea. Environmental science & technology, 50, 8722-8730. https://doi.org/10.1021/acs.est.6b01742

Prince George's County (Md.). Department of Environmental Resources. Programs, & Planning Division. (1999) Low-impact development: An integrated design approach. The Department.

Pyke, C., Warren, M. P., Johnson, T., LaGro Jr, J., Scharfenberg, J., Groth, P., ... & Main, E. (2011) Assessment of low impact development for managing stormwater with changing precipitation due to climate change. Landscape and Urban Planning, 103, 166-173. https://doi.org/10.1016/j.landurbplan.2011.07.006

Qiu, F., Zhao, S., Zhao, D., Wang, J., & Fu, K. (2019) Enhanced nutrient removal in bioretention systems modified with water treatment residuals and internal water storage zone. Environmental Science: Water Research & Technology, 5, 993-1003. https://doi.org/10.1039/c9ew00093c

Quinn, R., & Dussaillant, A. (2014) Predicting infiltration pollutant retention in bioretention sustainable drainage systems: model development and validation. Hydrology Research, 45, 855-867. https://doi.org/10.2166/nh.2014.146

Quynh, L. T. P., Billen, G., Garnier, J., Théry, S., Fézard, C., & Minh, C. V. (2005) Nutrient (N, P) budgets for the Red River basin (Vietnam and China). Global biogeochemical cycles, 19. https://doi.org/10.1029/2004GB002405

Radosavljevic, J., Slowinski, S., Shafii, M., Akbarzadeh, Z., Rezanezhad, F., Parsons, C. T., Withers, W., & Van Cappellen, P. (2022) Salinization as a driver of eutrophication symptoms in an urban lake (Lake Wilcox, Ontario, Canada). Science of the Total Environment, 846. https://doi.org/10.1016/j.scitotenv.2022.157336

Randelovic, A., Zhang, K., Jacimovic, N., McCarthy, D., & Deletic, A. (2016) Stormwater biofilter treatment model (MPiRe) for selected micro-pollutants. *Water research*, *89*, 180-191. https://doi.org/10.1016/j.watres.2015.11.046

RColorBrewer, S., & Liaw, M. A. (2018) Package 'randomforest'. University of California, Berkeley: Berkeley, CA, USA. https://peerj.com/articles/9945/Supplemental_Data_S11.pdf

Redfield, G. W. (2002) Atmospheric deposition of phosphorus to the Everglades: concepts, constraints, and published deposition rates for ecosystem management. The Scientific World Journal, 2, 1843-1873. https://doi.org/10.1100/tsw.2002.813

Rice, E.W., Baird, R. B., Eaton, A. D., & Clesceri, L. S. (2012) *Standard methods for the examination of water and wastewater* (Vol. 10). E. W. Rice (Ed.). Washington, DC: American public health association. 156-172. ISBN: 9780875532875. http://yabesh.ir/wp-content/uploads/2018/02/Standard-Methods-23rd-Perv.pdf

Riemersma, S., Little, J., Ontkean, G., & Moskal-Hébert, T. (2006) Phosphorus sources and sinks in watersheds: A review. 82 pp. Alberta soil phosphorus limits project, 5.

Robertson, W. D., Van Stempvoort, D. R., & Schiff, S. L. (2019) Review of phosphorus attenuation in groundwater plumes from 24 septic systems. Science of The Total Environment, 692, 640-652. https://doi.org/10.1016/j.scitotenv.2019.07.198

Romero-Lankao, P., Smith, J. B., Davidson, D. J., Diffenbaugh, N. S., Kinney, P. L., Kirshen, P., Kovacs, P., & Ruiz, L. V. (2014) IPCC 26. North America. In Fifth Assessment Report.

Roy, J. W., & Bickerton, G. (2014) Elevated dissolved phosphorus in riparian groundwater along gaining urban streams. Environmental science & technology, 48, 1492-1498. https://doi.org/10.1021/es404801y

Roy-Poirier, A., Champagne, P., & Filion, Y. (2010a) Bioretention processes for phosphorus pollution control. Environmental Reviews, 18, 159-173. https://doi.org/10.1139/A10-006

Roy-Poirier, A., Filion, Y., & Champagne, P. (2010b) Development of a Total Phosphorus Removal Model for Bioretention Systems. Journal of Water Management Modeling, 6062. https://doi.org/10.14796/JWMM.R236-20

Roy-Poirier, A., Filion, Y., & Champagne, P. (2015) An event-based hydrologic simulation model for bioretention systems. Water Science and Technology, 72, 1524-1533. https://doi.org/10.2166/wst.2015.368

Russell, K. L., Vietz, G. J., & Fletcher, T. D. (2017) Global sediment yields from urban and urbanizing watersheds. Earth-Science Reviews, 168, 73-80. https://doi.org/10.1016/j.earscirev.2017.04.001

Russell, K. L., Vietz, G. J., & Fletcher, T. D. (2019) Urban sediment supply to streams from hillslope sources. Science of the Total Environment, 653, 684-697. https://doi.org/10.1016/j.scitotenv.2018.10.374

Ruttenberg, K. C. (1992) Development of a sequential extraction method for different forms of phosphorus in marine sediments. Limnology and oceanography, 37, 1460-1482. https://doi.org/10.4319/lo.1992.37.7.1460

Rycewicz-Borecki, M., McLean, J. E., & Dupont, R. R. (2017) Nitrogen and phosphorus mass balance, retention and uptake in six plant species grown in stormwater bioretention microcosms. Ecological Engineering, 99, 409-416. https://doi.org/10.1016/j.ecoleng.2016.11.020

Ryther, J. H., & Dunstan, W. M. (1971) Nitrogen, phosphorus, and eutrophication in the coastal marine environment. Science, 171, 1008–1013. https://doi.org/10.1126/science.171.3975.1008

Sabo, R. D., Clark, C. M., Gibbs, D. A., Metson, G. S., Todd, M. J., LeDuc, S. D., Greiner, D., Fry, M. M., Polinsky, R., & Yang, Q. (2021) Phosphorus inventory for the conterminous United States (2002–2012). Journal of Geophysical Research: Biogeosciences, 126, e2020JG005684. https://doi.org/10.1029/2020JG005684

Sabur, M. A., Parsons, C. T., Maavara, T., & Van Cappellen, P. (2022) Effects of pH and Dissolved Silicate on Phosphate Mineral-Water Partitioning with Goethite. ACS Earth and Space Chemistry, 6, 34-43. https://doi.org/10.1021/acsearthspacechem.1c00197

Sakshi, S., & Singh, A. (2016) Modeling LID using SWMM5 and MIDS credit calculator: credit valley conservation's Elm Drive case study. *Journal of Water Management Modeling*. https://doi.org/10.14796/jwmm.c403

Sample, D. J., Grizzard, T. J., Sansalone, J., Davis, A. P., Roseen, R. M., & Walker, J. (2012) Assessing performance of manufactured treatment devices for the removal of phosphorus from urban stormwater. Journal of environmental management, 113, 279-291. https://doi.org/10.1016/j.jenvman.2012.08.039

Sansalone, J. J., & Ma, J. (2009) Parametric evaluation of batch equilibria for storm-water phosphorus adsorption on aluminum oxide media. Journal of Environmental Engineering, 135, 737-746. https://doi.org/10.1061/(ASCE)EE.1943-7870.0000041

Sartor, J. D., & Boyd, G. B. (1972) Water pollution aspects of street surface contaminants (Vol. 2). US Government Printing Office.

Schachtman, D. P., Reid, R. J., & Ayling, S. M. (1998) Phosphorus uptake by plants: from soil to

cell. Plant physiology, 116, 447-453. https://doi.org/10.1104/pp.116.2.447

Scherer, N. M., Gibbons, H. L., Stoops, K. B., & Muller, M. (1995) Phosphorus loading of an urban lake by bird droppings. Lake and Reservoir Management, 11, 317-327. https://doi.org/10.1080/07438149509354213

Schindler, D. W. (1974) Eutrophication and recovery in experimental lakes: implications for lake management. Science, 184, 897-899. https://doi.org/10.1126/science.184.4139.897

Schindler, D. W. (2009) Lakes as sentinels and integrators for the effects of climate change on watersheds, airsheds, and landscapes. Limnology and oceanography, 54, 2349-2358. https://doi.org/10.4319/lo.2009.54.6_part_2.2349

Schindler, D. W., Carpenter, S. R., Chapra, S. C., Hecky, R. E., & Orihel, D. M. (2016) Reducing phosphorus to curb lake eutrophication is a success. Environmental Science & Technology, 50, 8923-8929. https://doi.org/10.1021/acs.est.6b02204

Schipper, W. (2014) Phosphorus: Too big to fail. European Journal of Inorganic Chemistry, 2014, 1567-1571. https://doi.org/10.1002/ejic.201400115

Schroer, W. F., Benitez-Nelson, C. R., Smith, E. M., & Ziolkowski, L. A. (2018) Drivers of sediment accumulation and nutrient burial in coastal stormwater detention ponds, South Carolina, USA. Ecosystems, 21, 1118-1138. https://doi.org/10.1007/s10021-017-0207-z

Schueler, T. R. (1987) Controlling urban runoff: A practical manual for planning and designing urban BMPs. Washington, DC: Metropolitan Washington Council of Governments. https://hero.epa.gov/hero/index.cfm/reference/details/reference_id/2246147

Seitzinger, S., Harrison, J. A., Böhlke, J. K., Bouwman, A. F., Lowrance, R., Peterson, B., Tobias, C., & Drecht, G. V. (2006) Denitrification across landscapes and waterscapes: a synthesis. Ecological applications, 16, 2064-2090. https://doi.org/10.1890/1051-0761(2006)016[2064:DALAWA]2.0.CO;2

Semadeni-Davies, A., Hernebring, C., Svensson, G., & Gustafsson, L. G. (2008) The impacts of climate change and urbanisation on drainage in Helsingborg, Sweden: Suburban stormwater. Journal of hydrology, 350, 114-125. https://doi.org/10.1016/j.jhydrol.2007.11.006

Sercu, B., Van De Werfhorst, L. C., Murray, J. L., & Holden, P. A. (2011) Sewage exfiltration as a source of storm drain contamination during dry weather in urban watersheds. Environmental science & technology, 45, 7151-7157. https://doi.org/10.1021/es200981k

Sharma, A. K., Vezzaro, L., Birch, H., Arnbjerg-Nielsen, K., & Mikkelsen, P. S. (2016) Effect of

climate change on stormwater runoff characteristics and treatment efficiencies of stormwater retention ponds: a case study from Denmark using TSS and Cu as indicator pollutants. SpringerPlus, 5, 1-12. https://doi.org/10.1186/s40064-016-3103-7

Sharma, A., Vezzaro, L., Birch, H., Arnbjerg-Nielsen, K., & Mikkelsen, P. S. (2011) Effect of climate change on stormwater characteristics and treatment efficiencies of stormwater retention ponds. In Proceedings of the 12th International Conference on Urban Drainage.

Sharpley, A., Jarvie, H. P., Buda, A., May, L., Spears, B., & Kleinman, P. (2013) Phosphorus legacy: overcoming the effects of past management practices to mitigate future water quality impairment. Journal of environmental quality, 42, 1308-1326. https://doi.org/10.2134/jeq2013.03.0098

Shrestha, P., Hurley, S. E., & Wemple, B. C. (2018) Effects of different soil media, vegetation, and hydrologic treatments on nutrient and sediment removal in roadside bioretention systems. Ecological Engineering, 112, 116-131. https://doi.org/10.1016/j.ecoleng.2017.12.004

Singh, P., & Kumar, N. (1996) Determination of snowmelt factor in the Himalayan region. Hydrological sciences journal, 41, 301-310. https://doi.org/10.1080/02626669609491504

Skorobogatov, A., He, J., Chu, A., Valeo, C., & van Duin, B. (2020) The impact of media, plants and their interactions on bioretention performance: A review. Science of the Total Environment, 715, 136918. https://doi.org/10.1016/j.scitotenv.2020.136918

Slowinski, S., Radosavljevic, J., Graham, A., Ippolito, I., Thomas, K., Rezanezhad, F., et al. (2023) Contrasting impacts of agricultural intensification and urbanization on lake phosphorus cycling and implications for managing eutrophication. Journal of Geophysical Research: Biogeosciences, 128, e2023JG007558. https://doi.org/10.1029/2023JG007558

Small, G. E., Martensson, N., Janke, B. D., & Metson, G. S. (2023) Potential for high contribution of urban gardens to nutrient export in urban watersheds. Landscape and Urban Planning, 229, 104602. https://doi.org/10.1016/J.LANDURBPLAN.2022.104602

Smil, V. (2000) Phosphorus in the environment: natural flows and human interferences. Annual review of energy and the environment, 25, 53-88. https://doi.org/10.1146/annurev.energy.25.1.53

Smith, V. H., Wood, S. A., McBride, C. G., Atalah, J., Hamilton, D. P., & Abell, J. (2016) Phosphorus and nitrogen loading restraints are essential for successful eutrophication control of Lake Rotorua, New Zealand. Inland Waters, 6, 273-283. https://doi.org/10.5268/IW-6.2.998

Søberg, L. C., Al-Rubaei, A. M., Viklander, M., & Blecken, G. T. (2020) Phosphorus and TSS Removal by Stormwater Bioretention: Effects of Temperature, Salt, and a Submerged Zone and Their Interactions. Water, Air, and Soil Pollution, 231. https://doi.org/10.1007/s11270-020-04646-3

Sohn, W., Kim, J. H., Li, M. H., & Brown, R. (2019) The influence of climate on the effectiveness of low impact development: A systematic review. Journal of Environmental Management, 236, 365–379. https://doi.org/10.1016/j.jenvman.2018.11.041

Soldat, D. J., Petrovic, A. M., & Ketterings, Q. M. (2009) Effect of soil phosphorus levels on phosphorus runoff concentrations from turfgrass. Water, Air, and Soil Pollution, 199, 33–44. https://doi.org/10.1007/s11270-008-9857-y

Solomon, S., Plattner, G. K., Knutti, R., & Friedlingstein, P. (2009) Irreversible climate change due to carbon dioxide emissions. Proceedings of the National Academy of Sciences of the United States of America. https://doi.org/10.1073/pnas.0812721106

Song, K., Winters, C., Xenopoulos, M. A., Marsalek, J., & Frost, P. C. (2017) Phosphorus cycling in urban aquatic ecosystems: connecting biological processes and water chemistry to sediment P fractions in urban stormwater management ponds. Biogeochemistry, 132, 203–212. https://doi.org/10.1007/s10533-017-0293-1

Song, K., Xenopoulos, M. A., Buttle, J. M., Marsalek, J., Wagner, N. D., Pick, F. R., & Frost, P. C. (2013) Thermal stratification patterns in urban ponds and their relationships with vertical nutrient gradients. Journal of Environmental Management, 127, 317–323. https://doi.org/10.1016/j.jenvman.2013.05.052

Song, K., Xenopoulos, M. A., Marsalek, J., & Frost, P. C. (2015) The fingerprints of urban nutrients: dynamics of phosphorus speciation in water flowing through developed landscapes. Biogeochemistry, 125, 1–10. https://doi.org/10.1007/s10533-015-0114-3

Sorenson, J. R. (2013) Potential Reductions of Street Solids and Phosphorus in Urban Watersheds from Street Cleaning, Cambridge, Massachusetts, 2009-2011. US Department of the Interior, US Geological Survey. https://doi.org/10.3133/sir20125292

Sparkman, S. A., Hogan, D. M., Hopkins, K. G., & Loperfido, J. V. (2017) Modeling watershed-scale impacts of stormwater management with traditional versus low impact development design. JAWRA Journal of the American Water Resources Association, 53, 1081-1094. https://doi.org/10.1111/1752-1688.12559

Spraakman, S., Rodgers, T. F., Monri-Fung, H., Nowicki, A., Diamond, M. L., Passeport, E., ... & Drake, J. (2020) A need for standardized reporting: a scoping review of bioretention research 2000–2019. Water, 12, 3122. https://doi.org/10.3390/w12113122

Stammler, K. L., Taylor, W. D., & Mohamed, M. N. (2017) Long-term decline in stream total phosphorus concentrations: a pervasive pattern in all watershed types in Ontario. Journal of Great Lakes Research, 43, 930-937. https://doi.org/10.1016/j.jglr.2017.07.005

Stewart, R. D., Lee, J. G., Shuster, W. D., & Darner, R. A. (2017) Modelling hydrological response to a fully-monitored urban bioretention cell. *Hydrological Processes*, *31*(26), 4626-4638. https://doi.org/10.1002/hyp.11386

Stumm, W., & Morgan, J. J. (2012) Aquatic chemistry: chemical equilibria and rates in natural waters. John Wiley & Sons.

Symbol, E. S. C. N. E. (2007) METHOD 6010C INDUCTIVELY COUPLED PLASMA-ATOMIC EMISSION SPECTROMETRY. https://www.ssi.shimadzu.com/sites/ssi.shimadzu.com/files/pim/pim_document_file/ssi/others/14778/m_6010c.pdf

Taguchi, V. J., Olsen, T. A., Natarajan, P., Janke, B. D., Gulliver, J. S., Finlay, J. C., & Stefan, H. G. (2020) Internal loading in stormwater ponds as a phosphorus source to downstream waters. Limnology and Oceanography Letters, 5, 322-330. https://doi.org/10.1002/lol2.10155

Tarapchak, S. J. (1983) Soluble Reactive Phosphorus Measurements in Lake Water: Evidence for Molybdate-enhanced Hydrolysis (Vol. 12, No. 1, pp. 105-108). American Society of Agronomy, Crop Science Society of America, and Soil Science Society of America.

Taylor, A., Wetzel, J., Mudrock, E., King, K., Cameron, J., Davis, J., & McIntyre, J. (2018) Engineering analysis of plant and fungal contributions to bioretention performance. Water, 10, 1226. https://doi.org/10.3390/w10091226

Tebaldi, C., Hayhoe, K., Arblaster, J. M., & Meehl, G. A. (2006) Going to the extremes: an intercomparison of model-simulated historical and future changes in extreme events. Climatic change, 79, 185-211. https://doi.org/10.1007/s10584-006-9051-4

Teng, Z., & Sansalone, J. (2004) In situ partial exfiltration of rainfall runoff. II: Particle separation. *Journal of environmental engineering*, *130*(9), 1008-1020. https://doi.org/10.1061/(ASCE)0733-9372(2004)130:9(1008)

Therneau, T. M., & Atkinson, E. J. (1997) An introduction to recursive partitioning using the RPART routines (Vol. 61, p. 452). Mayo Foundation: Technical report.

Tirpak, R. A., Afrooz, A. N., Winston, R. J., Valenca, R., Schiff, K., & Mohanty, S. K. (2021) Conventional and amended bioretention soil media for targeted pollutant treatment: A

critical review to guide the state of the practice. Water Research, 189, 116648. https://doi.org/10.1016/j.watres.2020.116648

Tiveron, T., Gholamreza-Kashi, S., & Joksimovic, D. (2018) A USEPA SWMM integrated tool for determining the suspended solids reduction performance of bioretention cells. Journal of Water Management Modeling. https://doi.org/10.14796/JWMM.C443

Tolson, B. A., & Shoemaker, C. A. (2007) Dynamically dimensioned search algorithm for computationally efficient watershed model calibration. Water Resources Research, 43. https://doi.org/10.1029/2005WR004723

Tong, Y., Wang, M., Peñuelas, J., Liu, X., Paerl, H. W., Elser, J. J., Sardans, J., Couture, R.-M., Larssen, T., & Hu, H. (2020) Improvement in municipal wastewater treatment alters lake nitrogen to phosphorus ratios in populated regions. Proceedings of the National Academy of Sciences, 117, 11566–11572. https://doi.org/10.1073/pnas.1920759117

Toor, G. S., Occhipinti, M. L., Yang, Y.-Y., Majcherek, T., Haver, D., & Oki, L. (2017) Managing urban runoff in residential neighborhoods: Nitrogen and phosphorus in lawn irrigation driven runoff. PLoS One, 12, e0179151. https://doi.org/10.1371/journal.pone.0179151

Torgo, L. (2016) Data mining with R: learning with case studies. CRC press.

Totten, G. E., Shah, R., & Forester, D. (2019) Fuels and Lubricants Handbook: Technology, Properties, Performance, and Testing 2nd Edition.

Trenberth, K. E. (2011) Changes in precipitation with climate change. Climate Research. https://doi.org/10.3354/cr00953

Trimble, S. W. (1997) Contribution of stream channel erosion to sediment yield from an urbanizing watershed. Science, 278, 1442-1444. https://doi.org/10.1126/science.278.5342.1442

Troitsky, B., Zhu, D. Z., Loewen, M., van Duin, B., & Mahmood, K. (2019) Nutrient processes and modeling in urban stormwater ponds and constructed wetlands. Canadian Water Resources Journal, 44, 230-247. https://doi.org/10.1080/07011784.2019.1594390

Trommer, G., Poxleitner, M., & Stibor, H. (2020) Responses of lake phytoplankton communities to changing inorganic nitrogen supply forms. Aquatic Sciences, 82, 1-13. https://doi.org/10.1007/s00027-020-0696-2

Tufenkji, N., & Elimelech, M. (2004) Correlation Equation for Predicting Single-Collector Efficiency in Physicochemical Filtration in Saturated Porous Media. Environmental Science and Technology, 38, 529–536. https://doi.org/10.1021/es034049r

Tuppad, P., Kannan, N., Srinivasan, R., Rossi, C. G., & Arnold, J. G. (2010) Simulation of Agricultural Management Alternatives for Watershed Protection. Water Resources Management, 24, 3115–3144. https://doi.org/10.1007/s11269-010-9598-8

Turk, R. P., Kraus, H. T., Hunt, W. F., Carmen, N. B., & Bilderback, T. E. (2017) Nutrient sequestration by vegetation in bioretention cells receiving high nutrient loads. Journal of Environmental Engineering, 143, 06016009. https://doi.org/10.1061/(asce)ee.1943-7870.0001158

US Congress. (1972) Federal Water Pollution Control Act Amendments of 1972. https://www.govinfo.gov/content/pkg/STATUTE-86/pdf/STATUTE-86-Pg816.pdf

US EPA. (1982) Results of the nationwide urban runoff program (Vol. 1). Water Planning Division, US Environmental Protection Agency.

Uusitalo, R., Yli-Halla, M., & Turtola, E. (2000) Suspended soil as a source of potentially bioavailable phosphorus in surface runoff waters from clay soils. Water Research, 34, 2477–2482. https://doi.org/10.1016/S0043-1354(99)00419-4

Valenca, R., Le, H., Zu, Y., Dittrich, T. M., Tsang, D. C. W., Datta, R., Sarkar, D., & Mohanty, S. K. (2021) Nitrate removal uncertainty in stormwater control measures: Is the design or climate a culprit? Water Research, 190, 116781. https://doi.org/10.1016/j.watres.2020.116781

Valtanen, M., Sillanpää, N., & Setälä, H. (2014) The effects of urbanization on runoff pollutant concentrations, loadings and their seasonal patterns under cold climate. Water, Air, & Soil Pollution, 225, 1-16. https://doi.org/10.1007/s11270-014-1977-y

Van Meter, K. J., McLeod, M. M., Liu, J., Tenkouano, G. T., Hall, R. I., Van Cappellen, P., & Basu, N. B. (2021) Beyond the mass balance: watershed phosphorus legacies and the evolution of the current water quality policy challenge. Water Resources Research, 57, e2020WR029316. https://doi.org/10.1029/2020WR029316

Van Vliet, M. T. H., & Zwolsman, J. J. G. (2008) Impact of summer droughts on the water quality of the Meuse river. Journal of Hydrology, 353, 1-17. https://doi.org/10.1016/j.jhydrol.2008.01.001

Vaze, J., & Chiew, F. H. (2004) Nutrient loads associated with different sediment sizes in urban stormwater and surface pollutants. Journal of Environmental Engineering, 130, 391-396. https://doi.org/10.1061/(asce)0733-9372(2004)130:4(391)

Verschoor, M. J., Powe, C. R., McQuay, E., Schiff, S. L., Venkiteswaran, J. J., Li, J., & Molot, L. A. (2017). Internal iron loading and warm temperatures are preconditions for cyanobacterial

dominance in embayments along Georgian Bay, Great Lakes. Canadian Journal of Fisheries and Aquatic Sciences, 74, 1439-1453. https://doi.org/10.1139/cjfas-2016-0377

Vezzaro, L., Benedetti, L., Gevaert, V., de Keyser, W., Verdonck, F., de Baets, B., Nopens, I., Cloutier, F., Vanrolleghem, P. A., & Mikkelsen, P. S. (2014) A model library for dynamic transport and fate of micropollutants in integrated urban wastewater and stormwater systems. Environmental Modelling and Software, 53, 98–111. https://doi.org/10.1016/j.envsoft.2013.11.010

Vezzaro, L., Eriksson, E., Ledin, A., & Mikkelsen, P. S. (2011) Modelling the fate of organic micropollutants in stormwater ponds. Science of the Total Environment, 409, 2597–2606. https://doi.org/10.1016/j.scitotenv.2011.02.046

Vezzaro, L., & Mikkelsen, P. S. (2012) Application of global sensitivity analysis and uncertainty quantification indynamic modelling of micropollutants in stormwater runoff. Environmental Modelling and Software, 27–28, 40–51. https://doi.org/10.1016/j.envsoft.2011.09.012

Vezzaro, L., Sharma, A. K., Ledin, A., & Mikkelsen, P. S. (2015) Evaluation of stormwater micropollutant source control and end-of-pipe control strategies using an uncertainty-calibrated integrated dynamic simulation model. Journal of Environmental Management, 151, 56–64. https://doi.org/10.1016/j.jenvman.2014.12.013

Wallace, T. A., Ganf, G. G., & Brookes, J. D. (2008) A comparison of phosphorus and DOC leachates from different types of leaf litter in an urban environment. Freshwater Biology, 53, 1902-1913. https://doi.org/10.1111/j.1365-2427.2008.02006.x

Walpole, R. E., Myers, R. H., Myers, S. L., & Ye, K. (1993) Probability and statistics for engineers and scientists (Vol. 5). New York: Macmillan. https://books.google.ca/books/about/Probability_Statistics_for_Engineers_Sci.html?id=Th3aDAAAQBAJ&redir_esc=y

Walsh, C. J., Fletcher, T. D., & Burns, M. J. (2012) Urban stormwater runoff: a new class of environmental flow problem. https://doi.org/10.1371/journal.pone.0045814

Walsh, C. J., Roy, A. H., Feminella, J. W., Cottingham, P. D., Groffman, P. M., & Morgan, R. P. (2005) The urban stream syndrome: current knowledge and the search for a cure. Journal of the North American Benthological Society, 24, 706-723. https://doi.org/10.1899/04-028.1

Wang, J., Fu, Z., Qiao, H., & Liu, F. (2019) Assessment of eutrophication and water quality in the estuarine area of Lake Wuli, Lake Taihu, China. Science of the Total Environment, 650, 1392–1402. https://doi.org/10.1016/j.scitotenv.2018.09.137

Wang, J., Huang, J. J., & Li, J. (2020) Characterization of the pollutant build-up processes and concentration/mass load in road deposited sediments over a long dry period. Science of the Total Environment, 718, 137282. https://doi.org/10.1016/j.scitotenv.2020.137282

Wang, M., Zhang, D., Cheng, Y., & Tan, S. K. (2019) Assessing performance of porous pavements and bioretention cells for stormwater management in response to probable climatic changes. Journal of Environmental Management, 243, 157–167. https://doi.org/10.1016/j.jenvman.2019.05.012

Wang, R., Balkanski, Y., Boucher, O., Ciais, P., Peñuelas, J., & Tao, S. (2015) Significant contribution of combustion-related emissions to the atmospheric phosphorus budget. Nature Geoscience, 8, 48-54. https://doi.org/10.1038/NGEO2324

Wang, R., Zhang, X., & Li, M. H. (2019) Predicting bioretention pollutant removal efficiency with design features: A data-driven approach. Journal of Environmental Management, 242, 403-414. https://doi.org/10.1016/j.jenvman.2019.04.064

Waschbusch, R. J., Selbig, W. R., & Bannerman, R. T. (1999) Sources of phosphorus in stormwater and street dirt from two urban residential basins in Madison, Wisconsin, 1994-95 (Vol. 99, No. 4021). US Department of the Interior, US Geological Survey.

Weiss, P. T., LeFevre, G., & Gulliver, J. S. (2008) Contamination of soil and groundwater due to stormwater infiltration practices, a literature review. St. Anthony Falls Laboratory. Retrieved from the University of Minnesota Digital Conservancy, https://hdl.handle.net/11299/115341

Wilby, R. L., Whitehead, P. G., Wade, A. J., Butterfield, D., Davis, R. J., & Watts, G. (2006) Integrated modelling of climate change impacts on water resources and quality in a lowland catchment: River Kennet, UK. Journal of hydrology, 330, 204-220. https://doi.org/10.1016/j.jhydrol.2006.04.033

Williams, C. J., Frost, P. C., & Xenopoulos, M. A. (2013) Beyond best management practices: Pelagic biogeochemical dynamics in urban stormwater ponds. Ecological Applications, 23(6), 1384–1395. https://doi.org/10.1890/12-0825.1

Wironen, M. B., Bennett, E. M., & Erickson, J. D. (2018) Phosphorus flows and legacy accumulation in an animal-dominated agricultural region from 1925 to 2012. Global Environmental Change, 50, 88-99. https://doi.org/10.1016/j.gloenvcha.2018.02.017

Withers, P. J. A., & Jarvie, H. P. (2008) Delivery and cycling of phosphorus in rivers: a review. Science of the total environment, 400, 379-395. https://doi.org/10.1016/j.scitotenv.2008.08.002

Wolman, M. G., & Schick, A. P. (1967) Effects of construction on fluvial sediment, urban and suburban areas of Maryland. Water Resources Research, 3, 451-464. https://doi.org/10.1029/WR003i002p00451

Wong, T. H. F., Fletcher, T. D., Duncan, H. P., & Jenkins, G. A. (2006) Modelling urban stormwater treatment-A unified approach. Ecological Engineering, 27, 58–70. https://doi.org/10.1016/j.ecoleng.2005.10.014

World Health Organization. (2008) Guidelines for drinking-water quality: second addendum. Vol. 1, Recommendations. https://apps.who.int/iris/bitstream/handle/10665/204412/9789241547604_eng.pdf

Yang, Y. Y., Asal, S., & Toor, G. S. (2021) Residential catchments to coastal waters: Forms, fluxes, and mechanisms of phosphorus transport. Science of the Total Environment, 765. https://doi.org/10.1016/j.scitotenv.2020.142767

Yang, Y. Y., & Lusk, M. G. (2018) Nutrients in urban stormwater runoff: Current state of the science and potential mitigation options. Current Pollution Reports, 4, 112-127. https://doi.org/10.1007/s40726-018-0087-7

Yang, Y.-Y., & Toor, G. S. (2018) Stormwater runoff driven phosphorus transport in an urban residential catchment: Implications for protecting water quality in urban watersheds. Scientific Reports, 8, 11681. https://doi.org/10.1038/s41598-018-29857-x

Yangxin, Y. U., Jin, Z. H. A. O., & Bayly, A. E. (2008) Development of surfactants and builders in detergent formulations. Chinese Journal of Chemical Engineering, 16, 517-527. https://doi.org/10.1016/S1004-9541(08)60115-9

Yindong, T., Ziwei, C., Yingting, W., Miao, Q., Yuyi, W., Mengshi, Z., Yan, L., Jian, S., Hefeng, Z., & Ruonan, W. (2022) Exploring dynamics of riverine phosphorus exports under future climate change using a process-based catchment model. Journal of Hydrology, 605, 127344. https://doi.org/10.1016/j.jhydrol.2021.127344

Young, T. C., DePinto, J. V., Martin, S. C., & Bonner, J. S. (1985) Algal-available particulate phosphorus in the Great Lakes Basin. Journal of Great Lakes Research, 11, 434-446. https://doi.org/10.1016/S0380-1330(85)71788-1

Yuan, D. G., Zhang, G. L., Gong, Z. T., & Burghardt, W. (2007) Variations of soil phosphorus accumulation in Nanjing, China as affected by urban development. Journal of Plant Nutrition and Soil Science, 170, 244-249. https://doi.org/10.1002/jpln.200622035

Zahmatkesh, Z., Burian, S. J., Karamouz, M., Tavakol-Davani, H., & Goharian, E. (2015) Low-Impact Development Practices to Mitigate Climate Change Effects on Urban Stormwater

Runoff: Case Study of New York City. Journal of Irrigation and Drainage Engineering, 141, 04014043. https://doi.org/10.1061/(asce)ir.1943-4774.0000770

Zango, B.-S., Seidou, O., Sartaj, M., Nakhaei, N., & Stiles, K. (2022) Impacts of urbanization and climate change on water quantity and quality in the Carp River watershed. Journal of Water and Climate Change, 13, 786–816. https://doi.org/10.2166/wcc.2021.158

Zarnetske, J. P., Haggerty, R., Wondzell, S. M., & Baker, M. A. (2011) Dynamics of nitrate production and removal as a function of residence time in the hyporheic zone. Journal of Geophysical Research: Biogeosciences, 116. https://doi.org/10.1029/2010JG001356

Zeiger, S. J., & Hubbart, J. A. (2017) Quantifying flow interval–pollutant loading relationships in a rapidly urbanizing mixed-land-use watershed of the Central USA. Environmental Earth Sciences, 76, 1-13. https://doi.org/10.1007/s12665-017-6819-y

Zhang, B., Li, J., Li, Y., & Li, H. (2018) Adsorption characteristics of several bioretention-modified fillers for phosphorus. *Water*, *10*(7), 831. https://doi.org/10.3390/w10070831

Zhang, K., & Chui, T. F. M. (2017) Evaluating hydrologic performance of bioretention cells in shallow groundwater. Hydrological Processes, 31, 4122-4135. https://doi.org/10.1002/hyp.11308

Zhang, K., Liu, Y., Deletic, A., McCarthy, D. T., Hatt, B. E., Payne, E. G. I., Chandrasena, G., Li, Y., Pham, T., Jamali, B., Daly, E., Fletcher, T. D., & Lintern, A. (2021) The impact of stormwater biofilter design and operational variables on nutrient removal-a statistical modelling approach. Water Research, 188, 116486. https://doi.org/10.1016/j.watres.2020.116486

Zhang, K., Randelovic, A., Deletic, A., Page, D., & McCarthy, D. T. (2016) Stormwater biofilters: A new validation modelling tool. Ecological Engineering, 87, 53-61. https://doi.org/10.1016/j.ecoleng.2015.11.014

Zhang, M. K. (2004). Phosphorus accumulation in soils along an urban–rural land use gradient in Hangzhou, southeast China. Communications in soil science and plant analysis, 35, 819-833. https://doi.org/10.1081/CSS-120030360

Zhang, W., Brown, G. O., Storm, D. E., & Zhang, H. (2008) Fly-ash-amended sand as filter media in bioretention cells to improve phosphorus removal. *Water Environment Research*, *80*(6), 507-516. https://doi.org/10.2175/106143008x266823

Zhang, X., Friedl, M. A., Schaaf, C. B., Strahler, A. H., & Schneider, A. (2004) The footprint of urban climates on vegetation phenology. Geophysical research letters, 31. https://doi.org/10.1029/2004GL020137

Zhou, B., Shafii, M., Parsons, C. T., Passeport, E., Rezanezhad, F., Lisogorsky, A., & Van

Cappellen, P. (2023) Modeling multi-year phosphorus dynamics in a bioretention cell: Phosphorus partitioning, accumulation, and export. Science of The Total Environment, 876, 162749. https://doi.org/10.1016/j.scitotenv.2023.162749

Zinger, Y., Prodanovic, V., Zhang, K., Fletcher, T. D., & Deletic, A. (2021) The effect of intermittent drying and wetting stormwater cycles on the nutrient removal performances of two vegetated biofiltration designs. *Chemosphere*, *267*, 129294. https://doi.org/10.1016/j.chemosphere.2020.129294

Żychowski, J. (2012) Impact of cemeteries on groundwater chemistry: A review. Catena, 93, 29-37. https://doi.org/10.1016/j.catena.2012.01.009

Appendix A. Supplementary Material: Chapter 3

Supplementary Figures

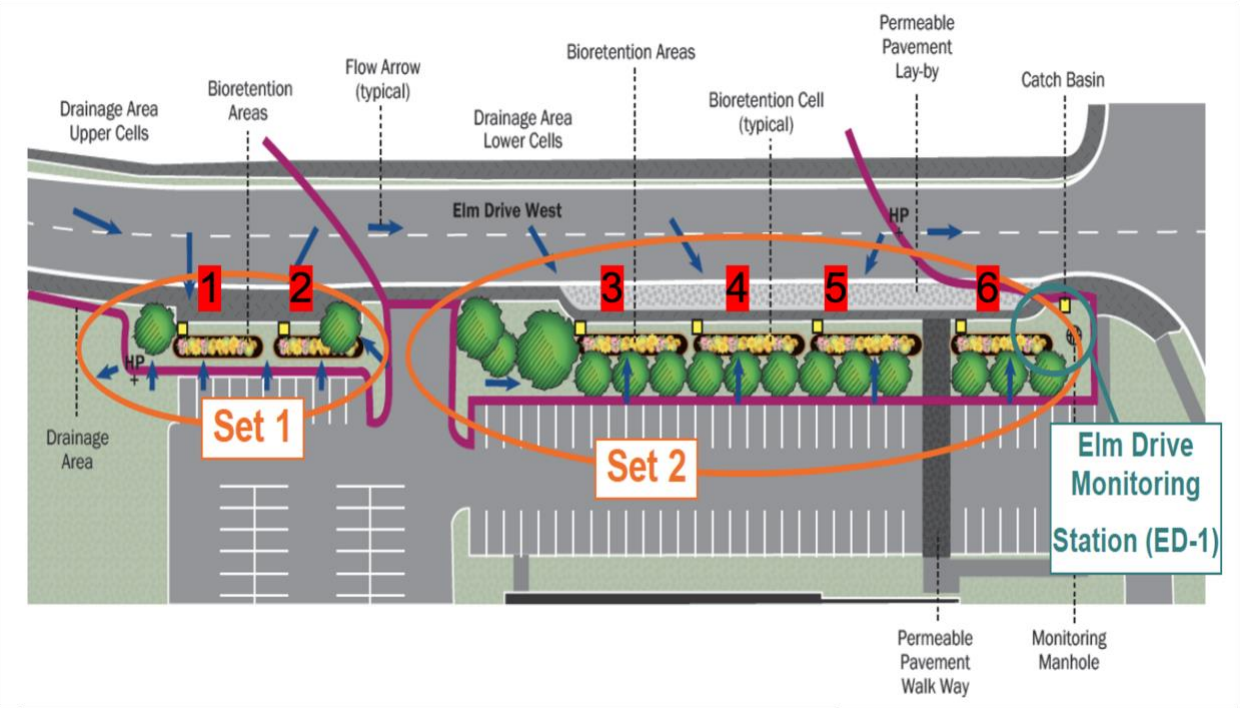

Figure AA1. Vertical view of Elm Drive bioretention cells. All 6 cells are connected by an underdrain pipe in the bedding storage layer through which water drains out of the system. Diagram adapted from CVC Technical Report (CVC Water and Climate Change Science Division, 2016).

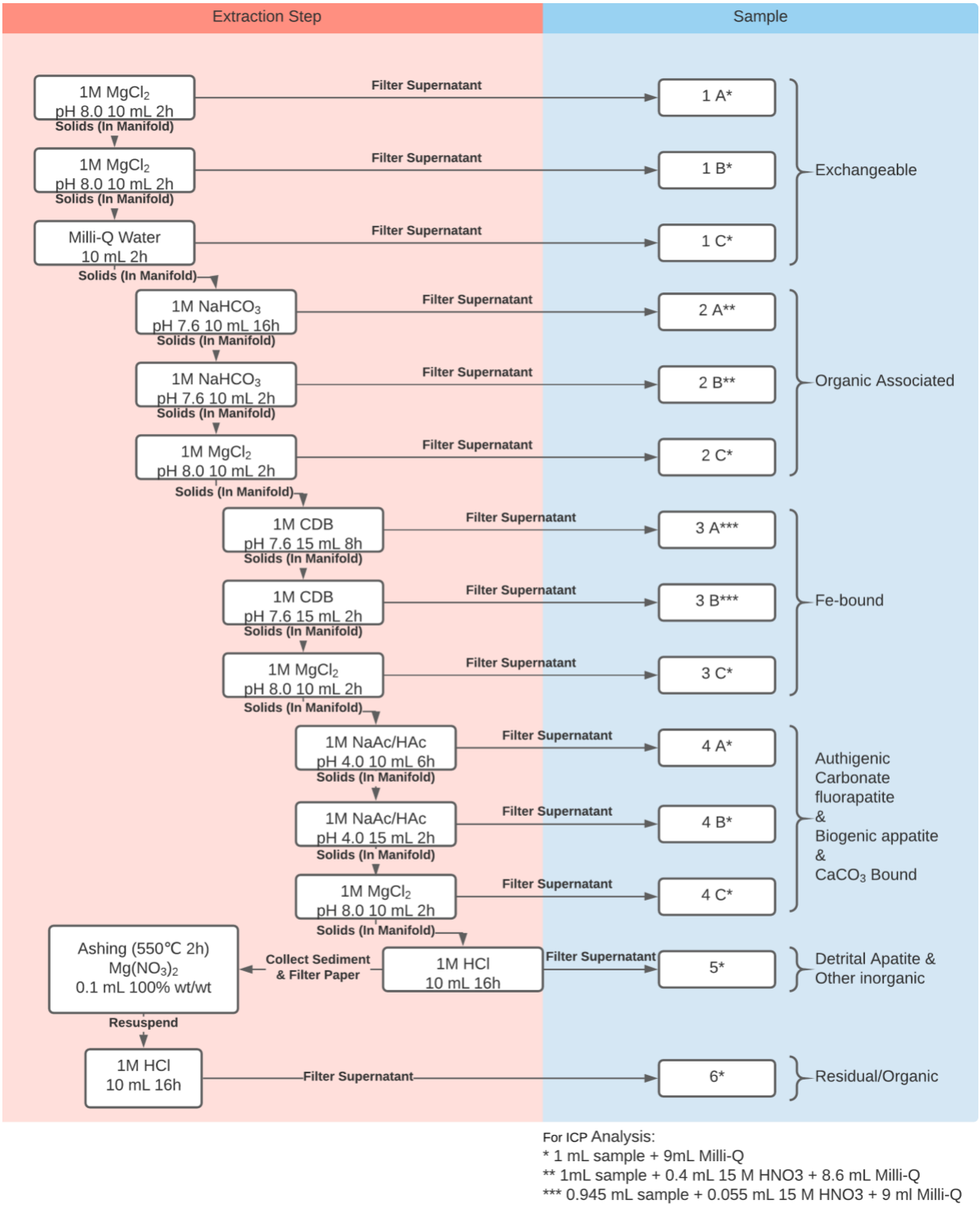

Figure AA2. Flow diagram of the modified SEDEX protocol used for the determination of phosphorus pools in filter media (modified by Parsons (2017) after Ruttenberg (1992)).

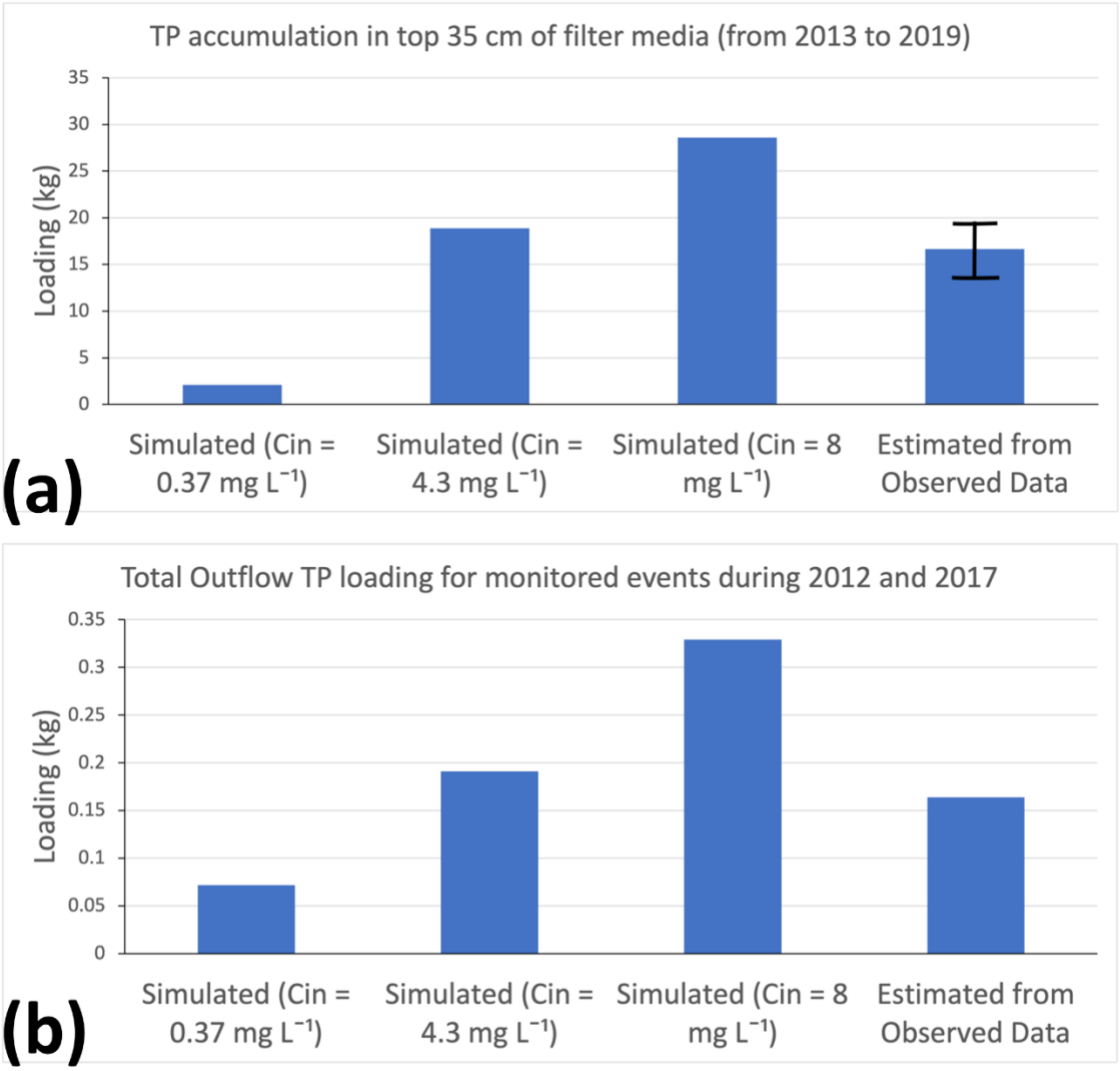

Figure AA3. (**a**) Estimated (based on observed data) versus simulated TP accumulation within the top 35 cm of filter media under different assumed inflow TP concentrations (0.37, 4.3 and 8 mg L^{-1}) during the period from 2013/10/02 to 2019/11/01. The error bar plotted in **a** shows the minimum (13 kg) and maximum (19.9 kg) possible accumulation of P loading. (**b**) Estimated (based on observed data) versus simulated total outflow TP loading for all monitored events between 2012 and 2017 under different assumed inflow TP concentrations (0.37, 4.3 and 8 mg L^{-1}).

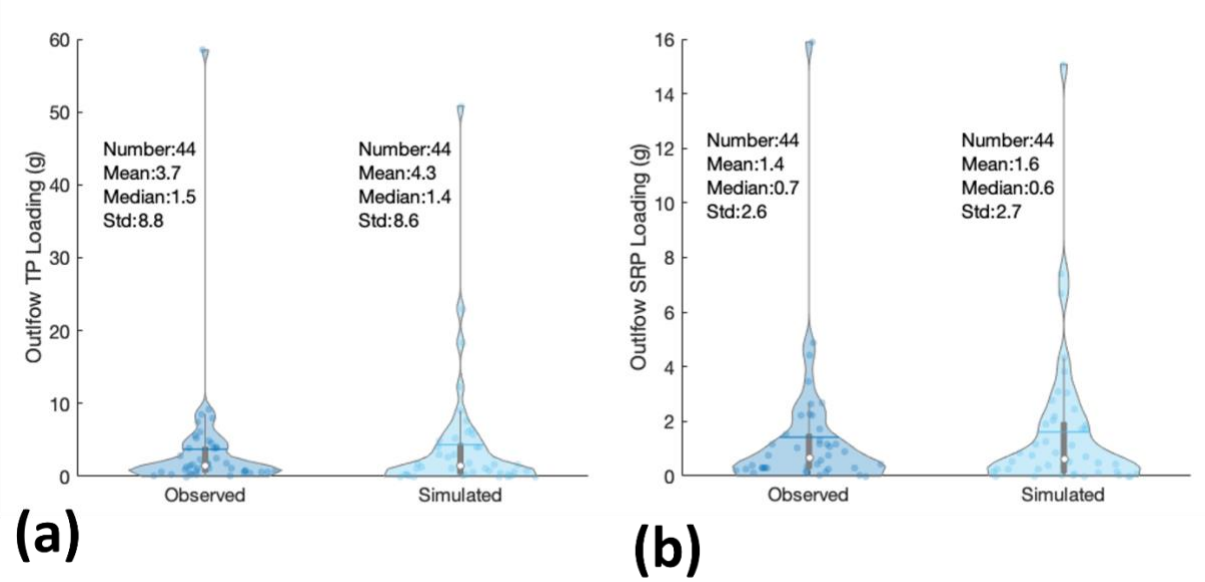

Figure AA4. Violin plots for outflow TP (**a**) and SRP (**b**) loadings of monitored events estimated from observed data and simulated results. Data number, mean, median and standard deviation (Std) values for each violin plot are shown in the figure.

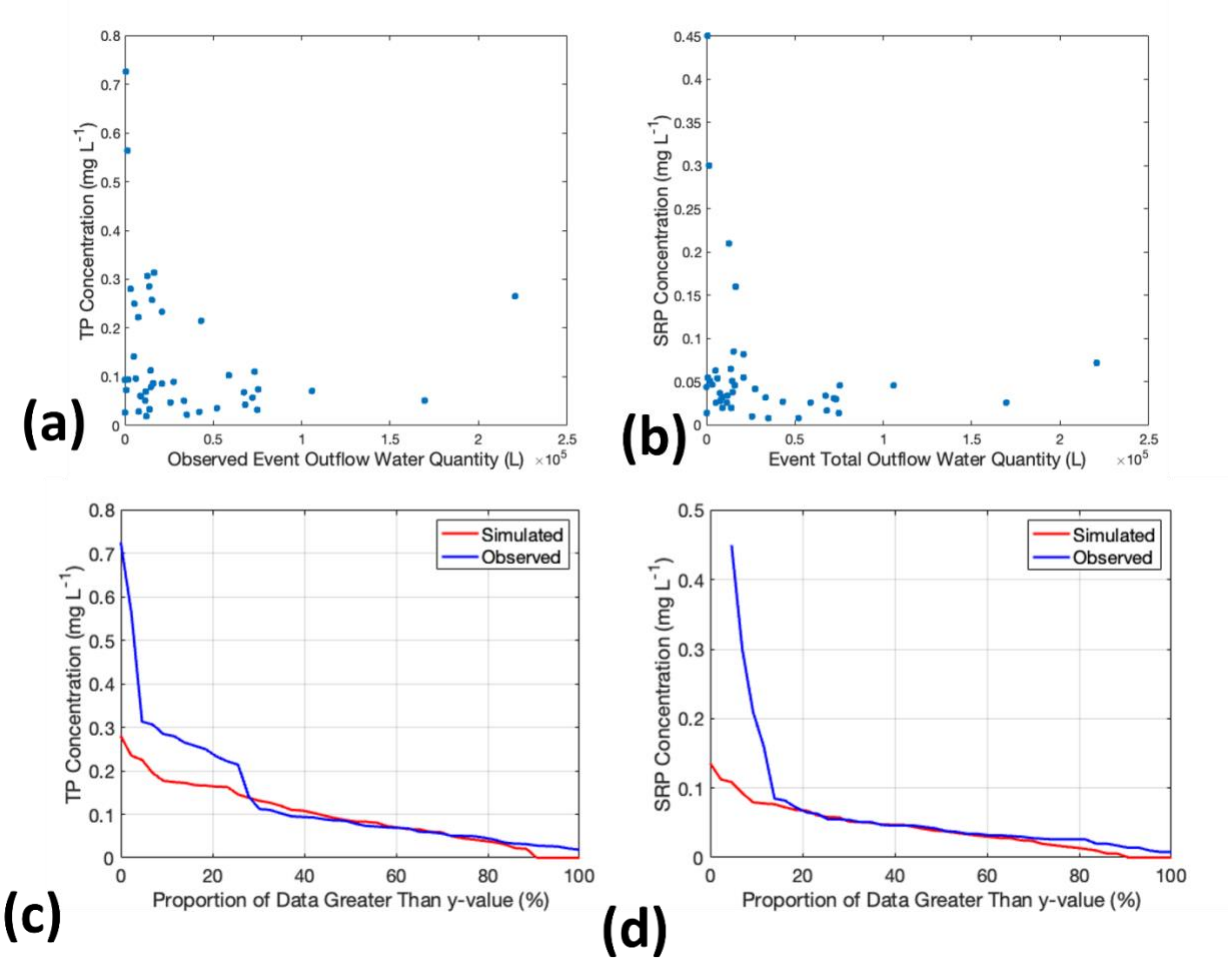

Figure AA5. (**a**) and (**b**): C-Q (concentration-flow) plot for observed EMC TP and SRP data, which shows that concentration may decrease as flow increases for both TP and SRP; (**c**) and (**d**): Duration curves of simulated and observed outflow TP and SRP concentration, which shows that model performance is superior when predicting events with lower outflow TP and SRP concentration.

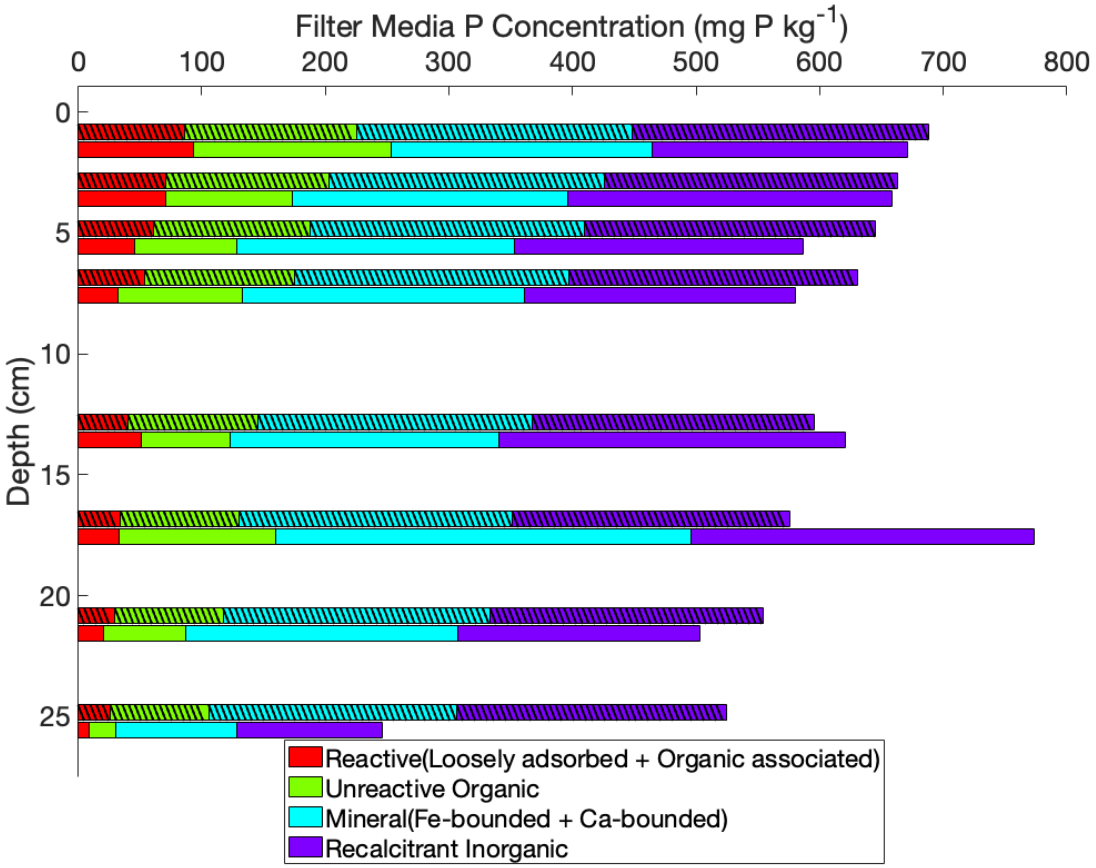

Figure AA6. Measured (bottom, unshaded bars) and modeled (top, shaded bars) concentrations of different P pools in the filter media layer (aka, the soil) as a function of depth. The measured results were obtained from the SEDEX extractions on core samples collected on November 1, 2019 (see section *3.3.1* in Chapter 3 for details).

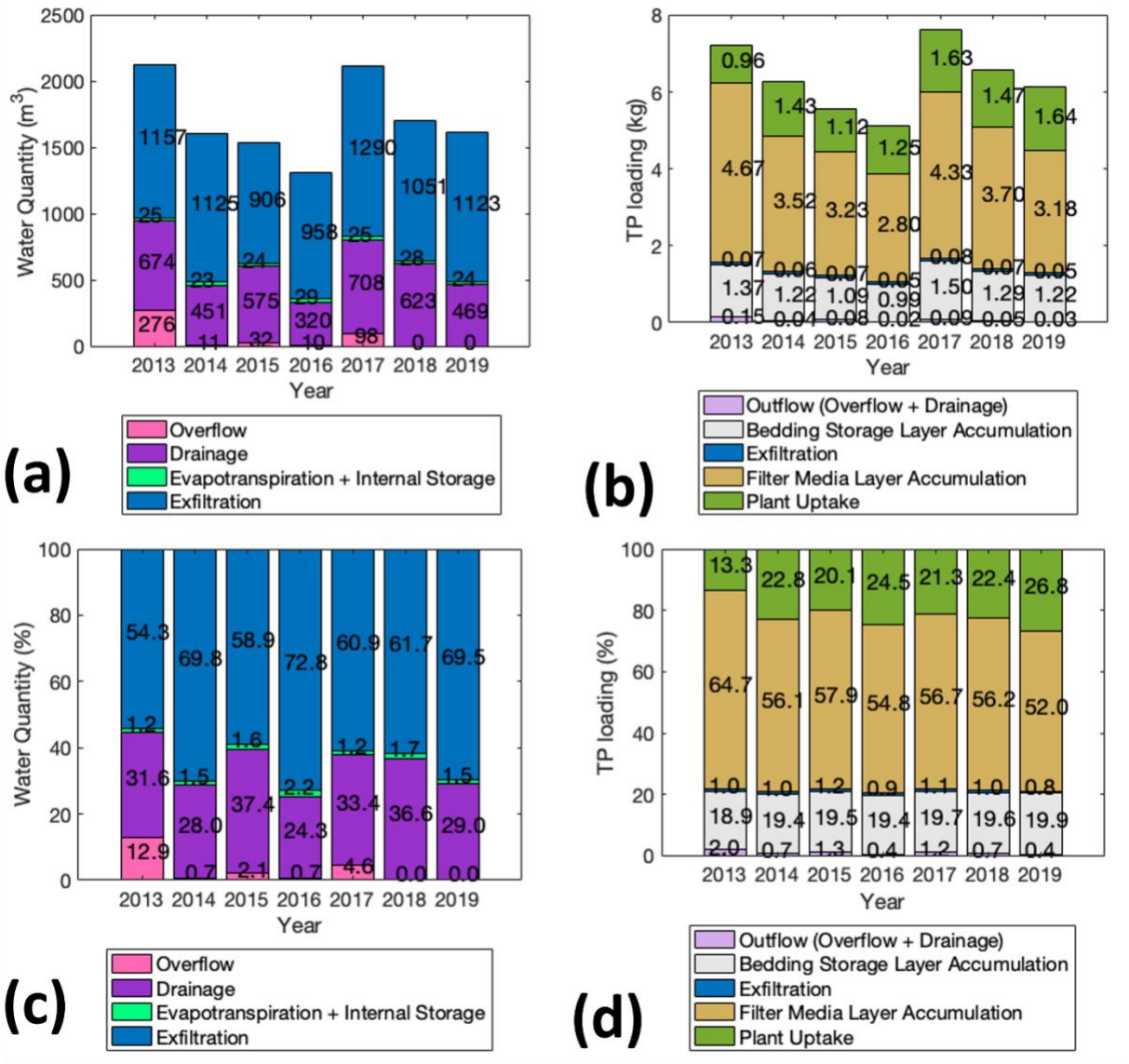

Figure AA7. Annual mass balance analysis results for Elm Drive bioretention cell. (**a**) Annual fate of water in volume (m^3); (**b**) Annual fate of P in loading (kg); (**c**) Annual fate of water expressed as a percentage; (**d**) Annual fate of P as a percentage.

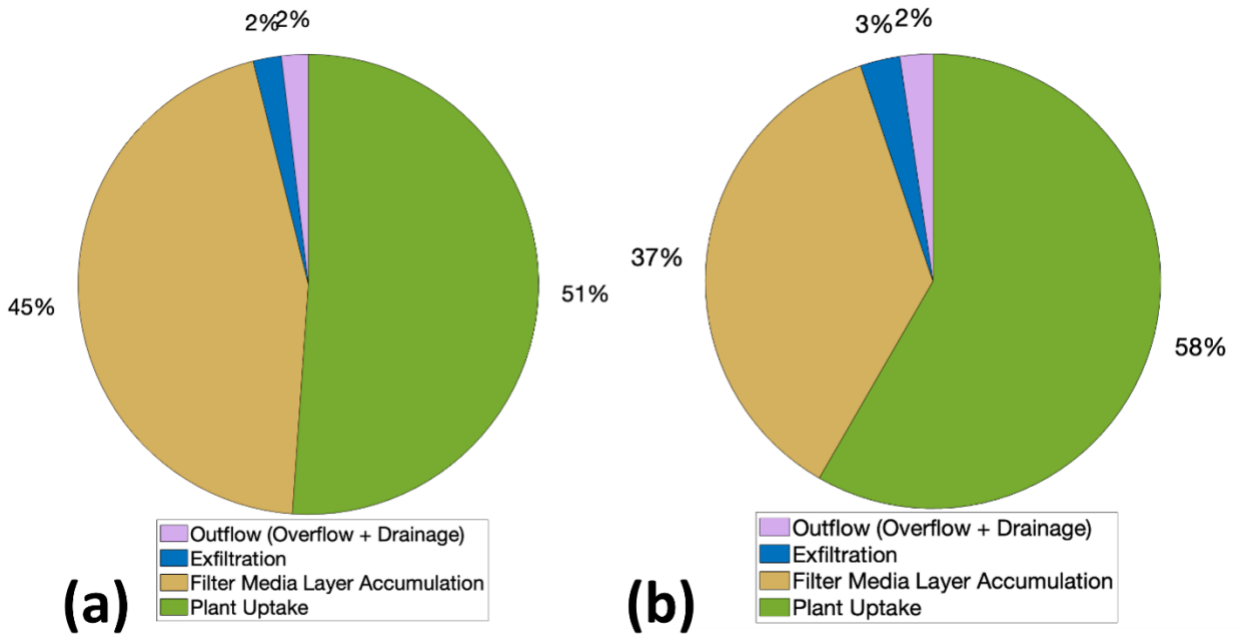

Figure AA8. Retention and export of SRP entering the bioretention cell under the scenarios with high inflow TP concentration (4.3 mg L^{-1}, with inflow SRP concentration as 0.86 mg L^{-1}) (**a**), and very high inflow TP concentration (15 mg L^{-1}, with inflow SRP concentration as 3 mg L^{-1}) (**b**). The percentages are model-calculated cumulative values for the period 2013-2019.

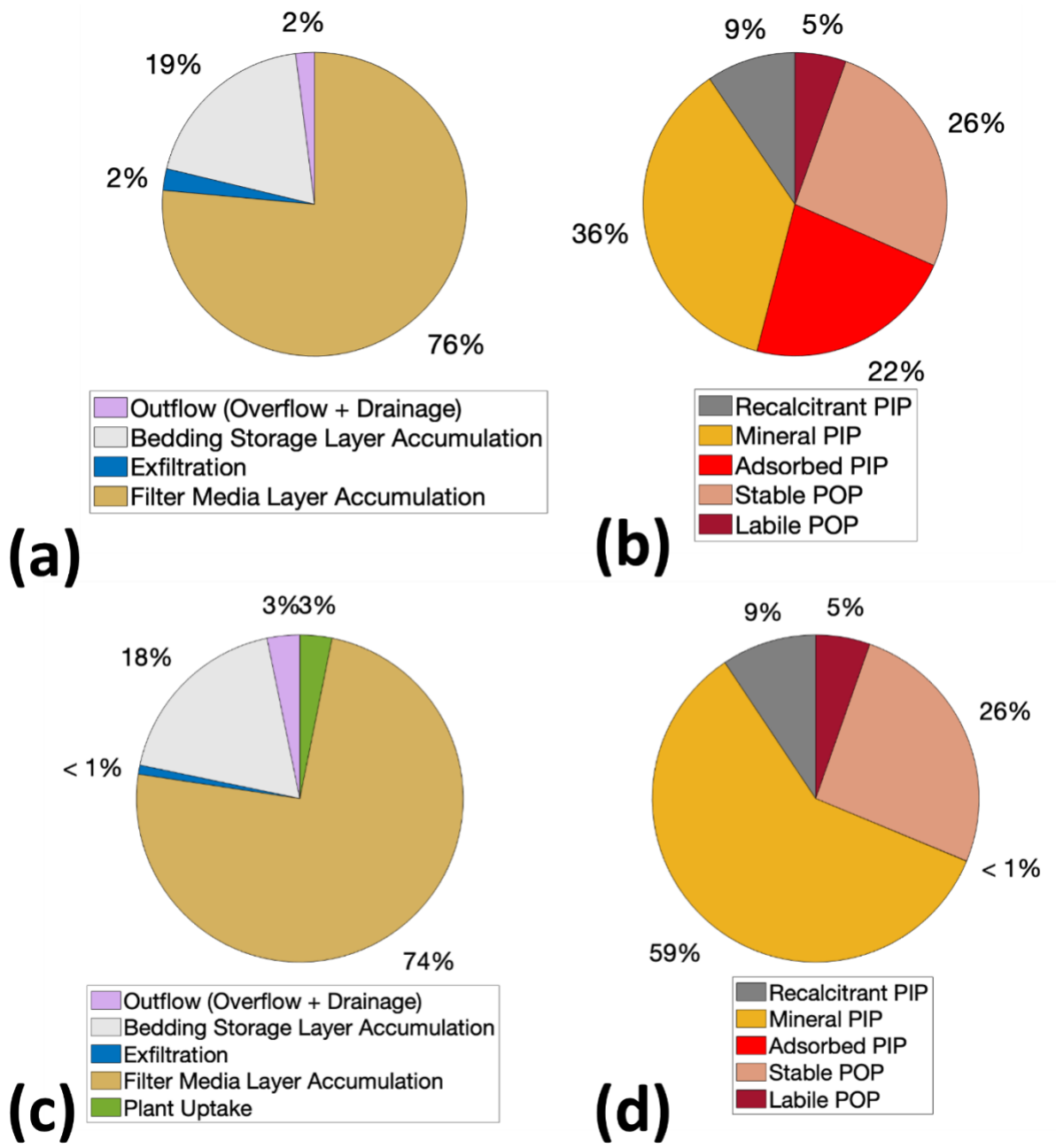

Figure AA9. Retention and export of P entering the bioretention cell (left panels, **a** and **c**), and (right panels, **b** and **d**) partitioning of P accumulated in the filter media layer between the different extracted pools under the scenarios without plant uptake (**a** and **b**) and the scenarios with low (0.37 mg L^{-1}) inflow TP concentration (**c** and **d**). The percentages are model-calculated cumulative values for the period 2013-2019.

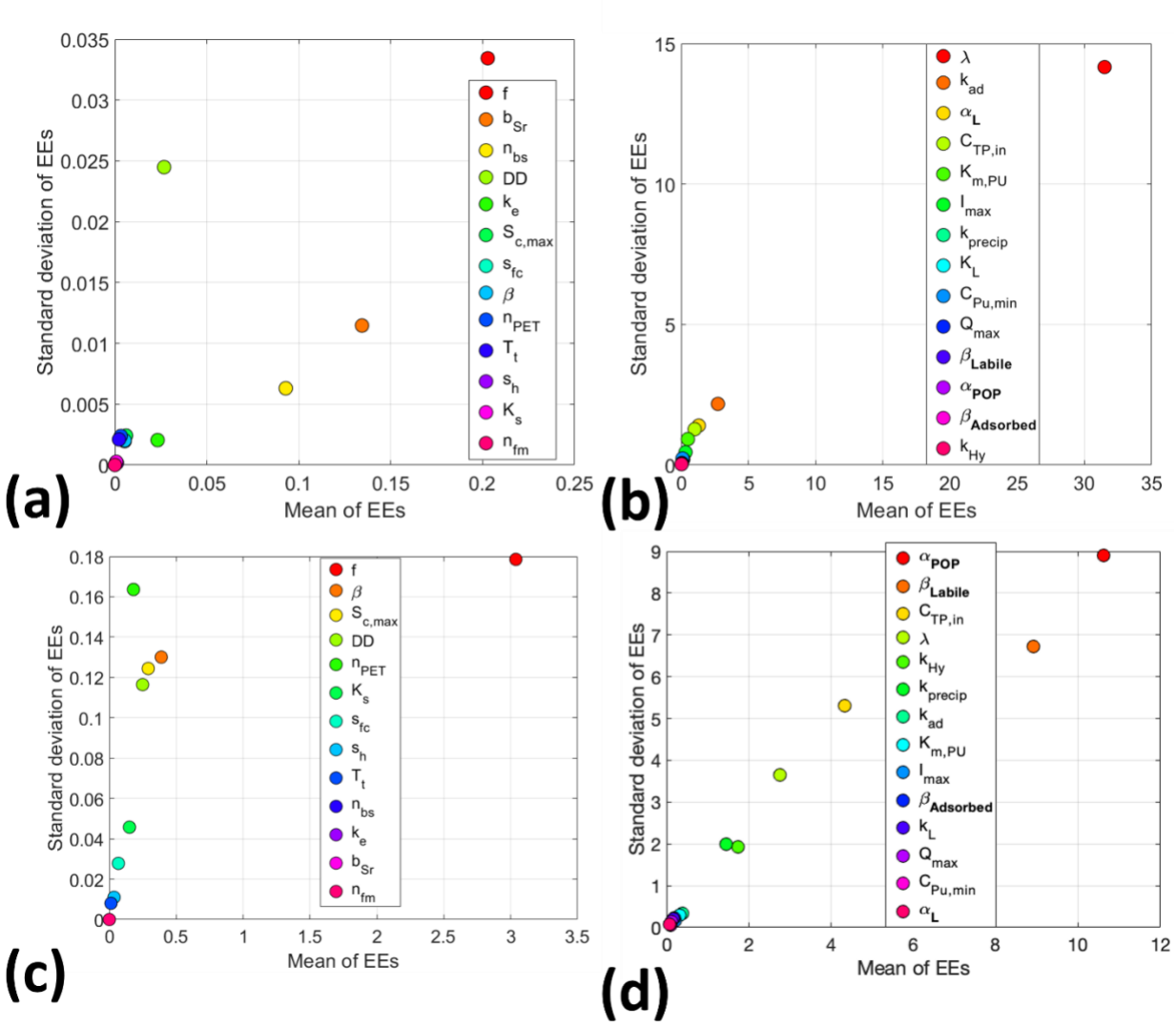

Figure AA10. Sensitivity analysis results. Sensitivity is quantified by elementary effect (EE, see Method S3) values. (**a**) Sensitivity of hydrologic model parameters (13 parameters) on runoff reduction efficiency; (**b**) Sensitivity of inflow P characteristics (concentration and fractions) and filter media P model parameters (14 parameters) on filter media TP retention efficiency; (**c**) Sensitivity of hydrologic model parameters (13 parameters) on filter media TP retention efficiency; (**d**) Sensitivity of inflow P characteristics (concentration and fractions) and filter media P model parameters (14 parameters) on filter media reactive P pool fraction;

Supplementary information for Methodology

Method AA1. Predict outflow drainage rate from bedding storage zone

We tried to use both a neural network regression model (Glorot & Bengio, 2010) and a traditional nonlinear regression model to predict outflow drainage rate from the bedding storage layer using hydraulic head (i.e., difference between bedding storage layer water level and bottom elevation of underdrain) when the bedding storage layer water level exceeds the bottom elevation of underdrain. For both of the methods, we trained the model using 80% of data (n = 106) and tested them on the remaining 20% (n = 28).

We trained the neural network regression model in Matlab through 'fitrnet' function, with layer sizes set as 30 outputs for the first fully connected layer and 10 outputs for the final fully connected layer. As default setting, 'fitrnet' function applies the rectified linear unit (ReLU) activation function to the first layer (for more information about 'fitrnet' function, please refer to the documentation of Matlab).

We also fitted the traditional nonlinear regression model in Excel, which provides equation:

$$Q_d = \begin{cases} 78 \cdot e^{28 \cdot (S_r - S_{r,crit})}, & when\ S_r > S_{r,crit} \\ 0, & when\ S_r \leq S_{r,crit} \end{cases}$$

We calculated the mean squared error (MSE) of prediction by both methods, and the results are shown in **Figure AA11**. It indicates that neural network regression model has significantly better prediction performance.

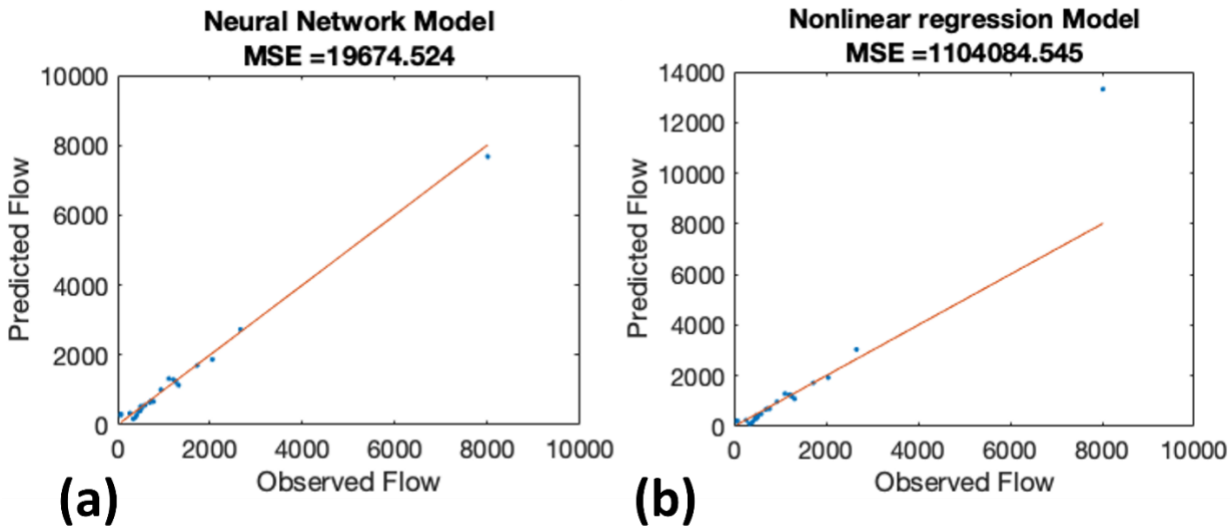

Figure AA11. Comparison between outflow drainage rate from bedding storage zone prediction performance (model test results) by (**a**) trained neural network regression model and (**b**) fitted traditional nonlinear regression model.

Method AA2. Methodology for loading and simulated flow-weighted average concentration calculation

The observed outflow P loading for each monitored event between November 2012 and December 2017 was calculated by multiplying the total measured outflow volume with the measured event mean concentration (EMC) from the corresponding composite sample (Eq AA2). The corresponding simulated outflow P loading is calculated by multiplying simulated outflow P concentration time series with the simulated outflow volume during the recorded start and end time of the ISCO water sampling program during the event (Eq AB1), as below:

$$M_{j\_P\_sim} = \sum_{j\_Start}^{j\_End} C_{P\_out\_Sim}(i) \cdot Q_{d\_Sim}(i) \qquad \text{(Eq AA1)}$$

$$M_{j\_P\_Ob} = C_{P\_out\_Ob}(j) \cdot \sum_{j\_Start}^{j\_End} Q_{d\_Ob}(i) \qquad \text{(Eq AA2)}$$

Where $M_{j\_P\_sim}$ and $M_{j\_P\_Ob}$ are simulated and observed loading for P species P (TP or SRP) during monitored event j. j_Start and j_End are the recorded start and end time of ISCO sampling program for composite sample during monitored event j. $C_{P\_out\_Sim}(i)$ and $Q_{d\_Sim}(i)$ are simulated outflow concentration of P and water quantity at time i, while $C_{P\_out\_Ob}(j)$ and $Q_{d\_Ob}(i)$ are measured outflow EMC of P during event j and monitored outflow water quantity

at time i, respectively. Simulated flow-weighted average concentration of monitored event j can also be calculated and compared with observed P concentration of composite samples, as below:

$$C_{P\_composite\_Sim\_j} = \frac{M_{j\_P\_sim}}{\sum_{j\_Start}^{j\_End} Q_{d\_Sim(i)}} \qquad \text{(Eq AA3)}$$

Where $C_{P\_composite\_Sim\_j}$ is the simulated flow-weighted average concentration of monitored event j.

Method AA3. Elementary effects (EES) method

The EES method assesses the change to model output in response to a small change to a particular parameter during each run. For a set of parameters $X = x_1, x_2, \dots, x_n$ to be analyzed, sensitivity of ith parameter (x_i) is measured as elementary effect ($EE_i(X)$) and it is expressed as follows (Morris et al., 2014):

$$EE_i(X) = \frac{y(x_1,\dots,x_i+\Delta,\dots,x_n) - y(x_1,\dots,x_i,\dots,x_n)}{\Delta} \qquad \text{(Eq AA4)}$$

Where Δ is the change of ith parameter in one run, y is the model output of interest (objective function). For sensitivity analysis of the hydrologic model the objective function was set as simulated runoff reduction efficiency over the simulation time span for hydrologic model calibration (November 2012 to December 2017). The sensitivity of 13 parameters calibrated in section 2.3 of main text were calculated via the EES method (Eq AA4) using 40 trials per parameter.

Method AA4. Simple mass balance calculation for minimum inflow TP concentration estimation

Unfortunately, the operator of the cell did not collect inflow P concentration data because of the difficulties associated with collecting samples in sheet flow. Nonetheless, a large value of the TP input concentration is required to account for the mass of accumulated P in the filter media, as shown by the following simple mass balance calculations:

1) The average TP concentration in the filter media increased from 331 mg kg^{-1} in 2013 to 534 mg kg^{-1} in 2019 (from the data shown in Figure 3.5). So, the total mass of P accumulated in the filter media over this time period is on the order of:

$$Increase\ of\ filter\ media\ P\ concentration \times\ volume\ of\ filtermedia\ \times$$
$$bulk\ density\ of\ filter\ media = (534\ -\ 331)\text{mg P kg}^{-1} \times 65250\ \text{L} \times\ 1.6\ \text{kg L}^{-1} =$$
$$\mathbf{21.2\ kg\ P}.$$

2) The total amount of water that passed through the filter media during the same period, which is directly derived from the monitored precipitation data, is 9.91×10^6 L. The P exported via surface overflow and exfiltration to the underlying native soil can be estimated from the corresponding outgoing water fluxes (based on the hydrological model of the cell) and the measured outflow TP concentration (assigning the same concentration for the exfiltrated water). Using the mean measured outflow TP concentration of 0.14 mg L^{-1}, the exported P loading amounts to:

$$0.14\ \text{mg/L} \times 9.91 \times 10^6\ \text{L} = \mathbf{1.4\ kg\ P}.$$

Even if we assume that no P accumulated in the bedding storage layer and no P plant uptake occurred (which is not realistic), the influent P concentration would still have to be at least:

$$(21.2 + 1.4)\ \text{kg P} \div 9.91 \times 10^6\ \text{L} = \mathbf{2.3\ mg\ L^{-1}}.$$

Our modeling results, supported by the vegetation maintenance practices of the operator of the cell, imply that plant uptake is a significant P removal process in this bioretention system. The 2.3 mg L^{-1} is thus an absolute minimum estimate of the average TP concentration loaded to the cell.

Method AA5. Details about collection and analysis of inflow, ponded water and mulch porewater samples during an event

To characterize the inflow P concentration to the filter media, we collected multiple water samples during an event on October 15th, 2021. We collected 3 water samples right at the inlet of 3 cells (cell 1, 4 and 5). For cell 1, water sample was collected during the first flush. For cell 4 and 5, water samples were collected after the first flush. We also collected 1 water sample from the ponded water in cell 4 before the water was infiltrated into the cell. All of the inflow and ponded water samples were further analyzed by to determine the TP and SRP concentration. We collected and centrifuged (3500 rpm for 30 minutes) the wet mulch samples from cell 1, 3, 4, 5 and 6 and further filtered the supernatants (i.e., mulch porewater) with 0.45 μm nylong filter and measured the SRP concentration. For TP concentration analysis, we extracted the water samples by persulfate extraction method (Dayton et al., 2017) followed by ICP-OES analysis. We used Thermo Scientific™ Gallery™ Discrete Analyzer to determine the SRP concentration, this method

is based on both EPA method 365.1 (Cabrera et al., 1982) and SM 4500-P E (Rice et al., 2012). P concentration of aforementioned water samples can be seen in Table AA1.

Table AA1. P concentrations of inflow water, ponded water and mulch porewater samples collected during the event of October 15th, 2021 in Elm Drive bioretention cells.

Sample Type	Cell Number*	SRP Concentration ($mg\ L^{-1}$)	TP Concentration ($mg\ L^{-1}$)
Inflow (during first flush)	1	0.08968834	5.431
Inflow	4	0.02347748	0.0962
Inflow	5	0.03573734	0.11875
Ponded water	4	0.08662933	2.8275
Mulch Porewater	4-U	0.1697	-
Mulch Porewater	1-U	0.2716	-
Mulch Porewater	4-D	0.4398	-
Mulch Porewater	4-M	0.8774	-
Mulch Porewater	5-U	1.167	-
Mulch Porewater	3-U	1.409	-
Mulch Porewater	5-M	2.152	-
Mulch Porewater	6-M	4.42	-
Mulch Porewater	5-D	5.908	-
Mulch Porewater	6-U	8.079	-

*Sampling location in the cell is labelled as: U—upstream, M—middle, D—downstream. For example, 4-U means the sample was collected at upstream of cell #2.

References in Appendix A

Cabrera, F., Diaz, E., Toca, C. G., & De Arambarri, P. (1982) A modification of the hydrogen peroxide method of determination of total phosphorus in natural waters. Water Research, 16(6), 1061-1064. https://doi.org/10.1016/0043-1354(82)90042-2.

CVC (2016) Elm Drive Low Impact development Infrastructure Performance and Assessment Technical Report (Issue May). Credit Valley Conservation (CVC) Water and Climate Change Science Division. https://files.cvc.ca/cvc/uploads/2016/06/TechReport_Elm_Drive_Final.pdf

Dayton, E. A., Whitacre, S., & Holloman, C. (2017) Comparison of three persulfate digestion methods for total phosphorus analysis and estimation of suspended sediments. Applied Geochemistry, 78, 357-362. https://doi.org/10.1016/j.apgeochem.2017.01.011.

Glorot, X., & Bengio, Y. (2010) Understanding the difficulty of training deep feedforward neural networks. Proceedings of the Thirteenth International Conference on Artificial Intelligence and Statistics, 249–256. https://proceedings.mlr.press/v9/glorot10a.

Parsons, C.T., Rezanezhad, F., O'Connell, D.W., Van Cappellen, P. (2017) Sediment phosphorus speciation and mobility under dynamic redox conditions. Biogeosciences 14 (14), 3585–3602. doi:10.5194/bg-14-3585-2017.

Rice, E.W., Baird, R. B., Eaton, A. D., & Clesceri, L. S. (2012) Standard methods for the examination of water and wastewater (Vol. 10). E. W. Rice (Ed.). Washington, DC: American public health association. 156-172. ISBN: 9780875532875. http://yabesh.ir/wp-content/uploads/2018/02/Standard-Methods-23rd-Perv.pdf.

Ruttenberg, K.C. (1992) Development of a sequential extraction method for different forms of phosphorus in marine sediments. Limnol. Oceanogr. 37 (7), 1460–1482. doi: 10.4319/lo.1992.37.7.1460.

Appendix B. Supplementary Material: Chapter 4

Supplementary Figures

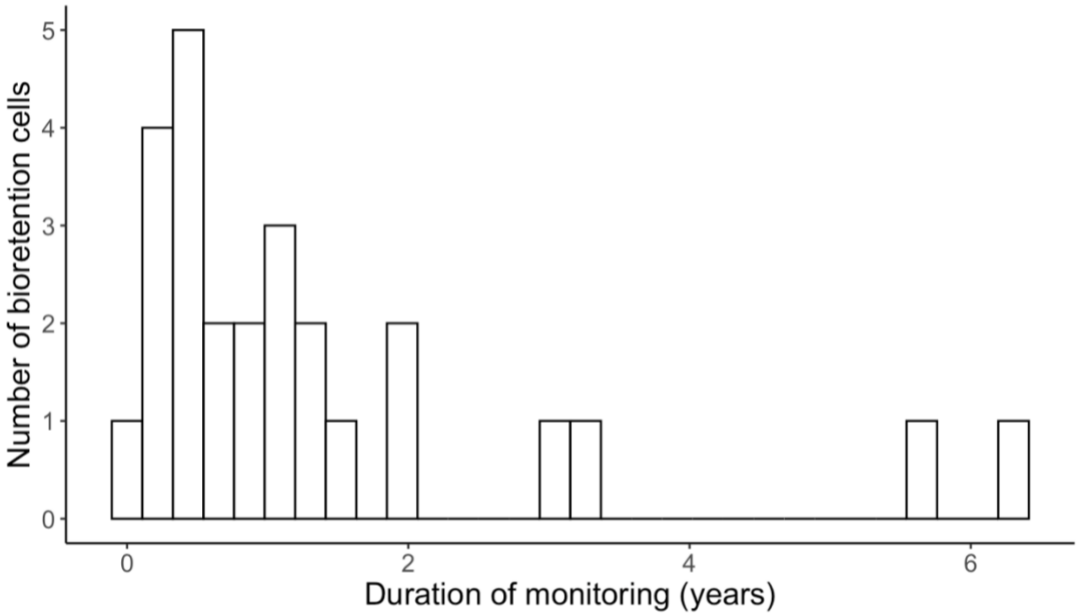

Figure AB1: Number of bioretention cells under different duration of monitoring for SRP concentrations in this analysis.

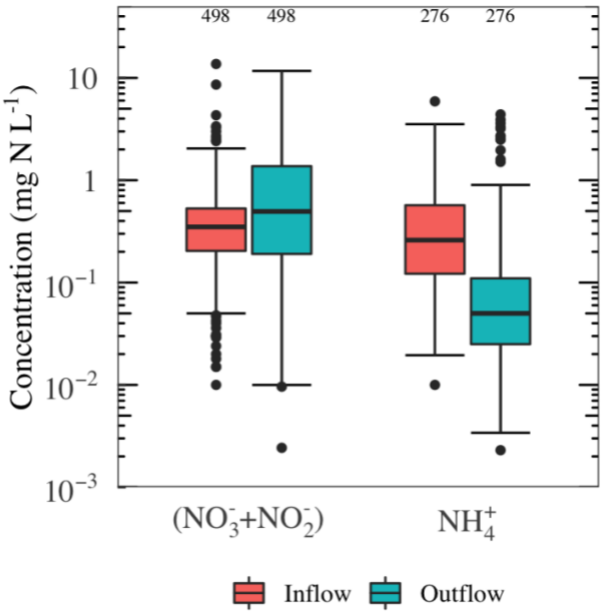

Figure AB2: Boxplot of inflow and outflow concentration of nitrite-N + nitrate-N (NO_3^--N+NO_2^--N) and ammonium-N (NH_4^+-N). The number of data points included in each box is shown on top of the plot.

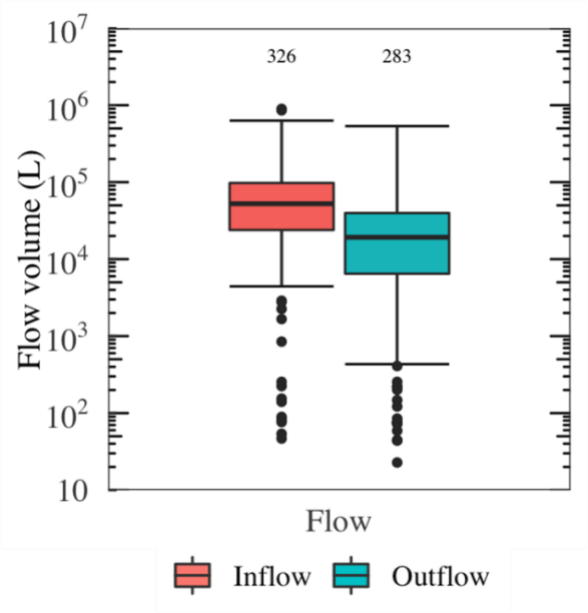

Figure AB3: Boxplot of total event volume inflow and outflow. The number of data points included in each box is shown on top of the plot. Note that some events did not generate any outflow; in these cases, the outflow volumes were 0. Because we used a logarithmic scale, zero values were excluded from the plot.

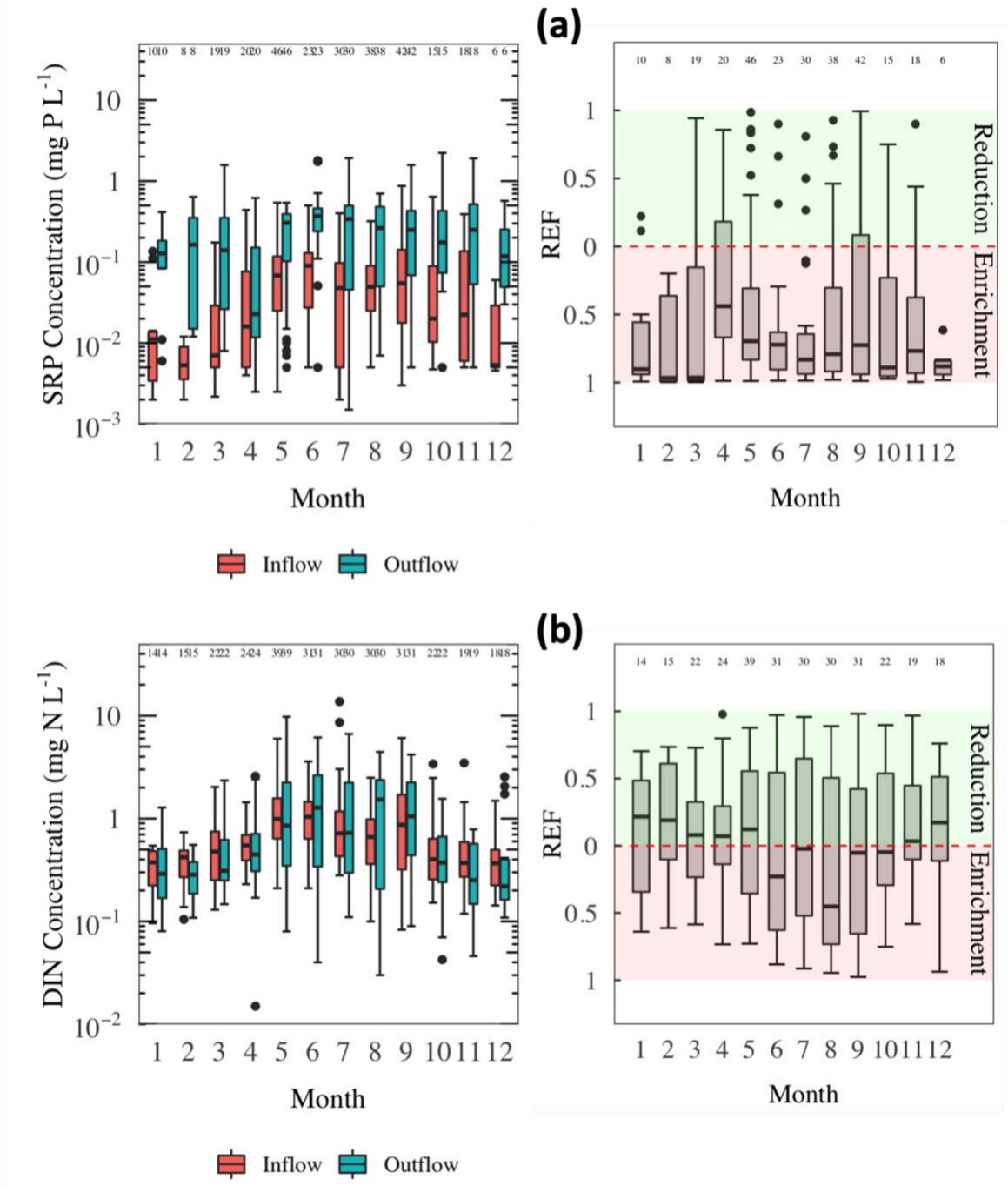

Figure AB4: Boxplot of inflow and outflow concentrations of SRP and DIN (data from all available sites) in different months (left panels of **a** and **b**), and the corresponding concentration REFs for the same parameters (right panels of **a** and **b**). Dashed line in the right panels shows the zero value, that is, no reduction or enrichment.. The number of data points included in each box is shown on top of the plot.

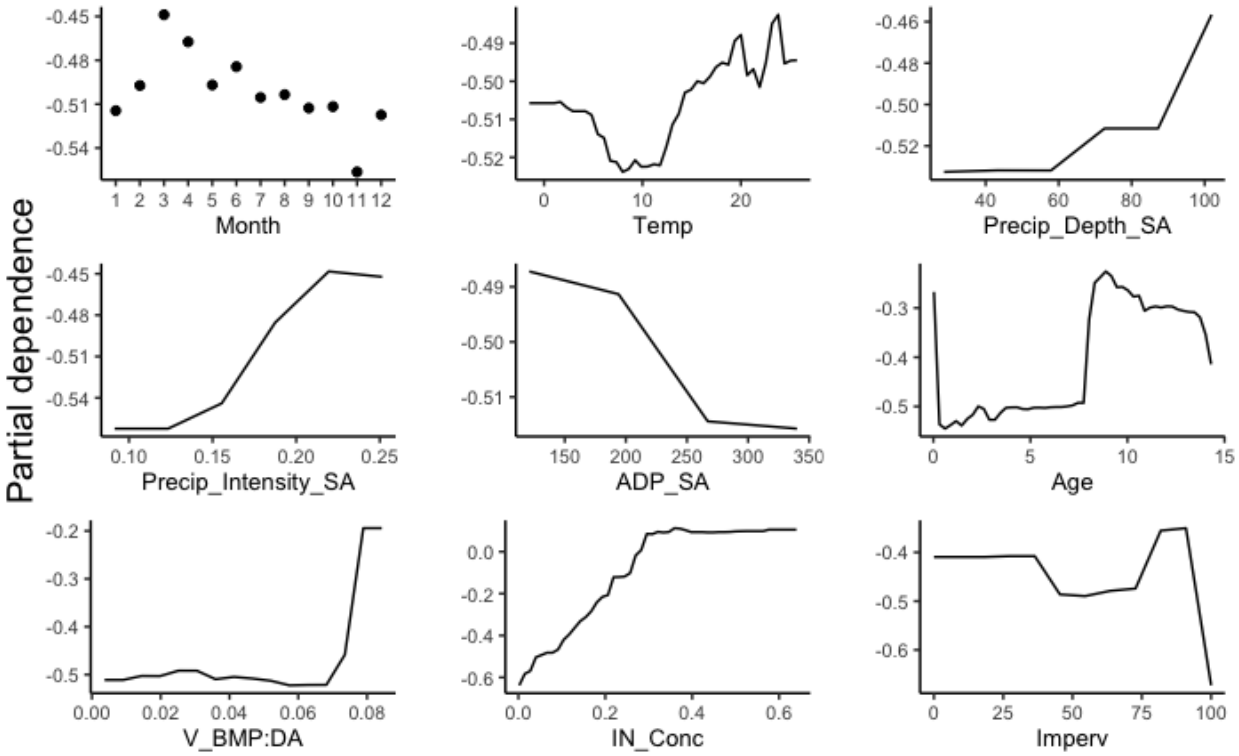

Figure AB5: Partial dependence plots for the explanatory variables included in the random forest modeling for the SRP concentration reduction and enrichment factors (REFs). Note that land use is not included because it is a categorical variable. Variables included: Month -- month of event date, Temp – local monthly average air temperature for the month when the event occurred (units: °C), P_Depth_SA -- site average annual total precipitation depth (units: cm), P_Intensity_SA -- site average precipitation intensity (units: cm hr^{-1}), ADP_SA -- site average inter-event dry duration (units: hour), Age -- bioretention cell age at event (units: years), V_BMP:DA -- Ratio of the bioretention cell (BRC) storage volume (filter media volume + ponding volume) to the drainage area of the BRC (units: m), IN_Conc -- influent concentration for a given event (units: mg L^{-1}), Imperv -- imperviousness of watershed (units: %). Note that positive values on the panels correspond to TP outflow concentration reduction while negative values represent TP outflow concentration enrichment.

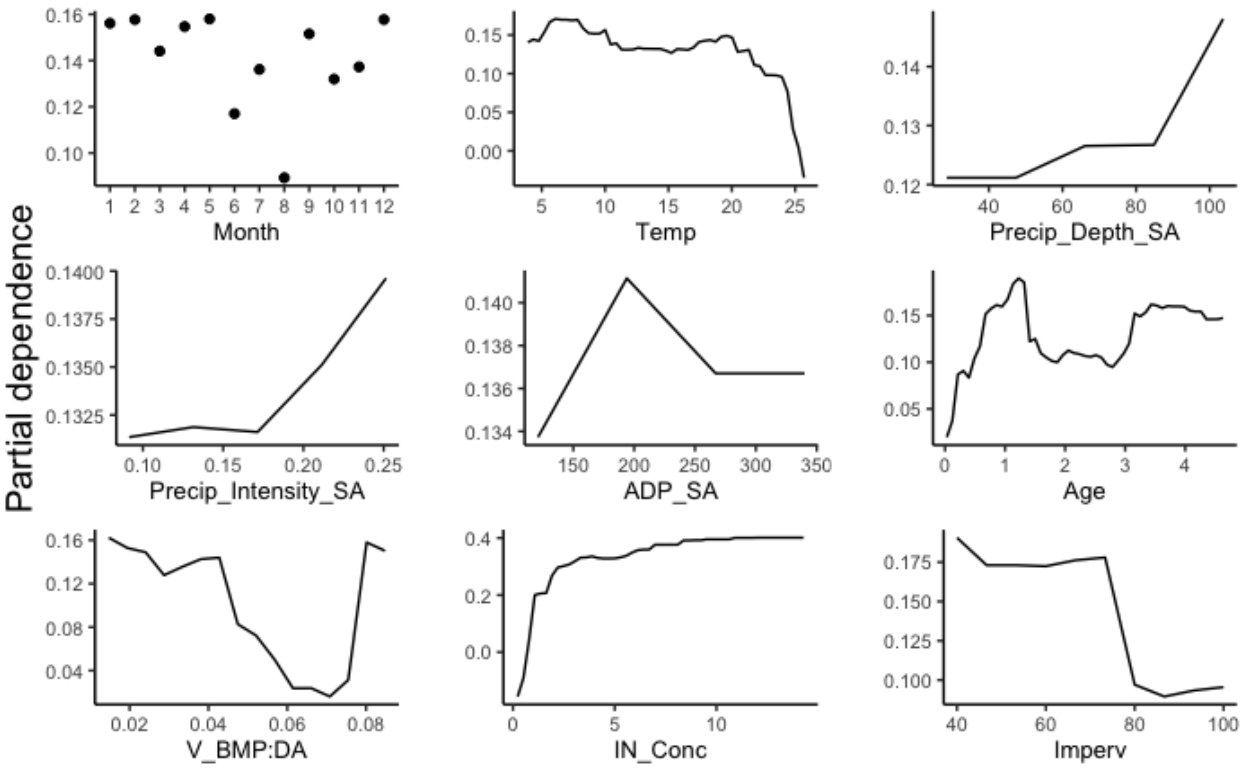

Figure AB6: Partial dependence plots for the explanatory variables included in the random forest modeling for the TN concentration reduction and enrichment factors (REFs). Note that land use is not included because it is a categorical variable. Variables included: Month -- month of event date, Temp – local monthly average air temperature for the month when the event occurred (units: °C), P_Depth_SA -- site average annual total precipitation depth (units: cm), P_Intensity_SA -- site average precipitation intensity (units: cm hr^{-1}), ADP_SA -- site average inter-event dry duration (units: hour), Age -- bioretention cell age at event (units: years), V_BMP:DA -- Ratio of the bioretention cell (BRC) storage volume (filter media volume + ponding volume) to the drainage area of the BRC (units: m), IN_Conc -- influent concentration for a given event (units: mg L^{-1}), Imperv -- imperviousness of watershed (units: %). Note that positive values on the panels correspond to TP outflow concentration reduction while negative values represent TP outflow concentration enrichment.

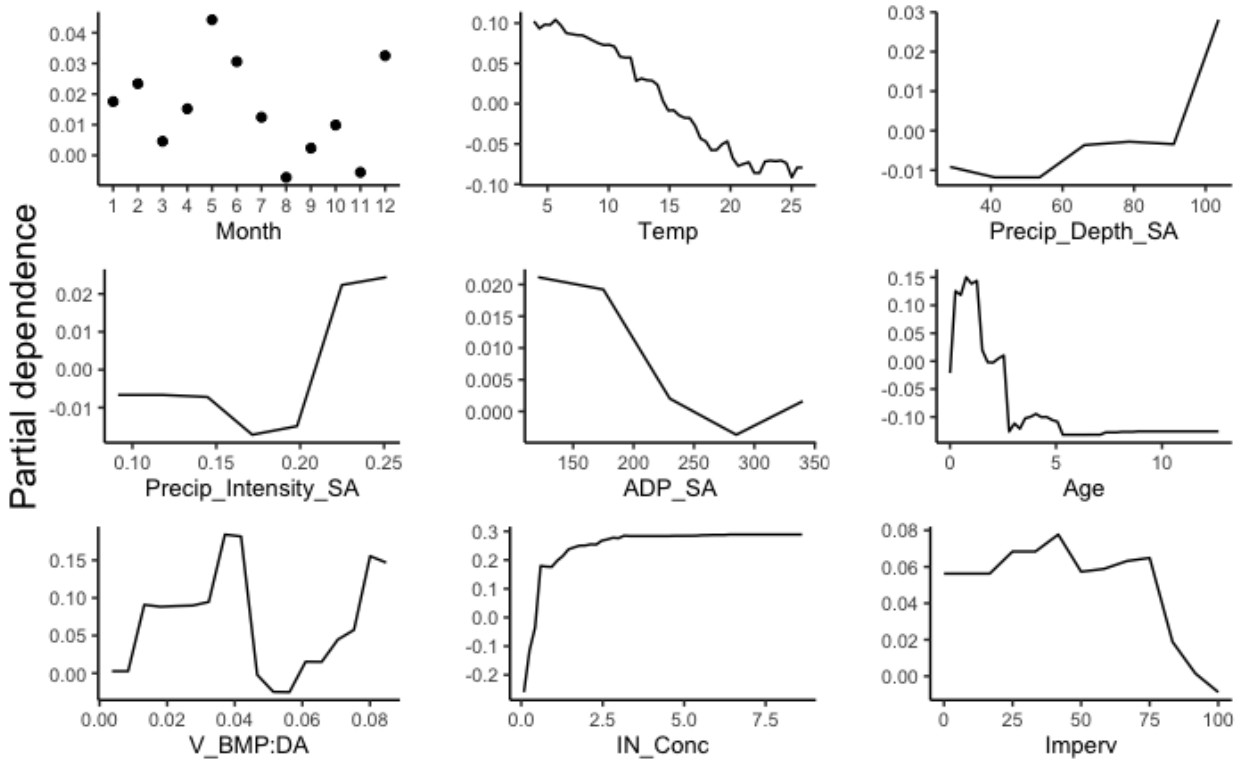

Figure AB7: Partial dependence plots for the explanatory variables included in the random forest modeling for the DIN concentration reduction and enrichment factors (REFs). Note that land use is not included because it is a categorical variable. Variables included: Month -- month of event date, Temp – local monthly average air temperature for the month when the event occurred (units: °C), P_Depth_SA -- site average annual total precipitation depth (units: cm), P_Intensity_SA -- site average precipitation intensity (units: cm hr^{-1}), ADP_SA -- site average inter-event dry duration (units: hour), Age -- bioretention cell age at event (units: years), V_BMP:DA -- Ratio of the bioretention cell (BRC) storage volume (filter media volume + ponding volume) to the drainage area of the BRC (units: m), IN_Conc -- influent concentration for a given event (units: mg L^{-1}), Imperv -- imperviousness of watershed (units: %). Note that positive values on the panels correspond to TP outflow concentration reduction while negative values represent TP outflow concentration enrichment.

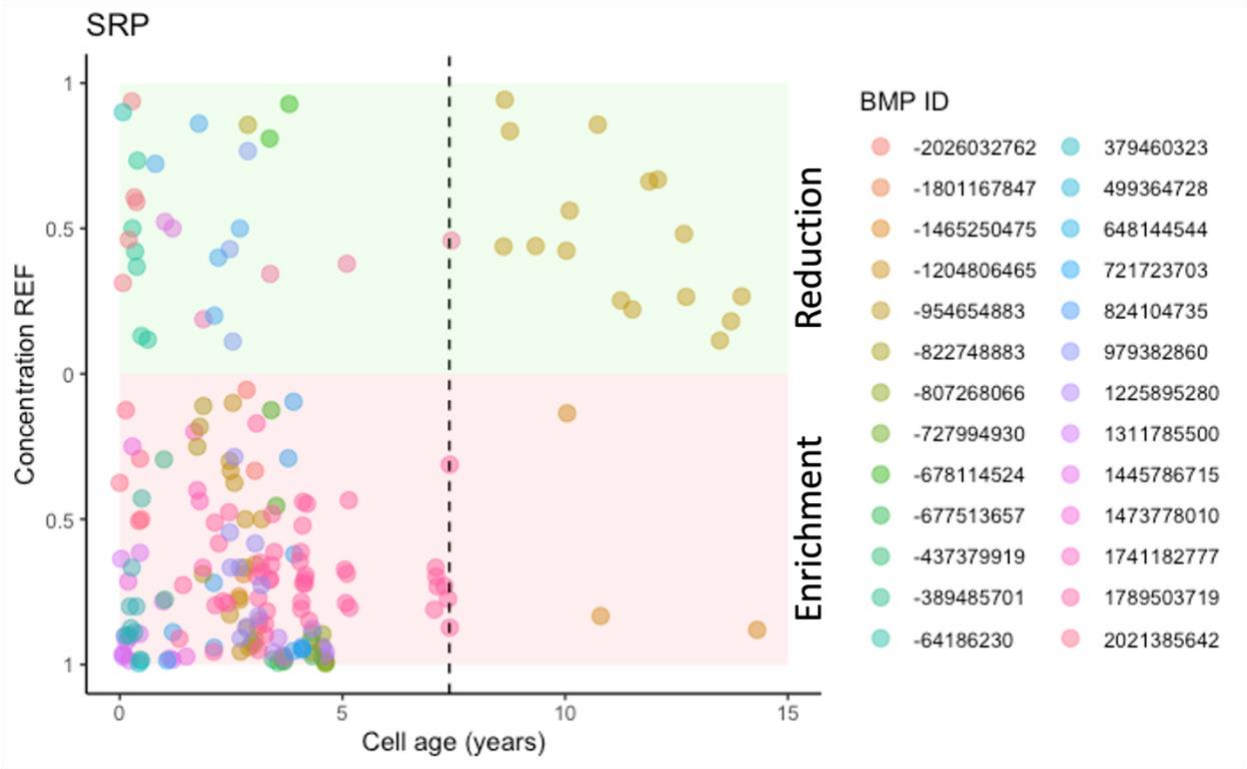

Figure AB8: Scatter plot of SRP concentration reduction or enrichment efficiency (*REF*) vs. bioretention cell (BRC) age for all available events for all BRCs (each BMP ID represents one BRC). The vertical dashed line corresponds to age 7.4 years, that is, the threshold age for improved SRP concentration control (*i.e*, lower enrichment *REF*) suggested by the partial dependence plots results in Figure AB5. Notice that only 2 bioretention cells in our analysis had hydrological event records for which SRP concentration was recorded after 7.4 years of age.

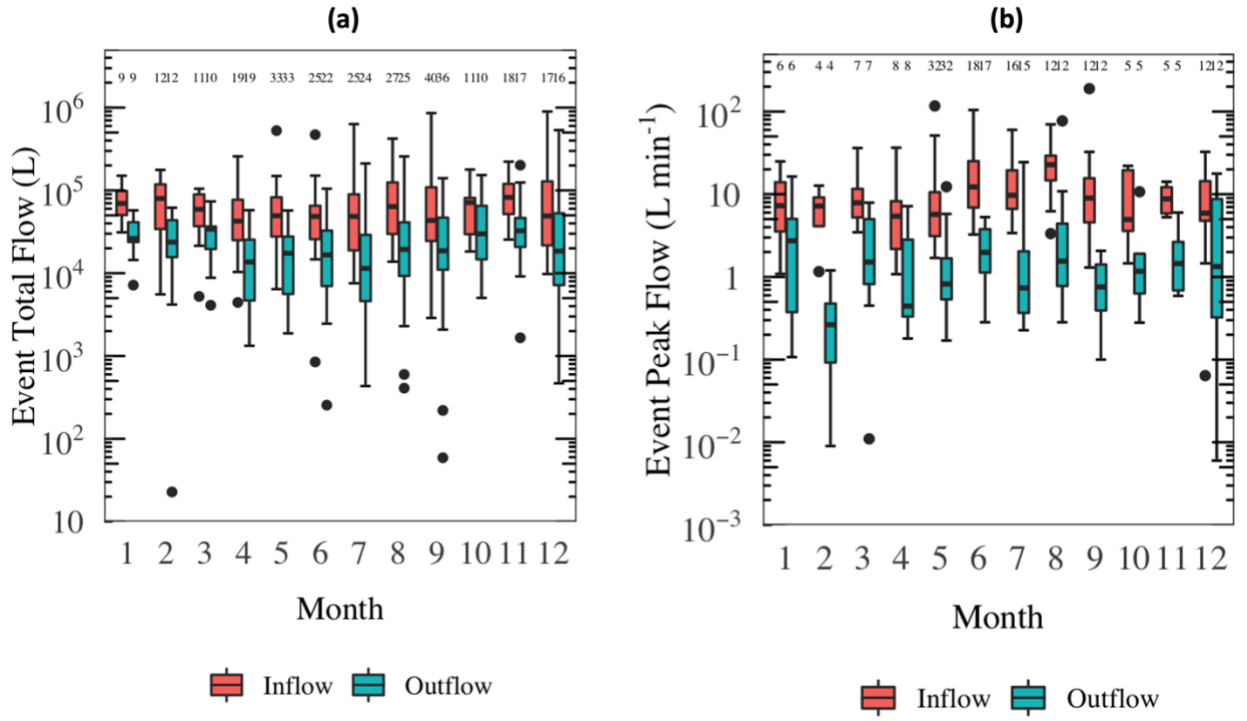

Figure AB9: Boxplot of inflow and outflow event peak flow rate (**a**) and event total flow (**b**) in different months. The number of data points included in each box is shown on top of the plot (some events did not generate any outflow, these result in outflow loads of 0 are therefore excluded from the plot (**b**) due to the logarithmic scale).

Supplementary Tables

Table AB1: Laboratory analysis methods and calculations for the water quality data reported in the International Stormwater BMP Database (ISBD).

Parameter	Laboratory analysis method	Calculation method
TP	EPA Method 365 (Cabrera et al., 1982) or Standard Method 4500 (American Public Health Association & American Water Works Association, 1995)	-
SRP	EPA Method 365 or Standard Method 4500	-
TN	Method ASTM D5176	TN = Total Kjeldahl N + nitrate-N + nitrite-N
DIN	-	DIN = Ammonium-N + Nitrate-N + nitrite-N (D. A. Chin, 2012)
Ammonium-N	EPA Method 350 (O'dell, 1993a) or Standard Method 4500	-
Nitrate-N and nitrite-N	EPA Method 300 (Pfaff, 1993), EPA Method 353 (O'dell, 1993b) or Standard Method 4500	-

Note: The laboratory analysis method is not reported for ~ 30% of the water quality records in ISBD. Although a variety of methods were used for a single water quality parameter within the database, methods usually remained unchanged at each site.

Table AB2. Number of bioretention cells (BRCs) exhibiting given long-term trends as identified by Mann Kendall test.

Water quality parameters	Concentration/Ratio REF (Increase: Decrease: No Trend*)	Flow REF (Increase: Decrease: No Trend*)	Loading REF (Increase: Decrease: No Trend*)
TP	1:2:36	0:1:38	1:1:37
SRP	0:0:27	1:0:26	3:1:23
NRP	0:2:24	0:0:26	1:0:25
TN	2:1:22	0:0:25	1:0:24
DIN	2:2:21	0:0:25	0:1:24
NRN	2:0:17	0:0:19	1:0:18
SRP:TP	0:0:26	-	-
DIN:TN	0:1:18	-	-
$(NO_3^-+NO_2^-):NH_4^+$	0:1:24	-	-
TN:TP	1:2:22	-	-
DIN:SRP	0:1:20	-	-

*Number of BRCs showing increasing trend (Increase): number of BRCs showing decreasing trend (Decrease): number of BRCs showing no statistically significant trend (No Trend).

Table AB3. Statistics for event inflow and outflow concentrations and molar ratios. EMC = event mean concentration.

Water Quality Parameter	Inflow EMC (mg L^{-1} or ratio)		Outflow EMC (mg L^{-1} or ratio)	
	Mean	**Median**	**Mean**	**Median**
TP	0.32	0.17	0.53	0.27
SRP	0.08	0.04	0.42	0.25
NRP	0.27	0.11	0.13	0.07
TN	1.7	1.2	1.8	1.0
DIN	0.88	0.54	1.1	0.50
NRN	0.83	0.57	0.89	0.47
SRP:TP	0.27	0.20	0.65	0.74
DIN:TN	0.45	0.44	0.46	0.46
$(NO_3^-+NO_2^-):NH_4^+$	5.9	1.2	30	4.8
TN:TP	32	24	30	17
DIN:SRP	230	49	65	13

References in Appendix B

American Public Health Association, & American Water Works Association. (1995) Standard methods for the examination of water and wastewater. In Standard methods for the examination of water and wastewater (pp. 1000-1000).

Cabrera, F., Diaz, E., Toca, C. G., & De Arambarri, P. (1982) A modification of the hydrogen peroxide method of determination of total phosphorus in natural waters. Water Research, 16(6), 1061-1064. https://doi.org/10.1016/0043-1354(82)90042-2

Chin, D. A. (2012) Water-quality engineering in natural systems: fate and transport processes in the water environment. John Wiley & Sons.

O'dell, J. (1993a) Environmental Protection Agency Method 350.1: Determination of Ammonia Nitrogen by Semi-Automated Colorimetry. United States Environmental Protection Agency: Washington, DC, USA, 45268.

O'dell, J. (1993b) Method 353.2, Revision 2.0: Determination of nitrate-nitrite nitrogen by automated colorimetry. Environmental Monitoring Systems Laboratory, US Environmental Protection Agency, Cincinnati, Ohio.

Pfaff, J. D. (1993) Method 300.0 Determination of inorganic anions by ion chromatography. US Environmental protection agency, Office of research and development, Environmental monitoring systems Laboratory, 28.

Appendix C. Supplementary Material: Chapter 5

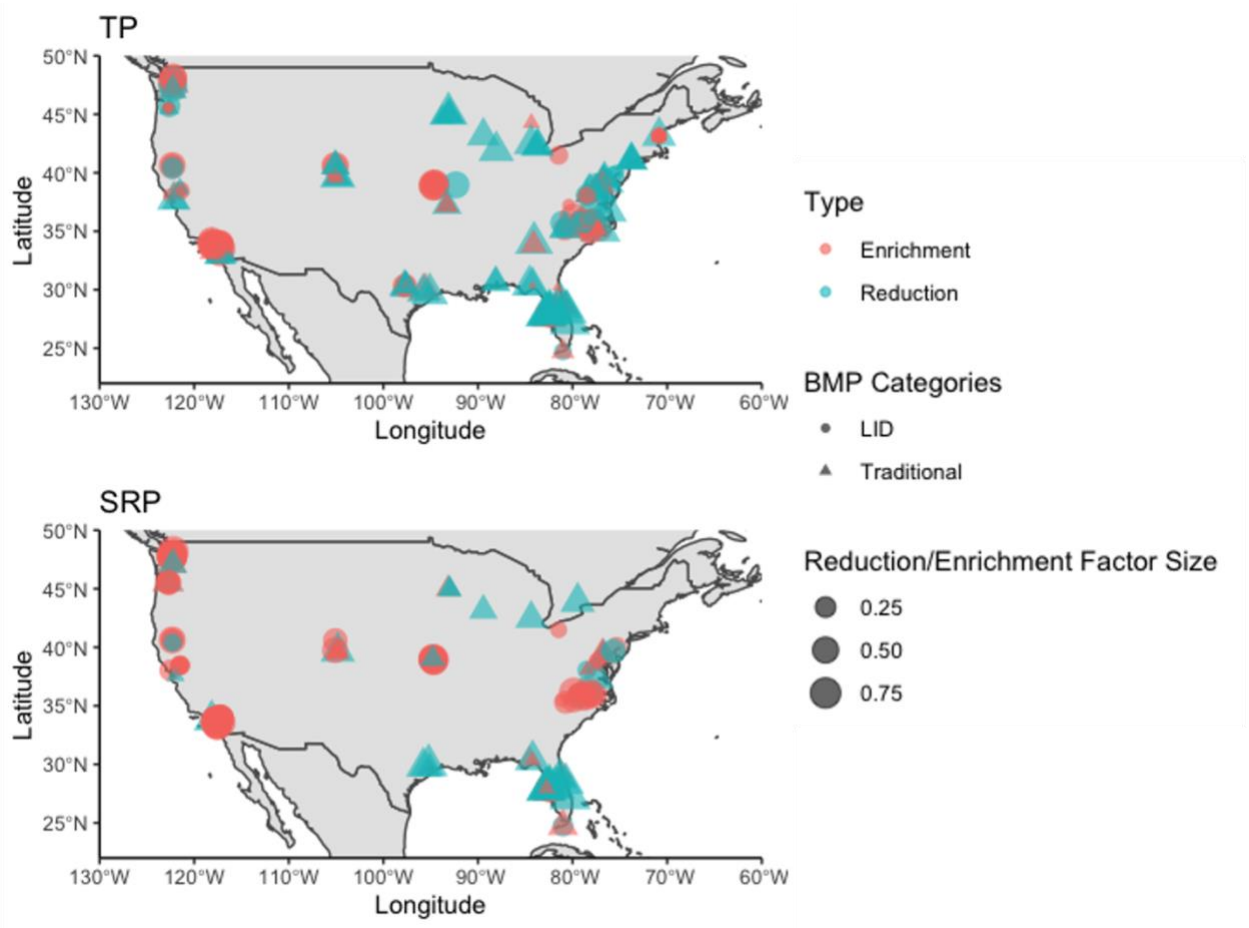

Figure AC1. Locations of BMPs with monitored TP and SRP concentration data available in International Stormwater BMP Database. Types (enrichment or reduction), categories (traditional or LID) and reduction/enrichment factor sizes of BMPs are specified as the color, shape and size of scatters in the plot, respectively.

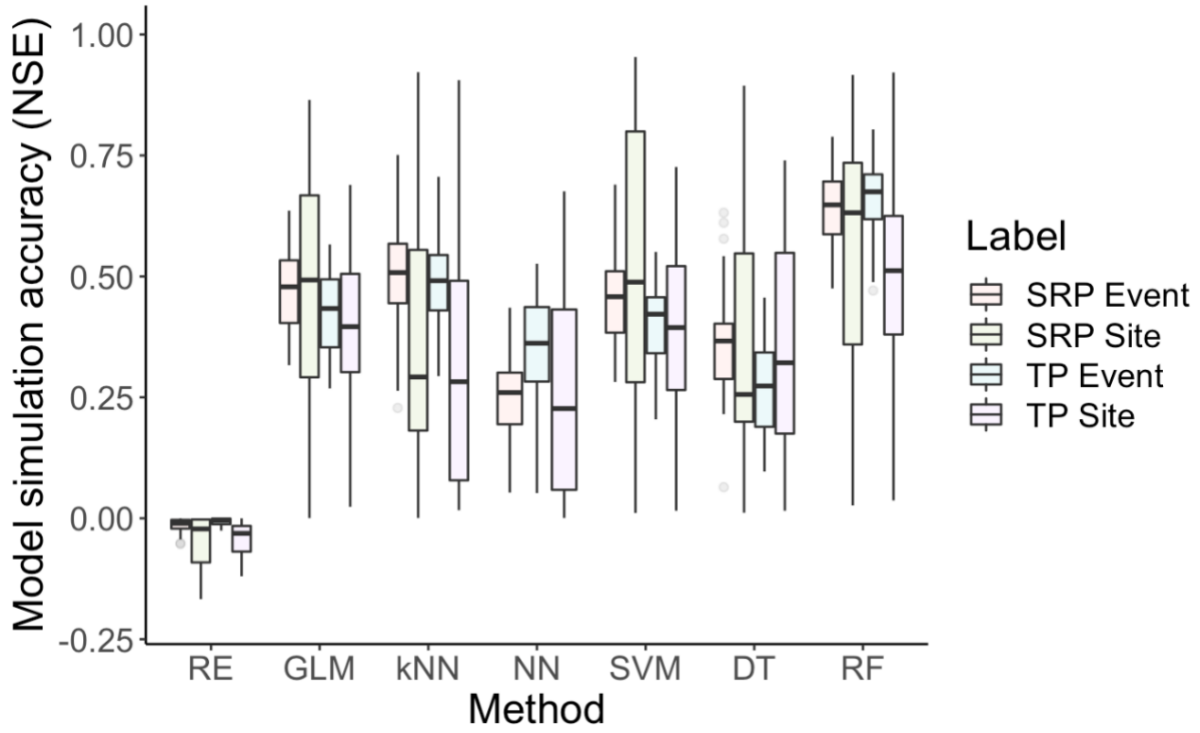

Figure AC2. Model simulation accuracy (quantified as NSE) under different types of model for event and site scale TP and SRP concentration reduction/elimination factors simulation. Traditional reduction efficiency method is labelled as 'RE', while abbreviations of ML modelling method (GLM, kNN, NN, SVM, DT and RF) are listed in Table 5.3.

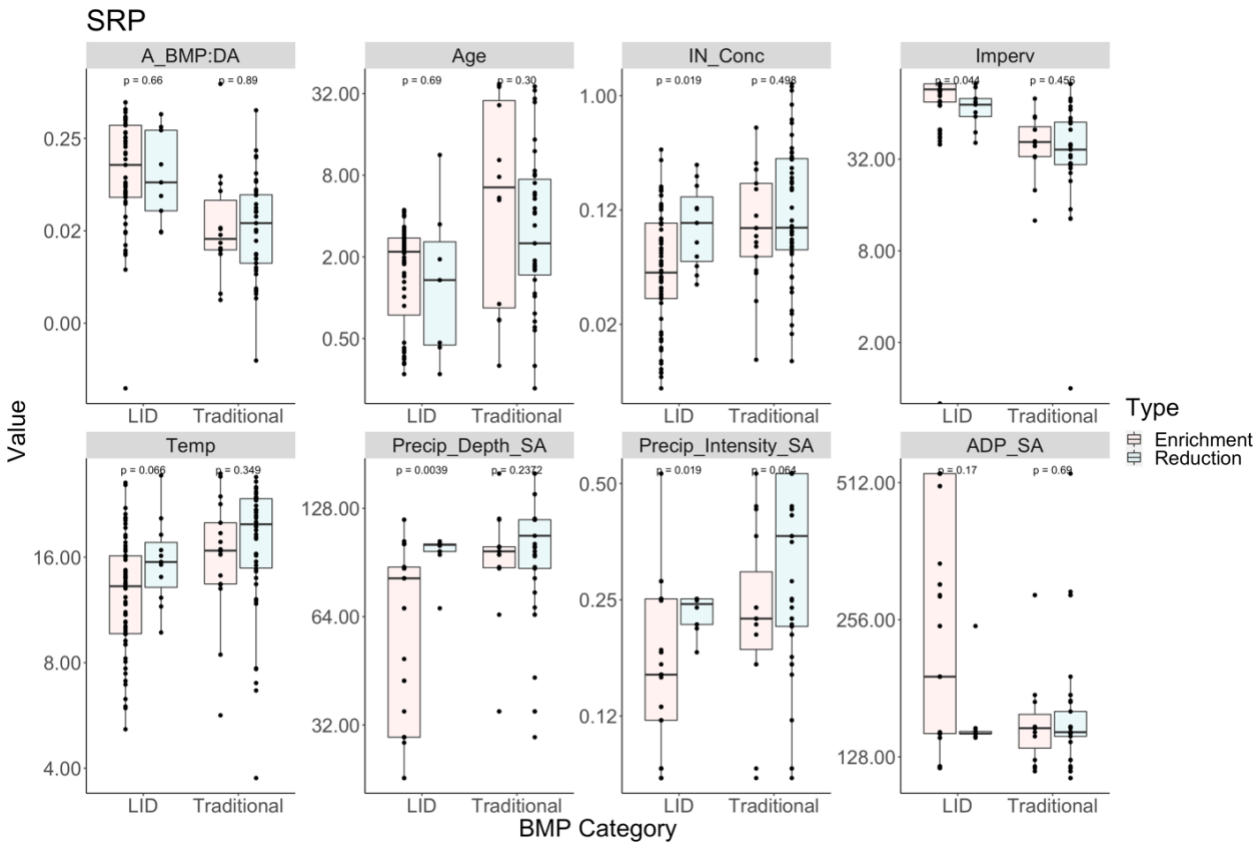

Figure AC3. Boxplots of factor values (site-scale results) under reduction or enrichment condition for traditional and LID BMPs. Significance (p value) of the difference of factor values under enrichment and reduction conditions under quantified by Wilcoxon Signed-Rank test. Difference of factor values between enrichment and reduction conditions can be considered as statistically significant if p value is lower than 0.05.

Table AC1. Categories of land uses

Land use categories labels used in this study	Key words in recorded land use categories labels in International Stormwater BMP Database
Institutional	Institutional, College Campus
Residential	Residential
Transportation	Highway, Ride, Parking, Automotive, Maintenance Station
Industrial	Industrial
Commercial	Commercial, Retail, Restaurants
Undeveloped	Open Space, Forest, Rangeland, Farming

Table AC2. Median model simulation accuracy (quantified as NSE) under different types of model for event and site scale TP and SRP concentration reduction/elimination factors simulation.

Method	Median NSE			
	SRP event	SRP site	TP event	TP site
Generalized linear model (GLM)	0.48	0.49	0.43	0.40
Nearest neighbour clustering (kNN)	0.51	0.29	0.49	0.28
Neural network (NN)	0.26	-*	0.36	0.23
Linear support vector machines (SVM)	0.46	0.49	0.42	0.39
Decision tree (DT)	0.37	0.26	0.27	0.32
Random forest (RF)	0.65	0.63	0.67	0.51
Reduction efficiency (RE)	-0.01	0.02	0	-0.04

*Data is insufficient for model validation.